Functional analysis of the 5' untranslated region of the c-*myc* proto-oncogene

by

Mark Stoneley M. A. (Cantab)

Thesis submitted for the degree of

Doctor of Philosophy

at the

University of Leicester

August 1998

UMI Number: U115896

Dissertation Publishing

Acknowledgements

Firstly, I would like to thank my supervisor, Anne Willis, for her ceaseless enthusiasm, encouragement and helpful advice. Her moto, "it'll be alright" helped me through even the worst failures and usually proved to be true.

Thanks also go to the members of "Lab 206", both past and present who provided illuminating discussions and made the laboratory an entertaining place to work. Those who have had to endure my unpredictable mood swings are; Fiona Paulin, Rebecca Whitney, Michelle West, Lucy Coles, John LeQuesne, Steve Chappell, and Mark Coldwell.

I would also like to thank Helen Plant for her unending support through the good times and the bad times. It is difficult to see how this thesis would have been completed without Helen's belief in me.

In addition, I would like to thank my parents, John and Carol, and my sister, Lisa, for their help and support throughout this project. Finally, I dedicate would like to dedicate this thesis to the memory of Bill Stoneley.

Abstract

Functional analysis of the 5' untranslated region of the c-*myc* proto-oncogene

Several mRNAs are expressed from the c-*myc* proto-oncogene, of which three have longer than average 5' untranslated regions (5' UTRs). These 5' leader sequences are GC-rich and consequently are predicted to contain stable RNA secondary structural motifs. Furthermore, the 5' UTR of the largest c-*myc* transcript P_0, contains four short open reading frames. Both of these features can reduce the translational efficiency of an mRNA and have been associated with regulated translational initiation. However, previous reports suggested that the predominant c-*myc* 5' UTRs did not alter the translational efficiency of the mRNA *in vivo*.

Expression of heterologous mRNAs fused to the principal c-*myc* 5' UTR (derived from the P2 transcript) in various cell lines confirmed that this element did not inhibit translation initiation. However, insertion of this sequence between the two cistrons of a dicistronic mRNA demonstrated that the 5' UTR stimulated the expression of the downstream cistron. Synthesis of the second cistron from the 5' UTR-containing dicistronic mRNA was shown to be independent of translation initiation at the upstream cistron start codon. In addition, the enhanced downstream cistron expression was shown to occur on intact dicistronic mRNAs. These data strongly suggest that the c-*myc* 5' UTR contains an internal ribosome entry segment capable of directing ribosomes to a site downstream of the 5' end of the mRNA.

Deletion analysis was used to define the minimum element required for c-*myc* IRES-directed translation. These experiments demonstrated that IRES is located between nucleotides -396 and -57 of the human c-*myc* P2 5' UTR. Interestingly, the activity of the c-*myc* IRES was found to vary in cell lines from different origins and was negligible if the dicistronic mRNAs were overexpressed. These observations imply that the efficiency of the c-*myc* IRES may depend on limiting factors. Furthermore, internal initiation directed by the c-*myc* 5' UTR was very inefficient on dicistronic mRNAs lacking a nuclear origin. Thus, a prior nuclear event may also be necessary for c-*myc* IRES-driven translation initiation.

Finally, the effect of the c-*myc* 5' leader sequences was analyzed in rabbit reticulocyte lysate. The 5' UTR was unable to promote internal ribosome entry in this system. In fact, both the P2 and P1 sequences reduced the translational efficiency of mRNAs. Furthermore, the P2 5' UTR displayed a strong dependence on the 5' cap structure.

Thus, the experiments herein suggest that the 5' UTR may modulate c-*myc* protein synthesis through both the cap-dependent and internal initiation mechanism of translation.

Contents

Abbreviations

AdML	adenovirus major late
ATP	adenosine 5'-triphosphate
ATPase	adenosine triphosphatase
bHLHzip	basic helix-loop-helix leucine zipper
BiP	immunoglobulin heavy chain binding protein
bp	base pairs
BSA	bovine serum albumin
Cad	Carbomyl-phosphate synthase (glutamine-hydrolysing)/asparatate carbamoyltransferase/dihydrooratase
CAT	chloramphenicol acetyltransferase
CDK	cyclin-dependent kinase
cDNA	complementary DNA
C/EBP	CCAAT/enhancer binding protein
CIAP	calf intestinal alkaline phosphatase
CMV	cytomegalovirus
cpm	counts per minute
CSFV	classic swine fever virus
CTP	cytidine 5'-triphosphate
dATP	deoxyadenosine 5'-triphosphate
dCTP	deoxycytidine 5'-triphosphate
ddNTP	dideoxynucleoside 5'-triphosphate
dGTP	deoxyguanosine 5'-triphosphate
DNA	deoxyribonucleic acid
DNase	deoxyribonuclease
dNTP	deoxyribonucleoside 5'-triphosphate
DTT	dithiothreitol
dTTP	deoxythymidine 5'-triphosphate
EBV	Epstein-Barr virus
E. Coli	*Escherischia coli*
EDTA	diaminoethanetetra-acetic acid

EGF	epidermal growth factor
eIF	eukaryotic initiation factor
EMCV	encephalomyocarditis virus
FCS	fetal calf serum
FGF2	fibroblast growth factor
Fluc	firefly luciferase
FMDV	foot and mouth disease virus
gas-1	growth-arrest specific gene
GDP	guanosine diphosphate
GSB	gel sample buffer
GST	glutathione-S-transferase
GTP	guanosine 5'-triphosphate
GTPase	guanidine triphosphatase
HCV	hepatitis C virus
HEPES	N-[2-hydroxyethyl]piperazine-N'-[2-ethanesulfonic acid]
HL60	human leukemic cell line 60
HLA	human leukocyte antigen
HLH	helix-loop-helix
HRV	human rhinovirus
HSP	heat shock protein
IGFII	insulin-like growth factor II
IgM	immunoglobulin class M
IL-3	interleukin-3
Inr	initiator element
IRE	iron response element
IRES	internal ribosome entry segment
IRP	iron regulatory protein
kB	kilobases
kcal	kilocalorie
kDa	kilodalton
LB	Luria-Bertani broth
LFA-1	leukocyte function-associated activity-1

MEL	murine erythroleukemia
met-tRNA$_i$	initiator methionyl tRNA
MHC	major histocompatibility complex
Miz-1	Myc-induced zinc-finger protein-1
MOPS	3-[N-morpholino]propanesulfonic acid
MrDb	Myc-regulated DEAD-box protein
mRNA	messenger ribonucleic acid
N-CAM	neural cell adhesion molecule
nt	nucleotide
ODC	ornithine decarboxylase
ORF	open reading frame
PABP	poly[A] binding protein
PAGE	polyacrylamide gel electrophoresis
PBS	phosphate buffered saline
PCBP1	poly(rC) binding protein 1
PCBP2	poly(rC) binding protein 2
PCR	polymerase chain reaction
PDGF2	platelet derived growth factor 2
Pfu	*Pyrococcus furiosus*
PIPES	piperazine-N, N'-bis[2-ethanesulfonic acid]
PNK	polynucleotide kinase
pRB	Retinoblastoma protein
PTB	polypyrimidine tract binding protein
PTF	poliovirus translation factor
Pwo	*Pyrococcus woesei*
Rluc	*Renilla* luciferase
RNA	ribonucleic acid
RNase	ribonucleic acid hydrolyase
RRL	rabbit reticulocyte lysate
RSV	rous sarcoma virus
s. d.	sample standard deviation
SDS	sodium dodecyl sulphate

TAD	transcriptional activation domain
Taq	*Thermophilus aquaticus*
TBP	TATA-box binding protein
TFIID	transcription factor IID
TFII-I	transcription factor II-I
4-thioUTP	4-thiouridine 5'-triphosphate
TLC	thin layer chromatography
TMEV	Theiller's murine encephalomyelitis virus
Tris	2-amino-2-(hydroxymethyl)-1, 3-propanediol
tRNA	transfer ribonucleic acid
UFR	unusual folding region
uORF	upstream open reading frame
USF	upstream binding factor 1
UTR	untranslated region
UTP	uridine 5'-triphosphate
UV	ultraviolet
VEGF	vascular endothelial growth factor
YY-1	ying-yang-1

Chapter 1

Introduction

1.1 General overview

A eukaryotic cell must be competent to respond to intracellular and extracellular signals and modulate gene expression accordingly. The multi-step nature of the pathway between DNA and gene product allows control to be exerted at numerous stages in this process. Consequently, the regulation of gene expression is both complex and diverse. Protein synthesis is an integral component of the pathway of gene expression and as such represents a target for regulation. Indeed, both the global rate of protein synthesis and the relative rates of synthesis of individual proteins can be influenced at the level of translation.

The c-*myc* proto-oncogene is a critical regulator of cell fate and is involved in the processes of cell proliferation, cell growth, differentiation, and apoptosis (see Henriksson and Lüscher, 1996). De-regulated expression of c-*myc* results in cellular transformation and contributes to a tumorigenic phenotype (Marcu *et al.*, 1992). Thus, c-*myc* gene expression is regulated at multifarious levels, involving both transcriptional and post-transcriptional processes, to avoid the inappropriate accumulation of the gene product. Numerous reports have suggested that the synthesis of the c-*myc* protein can contribute to the regulation of c-*myc* gene expression. Furthermore, much attention has focussed on the 5' untranslated region (5' UTR) of the c-*myc* mRNA and its potential role in modulating translation initiation (Nilsen and Maroney, 1984; Butnick *et al.*, 1985; Darveau *et al.*, 1985; Lazarus *et al.*, 1988; Fraser *et al.*, 1996; Nanbru *et al.*, 1997; Stoneley *et al.*, 1998).

1.2. Eukaryotic protein synthesis

Eukaryotic protein synthesis can be subdivided into three phases; initiation, elongation, and termination. During the initiation phase, the ribosome binds to the mRNA and identifies a start codon. Subsequently, polypeptide chain elongation is catalysed by the ribosomal peptidyl synthase activity. In this cyclic process, each round results in the addition of a single amino acid to the C-terminal end of the nascent polypeptide chain. Finally, termination

1

occurs when the ribosome encounters a stop codon, resulting in cleavage of the completed peptidyl-tRNA and dissociation of the ribosomal subunits.

The regulation of protein synthesis can contribute to changes in gene expression throughout cell growth, differentiation and development. The great majority of this control impinges on the initiation phase of translation. Furthermore, an alteration in the initiation efficiency can modulate both the global rate of protein synthesis and the relative rates of synthesis of different proteins.

1.3. Initiation of protein synthesis

The initiation of translation involves the sequential binding of the 40S and the 60S ribosomal subunits to the mRNA, culminating in the assembly of an 80S ribosomal initiation complex at a start codon. This process is catalysed by a set of initiation factors (eIFs), many of which are protein complexes (see Table 1.1).

The principal events of the initiation pathway occur in four major steps (fig. 1.1). After a termination event the ribosome dissociates into 40S and 60S ribosomal subunits (fig. 1.1; stage I). The initiator methionyl-tRNA (met-tRNA$_i$) can then associate with the 40S ribosomal subunit producing the 43S preinitiation complex (fig. 1.1; stage II). This complex subsequently binds to the mRNA and migrates to the initiation codon forming the 48S preinitiation complex (fig. 1.1; stage III). Finally, the 60S ribosomal subunit interacts with the 40S ribosomal subunit generating an 80S initiation complex (fig. 1.1; stage IV). The ribosome is now competent to translate the open reading frame (reviewed in Hershey, 1991; Pain, 1996).

1.3.1. Dissociation of 80S ribosomes

At physiological Mg^{2+} concentrations the formation of 80S ribosomes is strongly favoured compared to its dissociation into 40S and 60S subunits. However, following termination the spontaneous assembly of the 80S ribosome is prevented by two initiation factors, eIF1A and eIF3, binding to the 40S subunit (Goumans et al., 1980). Both factors have been detected in 43S preinitiation complexes following sucrose density gradient centrifugation demonstrating the stability of these interactions. However, a recent report suggests that eIF1A does not play

Factor	Function	Subunit mass (kDa)	
eIF1A	Stimulates transfer of ternary complex to the 40S ribosome.	Human 16.5	*S. cerevisiae* 17.4 (*TIF11*)
eIF2	GTP-dependent met-tRNA binding to the 40S ribosome.	Human α 36 β 38 γ 52	*S. cerevisiae* α 35 (*SUI2*) β 32 (*SUI3*) γ 58 (*GCD11*)
eIF2B	Exchanges eIF2-bound GDP for GTP	Rat α 34 δ 58 ε 80	*S. cerevisiae* α 34 (*GCD3*) β 43 (*GCD7*) γ 66 (*GCD1*) δ 71 (*GCD2*) ε 81 (*GCD6*)
eIF3	Stimulates the formation of 40S ribosomes. Provides link between 43S preinitiation complex and the cap binding complex, eIF4F	Human p170 p116 p110 (hNip1) p66 p47 p44 p40 p36 (TRIP-1) p35	*S. cerevisiae* p135 p90 (*PRT1*) p62 (*GCD10*) p39 (*TIF34*) p33 p29 p21 p16 (*SUI1*)
eIF4AI	ATP-dependent RNA helicase. Stimulates RNA binding.	Mouse 46	*S. cerevisiae* 45 (*TIF1*)
eIF4AII	ATP-dependent RNA helicase. Stimulates RNA binding.	Human 46	*S. cerevisiae* 45 (*TIF2*)
eIF4B	Stimulates helicase activity of eIF4A.	Human 69	*S. cerevisiae* 48 (*TIF3*)
eIF4E	Cap binding component of eIF4F.	Human 25	*S. cerevisiae* 24 (*CDC33*)
eIF4G	Provides bridging structure between eIF4E and 43S preinitiation complex.	Human 154	*S. cerevisiae* 107 (*TIF4631*) 104 (*TIF4632*)
eIF5	GTP-dependent formation of the 80S initiation complex.	Rat 49	*S. cerevisiae* 45 (*TIF5*)

Table 1.1: Details of the eukaryotic translation initiation factors.

(I) Dissociated ribosomal subunits
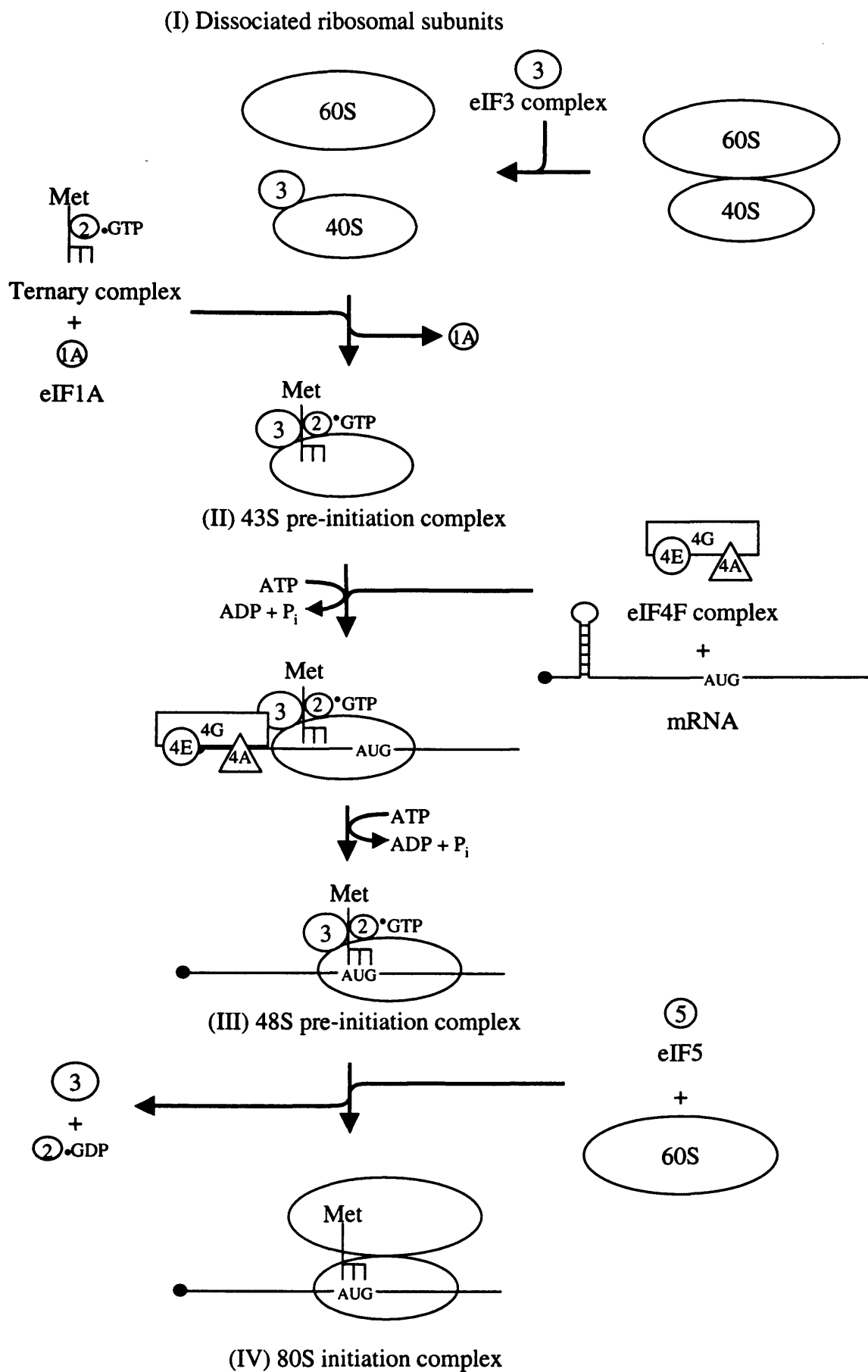
Figure 1.1: A schematic diagram illustrating the multi-step pathway of translation initiation. Initiation factors are represented by a shape containing the relevant number.

a role in the dissociation of 80S ribosomal subunits nor does it form a stable complex with the ribosome (Chaudhuri *et al.*, 1997).

1.3.2. Formation of the 43S preinitiation complex

The met-tRNA$_i$ is recruited to the 40S ribosomal subunit in a ternary complex whose other components are eIF2 and GTP. Binding of the ternary complex to the 40S ribosome results in the formation of the 43S preinitiation complex (reviewed in Pain, 1986). It has been suggested that eIF3 stabilises the interaction of the ternary complex with the 40S ribosome subunit (Trachsel *et al.*, 1977; Trachsel and Staehelin, 1979). Electron microscopy studies place eIF2 and eIF3 in close proximity on the 40S subunit providing a structural basis for this hypothesis (Bommer *et al.*, 1991). In addition, eIF1A substantially enhances the transfer of the ternary complex to the 40S ribosomal subunit *in vitro*. Nevertheless, eIF1A was not found to associate with the ribosome under these conditions suggesting that it performs a catalytic function in 43S preinitiation complex formation (Chaudhuri *et al.*, 1997).

1.3.3. mRNA binding to the 43S preinitiation complex

The 43S preinitiation complex (as detailed above) is believed to represent the active species of the 40S subunit recruited to the mRNA. Two separate models have been proposed for the assembly of the 48S preinitiation complex. For the majority of eukaryotic mRNAs, binding of the 40S subunit occurs at the 5' terminus and subsequently the ribosome migrates in a 5'-3' direction towards the initiation codon (the scanning model). Alternatively, the 40S subunit can bind a region downstream of the 5' end resulting in either direct recognition of the initiation codon or scanning (the internal initiation model) (Fig. 1.2).

1. The scanning model - cap-dependent initiation

Eukaryotic mRNAs are posttranscriptionally modified at their 5' terminus with a 7-methyl-guanylic acid residue, known as the cap structure (m^{7}GpppN). Although, uncapped transcripts can be translated *in vitro* and *in vivo* (Muthukrishnan *et al.*, 1976; Lodish and Rose, 1977; Hambridge and Sarnow, 1991; Gunnery and Matthews, 1995), the presence of a 5' cap structure dramatically stimulates protein synthesis *in vivo* (Drummond *et al.*, 1985; Hambridge and Sarnow, 1991). The initiation factor eIF4E interacts directly with the 5'cap

A. Cap-dependent mechanism of ribosome binding

43S preinitiation complex directed
to the mRNA by the eIF4F complex
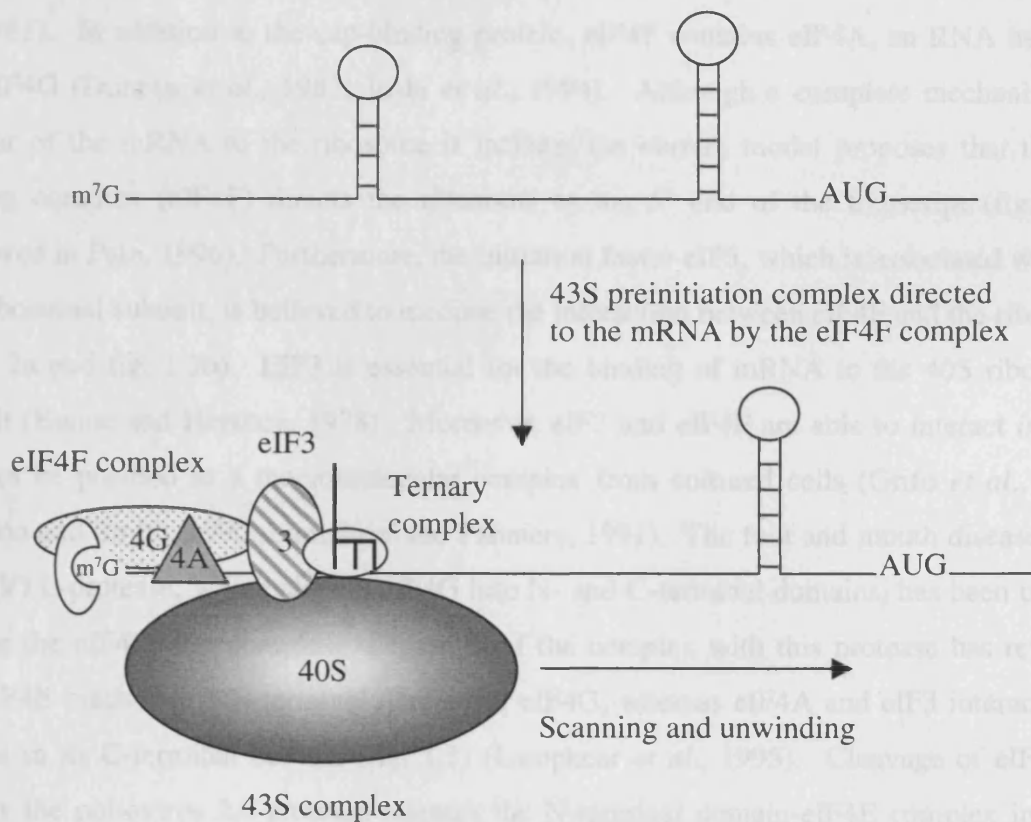
B. Internal initiation mechanism of ribosome binding
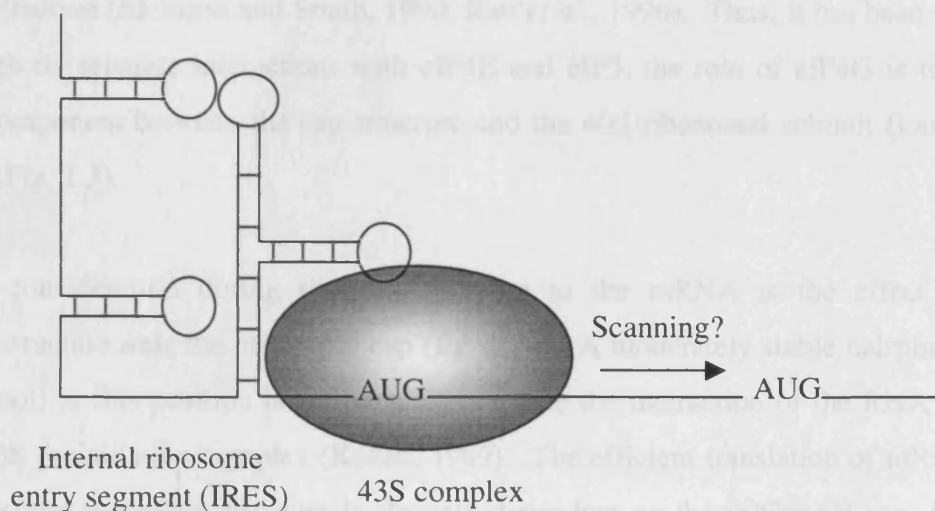
Figure 1.2: Alternative models for ribosome recruitment to the mRNA. (A) The conventional scanning model. The 43S preinitiation complex is recruited to the 5' end of the mRNA in a cap-dependent manner by the eIF4F complex. (B) The internal ribosome entry model. The ribosome is conducted to the mRNA at a site distal to the 5' end of the transcript by a complex structured element, known as an internal ribosome entry segment (IRES).

structure. This phosphoprotein can be isolated as a component of a high molecular weight cap-binding complex known as eIF4F. (Sonenberg *et al.*, 1978; Tahara *et al.*, 1981; Grifo *et al.*, 1983). In addition to the cap-binding protein, eIF4F contains eIF4A, an RNA helicase, and eIF4G (Duncan *et al.*, 1987; Joshi *et al.*, 1994). Although a complete mechanism for transfer of the mRNA to the ribosome is lacking, the current model proposes that the cap binding complex (eIF4F) directs the ribosome to the 5' end of the transcript (fig. 1.2a) (reviewed in Pain, 1996). Furthermore, the initiation factor eIF3, which is associated with the 40S ribosomal subunit, is believed to mediate the interaction between eIF4F and the ribosome (fig. 1.2a and fig. 1.3b). EIF3 is essential for the binding of mRNA to the 40S ribosomal subunit (Benne and Hershey, 1978). Moreover, eIF3 and eIF4F are able to interact *in vitro* and can be purified in a macromolecular complex from cultured cells (Grifo *et al.*, 1983; Etchison and Smith, 1990; Lamphear and Panniers, 1991). The foot and mouth disease virus (FMDV) L-protease, which cleaves eIF4G into N- and C-terminal domains, has been used to analyse the eIF4F-eIF3 complex. Digestion of the complex with this protease has revealed that eIF4E binds to the N-terminal domain of eIF4G, whereas eIF4A and eIF3 interact with regions in its C-terminal domain (fig. 1.3) (Lamphear *et al.*, 1995). Cleavage of eIF4G *in vivo* by the poliovirus 2A protease releases the N-terminal domain-eIF4E complex into the post-ribosomal supernatant, whilst the C-terminal domain remains associated with the ribosomal fraction (Etchison and Smith, 1990; Rau *et al.*, 1996). Thus, it has been suggested that through its separate interactions with eIF4E and eIF3, the role of eIF4G is to act as a bridging component between the cap structure and the 40S ribosomal subunit (Lamphear *et al.*, 1995) (Fig. 1.3).

A further consideration during ribosome binding to the mRNA is the effect of RNA secondary structure near the m⁷GpppN cap (fig. 1.2a). A moderately stable hairpin structure (-30 kcal/mol) in this position is sufficient to preclude the interaction of the RNA molecule with the 43S preinitiation complex (Kozak, 1989). The efficient translation of mRNAs with 5' cap-proximal secondary structure is strongly dependent on the m⁷GpppN cap, indicating that eIF4F is able to relieve local secondary structure and consequently promote ribosome binding (Morgan and Shatkin, 1980; Sonenberg *et al.*, 1981). This is achieved through eIF4A, which in combination with eIF4B exhibits ATP-dependent RNA helicase and ATPase activities (Pause and Sonenberg, 1992). Furthermore, the use of dominant negative eIF4A mutants indicates that this activity is essential for efficient cap-dependent translation (Pause *et al.*, 1994).

A. Domain structure of eIF4G

N-terminal domain

C-terminal domain

N

C

eIF4E binding

eIF3 binding

eIF4A binding

L-protease + 2A protease
cleavage sites
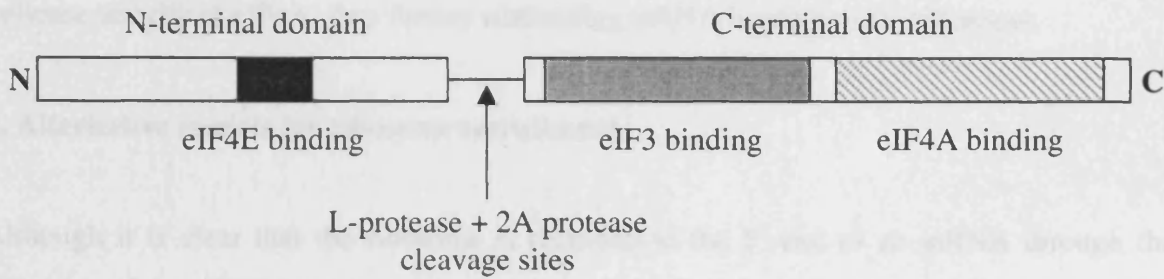
B. Result of eIF4G cleavage

4G

4E

4A

AUG

3

40S

Cleavage of eIF4G
with L- or 2A-protease

4A

3

40S

C-terminal domain associated
with eIF3 and eIF4A

4E

AUG

N-terminal domain associated
with eIF4E
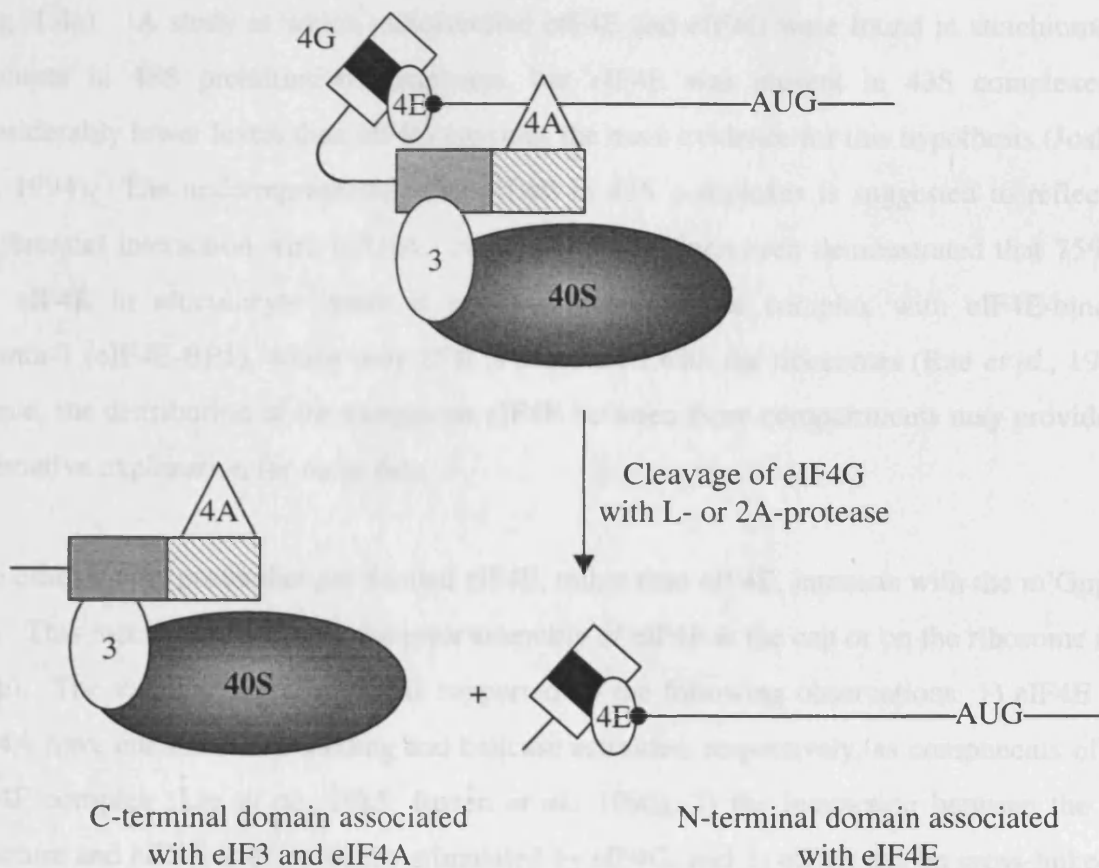
Figure 1.3: The interactions of eIF4G with eIF4E, eIF4A and eIF3. (A) The position of the eIF4G domains involved in protein-protein interactions with other initiation factors. Adapted from Morley *et al.*, 1997 (B) A model of the cap-dependent interaction of eIF4F with eIF3, demonstrating the bridging function of eIF4G. Cleavage of the eIF4G-eIF3 complex with the L-protease separates the N- and C-terminal domains as shown.

In summary, the components of eIF4F are believed to mediate the recruitment of the 43S preinitiation complex to the 5' end of the mRNA through protein-protein and RNA-protein interactions. In addition, eIF4F relieves 5' cap proximal secondary structure through the helicase activity of eIF4A, thus further stimulating mRNA binding to the ribosome.

2. Alternative models for ribosome recruitment

Although it is clear that the ribosome is recruited to the 5' end of an mRNA through the activities of the eIF4F complex, the exact order in which the components interact is unclear. Currently, two main models exist for the sequence of events that lead to ribosome binding (fig. 1.4). The first model suggests that eIF4E binds to the cap structure and subsequently recruits the 43S preinitiation complex, which is already associated with eIF4G, to the mRNA (Fig. 1.4a). A study in which radiolabelled eIF4E and eIF4G were found in stoichiometric amounts in 48S preinitiation complexes, but eIF4E was present in 43S complexes at considerably lower levels than eIF4G provides the main evidence for this hypothesis (Joshi *et al.*, 1994). The underrepresentation of eIF4E in 43S complexes is suggested to reflect its preferential interaction with mRNA. However, it has since been demonstrated that 75% of the eIF4E in reticulocyte lysate is present in an inactive complex with eIF4E-binding protein-1 (eIF4E-BP1), whilst only 25% is associated with the ribosomes (Rau *et al.*, 1996). Hence, the distribution of the exogenous eIF4E between these compartments may provide an alternative explanation for these data.

The other model posits that pre-formed eIF4F, rather than eIF4E, interacts with the m^7GpppN cap. This mechanism includes the prior assembly of eIF4F at the cap or on the ribosome (fig. 1.4b). The validity of this model is supported by the following observations: 1) eIF4E and eIF4A have enhanced cap-binding and helicase activities, respectively, as components of the eIF4F complex (Lee *et al.*, 1985; Rozen *et al.*, 1990), 2) the interaction between the cap structure and eIF4E is dramatically stimulated by eIF4G, and 3) eIF4B can be cross-linked to the mRNA provided eIF4F is assembled at the cap (Haghighat and Sonenberg, 1997). These data strongly favour the interaction of eIF4E with the cap structure as a part of the eIF4F complex, accompanied by localised relief of secondary structure and ribosome binding.

A. eIF4E binds alone to the cap

eIF4E-mRNA complex

eIF4G-43S complex

mRNA-43S complex

B. eIF4F binds to the cap

mRNA-eIF4F complex

43S complex

mRNA-43S complex

eIF4F-43S complex
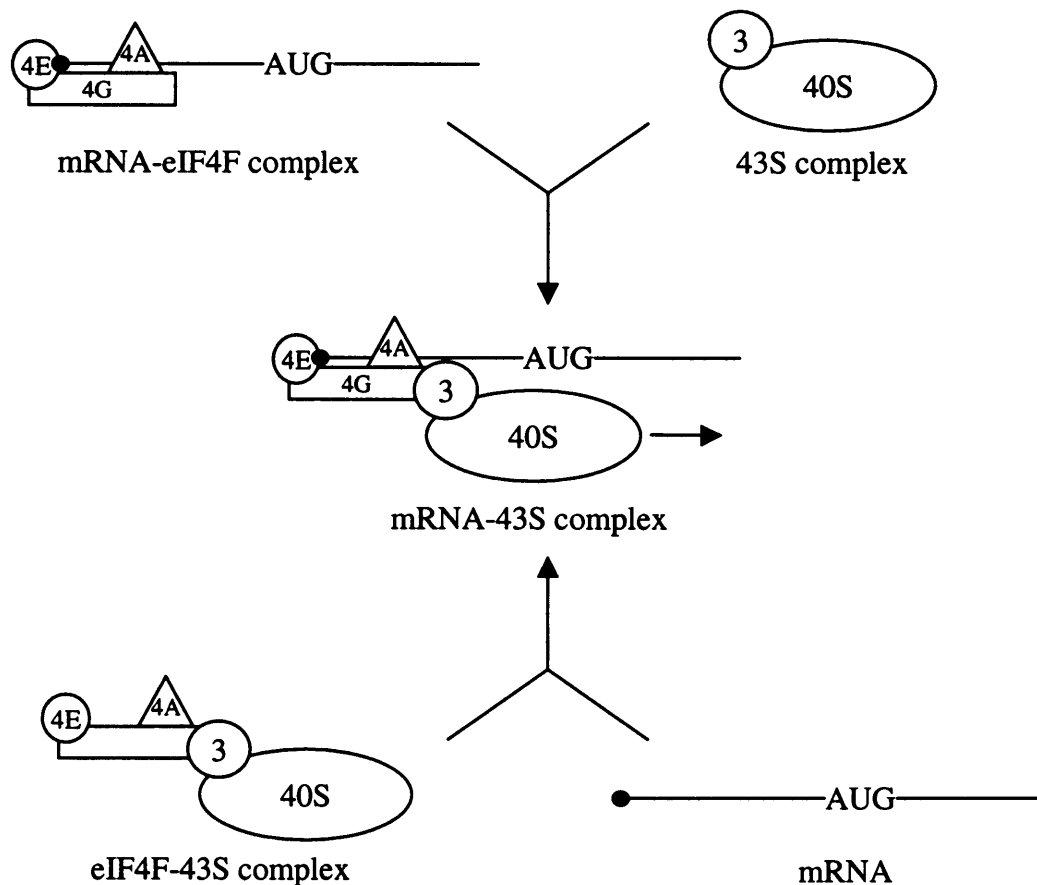
mRNA

Figure 1.4: Alternative models for the mechanism of ribosome recruitment during cap-dependent translation initiation. (A) EIF4E alone binds to the 5' cap and conducts the 43S complex, which is already associated with eIF4G, to the 5' end of the mRNA. (B) EIF4F is pre-assembled and interacts either with the 5' cap (upper) or the 43S complex (lower). The ribosome is then recruited to the mRNA through the activities of eIF4F.

1.3.4. Ribosome migration and start codon recognition

Interaction of the 43S preinitiation complex with the mRNA is followed by migration of the ribosome in a 5' to 3' direction by a process know as scanning. The presence of stable secondary structural elements (>50 kcal/mol) in the 5' UTR impedes ribosome scanning. However, structures with a lower free energy have considerably less effect on translation initiation. The implication of these results is that the 40S subunit has an associated helicase activity able to relieve downstream secondary structure. Nevertheless, very stable helices are refractory to this activity (Kozak, 1986a, 1989). It has been postulated that eIF4A, stimulated by eIF4B, may participate in this process (Altmann et al., 1993). However, whether it performs this task as a part of the eIF4F complex or separately is currently unknown.

It is a prediction of the scanning model of initiation that the scanning ribosome will encounter the most 5' AUG codon and initiate polypeptide chain elongation from this site (Fig. 1.2). Indeed, for the great majority of eukaryotic mRNAs this is the case (Kozak, 1987, 1991a). Studies in yeast have demonstrated that base-pairing between the met-tRNA$_i$ and the initiation codon contributes to start codon recognition (Cigan et al., 1988). In addition, mutations in each of the three subunits of eIF2 have been found to influence the fidelity of met-tRNA$_i$ interactions (Donahue et al., 1988; Cigan et al., 1989; Dorris et al., 1995). Nevertheless, it has become clear that sequences surrounding the start codon are also involved in specifying the initiation site. An examination of 699 vertebrate mRNAs revealed a consensus sequence (GCCGCCA/GCCAUGG) around the authentic initiation codon (Kozak, 1987). Furthermore, mutational analysis identified a purine at the -3 position and a G at the +4 position as critical determinants of initiation codon usage (Kozak, 1986b). Thus, the surrounding sequence context influences the efficiency of start codon recognition. This is particularly important for non-AUG initiation codons, such as CUG, ACG and GUG, where positions +4, +5 and +6 strongly enhance initiation from these sites (Boeck and Kolakofsky, 1994; Grünert and Jackson, 1994; Kozak, 1997).

It has been proposed that residues around the AUG are involved in interactions with either the 18S ribosomal RNA and/or trans-acting factors (McBratney and Sarnow, 1996; Kozak, 1986b). Whilst direct evidence for the former model is lacking, the La antigen and a protein of 100 kDa were found to bind specifically to the Kozak consensus sequence (McBratney and Sarnow, 1996). Both models suggest that these interactions would effectively slow the

progress of the ribosome in the region of the initiation codon and increase the probability of codon-anticodon recognition. Indeed, positioning a hairpin structure just downstream of a start codon in poor context inhibits ribosomal scanning and enhances the recognition of this start site (Kozak, 1991b).

1.3.5. Formation of the 80S initiation complex and eIF2 recycling

In order for the 40S and 60S ribosomal subunits to associate, the initiation factors that initially prevented the assembly of the 80S ribosome must be released. *In vitro* studies demonstrate that this step requires the hydrolysis of the eIF2 bound GTP in a process catalysed by eIF5 (Hershey, 1991). Although this factor contains motifs present in other GTPases, (Das *et al.*, 1993) it requires the presence of 40S subunits to promote GTP hydrolysis. Since eIF5 and eIF2 form a stable complex *in vitro*, this interaction is proposed to occur on the 40S ribosome and consequently stimulate eIF5 GTPase activity. The hydrolysis of GTP is followed by the release of initiation factors and as a result the association of the 40S and 60S ribosomal subunits (Chaudhuri *et al.*, 1994).

The formation of the 80S initiation complex represents the endpoint of translation initiation following which polypeptide synthesis occurs. However, the hydrolysis of the eIF2 bound GTP results in the generation of inactive eIF2-GDP binary complexes. Thus, in order for eIF2 to be incorporated into further ternary complexes, the GDP must be exchanged for GTP. This process is accomplished by eIF2B, a complex of five polypeptides, which has a guanine nucleotide exchange activity (Price and Proud, 1994).

1.3.6. Ribosome binding through internal initiation

The recruitment of ribosomes onto an RNA molecule can also occur through the mechanism of internal initiation. Unlike the scanning model of initiation, ribosome binding is independent of a cap structure and occurs at a site downstream of the 5' end of the transcript (Fig. 1.2). This mechanism was first proposed to account for the synthesis of the poliovirus and encephalomyocarditis virus (EMCV) polyproteins (Dorner *et al.*, 1984; Pelletier and Sonenberg, 1988a; Jang *et al.*, 1989). Both poliovirus and EMCV have been classified as picornaviruses and internal initiation has been demonstrated on the 5' leader sequences of all

the members of this family. Consequently, the picornaviruses have come to represent the paradigm for this mechanism (Jackson *et al.*, 1994; Jackson and Kaminski, 1995).

1. Internal initiation on picornavirus RNAs

Several features within the picornavirus RNA genome suggested that translation initiation by the conventional scanning mechanism would be extremely inefficient. The physical 5' end of the virion RNA is a covalently-linked virally-encoded protein (VPg). This protein is removed after infection and consequently translation occurs on an uncapped RNA molecule. Furthermore, the genomes have long 5' UTRs (610 to more than 1400 nt) that are predicted to contain a complex pattern of stable structural motifs. In addition, multiple AUG codons are present within the 5' leader sequences. These upstream AUGs are often poorly conserved between related virus species, within a virus species and even between isolates of the same serotype. Although some of these 'cryptic' AUG codons are located in a favourable sequence context, they do not appear to represent translation start sites (Jackson *et al.*, 1994; Jackson and Kaminski, 1995). Thus, the presence of both stable structural motifs and upstream AUG codons in the 5' leader sequence represents a considerable barrier to a scanning ribosome.

Dicistronic RNAs were employed to gain direct evidence of internal initiation (Dorner *et al.*, 1984; Pelletier and Sonenberg, 1988a; Jang *et al.*, 1989). Since the majority of ribosomes dissociate after translating the upstream cistron, the downstream cistron of such RNAs is translated inefficiently (fig. 1.5a). However, insertion of a picornavirus 5' UTR between the two cistrons results in efficient translation of the downstream open reading frame by internal initiation (fig. 1.5b). Indeed, enhanced expression of the downstream cistron occurs even when translation of the upstream cistron is strongly inhibited by the proteolytic cleavage of eIF4G (fig. 1.5c) (Pelletier and Sonenberg, 1988a).

Deletion analysis performed on picornavirus 5' UTRs has defined the minimum sequence required for internal initiation. These internal ribosome entry segments, as they have become known, are approximately 450 nt long and do not contain an obvious consensus sequence. However, they have been classified into three groups, the cardio- and aphthoviruses, the entero- and rhinoviruses, and hepatitis A virus, based on primary sequence conservation and more importantly secondary structure conservation (Jackson *et al.*, 1990; Jackson *et al.*,

A. Translation on a control dicistronic mRNA

upstream cistron   downstream cistron

m^7G
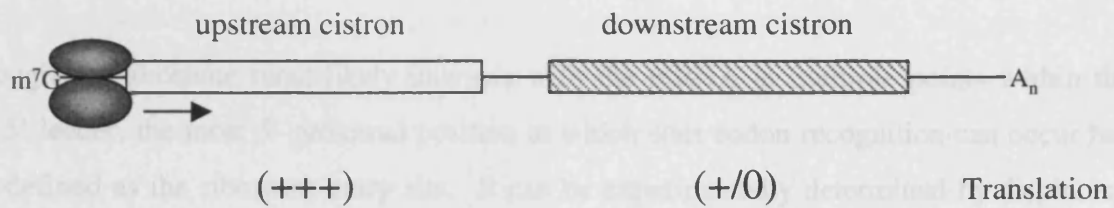
(+++)   (+/0)   Translation

B. Translation on a dicistronic mRNA containing an IRES

m^7G
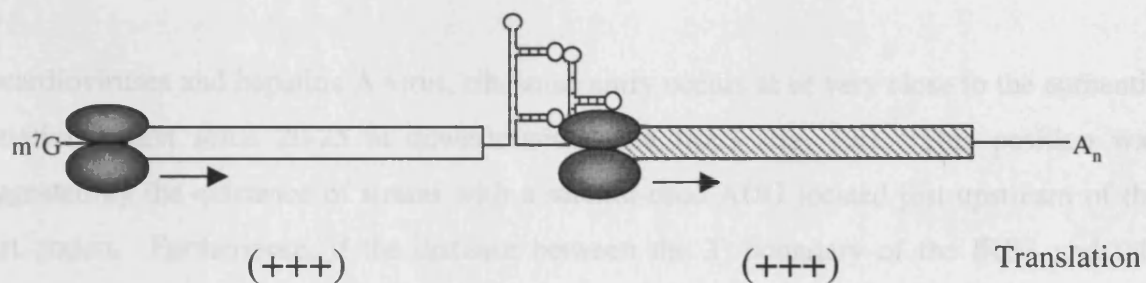
(+++)   (+++)   Translation

C. IRES-directed translation after poliovirus infection

m^7G
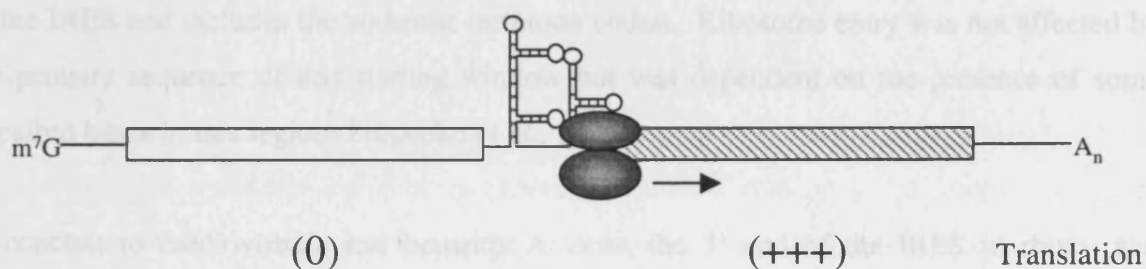
(0)   (+++)   Translation

Figure 1.5: Dicistronic mRNAs are employed to demonstrate internal initiation. (A) On the control dicistronic mRNA, the upstream cistron is translated efficiently by a cap-dependent mechanism whereas few ribosomes initiate translation at the downstream cistron. (B) Insertion of an IRES between the two cistrons results in efficient synthesis of upstream and downstream gene products by cap-dependent and internal initiation mechanisms, respectively. (C) Poliovirus infection inhibits cap-dependent translation initiation at the upstream cistron. However, the downstream cistron is translated efficiently by the cap-independent mechanism of internal initiation.

1994). The only conserved feature between these groups is a pyrimidine-rich tract approximately 25 nt upstream of the initiation codon (Jackson *et al.*, 1994).

2. The location of the ribosome entry site

Although the ribosome most likely interacts with the mRNA at multiple points within the viral 5' leader, the most 5' proximal position at which start codon recognition can occur has been defined as the ribosome entry site. It can be experimentally determined by displacing the start codon in a 3'-5' direction until it no longer acts as a translation start site. In picornaviruses this site has been localised to the 3' end of the IRES (Jackson and Kaminski, 1994). However, the position of ribosome entry relative to the authentic start site differs between the three major classes of picornaviruses.

In cardioviruses and hepatitis A virus, ribosome entry occurs at or very close to the authentic initiation codon some 20-25 nt downstream of the IRES (fig. 1.6). This position was suggested by the existence of strains with a seldom-used AUG located just upstream of the start codon. Furthermore, if the distance between the 3' boundary of the IRES and this cryptic AUG is increased the ribosome is able to initiate polypeptide synthesis from this site. This observation implies that the ribosome entry site is located a fixed distance from the IRES (Kaminski *et al.*, 1994). The ribosome entry site of Theiler murine encephalomyelitis virus (TMEV) has been mapped to a sequence that lies approximately 17 nt from the 3' end of the IRES and includes the authentic initiation codon. Ribosome entry was not affected by the primary sequence of this starting window but was dependent on the presence of some unpaired bases in this region (Pilipenko *et al.*, 1994).

In contrast to cardioviruses and hepatitis A virus, the 3' end of the IRES in rhino- and enteroviruses is located some distance upstream of the initiation codon, approximately 40 or 160 nts, respectively (Pelletier *et al.*, 1988b; Pilipenko *et al.*, 1992; Borman and Jackson, 1993). Ribosome entry occurs at or near to a conserved cryptic AUG located at the 3' end of the IRES (20-25 nts downstream of the polypyrimidine tract) (fig. 1.6). Indeed, the translational efficiency of poliovirus mutants lacking this AUG is severely compromised, suggesting a critical role for this element in internal initiation (Pelletier *et al.*, 1988b; Meerovitch *et al.*, 1991; Pestova *et al.*, 1994). Following its entry onto the RNA, the ribosome must be transferred downstream to the initiation codon. This is most likely

achieved through ribosome scanning since the intervening sequence is hypervariable and never includes an AUG codon. Indeed, insertion of an AUG codon or sequence predicted to form a stable hairpin in this region reduces infectivity or initiation at the authentic start (Pelletier and Sonenberg, 1988b; Kuge *et al.*, 1989). Ribosome scanning may also be involved in aphthovirus translation since some ribosomes begin translating from an AUG at the 3' end of the IRES (similar to cardioviruses and hepatitis A virus) and others initiate from the next downstream AUG (Jackson and Kaminski, 1995).

3. Structure-function relationships of the Picornavirus IRESes

Picornavirus IRESes have a complex secondary and presumably tertiary structure (Jackson *et al.*, 1994). The determination of a common secondary structure for the entero/rhinovirus and cardio/aphthovirus families has been facilitated by two factors: 1) The large number of virus species within each family, and 2) the high degree of genetic drift between different strains of the same species and different isolates of the same serotype. Thus, phylogenetic comparisons have provided evidence for secondary structure motifs that in many cases have been confirmed using biochemical probing (Jackson *et al.*, 1994). Viral function is often impaired by introducing mutations within the IRES that destabilise structural motifs. However, phenotypic revertants can be isolated that have compensatory mutations at a distant site which serve to restore the original structure. These observations underline the importance of IRES structure to the process of internal initiation (Haller and Semler, 1992).

A comparison of the conserved primary sequences in the entero/rhinovirus family has revealed that the majority of these are located in unpaired loops and bulges. Often mutation of one of these conserved residues results in a dramatic attenuation of internal initiation (Jackson *et al.*, 1995). It has been suggested that these primary sequences represent sites that interact with the protein and RNA components of the 43S preinitiation complex and other initiation factors. Thus, the ribosome is conducted to the RNA by a three dimensional arrangement of binding sites (fig. 1.6). Alternatively, another model postulates that *trans*-acting factors bind to some of these regions and promote ribosome binding (Fig. 1.6) (Jackson *et al.*, 1995).
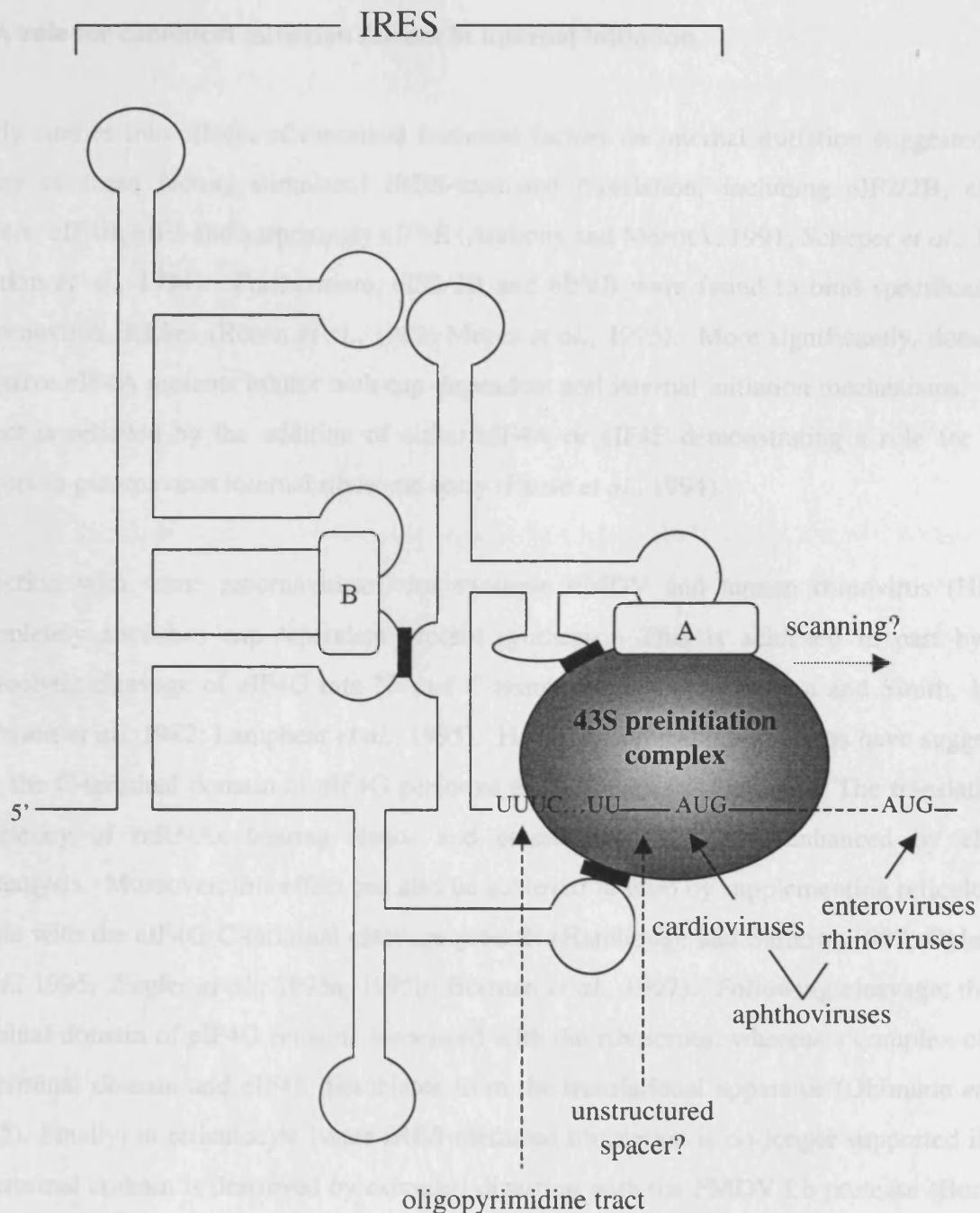
Figure 1.6: A general model for internal initiation of translation on picornavirus IRESes. The complex tertiary structure of the IRES presents a number of sequence elements in an orientation that allows their interaction with the 43S complex. In addition, some primary sequence motifs may be binding sites for specific RNA-binding proteins. These proteins either stabilise structural motifs (protein B) or are involved in interactions with the 43S complex (protein A). Through these interactions, the 43S complex is directed to the ribosome entry site which lies some 25 nt downstream of a conserved oligopyrimidine tract. In cardioviruses, the authentic initiation codon at the 3' end of the IRES is probably the ribosome entry site. In comparison, in entero/rhinoviruses a similar site may represent the point of ribosome entry, but it does not serve as an initiation codon; ribosomes migrate to a downstream AUG, most likely by a scanning mechanism. Finally, the aphthoviruses initiate at both the ribosome entry site and a downstream start site. Adapted from Jackson and Kaminiski (1995).

4. A role for canonical initiation factors in internal initiation

Early studies into effects of canonical initiation factors on internal initiation suggested that many of these factors stimulated IRES-mediated translation, including eIF2/2B, eIF4F, eIF4A, eIF4B, eIF3 and surprisingly eIF4E (Anthony and Merrick, 1991; Scheper *et al.*, 1992; Svitkin *et al.*, 1994). Furthermore, eIF2/2B and eIF4B were found to bind specifically to picornavirus IRESes (Rosen *et al.*, 1982; Meyer *et al.*, 1995). More significantly, dominant negative eIF4A mutants inhibit both cap-dependent and internal initiation mechanisms. This effect is relieved by the addition of either eIF4A or eIF4F demonstrating a role for both factors in picornavirus internal ribosome entry (Pause *et al.*, 1994).

Infection with some picornaviruses, for example FMDV and human rhinovirus (HRV), completely abolishes cap-dependent protein synthesis. This is achieved in part by the proteolytic cleavage of eIF4G into N- and C-terminal domains (Etchison and Smith, 1990; Etchison *et al.*, 1982; Lamphear *et al.*, 1995). However, several observations have suggested that the C-terminal domain of eIF4G performs a role in internal initiation. The translational efficiency of mRNAs bearing rhino- and enterovirus IRESes is enhanced by eIF4G proteolysis. Moreover, this effect can also be achieved *in vitro* by supplementing reticulocyte lysate with the eIF4G C-terminal cleavage product (Hambridge and Sarnow, 1992; Ohlmann *et al.*, 1995; Ziegler *et al.*, 1995a, 1995b; Borman *et al.*, 1997). Following cleavage, the C-terminal domain of eIF4G remains associated with the ribosomes, whereas a complex of the N-terminal domain and eIF4E dissociates from the translational apparatus (Ohlmann *et al.*, 1995). Finally, in reticulocyte lysate IRES-mediated translation is no longer supported if the C-terminal domain is destroyed by extended digestion with the FMDV Lb protease (Borman *et al.*, 1997). Thus, internal initiation appears to require an intact eIF4G C-terminal domain, whereas the N-terminal domain and eIF4E are not required. Since the C-terminal domain interacts with eIF3 and eIF4A, these data are also consistent with a function for eIF3 and eIF4A in internal initiation (Lamphear *et al.*, 1995; Ohlmann *et al.*, 1995).

The assembly of 48S preinitiation complexes onto the EMCV IRES *in vitro*, using purified canonical initiation factors, has provided direct evidence for their role in internal initiation. In addition to 40S subunits, met-tRNA$_i$ and EMCV RNA, this process required eIF2, eIF3, and eIF4F and was stimulated by eIF4B (Pestova *et al.*, 1996a). Furthermore, a stable interaction between an IRES secondary structure motif (the J-K domain) and eIF4F was

demonstrated. Thus, the proposed model for EMCV internal initiation involves direct binding of eIF4F to the IRES, followed by recruitment of the 43S preinitiation complex to the RNA (Pestova *et al.*, 1996a; Pestova *et al.*, 1996b). The interaction between eIF4F and the J-K domain is mediated by the central domain of eIF4G, which also contains the binding sites for eIF3 and eIF4A. Indeed, this domain in conjunction with eIF4A and eIF3 was sufficient to recruit the 43S preinitiation complex to the IRES (Pestova *et al.*, 1996b). However, unlike the intact C-terminal domain, the expression of this domain *in vivo* does not enhance EMCV-driven translation. This could be due to the presence of a second binding for eIF4A site on eIF4G that is required for internal ribosome entry *in vivo* (Imataka and Sonenberg, 1997).

Thus, the evidence suggests that the same canonical factors used in cap-dependent translation are also required for internal initiation, with the exception of eIF4E. However, since intact eIF4G is necessary for the activity of the IRES from hepatitis A virus, it remains possible that in some cases the N-terminus and eIF4E both play a part in internal initiation (Borman and Kean, 1997).

5. The hepatitis C virus and classic swine fever virus IRESes

IRESes are also found within the genomes of the non-picornaviral hepatitis C virus (HCV) and the pestiviruses, such as classic swine fever virus (CSFV) (Tsukiyama-Kohara *et* al., 1992; Poole *et al.*, 1995). Ribosome entry occurs at or immediately upstream of the authentic initiation codon and does not appear to involve scanning. In common with picornaviruses, these IRESes contain multiple upstream AUG codons and have a highly ordered secondary structure. However, they differ from those of the picornaviruses in the following respects: 1) they are approximately 100 nt shorter, 2) they include up to 30 nt of the coding region and, 3) they have distinct secondary structure motifs, such as a pseudoknot upstream of the initiation codon, that are functionally important (see Wang and Siddiqui, 1995).

Studies have suggested that the mechanism of ribosome entry for the HCV-like IRESes differs markedly from that of the picornaviruses. The 43S preinitiation complex is able to bind to the HCV and CSFV IRESes at the initiation site but does not require the activity of eIF4F, eIF4A, eIF4B or eIF3. Furthermore, internal initiation directed by HCV and CSFV IRESes was refractory to dominant negative eIF4A mutants, unlike picornavirus translation initiation (Pestova *et al.*, 1998).

The recruitment of the 43S preinitiation complex to the start site is mediated by direct interactions between the 40S subunit and the IRES. Indeed, these two components form a stable binary complex in the absence of any initiation factors. The S9 ribosomal protein was found to interact with both HCV and CSFV IRESes. Nevertheless, this interaction was also observed using a truncated IRES that was unable to form a binary complex with 40S ribosome. Therefore, although the S9 protein may have a role in ribosome transfer it does not provide the principle interaction between IRES and ribosome. Since, this was the only ribosomal protein found to cross-link to the IRESes, it has been suggested that the interaction between the IRES and the ribosome could involve the 18S rRNA (Pestova *et al.*, 1998).

Two models for HCV-like internal initiation have been proposed based on these observations. Either the 43S preinitiation complex binds directly to the IRES at the initiation site, or the 40S subunit and the ternary complex bind consecutively. Subsequently, the met-tRNA$_i$ interacts with the start codon forming the 48S preinitiation complex. These events do not require eIF4F, eIF4A, eIF4B or eIF3, however eIF3 may have a role in stabilising the 48S preinitiation complex. Furthermore, eIF3 is essential for the formation of the 80S initiation complex (Pestova *et al.*, 1998, Sizova *et al.*, 1998).

In conclusion, whilst the EMCV IRES functions by interacting with eIF4F, the HCV and CSFV IRESes are independent of this factor and appear to bind directly to the 40S ribosomal subunit.

6. A requirement for non-canonical *trans*-acting factors

The cardio- and aphthovirus IRESes function efficiently in reticulocyte lysate, whereas those of the hepatitis A virus and the entero/rhinoviruses are inefficient in this system. However, supplementation of reticulocyte lysate with cytoplasmic extracts from cultured cells or mouse liver stimulates internal initiation from entero/rhinovirus and hepatitis A IRESes, respectively (see Jackson and Kaminiski, 1995; Belsham and Sonenberg, 1996). Furthermore, the cardio/aphthovirus IRESes direct internal initiation efficiently in many cell lines, but the activity of entero/rhinoviruses IRESes varies considerably between cell lines (Borman *et al.*, 1997). Therefore, it appears that in addition to initiation factors, the activity of picornavirus IRESes depends on the presence of non-canonical *trans*-acting factors.

Two different approaches have been employed to characterise potential *trans*-acting factors. Gel retardation and UV crosslinking assays have identified specific RNA-protein complexes formed between cellular proteins and IRESes. Whilst using a more functional approach, fractions isolated from HeLa cytoplasmic extracts have been tested for their ability to stimulate internal initiation in rabbit reticulocyte lysate or *Xenopus* oocytes.

6a. The La autoantigen

A 52 kDa protein was found to bind to a region of the poliovirus IRES by a combination of mobility shift assays and UV crosslinking. This factor was subsequently purified and identified as the La autoantigen (Meerovitch *et al.*, 1989; Meerovitch *et al.*, 1993). The La autoantigen is an RNA binding protein believed to be involved in the maturation of RNA polymerase III transcripts. In addition, it is predominantly located in the nucleus, whilst picornavirus translation and replication occur exclusively in the cytoplasm. Nevertheless, following poliovirus infection its subcellular localisation alters, such that a significant fraction is present in the cytoplasm (Meerovitch *et al.*, 1993).

The addition of purified recombinant La protein to reticulocyte lysate both reduced aberrant initiation and enhanced internal initiation directed by the poliovirus IRES. These effects are also achieved using HeLa cell extract, however the amount of purified La added was approximately 10-fold higher than that present in HeLa extract (Meerovitch *et al.*, 1993; Belsham and Sonenberg, 1996). In addition, immunodepletion of La from HeLa cell lysate inhibited poliovirus translation. However, addition of purified, recombinant La could not relieve this effect (Svitkin *et al.*, 1994). Two arguments have been proposed to explain these discrepancies. The first posits that the recombinant La is in some way less active than endogenous La (Meerovitch *et al.*, 1993; Svitkin *et al.*, 1994; Belsham and Sonenberg, 1996). An alternative proposition suggests that the addition of La to reticulocyte corrects aberrant initiation events and consequently authentic initiation events are stimulated by default (Jackson *et al.*, 1995).

Thus, the role of La as a *trans*-acting factor for internal initiation is currently unclear. However, since La possesses an RNA helicase activity it has been postulated that it could function by influencing IRES secondary structure (Belsham and Sonenberg, 1996).

6b. Polypyrimidine tract binding protein

A protein doublet of 56-60 kDa can be cross-linked to all picornavirus IRESes and was identified as the polypyrimidine tract binding protein (PTB) (Borman *et al.*, 1993; Hellen *et al.*, 1993). PTB is predominantly a nuclear protein, but is more abundant in HeLa cytoplasmic extract than in reticulocyte lysate. Indeed, the addition of PTB to reticulocyte lysate stimulates internal initiation directed by the human rhinovirus IRES (Borman *et al.*, 1993).

Evidence of a direct role for PTB in picornavirus internal initiation has been provided by several observations. A stem loop was identified as a high affinity PTB binding site in the EMCV IRES. Mutations that destabilise this motif reduced both PTB binding and translation initiation. Moreover, when compensatory mutations were introduced to restore the RNA helix, both PTB binding and translation were rescued (Jang and Wimmer, 1990). In addition, a transcript containing this motif selectively inhibits EMCV IRES-driven translation (Kaminski *et al.*, 1995). Finally, a reticulocyte lysate depleted of PTB is unable to support internal initiation directed by the EMCV IRES, whilst cap-dependant translation is unaffected. However, this activity can be restored by the addition of purified, recombinant PTB at a physiologically relevant concentration (Kaminski *et al.*, 1995). Interestingly, despite the ability of PTB to interact with the TMEV IRES, the reticulocyte lysate depleted of PTB had no effect on its activity. Thus, it has been suggested that PTB could perform the role of an RNA chaperone by promoting the formation of active IRES structures in EMCV, whereas TMEV adopts the correct structure spontaneously (Kaminski *et al.*, 1995).

6c. Poly(rC) binding protein 2

A combination of RNA affinity chromatography and Northwestern blotting showed that three major polypeptides in the 39-42 kDa range specifically interact with stem-loop IV of the poliovirus IRES. The 39 kDa protein was identified as poly(rC) binding protein 2 (PCBP2), a nuclear protein believed to be involved in RNA metabolism (Blyn *et al.*, 1996; Leffers *et al.*, 1995). Furthermore, all three proteins are recognised by a PCBP2 specific antiserum indicating that they are post-translationally modified variants of PCBP2 (Blyn *et al.*, 1997).

The importance of the interaction between PCBP2 and stem-loop IV was implied by a small mutation in this region that abolished virus growth and formation of this RNA-protein complex. Furthermore, depletion of PCBP2 from a HeLa cell extract resulted in inefficient poliovirus RNA translation. This activity was restored by the addition of recombinant PCBP2, but not PCBP1, to a physiologically relevant concentration (Blyn et al., 1997). However, the role of PCBP2 in poliovirus internal initiation is not yet known.

6d. Functional approaches to identifying trans-acting factors

Two similar functional approaches have been adopted in the search for trans-acting factors involved in internal initiation, both of which rely on the stimulation of IRES activity in systems that normally translate entero/rhinovirus RNAs inefficiently.

The translation of poliovirus RNA in micro-injected *Xenopus* oocytes can be stimulated dramatically by either the co-injection of HeLa cytoplasmic extract or prior injection with total HeLa RNA. This effect is specific to the poliovirus IRES since neither cap-dependent translation nor mengovirus RNA translation is affected in this manner. Fractionation of HeLa cell extracts showed that this activity, termed poliovirus translation factor (PTF), is 300 kDa. Furthermore, PTF is localised almost exclusively in the cytoplasm and is distributed equally between the ribosomal fraction and the post-ribosomal supernatant (Gamarnik and Andino, 1996). However, the identity of PTF is currently unknown.

The activity of the HRV and the poliovirus IRESes in rabbit reticulocyte lysate can be greatly enhanced by the addition of HeLa cytoplasmic extract. Fractionation of this activity demonstrated that it co-purified with a 97 kDa protein and a quantity of PTB (Borman et al., 1993). Further purification of the 97 kDa protein drastically reduced the translation stimulatory activity and it was shown that p97 and PTB acted synergistically to stimulate HRV IRES activity. When purified from a ribosomal salt wash, the activity exists in a complex of greater than 400 kDa. It was suggested that this activity might represent a multi-subunit complex composed of p97, PTB and potentially other factors. Indeed, further characterisation of the HRV translation stimulatory activity has revealed that it also co-purifies with a 38 kDa protein (Jackson, 1996). However, the biochemical properties of p97 and p38 are not known at present.

In conclusion, although the existence of *trans*-acting factors that stimulate internal initiation has been demonstrated, little is know about how they perform this function. The model illustrated in figure 1.6 suggests that two of these roles could be either to act as RNA chaperones or to participate directly in the recruitment of the 43S preinitiation complex to the RNA.

1.4. The effect of the 5' UTR on the translation of cellular mRNAs

An analysis of polysomes isolated from eukaryotic cells reveals that the ribosomes are spaced along the mRNA at intervals of 80-100 nt. However, it has been demonstrated that ribosomes can be distributed every 30 nt when they stack up behind a pause site (Wolin and Walter, 1988). Therefore, under most physiological conditions, it is widely accepted that the rate-limiting step of protein synthesis is the initiation phase (Jagus *et al.*, 1981). Furthermore, kinetic studies indicate that the 43S preinitiation complex and eIF4F both contribute to the overall rate of protein synthesis (Lodish, 1974; Godefroy-Colburn and Thatch, 1981; Ray *et al.*, 1983; Sarkar *et al.*, 1984). However, joining of the 40S and 60S ribosomal subunits, to form the 80S initiation complex, has also been identified as near-limiting. Thus, it appears that a number of steps influence the rate of initiation, such that an increase in a single component is less likely to have a dramatic effect on protein synthesis (Hershey, 1991).

It is a corollary of the mechanisms of cap-dependent initiation and internal initiation that features within the 5' UTR will effect ribosome binding and initiation codon recognition. In doing so, they will modulate the translational efficiency of the mRNA.

1.4.1 Elements within the 5' UTR associated with inefficient translation

The 5' UTRs of some mRNAs, including many that encode for proteins involved in cell proliferation, are highly structured and/or contain small upstream open reading frames (uORFs). These elements are believed to be critical determinants of 80S initiation complex formation, and may play a crucial role in the regulation of cell growth (Kozak, 1991).

1. Secondary structure

Synthetic hairpin structures introduced into the 5' UTR of an RNA were shown to inhibit its translation in a manner dependent on the position and stability of the structure (Pelletier and Sonenberg, 1985a; Kozak, 1986; Kozak, 1989). Detailed *in vitro* analysis revealed that a modest amount of secondary structure (30 kcal/mol) near the m^{7}GpppN cap (12 nt) prevented its interaction with the 40S ribosomal subunit and consequently drastically impaired the translation of the RNA (Kozak, 1989). Moreover, a reduction in UV crosslinking of eIF4F components to the cap structure has been correlated with increased secondary structure near the 5' end of the RNA (Pelletier and Sonenberg, 1985b; Lawson *et al.*, 1988). These observations suggest that cap proximal structural elements interfere with eIF4F binding and consequently cap-dependent translation initiation.

In comparison, a structural element of at least 50 kcal/mol is required to inhibit translation if positioned further from the 5' cap. In this case, ribosome binding is unaffected, but the migration of the 43S preinitiation complex is impeded (Kozak *et al.*, 1989). Thus, secondary structure within the 5' UTR may inhibit translation by two mechanisms: 1) interfering with ribosome binding, and 2) obstructing the scanning ribosome.

The results of these studies are equally applicable to natural mRNAs. Indeed, extensive secondary structure within the 5' UTRs of many endogenous mRNAs elicits a reduction in their translational efficiency (Rao *et al.*, 1988; Grens and Scheffler, 1990; Hoover *et al.*, 1997). Furthermore, both mechanisms of translational repression appear to operate. For example, the major inhibitory element in the 5' UTR of platelet-derived growth factor 2 (PDGF 2) is a GC-rich region of 140 nt located immediately upstream of the start codon (Rao *et al.*, 1988). In contrast, secondary structure close to the m^{7}GpppN cap inhibits the translation of the ornithine decarboxylase (ODC) mRNA (Grens and Scheffler, 1990). These structured 5' UTRs impart translational inefficiency upon many mRNAs involved in the regulation of cell growth and may play a crucial role in maintaining regulated cell proliferation.

2. Secondary structure and the competition model

An overall increase in protein synthesis occurs after the stimulation of quiescent cells with hormones, growth factors or mitogens. In addition, the biosynthesis of many proteins is elevated over and above the general augmentation of translation (Standaert and Pollet, 1988). These effects correlate with enhanced eIF4F activity achieved through the phosphorylation or increased availability of eIF4F components.

Increased phosphorylation of both eIF4E and eIF4G is observed following growth stimulation (for reviews see Pain et al., 1996; Morley et al., 1997). In both cases this is suggested to enhance eIF4F complex formation (Morley et al., 1991; Morley and Pain, 1995; Lamphear and Panniers, 1990; Rau et al., 1996) and in the case of eIF4E may increase m⁷GpppN cap recognition (Minich et al., 1994). Furthermore, phosphorylation also contributes to the amount of eIF4E available for eIF4F assembly. EIF4E is also present in a low molecular weight complex in vivo associated with eIF4E-BP1 (Rau et al., 1996). This interaction prevents eIF4E from binding to eIF4G and participating in eIF4F complexes (Lin et al., 1994). However, after insulin stimulation eIF4E-BP1 is phosphorylated resulting in the release of eIF4E (Lin et al., 1994). Finally, increases in eIF4E mRNA and protein levels have been observed following mitogenic stimulation which further contribute to the elevation of eIF4F complex activity.

Several reports have suggested that the eIF4F complex is the limiting component of translation initiation (Hiremath et al., 1985; Duncan et al., 1987; Rau et al., 1996). Under these conditions, it has been proposed that competition exist between mRNAs. Those mRNAs with secondary structure in their 5' UTR will compete poorly for eIF4F and consequently are translated inefficiently. However, an increase in eIF4F activity would overcome this selection and accordingly have a greater effect on the translation of structured mRNAs. Indeed, the competition between mRNAs in rabbit reticulocyte lysate can be relieved by the addition of eIF4F (Ray et al., 1983; Sarkar et al., 1984). The competition model has been invoked to explain the preferential translation of certain mRNAs following growth stimulation. It is proposed that the increased eIF4F activity may relieve the translational repression of a group of mRNAs with highly structured 5' UTRs.

Ornithine decarboxylase has been suggested as one such mRNA subject to translational de-repression. The 5' UTR conferred an insulin-dependent preferential increase in translation on a heterologous reporter RNA. Furthermore, this effect correlated with the predicted secondary structure in the 5' UTR and was preceded by increased phosphorylation of eIF4E and eIF4B (Manzella et al., 1991). It was proposed that eIF4E activity is responsible for the translational derepression of ODC mRNA since enhanced translation initiation of endogenous ODC mRNA has been observed in cell lines overexpressing eIF4E (Shantz and Pegg, 1994; Rousseau et al., 1996). The constitutive expression of eIF4E is postulated to increase eIF4F activity and in two studies eIF4E was shown to be the limiting component of eIF4F (Hiremath et al., 1985; Duncan et al., 1987). Furthermore, overexpression of eIF4E in cell lines can overcome extensive secondary structure in synthetic 5' UTRs (Koromilas et al., 1992). However, there is some doubt about the validity of this model since overexpression of eIF4E did not increase the translational efficiency of a heterologous mRNA bearing the ODC 5' UTR (Shantz et al., 1996). In addition, a recent study of the cellular concentration of eIF4E demonstrates that it may not be the limiting component of translation initiation (Rau et al., 1996). Given the central position that eIF4F occupies during cap-dependent translation initiation its activity is likely to influence the synthesis of ODC. However, a number of modifications to this complex may be necessary to achieve translational de-repression rather than an increase in the activity of one component.

Other mRNAs, including pim-1 and c-myc, have been proposed as targets for translational regulation through the relief of structural inhibition (De Benedetti 1994; Hoover et al., 1997). However, the use of eIF4E overexpressing cell lines in these studies does not rule out the involvement of alternative mechanisms. This is clearly illustrated by the increased nucleocytoplasmic transport of the cyclin D_1 mRNA that occurs as a consequence of the deregulated expression of eIF4E (Rousseau et al., 1996).

3. Upstream AUG codons and reinitiation

The 5' UTRs of some mRNAs have one or more AUGs upstream of the authentic initiation codon (Kozak, 1991). An AUG in strong sequence context will be recognised by the scanning 40S ribosomal subunit and initiation at the downstream start site will be severely inhibited. It is often the case that an in-frame stop codon closely follows such an AUG resulting in a uORF. Following termination, the 40S ribosomal subunits remain associated

with the mRNA and continue scanning. The efficiency of reinitiation at the downstream start site is directly correlated with the distance between it and the uORF. Indeed, translational inhibition mediated by a uORF can be completely abrogated by increasing the intercistronic distance (Kozak, 1987). Obviously, in order to initiate at the downstream start site the 40S subunits must acquire another ternary complex. The effect of the intercistronic length on downstream cistron synthesis is believed to reflect the increased likelihood of the ternary complex interacting with the 40S subunit over time (Grant et al., 1994). Other factors influencing reinitiation include: 1) the sequence around the termination codon, 2) the peptide sequence of the uORF, and 3) the length of the uORF (for review see Geballe and Morris, 1994).

Translational regulation can be mediated by the presence of uORFs in the 5' UTR. A well-documented example is the activation of GCN4 under conditions of amino acid starvation in S. cerevisiae. GCN4 is a transcription factor that stimulates the expression of enzymes involved in de novo synthesis of amino acids. The presence of four uORFs in the 5' UTR ensure that it is not expressed in cells fed with amino acids. Following translation of the most 5' uORF, approximately 50% of 40S subunits acquire a new ternary complex before the third or fourth uORF. A consequence of the translation of uORF 3 and 4 is that few 43S ribosomal complexes reach the GCN4 initiation codon. However, during amino acid starvation the GCN2 kinase phosphorylates eIF2α and blocks the guanine nucleotide exchange activity of eIF2B. Consequently, the accumulation of eIF2/GDP makes it less likely that 40S ribosomes will interact with a new ternary complex before it reaches uORF3 or 4. Accordingly, some 40S subunits acquire a new ternary complex downstream of the inhibitory uORFs and hence the GCN4 ORF is translated (see Hinnebusch, 1996).

4. Interactions between structural elements and specific binding proteins

A class of mRNAs has been identified whose translation is regulated through structural motifs in the 5' UTR that interact with specific repressor RNA binding proteins. Furthermore, the formation of these inhibitory RNA-protein complexes can be modulated by intra/extracellular signals. The translation of ferritin mRNA, an intracellular iron storage protein, is controlled by iron concentrations in this manner (see Gray and Hentze, 1994). Regulation is achieved through the iron response element (IRE), a conserved stem-loop structure in the 5' UTR. The IRE has a free energy of approximately -5 kcal/mol, and hence

it is not sufficiently stable to affect ferritin translation. However, when intracellular iron concentrations are low, the IRE is recognised by specific RNA binding proteins, the iron regulatory proteins (IRPs). The assembly of the IRP-IRE complex inhibits ferritin translation by interfering with the formation of the 48S initiation complex. Translational inhibition mediated by IRPs is dependent on the position of the IRE and only occurs if the RNA element is within 60 nt of the cap structure. These observations suggest that the cap-dependent recruitment of the 43S preinitiation complex to the mRNA is sterically hindered by the IRP-IRE complex. Furthermore, this effect can be mimicked using heterologous mRNA binding proteins such as the MS2 coat protein and the U1A protein. These proteins inhibit the translation of an RNA *in vitro* and *in vivo* when their respective binding sites are located in a similar cap-proximal position (Stripecke and Hentze, 1992; Stripecke *et al.*, 1994).

Other examples of translational regulation through this mechanism are beginning to emerge. The 5' UTR of 5-aminolevulinate synthase, which is also involved in iron metabolism, contains an IRE that confers the same iron-dependent translational regulation on the mRNA (Melefors *et al.*, 1993). Furthermore, the auto-regulated translation of thymidylate synthase may be a result of the interaction between the protein and two elements within the mRNA, one in the 5' UTR and the other in the coding region (Chu *et al.*, 1993). In addition, poly[A]-binding protein (PABP) has been shown to repress its own translation through an oligo[A] element in the 5' UTR (DeMelo Neto *et al.*, 1995). This sequence is postulated to have a lower affinity for PABP than the poly[A] tails of cellular mRNAs and consequently translational inhibition only occurs when PABP levels are not limiting.

5. Oligopyrimidine tracts

Oligopyrimidine tracts (5-14 nt) are found at the extreme 5' end of mRNAs encoding the ribosomal proteins and other polypeptides involved in translation and growth regulation (Meyuhas *et al.*, 1996). These elements ensure the co-ordinate translation of the mRNAs and are predicted to form a hairpin structure (Meyuhas *et al.*, 1996). Transcripts bearing an oligopyrimidine tract undergo a selective shift to full-size polysomes during growth stimulation and a high proportion are present in inactive complexes even in growing cells. The recruitment of these mRNAs to the polysomes during growth stimulation is blocked by inhibition of the FRAP/TOR signalling pathway with the drug rapamycin (Jefferies *et al.*, 1994). This pathway appears to be exclusively involved in signalling to components of the

translational apparatus. Thus, it has been suggested that the regulation of mRNAs bearing these elements could involve a change in the phosphorylation of a specific binding protein mediated through the FRAP/TOR signalling pathway (Meyuhas *et al.*, 1996).

1.4.2 Elements within the 5' UTR conferring efficient translation

Some transcripts are translated significantly more efficiently than the majority of cellular mRNAs under conditions where the activity of eIF4F is compromised. Features located within the 5' leader sequences of these RNAs have been shown to be critical determinants of their enhanced translational efficiency. Examples include many viral mRNAs such as those encoding the alfalfa mosaic virus coat protein 4 (AMV 4), the late adenovirus mRNAs and the heat shock protein mRNAs.

1. Viral 5' leaders

The AMV 4 mRNA is capped and has a short 5' UTR, which is predicted to be unstructured. It is translated more efficiently in poliovirus-infected HeLa cell extracts than other capped RNAs, but with less than half the efficiency of EMCV IRES-driven translation (Sonenberg *et al.*, 1982). Furthermore, its translation *in vitro* is more resistant to reduced eIF4F activity than many capped RNAs (Sonenberg *et al.*, 1981). However, studies have shown that its translation does require eIF4F, albeit at a lower concentration than other cap-dependent mRNAs and it has been suggested that this effect is mediated by its unstructured 5' UTR (Fletcher *et al.*, 1990; Jackson *et al.*, 1995).

In the late phase of adenovirus infection host protein synthesis is downmodulated as a result of the near complete dephosphorylation of eIF4E. Furthermore, adenovirus mRNAs and chimaeric mRNAs bearing the adenovirus tripartite leader sequence were translated efficiently under these conditions (Huang and Schneider, 1991). However, the *in vitro* translation of these RNAs was dramatically inhibited in extracts having cleaved eIF4G (Thomas *et al.*, 1992). Thus, the adenovirus 5' UTR imparts efficient cap-dependent translation on its mRNA by a mechanism requiring a low level of eIF4F activity.

2. Heat shock protein mRNAs

In many cell-types, protein synthesis is downregulated after receiving a heat shock. This process involves phosphorylation/dephosphorylation of translation initiation factors, such as eIF4E (Duncan et al., 1987; Duncan and Hershey, 1984). However, against this background of translational inhibition, synthesis of the heat shock proteins (HSPs) is unaltered and in some cells can increase. This selective mechanism appears to be a consequence of the reduced eIF4F activity required for translational initiation on HSP mRNAs (Joshi-Barve et al., 1992). Furthermore, many observations suggest that the HSP mRNAs are translated by a relatively cap-independent mechanism. Expression of anti-sense eIF4E RNAs in cell lines dramatically reduces cap-dependent translation, but enhances the synthesis of HSPs. In addition, translational inhibition mediated by poliovirus infection has a reduced effect of on HSP synthesis when compare to most cap-dependent cellular mRNAs.

The preferential translation of HSP mRNAs under these conditions is a function of their 5' UTRs (reviewed by Linquist and Petersen, 1991; Rhoads and Lamphear, 1995). These elements are long and rich in A residues and consequently are predicted to be largely unstructured. Thus, according to the competition model HSP mRNAs are able to compete efficiently with other cellular messages even when eIF4F activity is greatly reduced. However, this is not the complete story since a synthetic unstructured leader cannot substitute for the HSP 5' UTR (Lindquist 1981; Linquist and Petersen, 1991). Indeed, the presence of a conserved 20 nt sequence near the 5' end of the mRNAs appears to be necessary but not sufficient for HSP synthesis (McGarry and Linquist, 1985). It has been suggested that the proximity of this element to the cap may contribute to an unstructured state at the extreme 5' end of the mRNA, thus drastically reducing its requirement for eIF4F activity (Jackson et al., 1995).

1.4.3 Internal ribosome entry segments in the 5' UTR of eukaryotic cellular mRNAs

The mechanisms of translational regulation described above all involve ribosome scanning from the 5' end of the mRNA. Indeed, it has been suggested that the overwhelming majority of cellular mRNAs are translated by a cap-dependent mechanism. Nevertheless, although most of IRESes studied thus far have been found in virus genomic RNAs, there is a growing body of evidence to support the use of internal initiation by cellular mRNAs (reviewed in

Iizuka *et al.*, 1995). Several studies have identified potential IRESes in the 5' UTRs of cellular transcripts encoding diverse proteins, these include immunoglobulin heavy chain binding protein (BiP), Antennapedia, TFIID, HAP4, basic fibroblast growth factor (FGF2), eukaryotic initiation factor 4G (eIF4G), insulin-like growth factor II (IGFII), platelet derived growth factor 2 (PDGF 2), c-Myc, and vascular endothelial growth factor (VEGF) (Macejak and Sarnow, 1991; Oh *et al.*, 1992; Iizuka *et al.*, 1994; Vagner *et al.*, 1995; Gan and Rhoads, 1996; Teerink *et al.*, 1995; Bernstein *et al.*, 1997; Nanbru *et al.*, 1997; Stoneley *et al.*, 1998; Stein *et al.*, 1998). In some cases, the evidence for an IRES in the mRNA is relatively strong, e. g. BiP and *antennapedia*, however further support is required in other instances (e. g. IGFII and PDGF2).

1. Glucose regulated protein 78/immunoglobulin heavy chain binding protein (BiP)

The translation of a 78 kDa protein, later identified as BiP, was found to be resistant to the general inhibition of cap-dependent protein synthesis subsequent to poliovirus infection (Sarnow, 1989). Furthermore, *in vitro* synthesised transcripts bearing the BiP 5' UTR can be translated in poliovirus-infected cells, indicating that such RNAs are translated by a cap-independent mechanism (Macejak *et al.*, 1990).

In mammalian cell lines, the expression of dicistronic mRNAs with the 220 nt BiP 5' UTR inserted between the two cistrons resulted in efficient translation of the downstream open reading frame, even after infection with poliovirus. Furthermore, the introduction of an RNA hairpin at the very 5' end of the first cistron completely abolished the translation of the first cistron but had no effect on the efficiency of downstream cistron translation. Thus, in conjunction with suitable controls this evidence demonstrates the presence of an IRES in the BiP 5' UTR (Macejak and Sarnow, 1991).

2. Antennapedia

Many mRNAs from *Drosophila melanogaster* have long 5' UTRs containing upstream AUGs that do not appear to function as initiation codons. Included amongst these is the mRNA encoding antennapedia, a gene product involved in development. The *antennapedia* gene has two promoters, P1 and P2, producing transcripts with upstream leader sequences of 1512 and 1727 nts respectively. The mRNA transcribed from P2 has 15 upstream AUGs of which 6 are

surrounded by favourable sequence context. Thus, it seems unlikely that these mRNAs are translated by the scanning mechanism. Indeed, the 5' UTR of the P2 mRNA mediates efficient translation of the downstream cistron on dicistronic RNAs either expressed in or transfected directly into *Drosophila* cell lines. Furthermore, such dicistronic RNAs remain associated with the polysomes when overall protein synthesis is inhibited by poliovirus infection. Hence, internal initiation occurs on the 5' UTR of the P2 mRNA demonstrating that an IRES is present within this sequence (Oh *et al.*, 1992). An element common to both P1 and P2 mRNAs was found to be partly responsible for this activity. This contains a 55 nt sequence, which is highly conserved between *Drosophila* species and is essential for IRES function (Iizuka *et al.*, 1995).

3. HAP4 and TFIID

The development of a translation extract from *Saccharomyces cerevisiae* capable of supporting both cap-dependent translation and cap-independent translation by internal initiation resulted in the identification of potential IRESes in the 5' UTRs of two yeast genes. The mRNAs of HAP4, a transcription factor, and TFIID, the TATA box binding protein, have long 5' UTRs that contain one or more short uORFs. The translation of chimeric RNAs containing these 5' UTRs is not stimulated by a m⁷GpppG cap structure and addition of the cap analogue to the extract did not inhibit their translation; thus the HAP4 and TFIID leader sequences confer cap-independent initiation of translation (Iizuka *et al.*, 1994). Furthermore, internal initiation mediated by these 5' UTRs *in vitro* was demonstrated on dicistronic RNAs confirming the presence of an IRES in the leader sequences of HAP4 and TFIID (Iizuka *et al.*, 1994). Whether these mRNAs are translated by the internal initiation mechanism *in vivo* has yet to be determined.

4. Human Fibroblast growth factor 2

Human fibroblast growth factor 2 is a cytokine involved in a number of cellular processes including, cell proliferation, differentiation, and wound healing (Rifkin and Moscatelli, 1989). The FGF2 coding region is preceded by a 318 nt 5' UTR that is predicted to have a highly ordered secondary structure. This sequence inhibits the translation of RNAs in a wheat germ extract, but not in a rabbit reticulocyte lysate or in COS7 cells. Consequently, it

has been postulated that *trans*-acting factors may be required for efficient FGF2 translation (Prats *et al.*, 1992).

In RRL, the presence of an m^7GpppN cap structure does not stimulate the translation of RNAs bearing the FGF2 5' UTR. Thus in this system, the 5' UTR directs translation by a relatively cap-independent mechanism (Vagner *et al.*, 1995). However, there is no supporting evidence for internal initiation mediated by this 5' UTR in RRL. Nevertheless, internal initiation driven by this sequence is observed on dicistronic mRNAs expressed in COS7 cells. However, translation of the downstream cistron is considerably less efficient than that which occurs on monocistronic mRNA preceded by this element (Vagner *et al.*, 1995). Thus, there is some evidence to suggest that the 5' UTR of FGF2 could contain an IRES.

Interestingly, another study demonstrated that the synthesis of FGF2 proteins is dramatically increased in cell lines overexpressing eIF4E. Furthermore, this effect appears to be due to an increase in the translation of FGF2 mRNAs (Kevil *et al.*, 1995). However, the authors did not determine whether the enhanced synthesis was due to a cap-dependent mechanism or internal initiation. Therefore, further work is necessary to determine the contribution of cap-dependent translation and internal initiation of translation to the synthesis of FGF2.

5. Vascular endothelial growth factor (VEGF)

Vascular endothelial growth factor plays a vital role in the formation of new blood vessels (Carmeliet *et al.*, 1996). The 5' UTR is long (1014 nt), GC-rich, and contains a short upstream open reading frame suggesting that translation by the conventional mechanism would be inefficient. However, despite these features the VEGF mRNA is translated efficiently *in vivo* (Stein *et al.*, 1998). Furthermore, the translation of a heterologous mRNA is enhanced 5-fold when it is fused to the VEGF 5' UTR. Insertion of the VEGF 5' leader sequence into the intercistronic region of a dicistronic mRNA results in a 70-fold stimulation of expression from the downstream cistron. Moreover, this effect is also observed under hypoxic conditions when cap-dependent translation is downmodulated (Stein *et al.*, 1998). These data indicate that internal entry of ribosomes occurs on the VEGF 5' UTR. Furthermore, deletion analysis suggests that the IRES is located within a 163 nt region of the 5' leader sequence (Stein *et al.*, 1998).

6. Insulin-like growth factor II

The human IGFII mRNA derived from promoter P1 has a 5' UTR of 598 nt and contains one upstream AUG codon. RNAs preceded by this sequence are translated extremely inefficiently both in RRL and HeLa cells (Teerink *et al.*, 1994; Teerink *et al.*, 1995). Nevertheless, there is limited evidence supporting a cap-independent mechanism of translational initiation for the IGFII mRNA. Heterologous RNAs bearing this leader sequence are translated equally efficiently in RRL whether they are capped or uncapped (Teerink *et al.*, 1994; Teerink *et al.*, 1995). In addition, the translation of these chimeric mRNAs is resistant to the downregulation of host protein synthesis accompanying the infection of HeLa cells by poliovirus (Teerink *et al.*, 1995). These data are consistent with either a cap-dependent mechanism of translation requiring little eIF4F activity or internal initiation of translation mediated by the IGFII 5' UTR.

The evidence for an IRES in the IGFII leader sequence is relatively weak. When dicistronic mRNAs are expressed in HeLa cells, translation of the downstream cistron is stimulated inefficiently by the IGFII 5' UTR when compared to the EMCV IRES (Teerink *et al.*, 1995). Furthermore, the presence of an element within this sequence that enhances reinitiation at the second cistron has not been addressed. Regardless, the apparently weak activity of this 5' UTR in the dicistronic assay could be due to its requirement for a *trans*-acting factor that is limiting in HeLa cells with respect to the expressed dicistronic mRNAs.

7. Eukaryotic initiation factor 4G (eIF4G)

The 5' UTRs of human and yeast eIF4G have several features reminiscent of the picornavirus leader sequences: 1) they are long compared to other cellular 5' UTRs, 2) they contain multiple cryptic AUG codons, and 3) a polypyrimidine tract is located a short distance upstream of the initiation codon. The human 5' UTR enhances the expression of reporter mRNAs in some cell lines despite the presence of four uORFs. Furthermore, mutation of the four upstream AUG codons has no effect on the translation of such mRNAs. In addition, this sequence was able to restore efficient translation to a cistron downstream of either an inhibitory hairpin structure or another open reading frame; a function characteristic of an IRES (Gan and Rhoads, 1996). Translation of the eIF4G mRNA through the mechanism of internal initiation is an attractive hypothesis since it would allow continued synthesis of this

protein subsequent to infection with viruses, such as poliovirus and adenovirus, that decrease eIF4F activity. However, the synthesis of eIF4G after poliovirus infection requires further investigation to substantiate this hypothesis.

8. PDGF2/c-*sis* - A differentiation inducible IRES

The 5' UTR of the platelet-derived growth factor 2/c-*sis* mRNA, which is 1022 nts long, represents a major barrier to the scanning 40S ribosomal subunit owing to its high GC content and the presence of 3 uORFs. Indeed, it strongly inhibits the translation of a downstream open reading frame in a number of cell lines (Rao *et al.*, 1988). This translational repression is greatly relieved during the megakaryocytic differentiation of human K562 cells (Bernstein *et al.*, 1995). However, the same effect is not achieved by the removal of the cryptic AUGs (Rao *et al.*, 1988) or overexpression of eIF4E (Bernstein *et al.*, 1995). Thus, this de-repression is unlikely to be due to enhanced reinitiation at the authentic AUG or the alleviation of structural inhibition. Instead, it has been postulated that differentiation may modulate PDGF2 translation by augmenting internal ribosome entry on the 5' UTR (Bernstein *et al.*, 1997). Upon differentiation, the translation of the downstream cistron of a dicistronic mRNA is enhanced. However, the increase in IRES activity is considerably lower than the stimulation that occurs on monocistronic mRNAs. Furthermore, an RNA hairpin structure positioned in the 5' leader of the 5' UTR-containing dicistronic mRNA reduced reporter gene expression from both cistrons. Thus, translation mediated by the PDGF2 5' UTR does not appear to be wholly cap-independent. In summary, these data are not entirely consistent with the presence of a conventional IRES in the 5' UTR of the PDGF2 mRNA. However, a relatively weak and differentiation inducible IRES-like element could explain these observations.

1.4.4. A comparison of virus and cellular IRESes

The cellular IRESes appear to share some common features with the virus IRESes, although a thorough comparison is hampered by the existence of only a handful of cellular examples and the limited studies performed on them thus far. Many of the cellular examples have cryptic AUGs within these elements, with the exception of FGF2 and BiP. Furthermore, the 5' UTRs of the cellular examples identified all contain predicted secondary structural motifs. Finally, in the case of the eIF4G IRES, the presence of a polypyrimidine tract located at the 3'

terminus is essential for efficient translation by internal initiation (Gan *et al.*, 1998). However, there appears to be considerably more variation in the size of cellular IRESes. The BiP and eIF4G IRESes have been mapped to sequences of only 92 nt and 101 nt, whilst the c-*myc* IRES is approximately 340 nt long (Yang and Sarnow, 1997; Stoneley *et al.*, 1998; Gan *et al.*, 1998).

There is limited evidence to suggest that like the picornavirus elements, ribosomes are also recruited to the 3' end of these cellular IRESes. The introduction of an AUG codon at the 3' end of the FGF2, eIF4G and antennapedia IRESes results in its use as a translation start site (Oh *et al.*, 1992; Gan *et al.*, 1998). In contrast, insertion of an AUG within the eIF4G IRES had little effect initiation at the authentic start codon (Gan *et al.*, 1998). However, further studies are required to definitively locate the ribosome entry sites on eukaryotic IRESes.

Attempts to align the virus and cellular IRESes demonstrate that there is no striking sequence conservation between these two groups of translational element. However, these RNA sequences are all predicted to contain complex secondary structure. Thus, the mechanism of ribosome binding could involve interactions between the translational apparatus and motifs within the tertiary structure of the IRES. In this regard, an unusual folding region (UFR) located just upstream of the BiP, FGF2 and antennapedia start codons has been predicted using an RNA folding algorithm that incorporates phylogenetic variations (Le and Maizel, 1997). This Y-shaped motif is also predicted to appear in a similar position in the cardio/aphthovirus and HCV-like IRESes (Le *et al.*, 1996). However, a comparison of this UFR to the more established secondary structural models reveals: 1) the J-K domain of the cardio/aphthovirus IRESes does form a Y-shaped motif but the helices are considerably longer than those predicted for the UFR, and 2) the UFR is not present in the HCV-like IRESes. Given the discrepancies between these models it remains to be determined whether this UFR exists in cellular IRESes.

1.4.5. A role for *trans*-acting factors in cellular internal initiation?

There are currently no reports of a cellular IRES directing internal initiation in rabbit reticulocyte lysate. Thus, it is possible that the cellular IRESes identified to date require non-canonical *trans*-acting factors, not present in RRL, in order to recruit the 43S preinitiation complex. Indeed, ultraviolet crosslinking assays have demonstrated that elements within the

BiP and FGF2 IRESes interact with proteins from HeLa cell extracts (Yang and Sarnow, 1997; Vagner *et al.*, 1996). The identity and biochemical functions of these factors are unknown, thus no conclusions can be draw about their role in internal initiation. However, it is noteworthy that two factors, p95 and p60, that interact with the BiP IRES are present in the nucleus. Moreover, the BiP IRES is significantly more efficient when transcribed in the nucleus compared to when introduced directly into the cytoplasm. Consequently, it has been proposed that *trans*-acting factors recruited in the nucleus may subsequently be involved in cytoplasmic internal initiation of translation (Iizuka *et al.*, 1995). This could represent a common mechanism to a subset of eukaryotic IRESes. However, since HAP4 and TFIID 5' UTRs promote internal initiation efficiently in a yeast cytoplasmic extract (Iizuka *et al.*, 1994) and the *antennapedia* IRES directs internal initiation when introduced into the cytoplasm by RNA transfection, it is not a mechanism utilised by all eukaryotic IRESes (Oh *et al.*, 1992).

1.4.6. The evolution of two mechanisms for initiation of translation

Although the majority of mRNAs are translated by a cap-dependent mechanism it is clear that some mRNAs utilise an alternative cap-independent pathway. This raises the question of why eukaryotic cells have evolved two mechanisms for initiation of translation? At present, only a few examples of cellular mRNAs translated by the internal initiation mechanism have been reported. Thus, it is difficult to arrive at any conclusions. However, one hypothesis suggests that these mRNAs encode a group of proteins that must continue to be synthesised when cap-dependent translation is downmodulated through a reduction in the activity or availability of eIF4F. This has been observed during mitosis, serum starvation, and as part of the cellular response to a heat shock/stress (Duncan and Hershey, 1984; Duncan and Hershey, 1985; Bonneau and Sonenberg, 1987; Vries *et al.*, 1997). Indeed, the synthesis of BiP and VEGF is maintained during either heat shock or hypoxic stress, respectively, supporting this argument (Haas, 1991; Stein *et al.*, 1998). For many of the mRNAs that support internal initiation this is an intellectually satisfying proposition, however direct evidence is currently lacking.

1.5. The c-*myc* proto-oncogene

1.5.1. The *myc* family of proto-oncogenes

The c-*myc* proto-oncogene was originally identified as the cellular homologue of the chicken v-*myc* oncogene (Vennström *et al.*, 1982; Dalla-Favera *et al.*, 1982). It has subsequently been cloned from many divergent species and displays a high degree of sequence conservation. Two other well characterised members of the *myc* family, the N-*myc* and L-*myc* genes, were identified as amplified coding sequences displaying a high degree of homology to c-*myc* in human neuroblastomas and small cell lung carcinomas, respectively (Swabb *et al.*, 1983; Nau *et al.*, 1985). The three *myc* genes share a three exon-two intron gene topology, with the major open reading frame residing in exons 2 and 3 (fig. 1.7). Homologous polypeptides are encoded by the family members and a number of highly conserved regions exist within exons 2 and 3.

In addition to c-, N-, and L-*myc*, two ill-characterised members of the *myc* family have been isolated. S-*myc* exhibits a high degree of homology to the second and third exons of N-*myc* but lacks the intervening intron (Sugiyama *et al.*, 1989); whilst B-*myc* is homologous to the second exon of c-*myc* and lacks the sequence corresponding to exon 3 (Ingvarsson *et al.*, 1988). To date, it has not been determined whether either gene expresses a functional polypeptide and it has been suggested that they could represent pseudogenes (Marcu *et al.*, 1992).

The N- and L-*myc* genes display a very restricted pattern of expression during mammalian development, with regulation occurring in both a tissue and developmental-stage specific manner (Zimmerman *et al.*, 1986; Downs *et al.*, 1989; Hirvonen *et al.*, 1990; Stanton *et al.*, 1992; Quéva *et al.*, 1998). In contrast, c-*myc* expression is more generalised and levels appear to correlate with cell proliferation and tissue folding during development (Schmid *et al.*, 1989; Stanton *et al.*, 1990). However, c-*myc* gene expression is not always restricted to proliferating cells, but is also found in some post-mitotic differentiating cells suggesting that it may play a role in other processes such as cell migration (Hirvonen *et al.*, 1990; Hurlin *et al.*, 1995).

A. C-*myc* genomic organisation
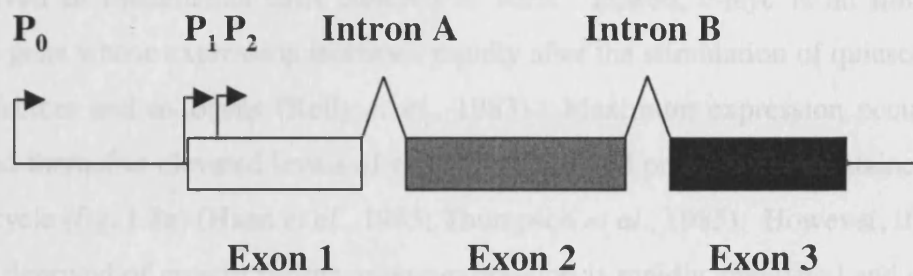
B. C-*myc* transcripts
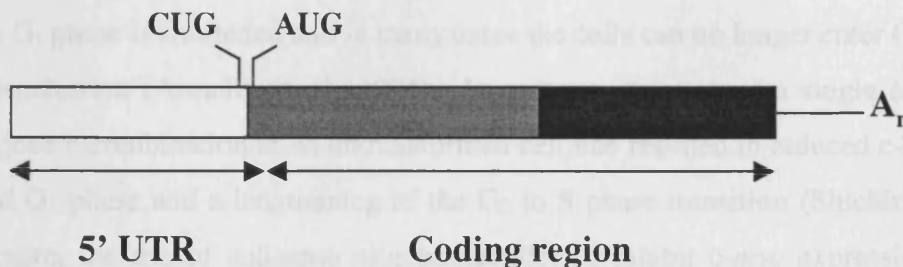
C. C-*myc* phosphoproteins
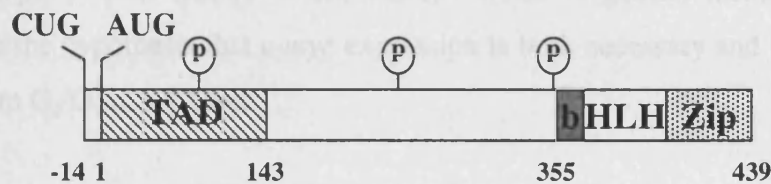
Figure 1.7: The organisation of the human c-*myc* genomic region, mRNAs and proteins. (A) Genomic organisation of the c-*myc* locus. The gene has a three exon-two intron topology and three promoters P_0, P_1 and P_2 are located in the upstream region. (B) Organisation of the c-*myc* mRNAs. Exon 1 is predominantly non-coding and consequently gives rise to the 5' UTR. The length of the 5' leader depends upon the promoter from which the transcript is derived and can be approximately 1000, 600 or 400 nt. Finally, the major translation site is an AUG codon located in exon 2, however a minor polypeptide is translated from a CUG located in exon 1. (C) Domain structure of the c-*myc* proteins. Myc-2 and Myc-1 are initiated at an AUG and a CUG codon, respectively. Both proteins contain a transcriptional activation domain (TAD) and a basic helix-loop-helix leucine zipper motif (bHLH/zip).

1.5.2. C-*myc* and cell proliferation

The correlation between c-*myc* expression and the proliferative status of cells *in vivo* can also be observed in mammalian cells cultured *in vitro*. Indeed, c-*myc* is an immediate early response gene whose expression increases rapidly after the stimulation of quiescent cells with growth factors and mitogens (Kelly *et al.*, 1983). Maximum expression occurs in mid-G_1 phase and thereafter elevated levels of c-*myc* mRNA and protein are maintained throughout the cell cycle (fig. 1.8a) (Hann *et al.*, 1985; Thompson *et al.*, 1985). However, if proliferating cells are deprived of growth factors, c-*myc* expression is rapidly attenuated and cells arrest in G_0 (fig. 1.8b) (Campisi *et al.*, 1984; Waters *et al.*, 1991).

Evidence has emerged suggesting that the progression of cells from the G_0/G_1 phase to S phase is regulated by the abundance of c-Myc. In cell lines that constitutively overexpress c-Myc the G_1 phase is shortened and in many cases the cells can no longer enter G_0 after growth factor deprivation (Armelin *et al.*, 1984). In contrast, deletion of a single c-*myc* allele by homologous recombination in an untransformed cell line resulted in reduced c-Myc levels, an extended G_1 phase and a lengthening of the G_0 to S phase transition (Shichiri *et al.*, 1993). Furthermore, the use of antisense oligonucleotides to inhibit c-*myc* expression in mitogen stimulated cells prevents their entry into S-phase and demonstrates that c-Myc is essential for progression from G_0/G_1 to S-phase (Heikkila *et al.*, 1987). Indeed, DNA synthesis can be activated in growth arrested cells, in the absence of any mitogens, through the activation of a conditional c-*myc* protein (Eilers *et al.*, 1991). Taken together, these observations are consistent with the hypothesis that c-*myc* expression is both necessary and sufficient for cells to progress from G_0/G_1 to S-phase.

In addition, to its role in regulating the G_0/G_1 to S-phase transition the invariant levels of c-Myc in proliferating cells suggest that its activity is required in other phases of the cell cycle (Henriksson and Lüscher, 1996). In support of this hypothesis, a considerable increase in c-Myc transactivation occurs during the S to G_2/M transition and is accompanied by changes in c-Myc phosphorylation (Seth *et al.*, 1993). However, the physiological effects of c-Myc in S, G_2 and M-phase are not yet known.

1.5.3. C-*myc* and differentiation

The expression of c-*myc* is altered in numerous cell types in response to diverse differentiation stimulating agents. Entry into a differentiation pathway is often accompanied by a rapid decrease in c-*myc* protein levels. Alternatively, the loss of c-*myc* expression may be delayed until the terminal stages of differentiation. Moreover, c-*myc* expression is generally low or undetectable in many differentiated adults tissues (Marcu *et al.*, 1992; Henriksson and Lüscher, 1996).

Direct evidence that c-Myc has a role in modulating cellular differentiation comes from exogenous expression of sense and antisense c-*myc* genes. Cells constitutively expressing c-*myc* are precluded from exiting the cell cycle and consequently are unable to differentiate (Coppola and Cole, 1986; Dmitrovsky *et al.*, 1986; Onclercq *et al.*, 1989; Freytag *et al.*, 1990). In contrast, abrogation of c-*myc* expression using antisense technology results in both growth arrest and differentiation in HL60 and MEL cells (Griep and Westphal, 1988; Holt *et al.*, 1988; Prochownick *et al.*, 1988). Thus, downregulation of c-*myc* expression is sufficient to initiate a program of differentiation in some cell types. However, U937 monoblastic cells constitutively expressing v-*myc* are able to differentiate in response to interferon-γ demonstrating that the loss of c-Myc activity is not obligatory in this case (Öberg *et al.*, 1991). Hence, although the loss of c-Myc is necessary for cell cycle withdrawal and the attainment of a terminally differentiated state, it is unclear whether this it is responsible for or merely a consequence of cellular conversion. Nevertheless, since differentiation and proliferation are mutually exclusive states it seems likely that c-Myc is a crucial regulator of these processes (Marcu *et al.*, 1992; Henriksson and Lüscher, 1996).

1.5.4. C-*myc* and apoptosis

The integrity of a multi-cellular organism is maintained by a dynamic equilibrium involving the processes of cell proliferation, differentiation and apoptosis or programmed cell death. In a population of cells, apoptosis will ensue when the appropriate cell survival factors become limiting. Alternatively, apoptosis may be triggered by stimulation with exogenous factors (Evan *et al.*, 1997; Wyllie, 1997).

A.
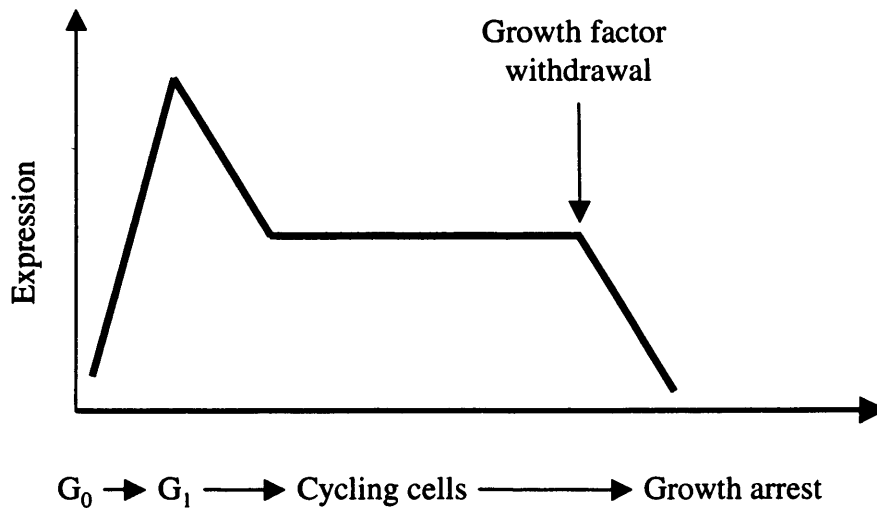
B.
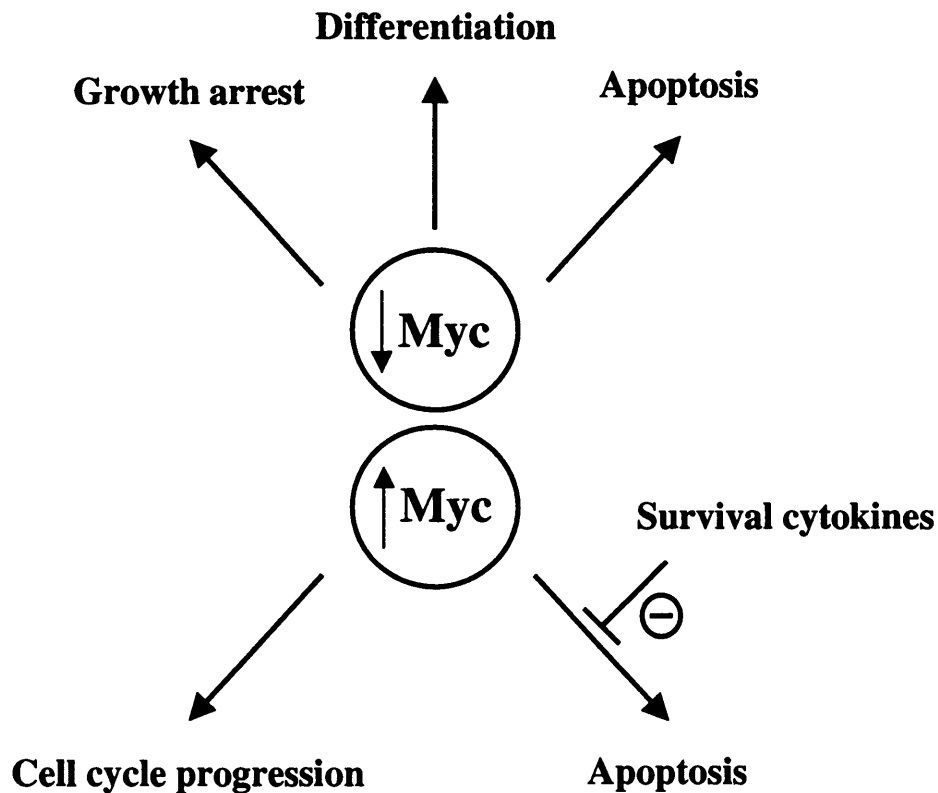
Figure 1.8: Expression and function of the c-*myc* proto-oncogene. (A) The effect of growth factors on c-*myc* expression. Stimulation of serum deprived cells with growth factors results in a rapid accumulation of c-*myc* mRNA and protein. Expression is maximal in mid-G_1 and drops to a level that is maintained throughout the cell cycle. Withdrawal of growth factors results in a rapid decrease in c-*myc* expression. Adapted from Henriksson and Lüscher, 1996. (B) The pivotal role occupied by the c-*myc* proto-oncogene in the determination of cellular fate. Increased expression can stimulate cell cycle progression or apoptosis. Whilst, decreased expression contributes to cell cycle arrest, differentiation and apoptosis.

A number of observations correlate the intracellular c-Myc concentration and the rate of apoptosis. Exogenous expression of high levels of c-Myc often results in an increased susceptibility to apoptosis (Wurm *et al.*, 1986; Wyllie *et al.*, 1987). Furthermore, in a myeloid cell line constitutively expressing c-Myc withdrawal of interleukin-3 (IL-3) stimulates entry into an apoptotic pathway (Askew *et al.*, 1991). Moreover, in cells arrested by serum deprivation or at various points in the cell cycle, the activation of a conditional allele induces apoptosis. Thus, the evidence points to a role for c-Myc in regulating the cells commitment into a program of cell death (Evan *et al.*, 1992). These observations seem somewhat paradoxical given the effects of c-Myc on cell cycle progression. However, it is proposed that c-Myc has a dual function; the induction of apoptosis can be regarded as a normal function of c-Myc that must be continually suppressed to promote cell survival and hence proliferation. In support of this hypothesis, the addition of cell survival factors such as IGF-I and PDGF abrogates c-Myc-induced apoptosis in growth arrested cells. Furthermore, this effect is not dependent on the mitogenic activity of these factors or the position of cell cycle arrest (Evan *et al.*, 1994). Thus, c-Myc appears to play a pivotal role in the commitment of cells to either an apoptotic or a proliferative pathway (fig. 1.8b). In addition, this model has profound implications for deregulated c-*myc* expression in tumour cells. It predicts that inappropriate expression of c-Myc not only results in increased cell proliferation but also apoptosis and consequently cell numbers will not increase dramatically. However, the cell population will expand if a concomitant suppression of apoptosis occurs. The observation that a large proportion of tumours with deregulated c-Myc expression either overexpress Bcl-2 or have lost p53 function provides circumstantial evidence for this hypothesis (Henriksson and Lüscher, 1996).

In stark contrast to the above model, stimulation of WEHI 231 lymphoma cells with IgM results in apoptosis and a reduction in c-Myc levels. Exogenous expression of c-*myc* abrogates IgM-induced apoptosis demonstrating that reduced c-*myc* expression mediates apoptosis in this case (Wu *et al.*, 1996). Furthermore, downmodulation of c-*myc* expression is associated with apoptosis in other B-cell lines suggesting that the regulation of c-*myc* mediated apoptosis may be cell-type specific (Warner *et al.*, 1992; Arsura *et al.*, 1996).

1.5.5. C-*myc*: a central regulator of cell fate?

To summarize the previous data, the expression of c-Myc is associated with both proliferation and apoptosis, whereas downmodulation can lead to growth arrest, differentiation or apoptosis. Clearly, multiple cellular pathways are modulated by c-Myc, suggesting that it plays a pivotal role in the determination of cellular fate (fig. 1.8b).

1.5.6. C-*myc* and tumorigenesis

The expression of c-*myc* is deregulated in a large number of tumour types. This often results from alterations at the c-*myc* locus such as chromosomal translocations and gene amplifications (Spencer and Groudine, 1991; Marcu *et al.*, 1992). In addition to genomic modifications, mechanisms have been described in tumour cell lines that increase c-Myc levels through enhanced translation or protein stabilization (Shindo *et al.*, 1993; West *et* al., 1995; Paulin *et al.*, 1996).

Deregulated c-*myc* expression in untransformed cell lines results in partial transformation reflecting the critical position that c-Myc occupies in transducing growth inhibitory and stimulatory signals. However, constitutive expression of c-*myc* alone does not induce a tumorigenic phenotype. Nevertheless, c-*myc* can cooperate with other oncogenes such as activated *ras* and Bcr-Abl in the transformation of many cell types suggesting that secondary genetic events are necessary to induce a malignant phenotype (Marcu *et al.*, 1992; Henriksson and Lüscher, 1996). Indeed, transgenic mice constitutively expressing c-*myc* in the B-lymphocyte compartment develop clonal lymphomas after a variable latency period and some of these tumors carry a mutated *ras* gene (Alexander *et al.*, 1989). These observations indicate that deregulated c-*myc* expression predisposes for but is not sufficient to induce tumorigenesis.

1.5.7. C-*myc* protein

The human c-*myc* gene encodes two polypeptides, Myc-1 and Myc-2, with apparent molecular masses of 67 and 64 kDa respectively. Translation of Myc-2, the major product is initiated at an AUG start codon at the 5' end of exon 2. Whereas, synthesis of Myc-1 commences at a CUG codon at the 3' end of exon 1 resulting in a 14 amino acid N-terminal

extension (Hann *et al.*, 1988) (fig. 1.7c). Both proteins are phoshorylated at multiple sites and localise to the nucleus. Furthermore, Myc-1 and 2 are degraded rapidly and exhibit a half-life of 15-30 minutes (Hann and Eisenman, 1984; Lüscher and Eisenman, 1990).

1.5.8. C-*myc* proteins are transcription factors

C-*myc* is a member of the basic helix-loop-helix leucine zipper (bHLHzip) family of transcription factors, having a contiguous arrangement of basic region, helix-loop-helix and leucine zipper motifs at its C-terminus (fig. 1.7c). Deletion analysis of the bHLHzip region revealed that this domain is essential and indicates that Myc functions through sequence specific binding (Landschulz *et al.*, 1988; Murre *et al.*, 1989; Lüscher and Eisenman, 1990). Structural homology between Myc and other bHLHzip proteins lead to the prediction that the basic region would recognise an E-box DNA sequence element (CANNTG). Furthermore, sequence-specific binding of a GST-Myc C-terminal domain fusion protein to the palindromic core sequence CACGTG confirmed this prediction (Blackwell *et al.*, 1990).

In addition to the DNA binding domain, a transcriptional activation domain (TAD) has been mapped to the N-terminus of c-Myc (Kato *et al.*, 1990) (fig. 1.7c). The TAD has three distinct regions; amino acids 1-41 (region A) are glutamine-rich, amino acids 42-103 (region B) are proline-rich and amino acids 104-143 (region C) do not resemble other transcriptional activation motifs (Kato *et al.*, 1990). Thus, the presence a DNA binding domain and a TAD strongly implicated the c-*myc* proteins as transcription factors.

1.5.9. Max: a dimerisation partner for Myc

Although c-*myc* proteins contain two dimerisation motifs, homo-dimerisation could only be detected at high and non-physiological protein concentrations (Dang *et al.*, 1989). Consequently, two separate studies demonstrated the existence of a Myc binding protein. Screening a primate cDNA library with a radiolabelled Myc bHLHzip domain identified a small and novel protein known as Max (Blackwood and Eisenman, 1991). Myn, the murine homologue of Max was amplified using a degenerate PCR approach based on the assumption that Myc would interact with a bHLHzip protein (Prendergast *et al.*, 1991). The human *max* gene encodes two polypeptides of 21 and 22 kDa (fig. 1.9a). The larger protein is generated by the retention of a small exon encoding a nine amino acid insertion in the basic region at

A.
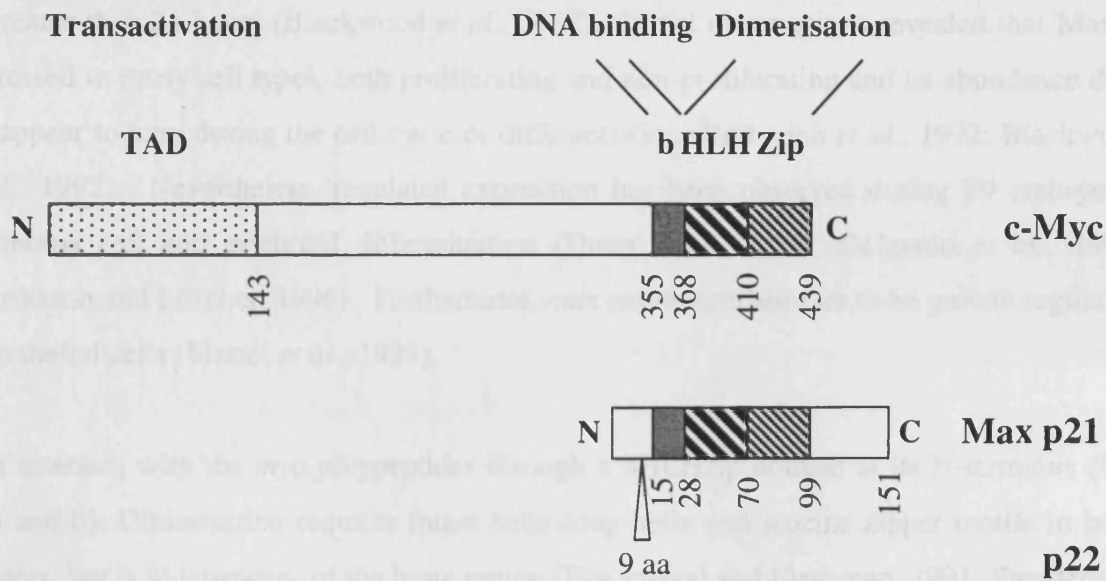
B.
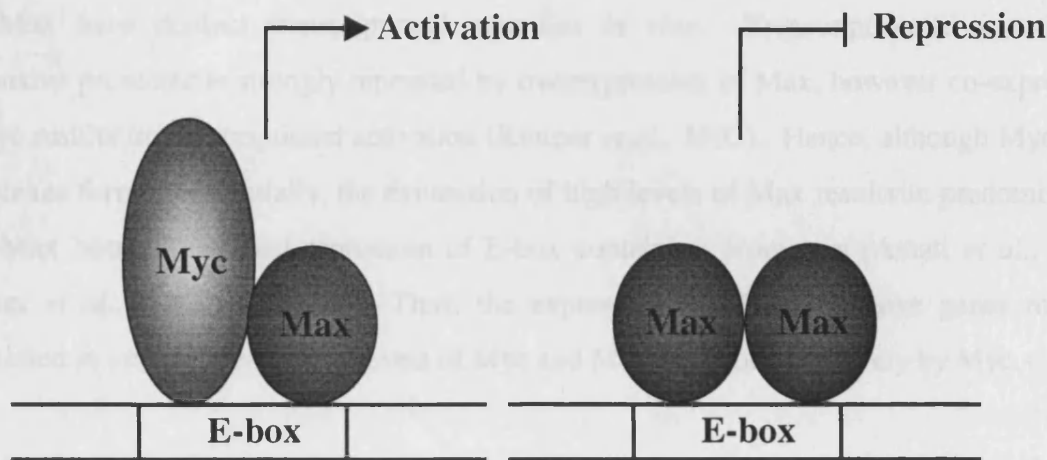
Figure 1.9: A comparison of the domain structure and transcriptional properties of the c-*myc* and max proteins. (A) A schematic comparison of the structures of c-Myc and Max. Both proteins contain a DNA binding/dimerisation domain (bHLH/zip). However, only c-Myc has a transactivation domain (TAD). Two isoforms of Max are generated by alternative splicing; the position of the additional exon in the p22 variant is indicated (Adapted from Henriksson and Lüscher, 1996). (B) Myc-Max heterodimers bind to and stimulate transcription from an E-box element. In contrast, the lack of a TAD in a Max-Max homodimer results in transcriptional repression by preventing a heterodimer from occupying this site.

the N-terminus (Blackwood and Eisenman, 1991) (fig. 1.9a). In common with Myc, Max is a nuclear phosphoprotein. However, *max* proteins are considerably more stable with a half-life of greater than 24 hours (Blackwood *et al.*, 1992). Initial observations revealed that Max is expressed in many cell types, both proliferating and non-proliferating and its abundance does not appear to vary during the cell cycle or differentiation (Berberich *et al.*, 1992; Blackwood *et al.*, 1992). Nevertheless, regulated expression has been observed during F9 embryonal carcinoma cell and erythroid differentiation (Dunn *et al.*, 1994; Delgardo *et al.*, 1995; Henriksson and Lüscher, 1996). Furthermore, *max* expression appears to be growth regulated in epithelial cells (Martel *et al.*, 1995).

Max interacts with the *myc* polypeptides through a bHLHzip domain at its N-terminus (fig. 1.9a and b). Dimerisation requires intact helix-loop-helix and leucine zipper motifs in both partners, but is independent of the basic region (Blackwood and Eisenman, 1991; Prendergast *et al.*, 1991). In addition to heterodimerisation with *myc* polypeptides, Max can form homodimers (fig. 1.9b). Both Myc-Max and Max-Max complexes bind specifically to the E-box sequence, however heterodimers have a considerably higher affinity for this site (Prendergast *et al.*, 1991). Unlike Myc, Max has no functional TAD and consequently Myc and Max have distinct transcriptional activities *in vivo*. Transcription from a E-box responsive promoter is strongly repressed by overexpression of Max, however co-expression of Myc results in transcriptional activation (Kretner *et al.*, 1992). Hence, although Myc-Max complexes form preferentially, the expression of high levels of Max results in predominantly Max-Max homodimers and repression of E-box containing promoters (Amati *et al.*, 1992; Kretner *et al.*, 1992) (fig. 19b). Thus, the expression of Myc-responsive genes may be modulated *in vivo* by the relative levels of Myc and Max, and not exclusively by Myc.

A body of evidence has emerged revealing that Myc does indeed exert its influence through dimerisation with Max. Studies in yeast, which have no endogenous Myc, demonstrated that Myc-Max complex formation is a prerequisite for Myc transcriptional activity (Amati *et al.*, 1992). In addition, a genetic complementation approach, utilising mutants of Myc and Max that bind to each other but not their wild-type partners, established that Max performs an essential role in Myc-dependent cellular transformation. Co-expression of both these mutant proteins co-operated with oncogenic Ras to induce a transformed phenotype, whilst expression of either protein alone had no effect (Amati *et al.*, 1993a). Finally, dimerisation is

essential for the *myc*-dependent stimulation of cell cycle progression and apoptosis, underlining the physiological significance of this interaction (Amati *et al.*, 1993b).

1.5.10. The Myc-recognition sequence

In vitro DNA binding studies identified a high affinity recognition site for Myc-Max heterodimers, an E box element (CACGTG), through which the complex stimulates transcription (Blackwell *et al.*, 1990; Prendergast and Ziff, 1991). Besides this canonical E box, a set of variant sites containing internal CG or TG dinucleotides bind the Myc-Max complex with somewhat lower affinity *in vitro* (Blackwell *et al.*, 1993). These 'non-canonical' binding sites include the following sequences: CATGTG, CATGCG, CACGCG, CACGAG and CAACGTG. However, the presence of an *in vitro* Myc-Max recognition site in a promoter or enhancer is not sufficient evidence for the occupation of this site *in vivo*. The majority of Myc-Max *in vitro* binding sites can also be recognised by more abundant transcription factors such as upstream binding factor (USF), transcription factor E3 (TFE3) and EB (TFEB); only a few such as CATGCG and CAACGTG appear to represent Myc-specific sites (Blackwell *et al.*, 1993). Indeed, a study designed to identify sequences bound by Myc-Max heterodimers *in vivo* suggested that the highest affinity site (CACGTG) does not represent the predominant *in vivo* binding element (Grandori *et al*, 1996). The majority of the core sites identified were 'non-canonical' and many of these sites are only recognised by Myc-Max heterodimers *in vitro*. Finally, Myc-Max DNA binding can be influenced *in vitro* by the nucleotides flanking the core site (Blackwell *et al.*, 1993; Solomon *et al.*, 1993). Indeed, a preference for G/C dinucleotides flanking the *in vivo* Myc binding sites further supports this notion (Grandori *et al.*, 1996). To summarise, whether a particular gene is transactivated by the Myc-Max complex may depend both on the nature of the DNA binding site and the abundance of other E box binding transcription factors. In addition, it is likely that the availability of Myc-Max sites will be restricted by DNA methylation, chromatin structure or competition with other transcription factors for overlapping binding sites.

1.5.11. Myc target genes

Myc responsive genes have been identified by several different approaches usually employing cells expressing either high or low levels of c-Myc. A valuable tool utilised in the quest for downstream genes is MycER; a chimeric polypeptide constructed from the oestrogen receptor

binding domain and c-Myc. In the absence of hormone, this conditional protein does not stimulate transcription, however binding of the ligand induces the activity of the TAD. Thus far, the potential target genes identified include the α-prothymosin gene, the ornithine decarboxylase gene, the p53 tumour suppressor gene, the cad gene, the cdc25A gene, the Myc-regulated DEAD box protein (MrDb) gene, the eukaryotic initiation factor 4E gene and the ECA39 gene (Eilers *et al.*, 1991; Benvenisty *et al.*, 1992; Bello-Fernandez *et al.*, 1993; Reisman *et al.*, 1993; Wagner *et al.*, 1993; Miltenberger *et al.*, 1995; Galaktionov *et al.*, 1996; Grandori *et al.*, 1996; Jones *et al.*, 1996).

1. Ornithine Decarboxylase

ODC is a rate-limiting enzyme in polyamine biosynthesis. A functional link between c-Myc and ODC was suggested by their similar biological activities. Both are required for entry into S-phase (Bowlin *et* al., 1986), are able to induce cellular transformation (Auvinen *et* al., 1992), and promote apoptosis in the absence of survival factors (Packham and Cleveland, 1994). During the G_0 to S-phase transition, ODC is induced in mid-G_1 and correlates with the *c-myc* expression pattern (Abrahamsen and Morris, 1990). Indeed, enforced *c-myc* expression and MycER activation both result in increased ODC expression (Dean *et al.*, 1987; Wagner *et al.*, 1993). Analysis of the human ODC promoter revealed an E-box element located upstream of the transcriptional start site that demonstrates serum dependent Myc-Max binding *in vitro*. This site is essential for the Myc-dependent serum stimulation of ODC expression (Peña *et al.*, 1993). In addition, two conserved E-boxes located in intron I bind Myc-Max heterodimers and confer Myc-responsiveness on heterologous promoter constructs (Bello-Fernandez *et al.*, 1993). However, binding of Myc-Max complexes to these sites is serum independent (Peña *et al.*, 1993).

2. Cdc25A

Cdc25A is a cell cycle regulated phosphatase that dephosphorylates cyclin-dependent kinases (CDKs) resulting increased CDK activity. It is expressed in early G_1 phase following the serum stimulation of quiescent fibroblasts (Jinno *et al.*, 1994). A role for c-Myc in the transcriptional regulation of *cdc25A* was suggested by its increased expression subsequent to MycER activation. Furthermore, Myc-Max DNA binding sequences are present in the first and second introns. These were shown to confer Myc-dependent transcriptional activation in

the context of the natural and heterologous promoters. Finally, the ability of Cdc25A to promote both cell transformation and apoptosis suggests that *cdc25A* is a physiological target of c-Myc (Galaktionov *et al.*, 1996). Therefore, it seems likely that the effects of c-Myc on cell cycle progression may be in part due to increased Cdc25A activity and its effects on the cell cycle machinery.

3. Eukaryotic initiation factor 4E (eIF4E)

Eukaryotic initiation factor 4E binds the m⁷GpppN cap of mRNAs during the process of translation initiation (Sonenberg *et al.*, 1978). In some systems, eIF4E is proposed to be the limiting component of the translation apparatus and consequently it plays a critical role in the regulation of protein synthesis (Hiremath *et al.*, 1985; Duncan *et al.*, 1987). The expression pattern of eIF4E during serum stimulation parallels that of c-*myc* and cell lines overexpressing c-*myc* demonstrate a marked increase in eIF4E levels. In addition, activation of the MycER chimera results in increased eIF4E transcription (Rosenwald *et al.*, 1993). Two E-box elements were identified in the eIF4E promoter and were found to regulate transcription in a Myc-dependent manner. Mutation of the proximal E-box inactivated the promoter, suggesting that this element is essential for eIF4E promoter function (Jones *et al.*, 1996). Therefore, c-*myc* proteins may contribute to the regulation of protein synthesis during the G_0 to S-phase transition through transcriptional activation of the eIF4E promoter.

4. p53

The tumour suppressor protein, p53, is a critical component of the cellular response to DNA damage (Vogelstein and Kinzler, 1992). Following its activation, p53 inhibits cell cycle progression from G_1 to S phase. This is mediated in part through its transcriptional stimulation of the gene encoding the CDK inhibitor, p21*CIP1* (El-Deiry *et al.*, 1993). Increased expression of the *p53* gene occurs in growth arrested cells stimulated with mitogens or in response to the activation of MycER (Hermeking and Eick, 1994; Wagner *et al.*, 1994). Furthermore, the human *p53* promoter can be activated by c-Myc through a Myc-Max binding site (Roy *et al.*, 1994). Since the effects of c-Myc and p53 on cell cycle progression are diametrically opposed, it seems counter-intuitive for *p53* to be a c-Myc target gene. However, the ability of c-Myc to promote apoptosis in growth arrested cells is ablated in *p53-/-* mouse embryo fibroblasts suggesting that c-Myc induced apoptosis is mediated

through transactivation of *p53* (Hermeking and Eick, 1994; Wagner *et al.*, 1994). Thus, the activation of *p53* gene expression may represent a checkpoint to prevent the pathological activation of c-*myc* gene expression (Henriksson and Lüscher, 1996). In this regard, it is interesting to note that a correlation between c-*myc* and *p53* expression has been observed in a number of tumour cell lines (Roy *et al.*, 1994).

5. Carbamoyl-phosphate synthase (glutamine-hydrolysing)/aspartate carbamoyltranferase/dihydroorotase (Cad).

The *cad* gene encodes a multifunctional biosynthetic enzyme which catalyses the first three steps in *de novo* pyrimidine biosynthesis (Evans, 1986). *Cad* is transcriptionally activated in late G_1 following the re-entry of serum deprived cells into the cell cycle. The upstream sequence responsible for this induction has been characterised and an E-box element is located within this element. Mutation of this E-box abolishes the growth-dependent increase in *cad* transcription. Furthermore, the expression of dominant-negative c-Myc proteins partially blocks the transactivation of a heterologous reporter gene linked to this element. Therefore, c-Myc may contribute to the regulation of *cad* expression during the G_0 to S-phase transition (Miltenberger *et al.*, 1995).

6. α-Prothymosin

α-Prothymosin is an acidic nuclear protein of unknown function whose expression appears to correlate with cell growth. It was identified as a c-Myc responsive gene in quiescent fibroblasts upon activation of MycER (Eilers *et al.*, 1991). In addition, the expression of α-prothymosin mRNA correlates with that of c-*myc* mRNA during mitogenic stimulation, the differentiation of HL60 promyelocytic cells and in primary human colon cancers (Dosil *et al.*, 1993; Mori *et al.*, 1993; Smith *et al.*, 1993). A c-Myc response element was localised to the first intron and contains a CACGTG consensus sequence (Gaubatz *et al.*, 1994). Interestingly, the expression of this gene cannot be induced by the activation of MycER in growing cells and the E-box is not c-Myc responsive under these conditions (Mol *et al.*, 1995). Thus, it appears that c-Myc regulates α-prothymosin expression during the G_0 to S-phase transition and differentiation but not in proliferating cells.

7. Myc-regulated DEAD box protein

MrDb was identified through immunoprecipitation of chromatin bound by Myc-Max complexes (Grandori *et al.*, 1996). The function of MrDb is unknown, however the protein contains motifs present in members of a family of RNA helicases. Increased expression of MrDb occurs during the G_0 to S-phase transition and following activation of the MycER chimera. Furthermore, MrDb mRNA levels fall during the granulocytic differentiation of the human leukemic cell line HL60 (Grandori *et al.*, 1996). The MrDb genomic clone through which the gene was identified contains an E-box element that binds Myc-Max heterodimers *in vivo*. This site confers Myc-dependent transactivation when cloned upstream of a heterologous reporter gene, however the location of this site within the gene structure is unknown (Grandori *et al.*, 1996).

8. *ECA39*

ECA39 was identified as a c-Myc target gene by differential screening of mRNA from a brain tumour induced through c-*myc* overexpression (Benvenisty *et al.*, 1992). A Myc-Max consensus sequence was located in the 5' untranslated region and mutational analysis demonstrates that this sequence is functional. However, the role of the *ECA39* gene product is unknown.

In conclusion, although the function of many c-Myc target genes is unclear, the evidence suggests that c-Myc participates in a spectrum of cell growth events through the activation of a specific set of target genes. These include genes encoding products that are directly involved in DNA synthesis (ODC and CAD), protein synthesis and RNA metabolism (eIF4E, eIF2α and MrDb), and cell cycle regulation (Cdc25A and p53).

1.5.12. Indirect effects of c-Myc on cell cycle regulators

Although the identification of c-Myc target genes has furthered our understanding of its function, with the exception of *cdc25A* none of these genes are candidates for the potent effect of c-Myc on cell cycle progression. Cells are restricted from entering S-phase in part by the retinoblastoma protein, pRB. The hypophosphorylated form of pRb, present in G_0 and early G_1, sequesters members of the E2F family of transcription factors and consequently

Growth factors and mitogens

**Activation of cyclin D1/cdk's
and cyclin E/cdk's** ⟶ **Cyclin A synthesis**

S-phase

E2F
pRB
Hypophosphorylated

pRB
E2F
Hyperphosphorylated

+

E2F
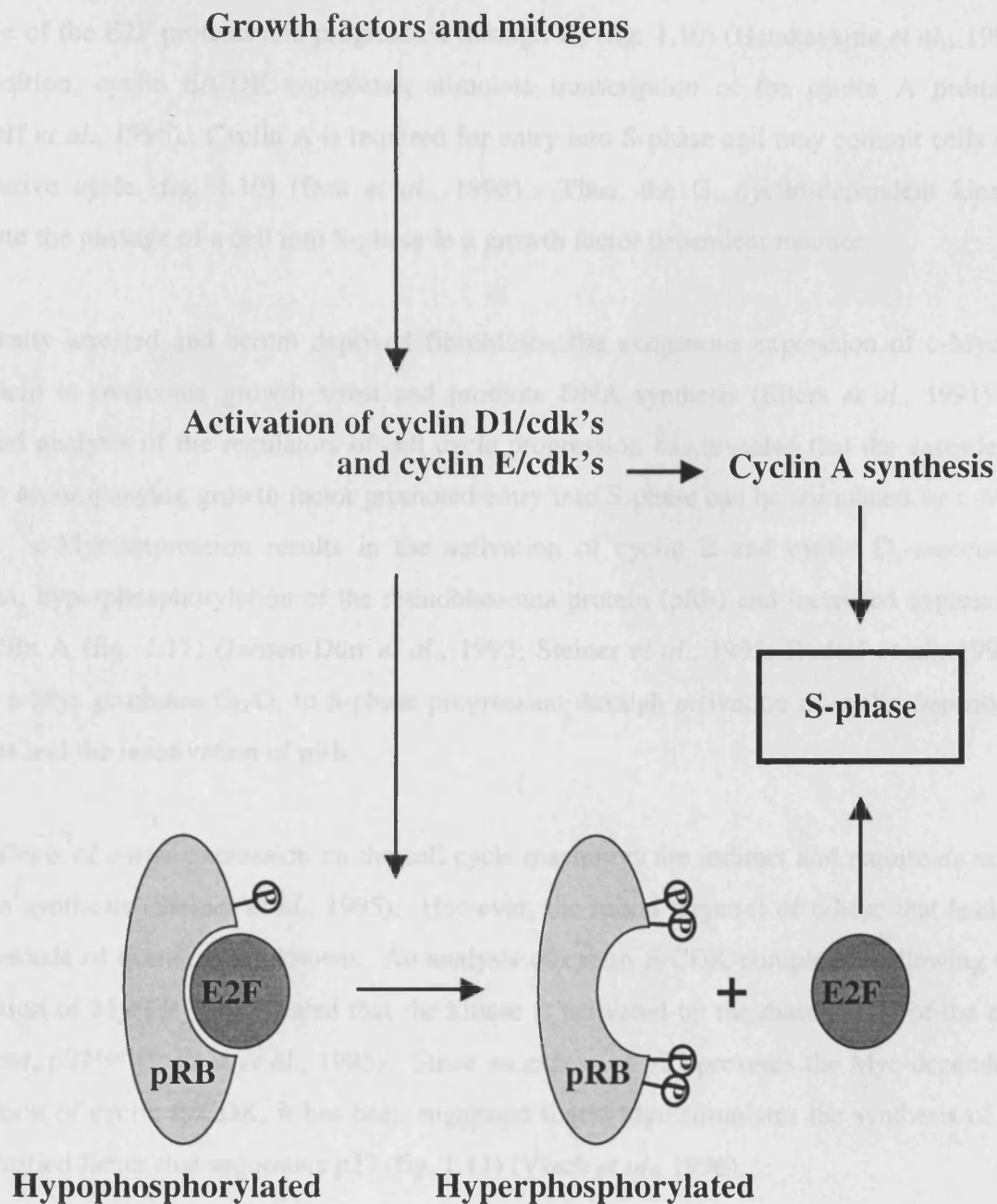
Figure 1.10: Diagrammatic representation of the cyclin D_1 and cyclin E-mediated events that promote DNA synthesis following growth factor stimulation. Growth factors and mitogens activate cyclin E and D_1-associated kinases. These kinases phosphorylate pRB, resulting in the release of E2F. Additionally, cyclin E/cdks stimulate the synthesis of cyclin A. Both E2F and cyclin A contribute to S-phase progression.

inhibits progression into S phase (see Weinberg, 1995). However, activation of cyclin D_1/CDK4/6 and cyclin E/CDK2 complexes results in the hyperphosphorylation of pRb, the release of the E2F proteins and progression through G_1 (fig. 1.10) (Hatakeyama et al., 1994). In addition, cyclin E/CDK complexes stimulate transcription of the cyclin A promoter (Rudolf et al., 1996). Cyclin A is required for entry into S-phase and may commit cells to a replicative cycle (fig. 1.10) (Dou et al., 1993). Thus, the G_1 cyclin-dependent kinases regulate the passage of a cell into S-phase in a growth factor dependent manner.

In density arrested and serum deprived fibroblasts, the exogenous expression of c-Myc is sufficient to overcome growth arrest and promote DNA synthesis (Eilers et al., 1991). A detailed analysis of the regulators of cell cycle progression has revealed that the cascade of events accompanying growth factor promoted entry into S-phase can be stimulated by c-Myc alone. c-Myc expression results in the activation of cyclin E and cyclin D_1-associated kinases, hyperphosphorylation of the retinoblastoma protein (pRb) and increased expression of cyclin A (fig. 1.11) (Jansen-Dürr et al., 1993; Steiner et al., 1995; Rudolf et al., 1996). Thus, c-Myc promotes G_0/G_1 to S-phase progression through activation of cyclin-dependent kinases and the inactivation of pRb.

The effects of c-myc expression on the cell cycle machinery are indirect and require de novo protein synthesis (Steiner et al., 1995). However, the initial target(s) of c-Myc that lead to this cascade of events are unknown. An analysis of cyclin E/CDK complexes following the activation of MycER has revealed that the kinase is activated by the dissociation of the cdk inhibitor, p27^{Kip1} (Steiner et al., 1995). Since an excess of p27 prevents the Myc-dependent activation of cyclin E/CDK, it has been suggested that c-Myc stimulates the synthesis of an unidentified factor that sequesters p27 (fig. 1.11) (Vlach et al., 1996).

Therefore, it appears that c-Myc promotes cell cycle progression through the de-repression of G_1 cyclin dependent kinases and the activation of the CDK activating phosphatase, Cdc25A (Jinno et al., 1994; Steiner et al., 1995).

1.5.13. C-Myc-mediated transrepression

A number of studies have described the repression of certain genes upon expression of high levels of c-Myc or N-Myc. These include genes encoding thrombospondin-1, leukocyte

Myc activity

↓

Synthesis of factor X

Sequestered p27^{KIP1}

p27 X

+

p27
Cdk2 Cyclin E

Inactive cdk complex

Cdk2 Cyclin E

Active cdk complex

pRB phosphorylation

Cyclin A expression

Cell cycle progression
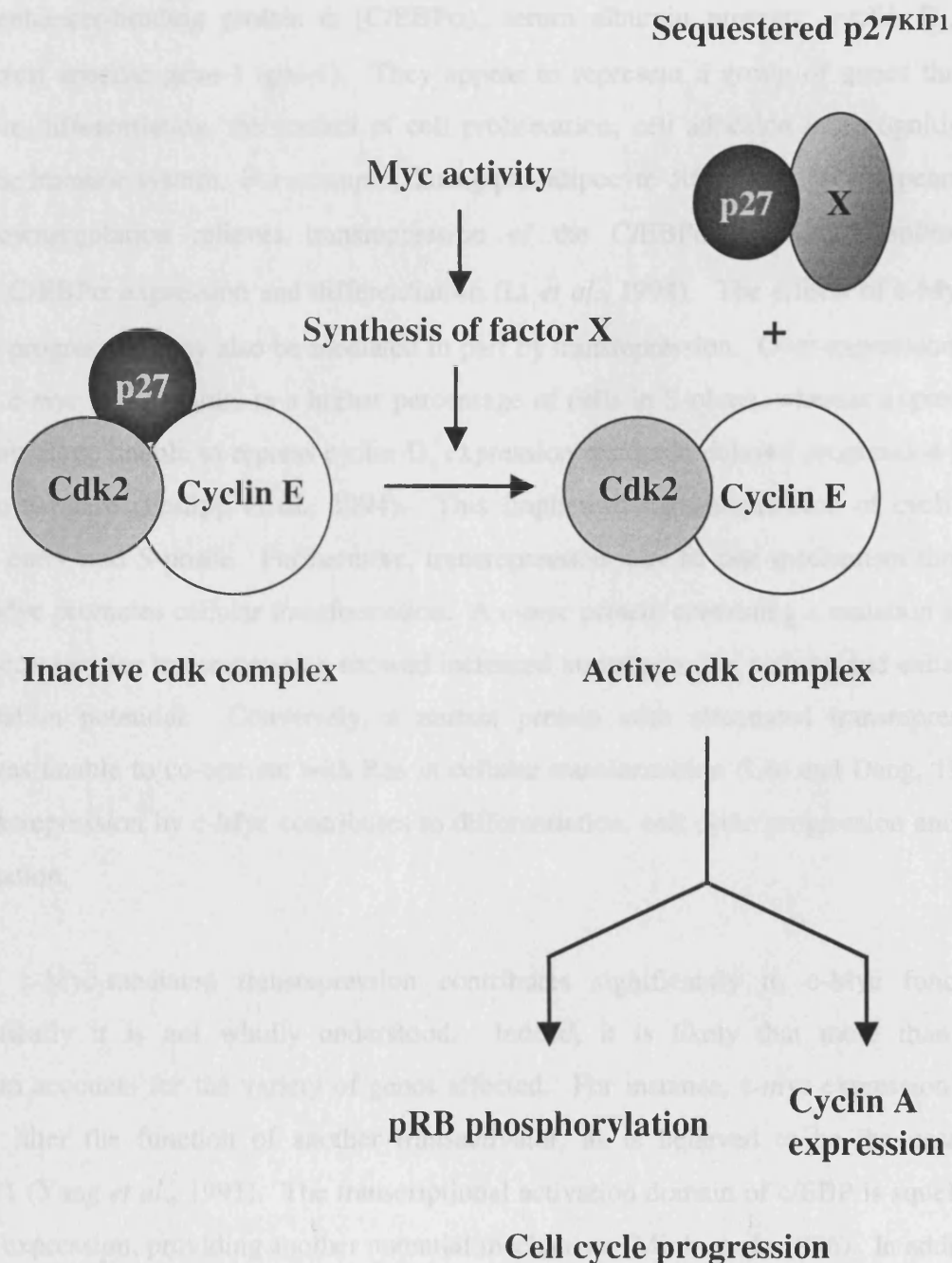
Figure 1.11: Activation of c-Myc in growth-arrested cells stimulates a cascade of events which result in cell cycle progression. Briefly, c-Myc synthesis results in the activation of cyclin E/cdk complexes through the release of the cdk inhibitor p27^{Kip1}. Consequently, cyclin E/cdk phosphorylates pRB and promotes cyclin A expression. Both events contribute to the G_0 to S-phase transition. It has been suggested that the initial c-*myc*-mediated event is the transactivation of a gene whose product sequesters p27.

function-associated activity-1 (LFA-1), neural cell adhesion molecule (N-CAM), collagen, major histocompatibility complex (MHC) class I antigens, human leukocyte antigens (HLAs), CCAAT/enhancer-binding protein α (C/EBPα), serum albumin proteins, cyclin D_1, and growth-arrest specific gene-1 (gas-1). They appear to represent a group of genes that are involved in differentiation, the control of cell proliferation, cell adhesion or recognition of cells by the immune system. For example, during pre-adipocyte differentiation it appears that c-Myc downregulation relieves transrepression of the C/EBPα promoter resulting in increased C/EBPα expression and differentiation (Li et al., 1994). The effects of c-Myc on cell cycle progression may also be mediated in part by transrepression. Over-expression of a wild type c-myc allele results in a higher percentage of cells in S-phase, whereas expression of a mutant allele unable to repress cyclin D_1 expression results in delayed progression from mitosis to S-phase (Philipp et al., 1994). This implies that transrepression of cyclin D_1 promotes entry into S-phase. Furthermore, transrepression may be one mechanism through which c-Myc promotes cellular transformation. A c-myc protein containing a mutation in the domain necessary for transrepression showed increased transrepression activity and enhanced transformation potential. Conversely, a mutant protein with attenuated transrepression activity was unable to co-operate with Ras in cellular transformation (Lee and Dang, 1997). Thus, transrepression by c-Myc contributes to differentiation, cell cycle progression and cell transformation.

Although c-Myc-mediated transrepression contributes significantly to c-Myc function, mechanistically it is not wholly understood. Indeed, it is likely that more than one mechanism accounts for the variety of genes affected. For instance, c-myc expression may indirectly alter the function of another transactivator, as is believed to be the case for CTF1/NF1 (Yang et al., 1991). The transcriptional activation domain of c/EBP is squelched by v-myc expression, providing another potential mechanism (Mink et al., 1996). In addition, it has been suggested that c-Myc may repress transcription through the initiator element (Inr) that can be found in many of the targets of Myc-mediated negative regulation. A basal promoter, containing the Inr, linked to a heterologous reporter gene was shown to confer Myc-mediated transrepression for the adenovirus major late (AdML), cyclin D_1 and c/EBPα promoters. Mutations within the Inr abolished this negative regulation (Li et al., 1994; Philip et al., 1994). Furthermore, c-Myc interacts with the general transcription factors, TFII-I and YY-1, that recruit the TATA-box binding protein (TBP) to the Inr. Consequently, c-Myc

A. Myc transrepression through YY-1 or TFII-I

YY-1/TFII-1
TBP
Inr

→ **Initiation complex assembly and transcription**

YY-1/TFII-1 | Myc | Max
Inr

→ **Myc-mediated transrepression**

B. Myc transrepression through Miz-1

Miz-1
Inr/Start site

→ **Transactivation of growth inhibitory genes**

Miz-1 | Myc
Inr/Start site

→ **Transrepression of growth inhibitory genes**
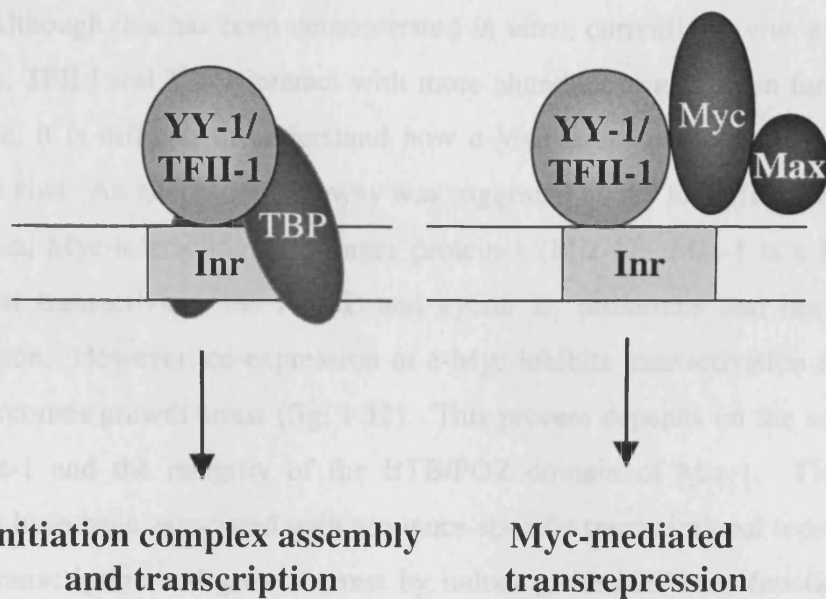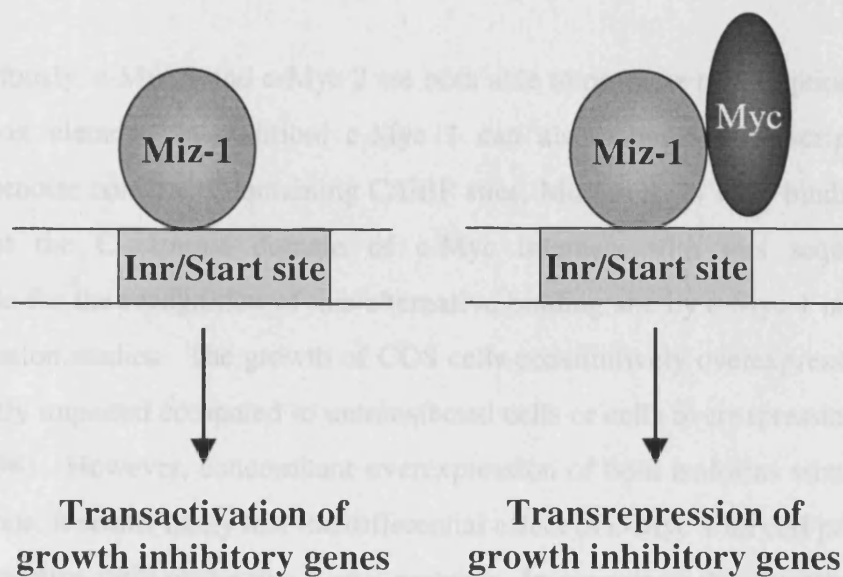
Figure 1.12: Alternative models for the mechanism of Inr-mediated transrepression by c-Myc. (A) YY-1 or TFII-I recruit the TATA-box binding protein (TBP) to the initiator element (Inr). A transcription preinitation complex assembles at this site and consequently the transcription is initiated. However, Myc can interact with TFII-I and YY-1, preventing complex assembly and therefore transcription initiation. (B) Miz-1 stimulates the transcription of growth-inhibitory genes through upstream Inr elements. However, interaction of Miz-1 with c-Myc could promote transrepression through the activation of the Miz-1 POZ domain.

precludes the formation of TBP-YY1 or TBP-TFII-I complexes and thereby inhibits transcription initiation from these sites (fig. 1.12) (Roy *et al*., 1993; Shrivastava *et al*., 1993; Li *et al*., 1994). Although this has been demonstrated *in vitro*, currently *in vivo* evidence is lacking. Moreover, TFII-I and YY-1 interact with more abundant transcription factors, such as USF. Therefore, it is difficult to understand how c-Myc could compete for binding to TFII-I and YY-1 *in vivo*. An alternative pathway was suggested by the identification of the c-Myc binding protein, Myc-interacting zinc-finger protein-1 (Miz-1). Miz-1 is a BTB/POZ domain protein that transactivates the AdML and cyclin D_1 promoters and has a potent growth arrest function. However, co-expression of c-Myc inhibits transactivation from both promoters and overcomes growth arrest (fig. 1.12). This process depends on the association of c-Myc and Miz-1 and the integrity of the BTB/POZ domain of Miz-1. Thus, since BTB/POZ domains have been associated with sequence-specific transcriptional repression, c-Myc may inhibit transcription and growth arrest by inducing the inhibitory function of the Miz-1 BTB/POZ domain (Chang *et al*., 1996; Peukert *et al*., 1997).

1.5.14. Differential transactivation mediated by the c-*myc* proteins

As detailed previously, c-Myc 1 and c-Myc 2 are both able to promote transcription initiation through an E-box element. In addition, c-Myc 1 can also stimulate transcription from heterologous promoter constructs containing C/EBP sites. Moreover, *in vitro* binding studies demonstrate that the C-terminal domain of c-Myc interacts with this sequence. A physiological role for the recognition of this alternative binding site by c-Myc 1 is suggested by *in vivo* expression studies. The growth of COS cells constitutively overexpressing c-Myc 1 was significantly impaired compared to untransfected cells or cells overexpressing c-Myc 2 (Hann *et al*., 1994). However, concomitant overexpression of both isoforms stimulates cell proliferation. Thus, it seems likely that the differential effect of c-Myc 1 on cell proliferation depends on the relative ratio of the two c-*myc* proteins. In support of this hypothesis, it has been reported that the relative levels of the c-*myc* proteins vary depending on the growth status of the cell. In growing cells, c-Myc 1 is normally considerably less abundant than c-Myc 2 (Hann *et al*., 1988; Hann *et al*., 1992). However, as cells approach high density in culture, c-Myc 1 accumulates to a level equal to or greater than c-Myc 2. This effect appears to be in response to methionine deprivation and may represent a cellular growth inhibitory response to the availability of nutrients (Hann *et al*., 1992). Furthermore, the disruption of c-Myc 1 protein synthesis in human Burkitt's lymphomas and avian bursal lymphomas, may

contribute to tumorigenicity through the loss of this growth suppressive response (Hann *et al.*, 1988). In summary, differential transactivation by the c-*myc* proteins through the E-box or C/EBP sites is likely to represent a mechanism through which the cell can respond appropriately to various growth conditions.

1.6. The regulation of c-*myc* gene expression

The expression of c-*myc* has profound implications for cellular fate and inappropriate expression can contribute to cell transformation. Consequently, c-*myc* expression is tightly regulated by transcriptional and post-transcriptional mechanism at multiple levels.

1.6.1. Trancriptional initiation and elongation

The stimulation of growth factor deprived cells with mitogens results in a rapid accumulation of c-*myc* mRNA (Kelly *et al.*, 1983; Dean *et al.*, 1986; Nepveu *et al.*, 1987). An increase in transcription initiation is in part responsible for this induction (Dean *et al.*, 1986; Nepveu *et al.*, 1987). Indeed, mitogen-responsive *cis*-acting elements have been identified in the c-*myc* promoter (Marcu, 1992). Nevertheless, the rate of c-*myc* transcription is relatively high in quiescent cells and consequently only a moderate increase in transcriptional initiation occurs on growth stimulation. Therefore, an alternative mechanism must account for the dramatic accumulation of c-*myc* mRNA in the cytoplasm (Blanchard *et al.*, 1985; Dean *et al.*, 1986; Nepveu *et al.*, 1987). Nuclear run-on assays assays demonstrate that a proportion of transcriptional complexes terminate at the 3' end of exon 1 (Bentley and Groudine, 1986; Nepveu and Marcu, 1986). Premature transcriptional termination has been identified as a major mechanism involved in the regulation of c-*myc* expression. The stimulation of quiescent fibroblasts with epidermal growth factor (EGF), human mononuclear cells with pokeweed mitogen or Ba/F3 cells with IL-3 partially relieves this block resulting in an increased rate of transcriptional elongation and the accumulation of c-*myc* mRNA (Eick *et al.*, 1987; Nepveu *et al.*, 1987; Chang *et al.*, 1991). In contrast, the rapid downregulation of c-*myc* expression during the differentiation of HL60 and MEL cells is due to the attenuation of transcriptional elongation (Bentley and Groudine, 1986; Watson, 1988).

A negative autoregulatory feedback mechanism is also implicated in the control of c-*myc* transcription. The overexpression of an exogenous c-*myc* allele in cultured cell lines

negatively regulates endogenous c-*myc* expression in a dose-dependent manner. This observation suggests that c-Myc is able to repress the activity of its own promoter (Grignani *et al.*, 1990). Furthermore, Max is also required for this effect implying that this is a transcriptional phenomenon (Penn *et al.*, 1990).

1.6.2 Evidence for post-transcriptional regulation

Clearly, the synthesis of c-*myc* mRNA is a major contributor to the regulation of c-*myc* expression. However, it has been observed that the level of c-*myc* protein does not always correlate with that of the cytoplasmic mRNA. The constitutive expression of the entire human c-*myc* gene in murine fibroblasts results in the accumulation of high levels of mRNA in the cytoplasm without a significant increase in the levels of c-*myc* protein (Ray *et al.*, 1989). Furthermore, in cell lines derived from patients with multiple myeloma and Bloom's syndrome c-*myc* expression is de-regulated by a translational mechanism (West *et al.*, 1995; Paulin *et al.*, 1996). In the case of multiple myeloma this is associated with a single point mutation in the 5' UTR of the mRNA (Paulin *et al.*, 1996).

1.6.3. Translational regulation mediated by the c-*myc* 5' untranslated region

The major translation start site in the c-*myc* gene is located within exon 2 and consequently exon 1 is predominantly non-coding (fig. 1.7b). Thus, the 5' untranslated region of the human c-*myc* mRNA is composed of exon 1 and 15 nt of exon 2. Multiple transcription initiation sites exist within the gene. Consequently, the length of the 5' UTR varies between approximately 1000 to 395 nt. There are two major promoters, P1 and P2, that are positioned 596 and 436 bp upstream of the AUG initiation codon, respectively (fig. 1.7) (Watt *et al.*, 1983; Saito *et al.*, 1983). P2 is the principle promoter, generating 75-90% of transcripts, whereas P1 only contributes 10-25% of the total c-*myc* mRNAs (Taub *et al.*, 1984; Bentley and Groudine, 1986a). In addition, two minor promoters, P0 and P3, each generate approximately 5% of c-*myc* transcripts. Both P0 and P3 lack TATA boxes and are located 550-560 bp upstream of P1 and near the 3' end of the first intron, respectively (fig. 1.7a) (Bentley and Groudine, 1986b; Ray and Robert-Lézéngés, 1989).

Chromosomal translocations can occur between the c-*myc* locus and one of the immunoglobulin loci, resulting in de-regulated c-*myc* expression. In approximately 70% of

murine plasmacytomas and 50% of human lymphomas the breakpoint occurs in the first exon or intron (Cory, 1986) suggesting that exon 1 could contribute to the normal regulation of c-*myc* expression. In support of this notion, the nucleotide sequence of exon 1 is well conserved between species (~70% between human and murine). It was proposed that the translation of c-*myc* mRNAs is repressed by a structural motif that results from base-pairing between sequences in exon 1 and exon 2. This model predicts that mRNAs derived from the translocated c-*myc* loci are efficiently translated since they lack this structure (Saito *et al.*, 1983).

Direct evidence that the 5' UTR can modulate the translational efficiency of c-*myc* mRNAs was provided by *in vitro* studies. In rabbit reticulocyte lysate, both murine and human c-*myc* transcripts bearing exon 1 sequences (441 and 502 nt respectively) are translated significantly less efficiently than those lacking the majority of exon 1 (Darveau *et al.*, 1985; Parkin *et al.*, 1988). Deletion analysis has revealed that exon 1-mediated translational repression is a property of the entire 5' noncoding region rather than a specific motif (Parkin *et al.*, 1988). Thus, the overall secondary structure of the 5' UTR is responsible for the translation inefficiency of the c-*myc* mRNA *in vitro*.

A comparison of the distribution of endogenous c-*myc* mRNAs between the monosome and polysome fractions in Burkitt's lymphoma cell lines demonstrated that exon 1 sequences do not appear to affect the *in vivo* translational efficiency of c-*myc* mRNAs (Nilsen and Maroney, 1984). Furthermore, exon 1 does not inhibit the translation of exogenously expressed c-*myc* mRNAs in cultured cell lines or in HeLa cell extracts (Butnick *et al.*, 1985; Parkin *et al.*, 1988). Nevertheless, sequences from both the murine and human exon 1 repress the translation of heterologous reporter mRNAs micro-injected into *Xenopus* oocytes (Parkin *et al.*, 1988; Fraser *et al.*, 1992). Thus, the effect of the c-*myc* 5' UTR on translation initiation depends on the assay system. This phenomenon may reflect the competence of these systems to translate mRNAs with structured leader sequences. Alternatively it has been suggested that the translation of c-*myc* mRNAs may require a non-canonical *trans*-acting factor present in cultured cells but lacking in reticulocyte lysate and *Xenopus* oocytes (Parkin *et al.*, 1988).

1.6.4. Developmental regulation of translation by the c-*myc* 5' UTR in *Xenopus laevis*

Differential translational regulation mediated by the c-*myc* 5' UTR has been observed during *Xenopus* oocyte maturation. In contrast to their reduced translational efficiency in oocytes, heterologous mRNAs bearing 360 nt of the murine c-*myc* 5' UTR are translated as efficiently as control mRNAs in fertilised eggs (Lazarus *et al.*, 1988). This effect correlates with a smaller enhancement of general protein synthesis during this period. Moreover, the translational repression of a reporter mRNA conferred by a synthetic hairpin in *Xenopus* oocytes was completely relieved in fertilised eggs (Fu *et al.*, 1991). Thus, the general increase in protein synthesis during oocyte maturation could alleviate the translational inhibition caused by secondary structure in the c-*myc* 5' UTR. However, a recent study demonstrated that translational potentiation mediated by structured 5' UTRs, including a synthetic hairpin, the human c-*myc* 5' UTR and the *Xenopus laevis* c-*myc* 5' UTR, does not occur in early embryos (Fraser *et al.*, 1996). Hence, these conflicting data must be resolved before any conclusions can be drawn on the role of the c-*myc* 5' UTR during development.

1.7 Project background and aims

In common with many genes involved in the regulation of cell proliferation, the c-*myc* mRNAs have GC-rich 5' leader sequences with the potential to form secondary structural motifs. Interestingly, in cell lines derived from patients with the B-cell neoplasia, multiple myeloma, a consistent point mutation in the c-*myc* 5' UTR is associated with de-regulated expression by a translational mechanism. Furthermore, this single alteration results in the 5' UTR having an increased affinity for a number of RNA binding proteins (Paulin *et al.*, 1996, 1997, 1998). These observations strongly suggested that the 5' UTR might be involved in the translational regulation of the c-*myc* proto-oncogene. However, a number of previous investigations into the role of the 5' UTR in translational modulation have proved somewhat inconclusive.

Recently, it has become clear that in addition to the conventional cap-dependent mechanism of translation initiation some eukaryotic cellular mRNAs utilise an alternative mechanism. These mRNAs have structured 5' UTRs that contain an internal ribosome entry segment (IRES). The IRES conducts the ribosome to the mRNA by the mechanism of internal initiation. Since the c-*myc* mRNAs are translated efficiently *in vivo* despite the presence of a long and structured 5' leader sequence, it seemed possible these mRNAs can be translated by internal ribosome entry. Thus, the aim of this project was to investigate the mechanism of c-*myc* mRNA translation and the role of the 5' UTR in regulating translation initiation.

Chapter 2

Materials and methods

2.1 General Reagents

Unless otherwise stated all chemical reagents were of analytical grade and most were obtained from BDH laboratory supplies (Lutterworth, Leicestershire, UK), Fisons (Loughborough, Leicestershire, UK), ICN Flow Ltd (Thame, Oxfordshire, UK) or Sigma Chemical company Ltd (Poole, Dorset, UK). Products for molecular biological techniques were routinely purchased from Boehringer Mannheim UK Ltd (Lewes, East Sussex, UK), Gibco-BRL (Paisley, Scotland), Stratagene Ltd (Cambridge, UK), New England Biolabs (NEB) (c/o CP Labs, Bishops Stortford, Hertfordshire, UK), MBI Fermentas (c/o Helena Biosciences, Sunderland, UK) and Pharmacia Biotech (Milton Keynes, Buckinghamshire, UK). Reagents for bacterial cell culture were obtained from Oxoid (Unipath, Basingstoke, Hampshire, UK). Foetal calf serum (FCS) for mammalian tissue culture was obtained from Advanced Protein Products (APP) (Brierly Hill, UK) and Wolf laboratories (High Wycombe, UK). All tissue culture plastic was supplied by Nunc products (Gibco-BRL) with the exception of six-well plates, which were obtained from Greiner Laboratories (Stonehouse, UK). Nitrocellulose membranes for blotting procedures were obtained from Bio-Rad laboratories (Hemelhempstead, Hertordshire, UK). Radiolabelled chemicals were obtained from Amersham International Plc (Little Chalfont, Buckinghamshire, UK) and NEN Dupont (Hounslow, UK).

2.2 Tissue Culture Techniques

2.2.1 Tissue culture media and supplements

RPMI 1640 medium; Rose Park Memorial Institute 1640 medium, with L-glutamine (Gibco-BRL) was supplemented with 10% FCS (Advanced protein products).

DMEM medium; Dulbecco's modified eagle medium, without sodium pyruvate (Gibco-BRL) was supplemented with 10% FCS.

Opti-MEM I; Reduced serum medium (Gibco-BRL)

2.2.2 Cell Lines

Details of the cell lines employed are given in Table 2.1.

Name	Cell Type	Growth Medium	Source
HeLa S3	Human cervical epitheloid carcinoma	DMEM (10% FCS)	ATCC
HepG2	Human hepatocyte carcinoma	DMEM (10% FCS)	ATCC
HK293	Human embryonic kidney cell line immortalised with adenovirus DNA	DMEM (10% FCS)	ATCC
Balb/c-3T3	Murine embryonic fibroblast cell line	DMEM (10% FCS)	ATCC
MCF7	Human breast carcinoma	DMEM (10% FCS)	ATCC
COS7	Monkey epithelial cell line (CV-1) immortalised with SV40 DNA	DMEM (10% FCS)	ATCC
GM03201	Human EBV immortalised lymphoblastoid cell line	RPMI 1640 (10% FCS)	NIGMS

Table 2.1: Cell lines utilised with details of their origin and *in vitro* growth requirements.

2.2.3 Maintenance of cell lines

All of the above cell lines were cultured in the appropriate growth media (Table 2.1) in sterile plasticware (Nunclon, Gibco-BRL). The adherent cells were grown to confluence in 10 cm petri-dishes and treated with 1X trypsin solution (Gibco-BRL) supplemented with 0.5 mM EDTA, pH 8.0. Approximately, 1×10^6 cells were diluted into fresh medium and replated into a new dish. Cells grown in suspension were maintained at concentrations between 5×10^5-1×10^6 cells/ml. All cells were routinely grown at 37^0C in a humidified atmosphere containing 5% CO_2.

2.2.4 Calcium phosphate-mediated DNA transfection

Calcium phosphate-mediated DNA transfection of mammalian cells was performed essentially as described by Jordan *et al.* with minor modifications (Jordan *et al.*, 1996). Approximately 20 hours before transfection, 1×10^6 cells were seeded onto a 10 cm plate in 9 ml of complete medium. A solution of 50 µl of 2.5 M $CaCl_2$ and 25 µg of plasmid DNA (20 µg of luciferase

plasmid and 5 µg of pcDNA3.1/HisB/*lacZ*) was diluted with sterile de-ionised water to a final volume of 500 µl. This 2X Ca/DNA solution was added in a dropwise manner to an equal volume of 2X HEPES buffered saline (50 mM HEPES, pH 7.05, 1.5 mM Na₂HPO4, 140 mM NaCl) whilst bubbling air through the mixture. The calcium phosphate-DNA co-precipitate was allowed to form for 5 min and was then added slowly to the 9 ml of medium covering the cells. After exposing the cells to the precipitate for 15-20 hours at 37^0C, the medium was removed and the cells were washed twice with phosphate buffered saline (4.3 mM Na_2HPO_4, 1.5 mM KH_2PO_4, 137 mM NaCl, 2.7 mM KCl, pH 7.4). Subsequently, fresh medium was added and the cells were grown for a further 24 hours before harvesting.

2.2.5 Cationic liposome-mediated RNA transfection

Cationic liposome-mediated RNA transfection of mammalian cells was performed as described by Dwarki *et al.* (Dwarki *et al.*, 1993). Capped and polyadenylated transcripts were synthesised using *in vitro* run-off transcription on an *Eco*RI linearised pSP64R(x)L Poly(A) template and subsequently purified. Approximately $2x10^5$ HeLa cells were diluted into 2 ml of fresh medium and grown in a 6-well plate. The cells were transfected as they approached confluence. The medium was aspirated and cells were washed once with Opti-MEM I reduced serum medium. During the preparation of the liposome-RNA complexes, the cells were returned to the 37^0C incubator covered in this medium. A mixture of 1ml of Opti-MEM I medium and 12.5 µg of lipofectin (Gibco-BRL) was incubated at room temperature for 20 min. 5 µg of capped mRNA was added directly to the media-lipid mixture and the solution was mixed. After a further incubation of 10 min at room temperature the Opti-MEM I medium was removed from the cells and replaced with the media-lipid-RNA solution. Finally, the cells were returned to the 37^0C incubator and harvested after 8 hours of transfection.

2.3 Bacterial Methods

2.3.1 Bacterial media and supplements

LB medium; 10 g Bacto-tryptone, 5 g bacto-yeast extract, 10 g NaCl dissolved in 1 l of deionised water.

LB agar plates; 10 g Bacto-tryptone, 5 g bacto-yeast extract, 10 g NaCl dissolved in 1 l of

deionised water and supplemented with 15 g of agar.

SOC medium; 2 g Bacto-tryptone, 0.5 g Bacto-yeast extract, 1 ml of 1 M NaCl, 0.25 ml of 1 M KCl, 1 ml of 2 M MgCl$_2$, 1 ml of 2 M glucose.

Ampillicin; a stock solution of 50 mg/ml was prepared using sterile deionised water. Ampicillin was used at a final concentration of 50 µg/ml.

2.3.2 Bacterial strains

The *E. coli* strain JM109 was used in most bacterial manipulations

JM109; e14$^-$(*mcrA*)*recA1*, *endA1*, *gyr A96*, *thi-1*, *hsdR17*, *supE44*, *relA1*, *Δ(lac-proAB)*, F', *traD36, proAB, lacZΔM15*.

To prevent the methylation of the *Eco*R09011 site in c-*myc* exon 1, the plasmid pSKutr2 was transformed into the *E. coli* strain BL21(DE3)

BL21(DE3); F$^-$, *ompT*, *hsdS$_B$*, (r$_B^-$, m$_B^-$), *dcm*, *gal*, λ(DE3)

2.3.3 Preparation of competent cells

A single colony from an LB plate was inoculated into 2.5 ml of LB medium and incubated overnight at 37^{0}C with shaking. The entire overnight culture was inoculated into 250 ml of LB medium supplemented with 20 mM MgSO$_4$ and incubated at 37^{0}C until the A$_{600}$ reached 0.4-0.6. Cells were collected by centrifugation at 4,500 x *g* for 5 min at 4^{0}C using a GSA rotor (Sorvall). Following centrifugation, the pellet was gently resuspended in 100 ml of ice-cold filter sterile TFB1 (30 mM KAc, 10 mM CaCl$_2$, 50 mM MnCl$_2$, 100 mM RbCl, 15% (v/v) glycerol, adjust to pH 5.8 with 1 M glacial acetic acid). After incubating on ice for 5 min, the cells were collected by centrifugation at 4,500 x *g* for 5 min at 4^{0}C. The pellet was resuspended in 10 ml of ice-cold filter sterile TFB2 (1 mM MOPS, pH 6.5, 75 mM CaCl$_2$, 10 mM RbCl, 15% (v/v) glycerol, adjust to pH 6.5 with 1 M KOH) and the cells were incubated on ice for 1 hour. Finally, the cells were rapidly frozen in an isopropanol/dry ice bath in 200 µl aliquots and stored at –70^{0}C.

2.3.4 Transformation of competent cells

Ligation products or plasmid DNA (10 ng) were added to 50 µl of competent cells and

incubated on ice for 20 min. After heating the mixture at 42^0C for 2 min, 150 µl of SOC medium was added. Subsequently, the cells were incubated with shaking at 37^0C for 45 min. Finally, the sample was spread onto a pre-warmed LB agar plate containing ampicillin and then incubated at 37^0C for 16-20 hours.

2.4 Molecular Biology Techniques

CsCl₂-saturated isopropanol (ITC); Mix 10 g of $CsCl_2$, 10 ml TES, and 40 ml isopropanol. Shake thoroughly to obtain a saturated solution and use the upper isopropanol phase.

OLB; Mix solutions A, B, and C in the ratio 2:5:3

A) 1.2 M Tris-HCl, pH 8.0, 0.12 M $MgCl_2$, 1.75%(v/v) β-mercaptoethanol, and 0.5 mM of dATP, dGTP and dTTP

B) 2 M HEPES-NaOH, pH 6.6

C) 1.6 mg/ml Hexadeoxyribonucleotides in 3 mM Tris-HCl, 0.2 mM EDTA, pH 7

0.5X TAE; 20 mM Tris-acetate, pH 7.5, 0.5 mM EDTA

TES; 50 mM Tris-HCl, pH 8.0, 5 mM NaCl, 50 mM EDTA

1X TBE; 89 mM Tris base, 89 mM Boric acid, 2.5 mM EDTA, pH 8.0

5X TBE loading buffer; 30%(v/v) glycerol, 0.25% Bromophenol blue, 0.25% Xylene cyanol

TE; 10 mM Tris-HCl pH 8.0, 1 mM EDTA

2.4.1 Plasmids

pGL3con (Promega)

pRLCMV (Promega)

pCAT3con (Promega)

pSK+bluescript (Stratagene)

pcDNA3.1/HisB/*lac*Z (Invitrogen)

pXLJ(10-605) (A kind gift from Dr. R. J. Jackson)

2.4.2 Ethanol precipitation of DNA

DNA was precipitated by adding 0.1 volume of 3 M sodium acetate, pH 5.2 and 2 volumes of absolute ethanol. The sample was incubated on ice or at -20^0C for 15-30 minutes following which the DNA was collected by centrifugation at 12,000 x *g* for 10 min. Excess salt was removed from the pellet by washing with 70% ethanol, then the DNA was dried briefly and

resuspended in either TE or sterile deionised water.

2.4.3 Phenol/chloroform extraction

Solutions of nucleic acid were separated from contaminating proteins by the addition of an equal volume of phenol:chloroform:isoamyl alcohol (25:24:1). After vigorous mixing, the phases were separated by centrifugation at 12,000 x g for 5 min. The upper aqueous phase was removed to a separate tube, to which an equal volume of chloroform:isoamyl alcohol was added. Following extraction and separation of the phases, the aqueous layer was transferred to new tube and the nucleic acid was precipitated.

2.4.4 Purification of DNA using glassmilk

Glassmilk was used to purify DNA fragments amplified by PCR, or to isolate DNA when a change of reaction buffer was required. Up to 5 μg of DNA was incubated with 3 volumes of 6 M NaI and 5 μl of glassmilk for 5 min at room temperature. The glassmilk was collected by centrifugation and washed two times in 0.5 ml of wash solution (10 mM Tris-HCl, pH 7.5, 100 mM NaCl, 52.6% ethanol). After the glassmilk was resuspended in 10 μl of sterile deionised water, it was incubated at 45-55^{0}C for 5 min to elute the DNA. Following centrifugation, the supernatant was removed to a fresh tube and the elution process was repeated.

2.4.5 Agarose gel electrophoresis

Fragments of DNA were fractionated according to their molecular weight by electrophoresis through agarose gels. Agarose was melted in 1X TBE buffer, cooled and cast into a gel. After which the gel was submerged in 1X TBE in a horizontal electrophoresis tank. Samples were mixed with 0.2 volume of 5X TBE loading buffer and separated in the gel at up to 8 V/cm. After electrophoresis, the gel was stained with ethidium bromide (1.3 mg/l in 1x TBE) for 15-20 min and the DNA was visualised on a UV transilluminator.

2.4.6 Gel isolation of DNA fragments

Initially, DNA fragments were separated by agarose gel electrophoresis as described in section

2.4.5, except the gel was prepared and submerged in 0.5X TAE. After staining with ethidium bromide, the fragments were visualised using a low intensity UV lamp. Agarose containing the required fragment was excised from the gel and melted at 55^0C in 3 volumes of 6 M NaI. DNA was isolated from this solution using the glassmilk procedure described in section 2.4.4.

2.4.7 Synthesis and purification of oligonucleotides

Oligonucleotides were synthesised on an Applied Biosystems model 394 machine (Protein and Nucleic Acid Sequencing Laboratory, Leicester University) at a 0.2 µM scale. Oligonucleotides were purified by ethanol precipitation with 0.1 volume of 3M sodium acetate, pH 5.2 and 3 volumes of absolute ethanol. Samples were incubated at -20^0C for 30 min and the precipitate was collected by centrifugation at 12,000 x g for 20 min. After washing with 70% ethanol the pellet was dried and then resuspended in 100 µl of TE. The concentration of the oligonucleotide was determined by measuring the absorbance at 260 nm.

2.4.8 Oligonucleotides

FP2501	5' TAATTCCAGCGAGAGGCAGA 3'
JLQ1	5' GAAGCCCCCTATTCGCTCC 3'
FP2670	5' TGCCGCATCCACGAAACTTT 3'
MS4526	5' GGGCATCGTCGCGGGAGGCTG 3'
MS4527	5' CTCAACGTTAGCTTCACCAAC 3'
MS4519	5' TATACCATCGTCGCGGGAGGCTGCTG 3'
MS7216	5' CGGAATTCTTACGCACAAGAGTTGCCGAT 3'
5'CUG	5' CTGCTTAGACGCTCGATTTTTTTCGGGTAGTGGAAAACCA 3'
KS	5' TCGAGGTCGACGGTATC 3'
T7	5' GTAATACGACTCACTATAGGGC 3'
Luc3'	5' GCGTATCTCTTCATAGCCTT 3'
ECLuc3	5' GTACGAATTCGTTGGTAAAGCCACCATGGA 3'
ECLuc5	5' GTACGAATTCAGTACCGGAATGCCAAGCTT 3'
ESP5	5' GATATCACTAGTCAGCTGG 3'
ESP3	5' CCAGCTGACTAGTGATATC 3'
LOOP1	5' AGATCTGGTACCGAGCTCCCCGGGCTGCAGGAT 3'
LOOP2	5' ATCCTGCAGCCCGGGGAGCTCGGTACCAGATCT 3'
RNaseF	5' GCAAGAAGATGCACCTGATG 3'

2.4.9 Restriction enzyme digestion

DNA was digested with restriction enzymes in a total volume of 10-50 µl under the conditions recommended by the suppliers. Reactions were incubated at the appropriate temperature for 1-2 hours.

2.4.10 Filling in recessed 3' ends

The large (Klenow) fragment of *E. coli* DNA polymerase I was used to fill in the recessed 3' ends of DNA fragments. The reaction was performed in a final volume of 25 µl, containing 80 µM of each dNTP, a maximum of 2 µg of DNA and 1X Fill-in buffer (50 mM Tris-HCl, pH 7.5, 10 mM $MgCl_2$, 0.1 mM DTT, 50 µg/ml BSA) or 1X Restriction enzyme buffer supplemented with 100 µg/ml of BSA. 1-5 units of Klenow DNA polymerase were added and the reaction was incubated at 30^0C for 15 min. The reaction was stopped by heating at 75^0C for 10 min, following which the DNA was purified.

2.4.11 Removal of overhanging 3' ends

The 3' exonuclease activity of T4 DNA polymerase was used to remove the overhanging 3' termini of DNA fragments generated by restriction digestion or *Taq* DNA polymerase. The reaction was performed in a final volume of 20 µl containing 1X T4 DNA polymerase buffer (33 mM Tris-acetate, pH 7.9, 66 mM KAc, 10 mM $Mg(Ac)_2$, 0.5 mM DTT, 100 µg/ml BSA), 100 µM of each dNTP and 2 µg of DNA. 10 units of enzyme were added and the reaction was incubated at 37^0C for 5 min. The reaction was stopped by heating at 75^0C for 10 min and then the DNA was purified.

2.4.12 Radiolabelled DNA markers

1 µg of pBR322 was digested with 5 units of *Hpa*I for 20 min in a volume of 10 µl and the reaction was stopped by heating at 90^0C for 2 min. The DNA fragments were radiolabelled using Klenow DNA polymerase in a reaction volume of 15 µl containing 1X Restriction enzyme buffer, 100 µg/ml of BSA, 1 mM dGTP, 10 µCi of $[\alpha\text{-}^{32}P]$ dCTP (800 Ci/mmol) and 5 units of Klenow DNA polymerase. The reaction was incubated at 30^0C for 15 min and stopped by the addition of formamide loading dyes.

2.4.13 Alkaline phosphatase treatment of DNA

Linearised plasmids were treated with calf intestinal alkaline phosphatase (CIAP) to remove the terminal phosphate group from the 5' ends and prevent self-ligation. Following restriction digestion, the restriction enzyme was inactivated by heating the reaction at 65^0C for 15 min. Dephosphorylation was performed in a final volume of 50 µl in 1X Restriction enzyme buffer. For DNA fragments with overhanging 5' ends the reaction was incubated for 30 min at 37^0C using 1 unit of CIAP, after which another unit of enzyme was added and the incubation was repeated. Whilst for DNA fragments with blunt ends, the reaction was incubated at 37^0C for 15 min followed by 56^0C for 15 min using 1 unit of CIAP, and these incubations were repeated after the addition of another unit of CIAP. The reaction was terminated by heating at 75^0C for 10 min and the DNA was purified using glassmilk. For those restriction enzymes that are resistant to heat-inactivation, the DNA was first purified using glassmilk and resuspended in 50 µl of 1X CIAP reaction buffer (50 mM Tris-HCl, pH 9.3, 1 mM $MgCl_2$, 0.1 mM $ZnCl_2$). The reactions were then performed as described above.

2.4.14 Phosphorylation of nucleic acids using T4 polynucleotide kinase

PCR products and oligonucleotides that were used in ligations were first treated with T4 polynucleotide kinase (T4 PNK) to add a 5' terminal phosphate group. For oligonucleotides, a reaction containing 5 µg of nucleic acid, 1X T4 PNK buffer (70 mM Tris-HCl, pH 7.6, 10 mM $MgCl_2$, 5 mM DTT) and 100 µM ATP in a final volume of 50 µl was incubated at 37^0C for 30 min with 10 units of T4 PNK. Similar conditions were used for PCR products, however prior to the addition of enzyme the reaction was heated at 65^0C for 10 min. Finally, the kinase reaction was terminated by heating at 75^0C for 10 min.

2.4.15 Annealing complementary oligonucleotides

The complementary oligonucleotides ESP5 and ESP3 or Loop1 and Loop2 were annealed to create an oligonucleotide cassette that was subsequently used in a ligation reaction. Initially, the oligonucleotides were treated with T4 PNK as described above. Subsequently, equimolar amounts of oligonucleotide (5 µg of each) were combined and heated at 75^0C for 10 min. The oligonucleotides were then annealed by incubating the mixture at 37^0C for 10 min followed by incubation on ice for 10 min. Finally, the concentration of the oligonucleotide cassette was

adjusted to approximately 40 nM.

2.4.16 Ligations

Ligations were performed in a total volume of 10 µl. Vector DNA (50 ng) was mixed in a 1:3 molar ratio with insert DNA in a reaction containing 1X T4 DNA ligase buffer (MBI Fermentas) and T4 DNA ligase. For ligations involving fragments with overhanging termini, the reaction was incubated at 16°C for 2-16 hours. Polyethylene glycol 8000 (4%(w/v)) was included in reactions in which all DNA termini were blunt. The efficiency of these blunt-ended ligations was further improved by incubating the reaction for at least 16 hours at 16°C. Alternatively, a cycle ligation was performed in which the temperature was alternated between 10°C and 30°C over 16 hours. The sample was incubated for 10 s at each temperature. After the appropriate incubation, 5 µl of the ligation reaction was transformed in competent *E.coli*.

2.4.17 Small scale preparation of plasmid DNA

A single colony of *E.coli* was inoculated into 5 ml of LB media containing ampicillin and incubated overnight at 37°C in a shaking incubator. Approximately 1.5 ml of the culture was decanted into a labelled tube and the bacteria were collected by centrifugation. The pellet was resuspended in 100 µl of ice-cold solution I (25 mM Tris-HCl, 10 mM EDTA, 50 mM Glucose, pH 8.0). After a 5 minute incubation at room temperature, 200 µl of solution II (1%(w/v) SDS, 0.2 M NaOH) was added and the solutions were mixed gently. The sample was incubated on ice for 5 min, following which 150 µl of 7.5 M NH₄Ac, pH 7.6 was added. After briefly mixing the solutions using a vortex, the sample was incubated on ice for a further 5 min. The precipitated matter was collected by centrifugation at 12,000 x *g* for 5 min and the supernatant was removed to a fresh tube. Plasmid DNA was ethanol precipitated from this solution as described in section 2.4.2. Finally, the washed and dried pellet was resuspended in 30 µl of TE. Diagnostic restriction digests were performed using 5 µl of this solution.

2.4.18 Large scale preparation of plasmid DNA

The ammonium acetate method described by Saporito-Irwin *et al.* was used to prepare milligram quantities of plasmid DNA (Saporito-Irwin *et al.*, 1997). An overnight culture of *E. coli* containing the plasmid was inoculated into 250 ml of LB media supplemented with

ampicillin. The culture was grown for 12-16 hours in a 37^0C shaking incubator. Cells were harvested by centrifugation at 4,000 x g for 10 min at 4^0C. The pellet was resuspended in 3 ml of ice-cold solution I and incubated at room temperature for 5 min. Following which, 6 ml of solution II was added and the sample was incubated on ice for 10 min. This solution was neutralised with 4.5 ml of 7.5M NH_4Ac, pH 7.6 and incubated for a further 10 min on ice. The precipitated matter was collected by centrifugation at 12,000 x g for 10 min at 4^0C and the supernatant was removed to a fresh tube. Isopropanol (0.6 volumes) was added and the solution was incubated at room temperature for 10 min. The insoluble material was collected by centrifugation (12,000 x g) for 10 min at room temperature. The plasmid DNA in the pellet was resuspended thoroughly in 2 M NH_4Ac, pH 7.4. The insoluble matter was separated from the supernatant as before, and the supernatant removed to a fresh tube. After the addition of 1 volume of isopropanol, the solution was incubated at room temperature for 10 min and the plasmid DNA was collected by centrifugation. Following resuspension of the pellet in 1ml of sterile deionised water, contaminating RNA was removed by adding 100 μg of RNase A and incubating the solution at 37^0C for 15 min. Proteins were then precipitated by the addition of 0.5 volume of 7.5M NH_4Ac, pH 7.6 and incubating at room temperature for 5 min. The precipitated proteins were collected by centrifugation and the supernatant was removed to a fresh tube. Finally, the plasmid DNA was precipitated using 1 volume of isopropanol, harvested by centrifugation and washed with 70% ethanol. The resulting pellet was resuspended in a volume of 0.5-1 ml of TE.

2.4.19 Caesium chloride gradient purification of plasmid DNA

To achieve efficient transfection of some cell lines (e. g. Balb/c-3T3) using a calcium phosphate/DNA co-precipitate, the DNA was further purified on a $CsCl_2$ gradient. Plasmid DNA was resuspended in 8 ml of TE, into which 10 g of $CsCl_2$ were subsequently dissolved. The $CsCl_2$/DNA solution was transferred to an 11.5 ml polyallomer tube (NEN-Sorvall) and supplemented with 0.5 ml of 10 mg/ml ethidium bromide. If necessary, additional TE was added to give a final volume of 11.5 ml and the tube was sealed. Plasmid DNA was fractionated on a $CsCl_2$ gradient by centrifugation of the sample in a Sorvall Ti270 rotor at 50,000 rpm for 20 hours at 4^0C. The supercoiled plasmid DNA was removed from the gradient using a syringe and separated from the ethidium bromide by repeated extraction with an equal volume of $CsCl_2$-saturated isopropanol (ITC). The aqueous solution was diluted with 2 volumes of deionised water and the plasmid DNA was precipitated by the addition of an equal volume of isopropanol and 0.1 volume of 3 M NaAc, pH 5.2. After centrifugation at

12,000 x *g* for 10 min the pellet was resuspended in 0.5 ml of deionised water and plasmid DNA was ethanol precipitated as described previously. The final pellet was resuspended in 0.25-1 ml of 0.1X TE.

2.4.20 Double stranded DNA sequencing

Plasmid DNA was isolated using the small scale method and contaminating RNA was digested with 1 μg of RNase A at 37^0C for 30 min. After RNase treatment, the DNA was ethanol precipitated and resuspended in 10 μl of sterile deionised water. The plasmid DNA was denatured by incubating this solution with 0.1 volumes of 2 mM NaOH, 2 mM EDTA, pH 8.0 at 37^0C for 15 min. After which, the solution was neutralised with 0.1 volumes of 3 M KAc, pH 4.8 and 1 volume of isopropanol was added. Following incubation at room temperature for 10 min, the single stranded DNA was collected by centrifugation at 12,000 x *g* for 10 min and the pellet was dried. The pellet was resuspended in 10 μl of a 2.5 ng/μl solution of sequencing primer and 2 μl of annealing buffer (280 mM Tris-HCl, pH 7.5, 100 mM $MgCl_2$, 350 mM NaCl). The plasmid DNA/primer solution was heated at 75^0C for 10 min, and then incubated at 37^0C for 10 min, followed by 5 min on ice to achieve primer annealing. Samples were labelled at 20^0C for 5 min, in a reaction containing 0.4 μl [α-^{35}S] dATP (12.5 mCi/ml), 3 μl of labelling mix A (2 μM dGTP, 2 μM dCTP, 2 μM dTTP), and 1 unit of T7 DNA polymerase. Labelling was terminated by the addition of 2-4 μl of each termination mix (150 μM of each dNTP, 10 mM $MgCl_2$, 40 mM Tris-HCl, pH 7.5, 50 mM NaCl, 15 μM ddNTP G, A, T, or C) and incubated at 42^0C for 5 min. Finally, the reaction was stopped by adding 4 μl of formamide loading dyes (100% deionised formamide, 0.1%(w/v) Xylene cyanol FF, 0.1%(w/v) Bromophenol blue, 1 mM EDTA). The labelled DNA fragments were fractionated on a 6% polyacrylamide/7 M urea gel following which the gel was dried for 1 hour at 80^0C and exposed to Fuji medical X-ray film for 16-48 hours.

2.4.21 Standard PCR reaction

Standard PCR reactions were performed in a final volume of 50 μl containing 1X PCR reaction buffer (Gibco-BRL), 1.5 mM $MgCl_2$, 0.2 mM of each dNTP, 25 pmol of both the upstream and downstream primers, 1 unit of *Taq* DNA polymerase (Gibco-BRL) and 100 ng of template DNA. Samples were overlaid with paraffin oil to minimise evaporation. Reactions were performed in a Perkin Elmer Cetus, or a Techne Genius Thermal Cycler.

DNA was initially denatured by heating at 94^0C for 3 min, following which the samples were heated at 94^0C for 30 s (denature), 57-65^0C for 30 s (anneal) and 72^0C for 60 s (extend) sequentially, for 25-30 cycles.

2.4.22 RT-PCR

When amplifying a DNA fragment using single stranded DNA from a reverse transcription (RT) reaction as a template, the entire RT reaction was used. The PCR reaction conditions were adjusted to account for the dNTPs, $MgCl_2$ and RT buffer already present. A fragment encoding the c-*myc* cDNA sequence from -396 to $+6$ was amplified using the primer set FP2501 and MS4526.

2.4.23 The construction of pGL3E using long PCR

An *Eco*RI site was engineered into the plasmid pGL3con by amplifying the whole plasmid using the primers ECLuc5 and ECLuc3. The PCR reaction was performed using the Expand™ kit (Boehringer Mannheim) according to the manufacturers instructions. Essentially, two mixes were prepared: Mix 1 contained 300 nM of each primer, 200 µM of each dNTP and 100 ng of pGL3con in a final volume of 25 µl, and Mix 2 contained 2X Expand™ reaction buffer and 0.75 µl of a *Taq/Pwo* DNA polymerase mix in a final volume of 25 µl. The two mixes were combined immediately before incubation and overlaid with mineral oil. The plasmid DNA was denatured by heating at 94^0C for 2 min, following which the reaction was incubated at 94^0C for 30 s (denature), 62^0C for 30 s (anneal) and 68^0C for 4 min (extend) sequentially for 10 cycles. Thereafter, the extension time was increased by 20 s each cycle for a further 15 cycles. Finally, the reaction was completed by heating at 72^0C for 7 min. The PCR product was purified using size exclusion chromatography on a chromaspin+TE-400 column (Clontech) and digested with *Eco*RI. The resulting linear DNA fragment was circularised by self-ligation for 2 hours at 16^0C thus creating pGL3E.

2.4.24 PCR mutagenesis

"One-tube, two-stage" PCR-directed *in vitro* mutagenesis was performed as described by Ekici *et al.* (1997). In the first stage, the mutagenic megaprimer was synthesised in a reaction containing 1X *Pfu* reaction buffer, 100 ng of pSKutr2, 50 pmol of the mutagenic primer

5'CUG, 25 pmol of the downstream primer KS, 200 μM of each dNTP and 2.5 units of *Pfu* DNA polymerase. After heating at 94^{0}C for 3 min, the reaction was incubated for 30 s at 94^{0}C (denature), 60 s at 60^{0}C (anneal) and 30 s at 72^{0}C (extend) sequentially for 20 cycles. In the second stage, a previously prepared mix containing 100 pmol of the upstream primer FP2501, 2.5 units of *Pfu* DNA polymerase, 200 μM of each dNTP in a final volume of 25 μl of 1X *Pfu* reaction buffer was added to the first reaction. The incubation conditions for the second reaction were identical to those of the first except that the annealing temperature was increased to 65^{0}C. After fractionation through an agarose gel, a DNA fragment of the appropriate size was isolated as described in section 2.4.6. The fragment was then treated with T4 PNK, digested with *Nco*I and ligated into pGL3R. The introduction of a *Taq*I restriction site was used to screen for clones containing the mutant plasmid and the presence of a single mutation was confirmed by sequencing.

2.4.25 Isolation of total cellular RNA

Total cellular RNA was isolated using the guanidium isothiocyanate method (Chomczynski and Sacchi, 1987). Adherent cells were lysed by scraping with a "rubber policeman" in 1 ml of TriReagent™ (Sigma), whilst suspension cells were first harvested by centrifugation before addition of the reagent. Once the lysate was transferred to a fresh tube, 200 μl of chloroform was added and the mixture was vigorously mixed using a vortex for at least 30 s. The aqueous and inorganic phases were separated by centrifugation at 12,000 x *g* for 15 min at 4^{0}C and the upper aqueous phase was transferred to a fresh tube. An equal volume of isopropanol was added to this solution and the sample was incubated at room temperature for 10 min. The precipitate was collected by centrifugation at 12,000 x *g* for 15 min and the pellet was washed with 75% ethanol. After briefly drying the pellet, it was resuspended in 30 μl of filter sterile deionised water. A 1 μl sample was subjected to agarose gel electrophoresis to ensure that degradation had not occurred. Finally, prior to storage at –20^{0}C, the concentration of the RNA was determined by measuring its absorbance at 260 nm.

2.4.26 Purification of poly[A]$^+$ mRNA from total cellular RNA

Poly[A]$^+$ mRNA was purified from total mRNA using oligo[dT] magnetic beads (Dynatec Inc.) according to the manufacturers instructions. Initially, 134 μl of oligo[dT] beads were washed in 100 μl of 2X Binding buffer (20 mM Tris-HCl, pH7.5, 1 M LiCl, 2 mM EDTA)

and then suspended in a further 100 µl of 2X Binding buffer. Filter sterile deionised water was used to increase the volume of 50 µg of total cellular RNA to 100 µl. After heating the RNA solution at 65^0C for 2 min, it was combined with the bead suspension. The RNA was bound to the beads by continuously mixing the solution at room temperature for 5 min. Following which, the beads were collected using the magnet provided and the supernatant was removed. Unbound material was removed by washing the beads twice with 200 µl of wash solution (10 mM Tris-HCl, pH 7.5, 0.15 M LiCl, 1 mM EDTA). Finally, 10 µl of elution solution (2 mM EDTA, pH 8.0) was added to the beads and the poly[A]$^+$ mRNA was eluted by heating at 65^0C for 2 min.

2.4.27 *In vitro* run-off transcription

10 µg of vector DNA was linearised by restriction digestion using a site downstream of the sequence of interest. Subsequently, the protein was removed by phenol/chloroform extraction and following ethanol precipitation, the DNA was resuspended in 10 µl of filter sterile deionised water. To synthesise uncapped transcripts, a reaction was set up containing 1X Transcription buffer (80 mM Hepes-KOH, pH 7.5, 24 mM $MgCl_2$, 2 mM spermidine, 40 mM DTT), 80 mM KOH, 40 units of recombinant RNasin ribonuclease inhibitor, 10 mM of each NTP, 1.5 µg of DNA template, and 40 units of T7, T3, or SP6 RNA polymerase in a final volume of 50 µl. After incubation at 37^0C for 2 hours, the DNA template was digested with 10 units of RNase-free DNase I for 15 min at 37^0C. Immediately following digestion, the RNA was phenol/chloroform extracted and unincorporated nucleotides were removed by passing the solution through a Sephadex G-50 column. The RNA was precipitated by the addition of 0.5 volume of 7.5 M NH_4Ac and 2.5 volumes of ethanol. After incubation at – 70^0C for 30 min, the RNA was collected by centrifugation and washed with 75% ethanol. The pellet was resuspended in 30 µl of filter sterile 0.1X TE and the concentration was determined using the absorbance at 260 nm. In addition, 0.5 µl of the RNA was subjected to agarose gel electrophoresis to ensure the product was not degraded.

Capped transcripts were synthesised in a reaction containing 1X Transcription buffer, 7 mM KOH, 40 units of RNasin, 1 mM ATP, 1 mM UTP, 1 mM CTP, 0.5 mM GTP, 2 mM $m^7G(5')ppp(5')G$, 1 µg of DNA template and 20 units of T7, T3, or SP6 RNA polymerase in a final volume of 50 µl. After incubating the reaction for 1 hour at 37^0C, the RNA was isolated as described above.

Radiolabelled transcripts were synthesised in a reaction containing 1X Transcription buffer, 6 mM KOH, 20 units of RNasin, 50 µCi of [α-^{32}P]CTP (400 Ci/mmol), 1 mM of ATP, UTP and GTP, 1 µg of template DNA and 20 units of T3 RNA polymerase in a final volume of 10 µl. For the radiolabelled transcripts used in UV cross-linking assays, a combination of 0.75 mM UTP and 0.25 mM 4-thioUTP was used instead of 1 mM UTP. After incubation for 1 hour at 37^{0}C, the template DNA was removed as described previously and the protein was extracted using phenol/chloroform. The RNA was precipitated by incubating the sample at –70^{0}C for 30 min with 0.5 volume of 7.5 M NH$_4$Ac and 2.5 volumes of ethanol. After collecting the RNA by centrifugation, it was resuspended in 10 µl of loading dyes (80% deionised formamide, 10 mM EDTA, 0.1% SDS, 0.1% Xylene cyanol FF, 0.1% Bromophenol blue) and the sample was heated at 85^{0}C for 5 min. Subsequently, transcripts were fractionated on a 4% polyacrylamide/7 M urea gel and detected by exposure to Fuji medical X-ray film for 30 s. A slice of polyacrylamide containing only full length transcripts was excised from the gel, and RNA was extracted by incubating with 0.5 ml of extraction buffer (0.5 M NH$_4$Ac, 1 mM EDTA, 0.2% SDS) for 16 hours at 4^{0}C. Radiolabelled RNA was precipitated from the supernatant using 0.1 volume of 7.5 M NH$_4$Ac and 2.5 volumes of ethanol, collected by centrifugation, washed with 75% ethanol and resuspended in 50 µl of filter sterile deionised water. RNA concentrations were then determined by Cerenkov scintillation counting in a Tri-Carb 2000CA scintillation counter (Packard).

2.4.28 Reverse transcription of total cellular RNA

RNA was isolated by the method described previously and 1 µg was diluted into a total volume of 5 µl using filter sterile deionised water. The sample was heated at 65^{0}C for 3 min and then incubated on ice for 5 min. The RNA was then added to a 15 µl reaction containing 1X Superscript reaction buffer (Gibco-BRL), 1 mM of each dNTP, 160 ng/µl of random hexanucleotides, 40 units of RNasin and 200 units of Superscript reverse transcriptase (Gibco-BRL). After which, the sample was incubated at 20^{0}C for 15 min to allow annealing to occur. Subsequently, reverse transcription was performed at 42^{0}C for 1 hour and the enzyme was inactivated by heating at 95^{0}C for 5 min. The sample was either used immediately to amplify a DNA fragment or stored at –20^{0}C.

2.4.29 RNase protection

The RNA samples were combined with 5×10^5 cpm of radiolabelled riboprobe and precipitated with 2.5 volumes of ethanol for 30 min at -20^0C. After the RNA was collected by centrifugation, washed with 75% ethanol, and briefly dried, it was resuspended in 30 µl of hybridisation buffer (80% deionised formamide, 40 mM PIPES, pH 6.4, 0.4 M NaCl, 1 mM EDTA). Samples were then heated at 85^0C for 5 min and subsequently incubated at 45^0C for 16 hours to allow annealing to occur. 300 µl of RNase digestion buffer (10 mM Tris-HCl, pH 7.5, 5 mM EDTA, 200 mM sodium acetate) were then added to each sample and the single stranded RNA was digested with RNase ONE™ (Promega) at a concentration of 1 unit/µg of RNA. The reaction was terminated by the addition of 10 µl of 20%(w/v) SDS and proteins were digested with 2.5 µl of 20 mg/ml proteinase K at 37^0C for 15 min. The sample was extracted once with phenol/chloroform and the aqueous phase was removed to a separate tube containing 10 µg of carrier tRNA. RNA was precipitated by incubating the sample with 825 µl of 100% ethanol at -20^0C for 30 min. After collecting the insoluble material by centrifugation and washing the pellet with 75% ethanol, the sample was dried and resuspended in 5 µl of formamide RNA loading dye. RNA was denatured by heating at 85^0C for 5 min and fractionated by electrophoresis through a 4% polyacrylamide/7 M urea gel. Finally, radiolabelled RNA fragments were detected by analysing the dried gel using a Molecular Dynamics phosphorimager.

2.4.30 Denaturing RNA agarose gel electrophoresis and Northern blotting

Samples of RNA were denatured by incubation in 1X Gel buffer (20 mM MOPS, pH 7.0, 5 mM NaAc, and 1 mM EDTA), 6.5% formaldehyde, and 50% deionised formamide at 55^0C for 15 min in a final volume of 20 µl. Denatured RNA was fractionated by electrophoresis through a 1% agarose gel containing 1X Gel buffer and 6% formaldehyde. The gel was submerged in 1X Gel buffer and run at 100 V for 3-4 hours. After electrophoresis was complete, the portion of gel containing the RNA markers (Gibco-BRL) was removed, stained with ethidium bromide (5 µg/ml) for 10 min and destained for 10 min using filter sterile deionised water. The markers were visualised using a UV transilluminator and photographed for later reference. The remainder of the gel was soaked in filter sterile deionised water for 15 min to remove any formaldehyde. After which, the gel was incubated in 20X SSC (3 M NaCl, 0.3 M tri-sodium citrate) for 20 min. The RNA was transferred from the gel to a Zetaprobe™

nitrocellulose membrane (Biorad) using capillary blotting. After transferring for 16 hours, the RNA was fixed to the membrane by baking at 80^0C for 2 hours. The filter was then ready for hybridisation with a random-primed radiolabelled probe.

2.4.31 Synthesis of a radiolabelled DNA probe and hybridisation to immobilised RNA

The plasmid pGL3 was digested with *Nco*I and *Ava*I and the 1058 bp luciferase encoding fragment was isolated as described previously. To prepare a random primed radiolabelled DNA probe, 30 ng of the DNA fragment was heated at 95^0C for 5 min in 10 µl of sterile deionised water. After the DNA was denatured, 3 µl of OLB, 0.5 µl of 10 mM BSA, 1 µl of $[\alpha-^{32}P]dCTP$ (800 Ci/mmol) and 5 units of Klenow DNA polymerase were added and the reaction was incubated at 37^0C for 1-2 hours. Unincorporated nucleotides were then removed by passing the probe through a Sephadex G-50 column.

The nitrocellulose filter containing the RNA was pre-hybridised with 10 ml of Church-Gilbert buffer (0.25 M Na_2HPO_4, pH 7.2, 7%(w/v) SDS) supplemented with 0.2 mg/ml of denatured Salmon sperm DNA and 50 µg/ml of bakers yeast tRNA (Sigma) for 1 hour at 65^0C. The random-primed radiolabelled DNA probe was denatured by heating at 95^0C for 5 min and added directly to the hybridisation buffer. Hybridisation was then performed at 65^0C for 16-24 hours after which the filter was washed twice for 30 min at 65^0C with Church buffer 1 (20 mM Na_2HPO_4, pH 7.2, 5%(w/v) SDS) and Church buffer 2 (20 mM Na_2HPO_4, pH 7.2, 1%(w/v) SDS), respectively. Further washes using Church buffer 2 were performed if the background counts on the filter remained high after the initial washes. Excess moisture was then removed from the filter and radiolabelled probe was detected by phosphorimager analysis.

2.5 Biochemical Techniques

2.5.1 *In vitro* translation reactions

In vitro translation reactions were performed using a standard reticulocyte lysate system (Promega) with minor modifications to the manufacturer's recommendations. Briefly, a reaction contained 8.25 µl of reticulocyte lysate, 0.25 µl of RNasin (40 units/µl), 1 µl of 1 mM amino acid mixture (minus methionine), 1 µl of $[^{35}S]$methionine (1,200 Ci/mmol) and RNA

substrate (0.125-20 ng/µl) in a final volume of 12.5 µl. The reaction was incubated at 30^0C for 1 hour and terminated by the addition of 1 volume of 2X GSB (100 mM Tris-HCl, pH 6.8, 8%(w/v) SDS, 20%(v/v) glycerol, 10%(v/v) β-mercaptoethanol, 5 mM EDTA, 0.02% Bromophenol blue). The radiolabelled proteins were then fractionated according to their molecular mass by SDS-polyacrylamide gel electrophoresis (SDS-PAGE). The resulting gel was stained with Coomassie brilliant blue, dried at 80^0C for 1 hour and subjected to phosphorimager analysis.

2.5.2 SDS-PAGE

Protein extracts were denatured by the addition of an equal volume of 2X SDS sample buffer and, with the exception of *in vitro* translation products, were heated at 95^0C for 5 min prior to loading onto a 10% SDS-polyacrylamide gel. Proteins were separated according to standard procedures (Laemelli, 1970). Typically, vertical gels were run at a constant current of 35 mA until the Bromophenol blue dye front reached the bottom of the gel.

2.5.3 Coomassie staining of SDS-polyacrylamide gels

Gels were stained in a solution of methanol, acetic acid, and water at a ratio of 5:1:5, respectively, containing 0.1% Coomassie Brilliant Blue R-250 for 30 min at room temperature. Subsequently, a solution of 10%(v/v) acetic acid was used to destain the gel for between 3-5 hours. Gels were then incubated in deionised water for 30 min to remove acetic acid before drying.

2.5.4 Nuclear extracts

Nuclear extracts were prepared according to the method of Dignam *et al.* (Dignam *et al.*, 1983) and were a kind gift from Dr. I. C. Eperon.

2.5.5 Protein concentration determination-Bradford Assay

Nuclear extracts were diluted by 5 and 10-fold in sterile deionised water. Likewise, stock BSA (2 mg/ml) was diluted to concentrations of between 0.1-1.5 mg/ml. Bradford reagent was added according to the manufacturers instructions (Pierce and Warriner) and the

absorbance at 630 nm was monitored using a microtitre plate reader (Bio-tek instruments). The concentration of the extracts was typically between 5-10 mg/ml.

2.5.6 UV-cross-linking reactions

Samples containing 30 μg of nuclear extract were incubated with 4-thioUTP-containing radiolabelled transcripts (5×10^5 cpm) in the absence or presence of unlabelled competitor RNAs for 15 min at 30^0C. The reaction was performed in a final volume of 30 μl in 1X UV cross-linking buffer (10 mM Hepes-NaOH, pH 7.4, 3 mM $MgCl_2$, 1.3 mM ATP, 5 mM creatine phosphate, 1 mM DTT, 100 mM KCl, 6%(v/v) glycerol and 0.1 μg/μl yeast tRNA). The reaction mixes were then irradiated at 302 nm using a UV source (UVP) at a distance of 5 cm for 30 min at 4^0C. After irradiation, the samples were digested with 0.2 mg/ml pancreatic RNase A (Sigma) for 20 min at 37^0C. An equal volume of 2X SDS sample buffer was added to each sample. The cross-linked RNA-protein complexes were analysed after separation on a 10% SDS polyacrylamide gel using a phosphorimager.

2.5.7 Preparation of cell lysates from transfected cells

After transfection, the medium was aspirated and the adherent cells were washed twice with phosphate buffered saline (PBS). Cells were lysed by the addition of 800 μl of either 1X Reporter lysis buffer (Promega) or 1X Passive lysis buffer (Promega) and plates were scraped with a "rubber policeman". The lysate was transferred to a tube and the insoluble matter was collected by centrifugation. The supernatant was removed to a fresh tube and either enzyme activity was assayed or the lysate was stored at -70^0C.

2.5.8 Luciferase assays

The activity of Firefly luciferase in lysates prepared from cells transfected with pGL3 or pGL3utr was measured using a luciferase reporter assay system (Promega). Lysates were prepared using 1X Reporter lysis buffer as described in section 2.5.7. 5 μl of lysate was added to 25 μl of luciferase assay reagent and light emission was measured over 1 second using a 1253 luminometer (Bio-Orbit) or over 10 seconds using an OPTOCOMP I luminometer (MGM instruments). The activity of both Firefly and *Renilla* luciferase in cell lysates transfected with dicistronic luciferase plasmids was measured using a Dual-luciferase reporter

assay system (Promega). Cell lysates were prepared using 1X Passive lysis buffer and 5 µl of lysate was used for each assay. Assays were performed according to the manufacturers recommendations except that only 25 µl of each reagent was used. Light emission was measured in the manner described previously.

2.5.9 β-Galactosidase assays

The activity of β-galactosidase in lysates prepared from cells transfected with pcDNA3.1/HisB/lacZ was measured using a Galactolight plus assay system (Tropix). 5 µl of cell lysate was added to 100 µl of Galactolight reagent (1:100 dilution in Galactolight buffer) and incubated at room temperature for 1 hour. After which, 150 µl of Accelerator was added and the reaction was incubated at room temperature for 30 seconds. Enzyme activity was then determined by measuring the light emission from the reaction in a luminometer, as previously described.

2.5.10 Chloramphenicol acetyltransferase (CAT) assays

Lysates were prepared from cells transfected with either pCAT3 (Promega), pRCAT or pRMCAT using 1X Passive lysis buffer and were subsequently heated at 60^0C for 10 min to inactivate endogenous deacetylase activity. Reactions were set up containing 100 µl of cell lysate, 0.15 µCi of [^{14}C]chloramphenicol (0.05 mCi/ml), and 5 µl of n-butyrlCoenzyme A (5 mg/ml) in a final volume of 233 µl. After incubating the samples at 37^0C for 20 hours, the reaction was terminated by the addition of 300 µl of mixed xylenes (Sigma). The samples were mixed thoroughly using a vortex and the inorganic phase was transferred to a fresh tube. Contaminating [^{14}C]chloramphenicol was removed from the solvent by extracting twice with 100 µl of 0.25 M Tris-HCl, pH 8.0. The amount of butyrylated [^{14}C]chloramphenicol in the xylene phase was measured by scintillation counting using Emulisifer-Safe™ scintillant (Packard) in an Tri-Carb 2000CA scintillation counter (Packard). In addition, to confirm the results visually, the samples were subjected to thin layer chromatography (TLC) on a Baker-flex® silica gel TLC plate (Baker Inc.) in a 97:3 mix of chloroform/methanol. After separation, the radioactive products were detected using phosphorimager analysis.

Chapter 3

The role of the c-*myc* 5' untranslated region

3. 1 Introduction

Previous studies have demonstrated that the translational efficiency of c-*myc* mRNAs in rabbit reticulocyte lysate (RRL) and *Xenopus* oocytes is significantly reduced by structural elements within the 5' UTR (Darveau *et al.*, 1985; Parkin *et al.*, 1988). However, in Burkitt's lymphoma cell lines, endogenous c-*myc* mRNAs are translated efficiently, irrespective of the presence or absence of the 5' UTR (Nilsen and Maroney, 1984). In addition, when expressed in established cell lines, the translation of heterologous mRNAs is not impaired by c-*myc* upstream sequences (Butnick *et al.*, 1985; Parkin *et al.*, 1988). These conflicting data could reflect differences in the capacity of these systems to relieve structural inhibition. Alternatively, c-*myc* translation may require non-canonical *trans*-acting factors not present in either *Xenopus* oocytes or RRL (Parkin *et al.*, 1988). Interestingly, in cell lines derived from patients with multiple myeloma, c-*myc* expression is deregulated by a translational mechanism. Moreover, a single point mutation was identified in the 5' UTR of c-*myc* mRNAs isolated from these cell lines (Paulin *et al.*, 1996). These observations prompted a further investigation into the effect of the 5' UTR on the translation of c-*myc* mRNAs.

3.2 The effect of the 5' UTR on a heterologous reporter mRNA expressed in cell lines

A 360 nt segment of the murine c-*myc* 5' UTR did not affect the translational efficiency of a heterologous mRNA when expressed in a variety of cell lines (Parkin *et al.*, 1988). Likewise, the translation of a human c-*myc* mRNA was not influenced by a 502 nt region of the 5' UTR (Butnick *et al.*, 1985). However, in the latter report the mRNA was expressed in a COS system under the control of the powerful RSV promoter/enhancer at levels vastly in excess of the endogenous transcript. It has been suggested that such overexpression may saturate the translational capacity of these cells (Parkin *et al.*, 1988). Consequently, any differences in translational efficiency would not be observed. Accordingly, the effect of the human c-*myc* 5' UTR on the translation of a heterologous mRNA was analysed in various cell lines using the considerably weaker SV40 promoter/enhancer. The strategy for the construction of the

reporter plasmids used to determine the effect of the 5' UTR on translation is shown in figures 3.1 and 3.2.

3.2.1 Construction of pGL3 and pGL3utr

When transfected into cell lines, the plasmid pGL3con (Promega) expresses firefly luciferase under the control of the SV40 promoter/enhancer elements. In order to transform this plasmid into a more powerful tool for the analysis of the effects of 5' UTRs, a small polylinker region was engineered between the promoter and the translation initiation codon. The primers ECLuc5 and ECLuc3 were used to amplify pGL3con by long-PCR (Barnes, 1994) and consequently introduce an EcoRI site at the 5' and 3' ends of this fragment. Digestion of this product with EcoRI followed by self-ligation created the plasmid pGL3E (fig. 3.1). Subsequently, an oligonucleotide cassette containing the EcoRV, SpeI and PvuII sites was blunt-end ligated into pGL3E at the EcoRI site. Thus, the new plasmid, pGL3, has unique HindIII, EcoRV, SpeI, PvuII, EcoRI and NcoI sites in the region immediately upstream of the luciferase coding region (fig. 3.1).

The principle c-myc promoter (P2) has been mapped to a TATA box 437 nt upstream of the AUG initiation codon (Watt et al., 1983; Saito et al., 1983). The 5' end of the P2 mRNA is located between 31 and 43 nt downstream of the TATA box; thus, the predominant 5' UTR is in the range of 406-395 nt long. The small variation in the length of the leader may reflect the difficulty in mapping the transcription initiation site accurately, or the different cell lines used in each study. Furthermore, it is possible that the synthesis of a proportion of mRNAs is initiated downstream of this region indicating that a certain heterogeneity exists at the 5' end of the P2 transcripts (fig. 3.20b).

The DNA sequence encoding the 5' UTR of the P2 mRNA was obtained from the plasmid pSKutr2 (fig. 3.2). This contains 394 bp of authentic 5' UTR sequence immediately followed by an NcoI site at the 3' end. Therefore, the sequence from 1114 to 719 bp in the plasmid pSKutr2 is identical to the endogenous human c-myc 5' UTR sequence, with the exception of a single G to C transition introduced by the NcoI site. PSKutr2 was digested with BamHI and the 3' recessed ends were filled in using Klenow DNA polymerase. Subsequently, a DNA fragment was excised from pSKutr2 by digesting this product with NcoI. After purification, the 403 bp fragment was ligated into pGL3 at the NcoI and PvuII sites, thus creating pGL3utr.
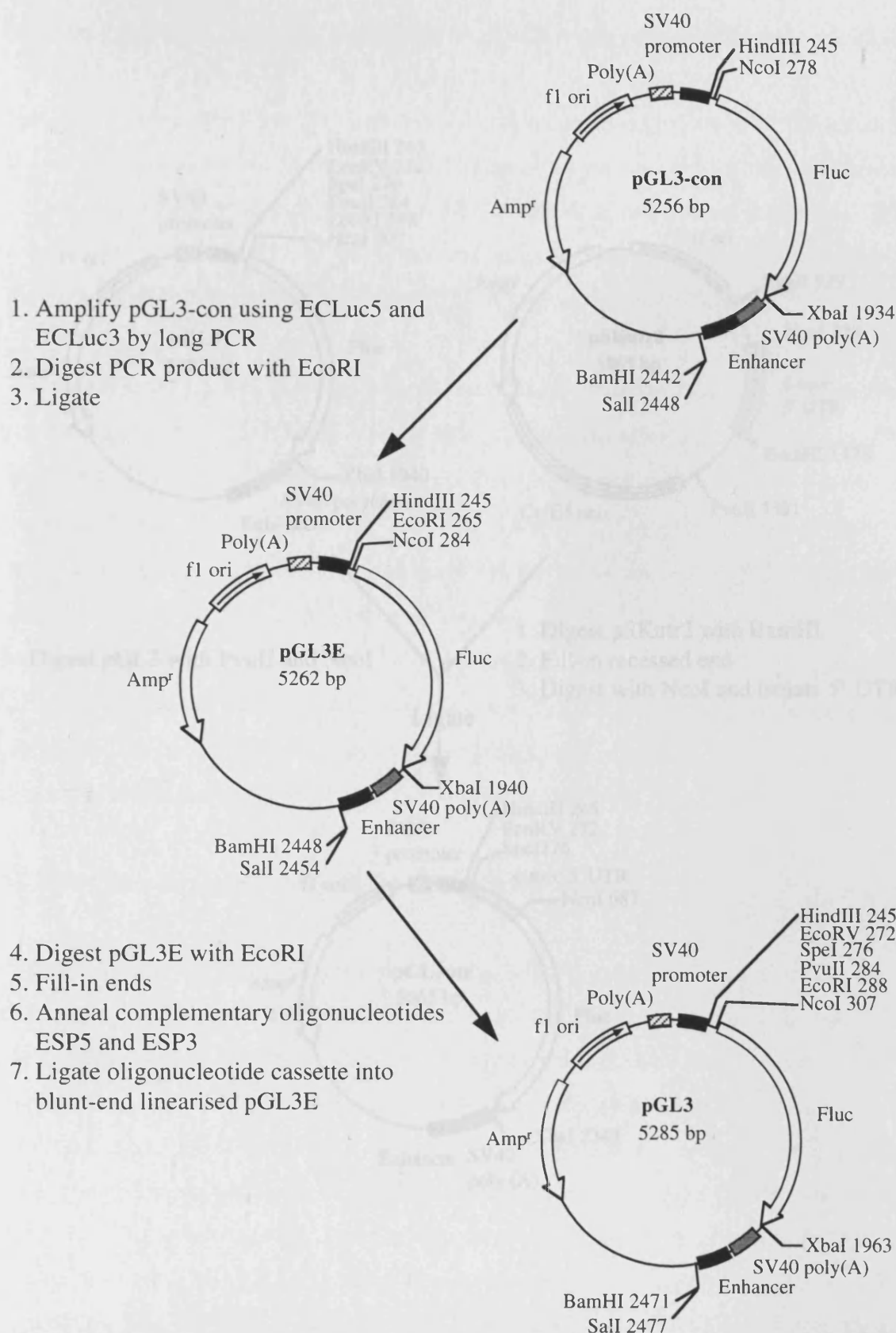
Figure 3.1: Construction of the firefly luciferase reporter plasmid pGL3. A polylinker region containing the recognition sites for *Eco*RV, *Spe*I, *Pvu*II, and *Eco*RI was inserted into the plasmid pGL3con (Promega) between the SV40 promoter and the Fluc open reading frame (see text). The sequences of the oligonucleotides ECLuc5, ECLuc3, ESP5 and ESP3 are detailed in Materials and Methods.

The mRNA transcribed from pGL3utr has a 5' UTR composed of 104 nt of luciferase leader sequence followed by 384 nt of the c-myc 5' noncoding region. While the control plasmid pGL3 contains the transcript with 104 or 426 nt of luciferase leader sequence. Thus, a comparison of luciferase expression synthesized from these reporter mRNAs when transfected into cells allow the effect of the 5' UTR on translational efficiency...

The plasmids pGL3 and pGL3utr were cotransfected with the β-galactosidase expression plasmid pCH110/Med into Hep3B liver carcinoma, HepG2 hepatoma, HK293 embryonic kidney and COS7 monkey kidney cells. Luciferase units compared two days post-transfection and the activities of both luciferase and β-galactosidase enzymes were determined. A different expression was essential for variation in transfection efficiency or translating luciferase to β-galactosidase activity...

Figure 3.2: Construction of the c-*myc* 5' UTR-containing firefly luciferase reporter plasmid pGL3utr. The plasmid pSKutr2 was digested with *Bam*HI and the recessed ends were filled in. Subsequently, a fragment containing the P2 c-*myc* 5' UTR was released by digesting the plasmid with *Nco*I. Finally, this fragment was inserted into pGL3 directly upstream of the firefly luciferase (Fluc) open reading frame between the *Pvu*II and *Nco*I sites.

3.2.2 An analysis of luciferase expression from pGL3 and pGL3utr in various cell lines

The mRNA transcribed from pGL3utr has a 5' UTR composed of 104 nt of luciferase leader sequence followed by 396 nt of the c-*myc* 5' noncoding region. Whilst the control plasmid, pGL3, generates a transcript with only 120 nt of luciferase leader sequence. Thus, a comparison of the amount of luciferase synthesised from these reporter mRNAs when expressed *in vivo* reveals the effect of the 5' UTR on translational efficiency.

The plasmids pGL3 and pGL3utr were co-transfected with the β-galactosidase expression plasmid, pcDNA3.1/HisB/*lacZ*, into HeLa (epithelial), HepG2 (hepatocyte), HK293 (embryonic kidney) and COS7 (epithelial) cells. Cell lysates were prepared two days post-transfection and the activities of both luciferase and β-galactosidase enzymes were determined. Luciferase expression was corrected for variations in transfection efficiency by normalising luciferase to β-galactosidase activity. Figure 3.3 shows a comparison of the average luciferase expression from pGL3 and pGL3utr in the four cell lines. It is clear that luciferase expression was not reduced by the c-*myc* 5' UTR *in vivo* (fig. 3.3; compare –UTR to +UTR). In fact, luciferase expression was enhanced 1.6, 1.3, 1.4, and 1.1-fold by this element in HeLa, HepG2, HK293, and Cos-7 cells, respectively.

3.2.3 Northern analysis of monocistronic luciferase mRNAs

Northern analysis of RNA isolated from HeLa, HK293, and COS7 cells transfected with pGL3 and pGL3utr was performed to determine the size and relative abundance of the transcripts generated from these plasmids. Total RNA was isolated from transfected cells and treated with DNase I to remove plasmid DNA. After fractionation using denaturing agarose gel electrophoresis, the RNA was transferred to a nitrocellulose membrane. A radiolabelled DNA probe, complementary to the luciferase coding region, was used to detect the luciferase transcripts. The representative northern blots shown in figure 3.4 demonstrate that one major species of either 2 kB or 2.4 kB was synthesised in cells transfected with pGL3 or pGL3utr, respectively (fig. 3.4; pGL3 and pGL3utr). Since the predicted length of these transcripts (minus poly[A] tail) is 1923 and 2302 bp, both plasmids expressed mRNAs of the expected size. Furthermore, both mRNAs accumulated to an equivalent level demonstrating that the 5' UTR does not affect either the rate of transcription or the stability of the luciferase mRNA.
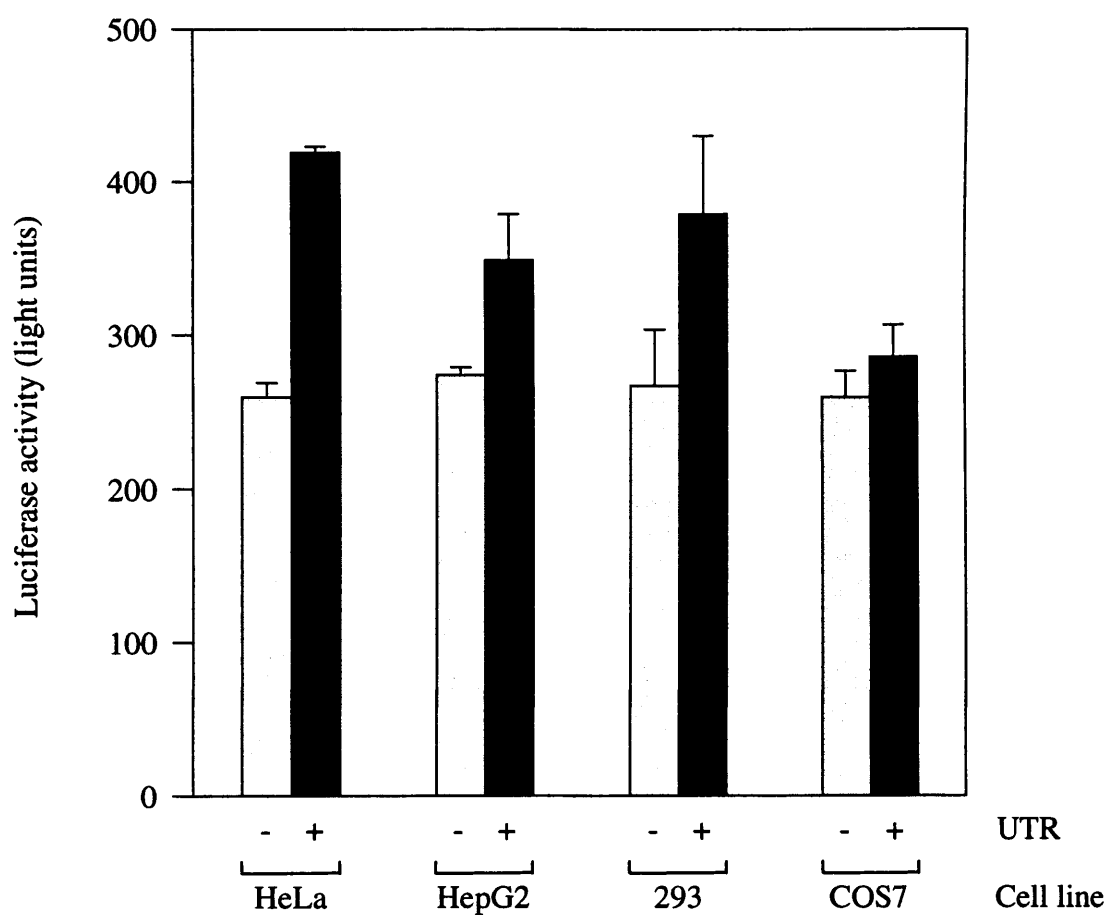
Figure 3.3: The effect of the human c-*myc* P2 5' UTR on luciferase expression. HeLa, HepG2, HK293, and COS7 cells were transfected with pGL3 (-UTR) or pGL3utr (+UTR). Firefly luciferase activity was measured using a luciferase assay system (Promega) and normalised to the transfection control, β-galactosidase.

Two minor species also hybridised to this probe: a species of 3.5 kB that may represent plasmid DNA not digested by DNase I treatment, and a smaller species of approximately 1.3 kB. The latter may arise through aberrant transcriptional or RNA processing events since it can also be isolated using oligo(dT) magnetic beads (see fig. 3.17).

Thus, the expression of approximately equivalent amounts of luciferase from both pGL3 and pGL3utr coupled with the Northern analysis indicated that the 5' UTR from the P2 transcript does not significantly alter the translational efficiency of a heterologous reporter mRNA.

3.3 Dicistronic mRNAs-an analysis of the effect of the c-myc 5' UTR

Secondary structure in the 5' UTR can reduce the rate of protein synthesis by impeding both ribosome binding and ribosome scanning (Kozak, 1989). However, the structured 5' UTRs of the picornavirus RNA genomes promote efficient translation through internal initiation (Jackson et al., 1995). In this mechanism, an internal ribosome entry segment (IRES) located in the upstream leader sequence directs ribosomes to a site at the 3' end of the 5' UTR. The great majority of cellular mRNAs are translated by the cap-dependent mechanism, however it has become clear that a group of mRNAs exist that utilise the alternative mechanism of internal initiation (Iizuka et al., 1995).

The 5' UTR of the human c-myc gene is 67% GC rich and is predicted to have a highly ordered secondary structure (Saito et al., 1983; Nanbru et al., 1997; Stoneley et al., 1998). Furthermore, its nucleotide sequence is well conserved between species. The efficient translation of heterologous mRNAs bearing the c-myc 5' UTR in vivo suggested that this sequence could contain an IRES. Direct evidence of the presence of an IRES is obtained using dicistronic mRNAs. The downstream cistron of a dicistronic mRNA is translated inefficiently, however an IRES promotes efficient translation of the downstream cistron when inserted into the intercistronic region (see chapter 1; fig 1.5). Thus, to test the hypothesis that the c-myc 5' UTR contains an IRES, plasmids were constructed that express dicistronic reporter mRNAs when transfected into cell lines.
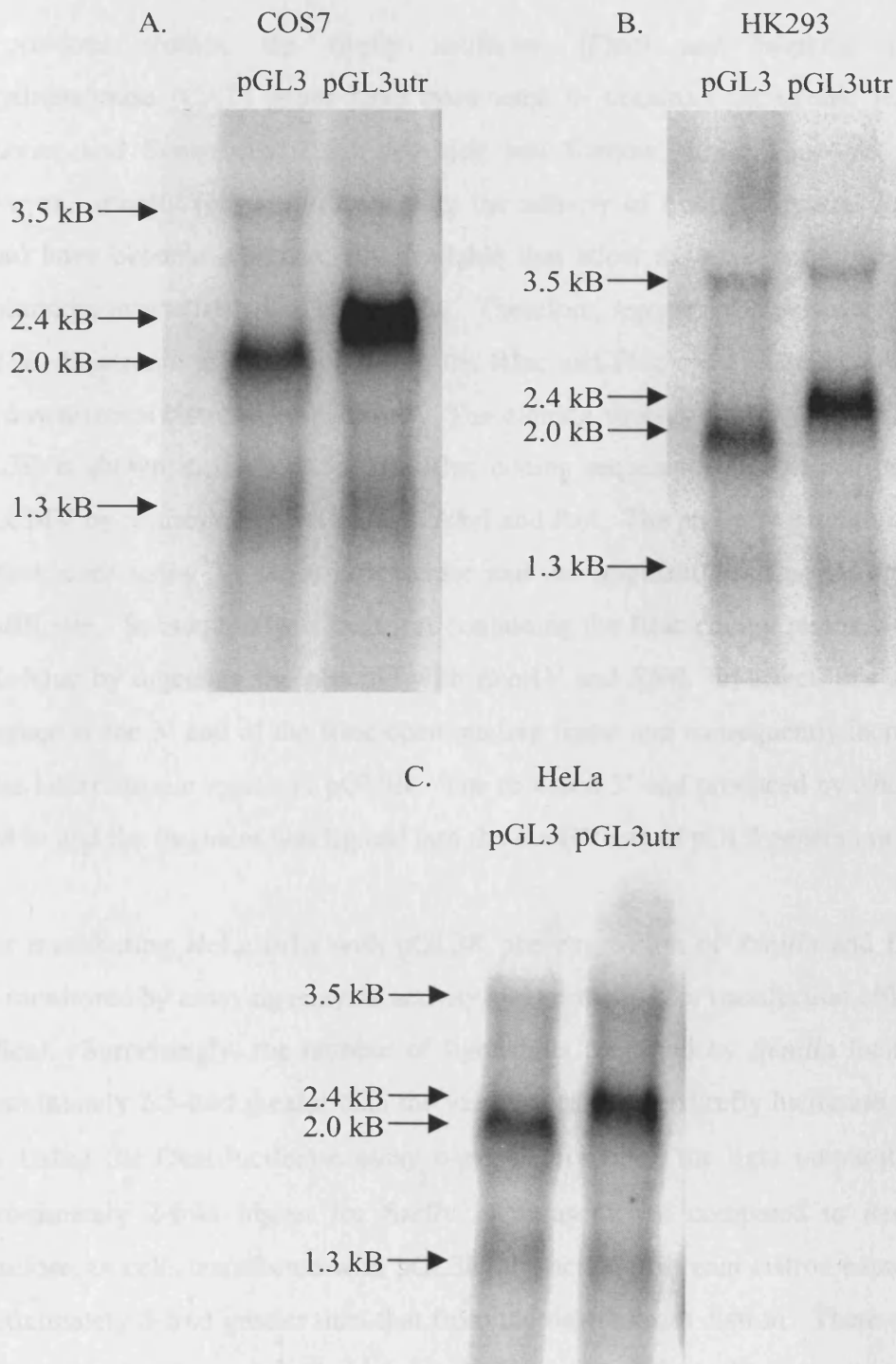
Figure 3.4: Northern analysis of the mRNAs transcribed from pGL3 and pGL3utr. Northern blotting was performed using 10 µg of total RNA isolated from a. COS7, b. HK293, and c. HeLa cells, transfected with pGL3 or pGL3utr. Luciferase transcripts were detected using a randomly-primed radiolabelled firefly luciferase probe (see text). The sizes of complementary species were determined using RNA markers (Gibco-BRL) and are indicated with arrows

3.3.1 Construction of the dicistronic reporter plasmids pGL3R and pGL3Rutr

In previous studies, the firefly luciferase (Fluc) and bacterial chloramphenicol acetyltransferase (CAT) genes have been used to construct dicistronic reporter plasmids (Pelletier and Sonenberg, 1988; Macejak and Sarnow, 1991; Gan and Rhoads, 1996). However, recently reagents for assaying the activity of both firefly and *Renilla* luciferase (Rluc) have become commercially available that allow the expression of both genes to be monitored consecutively in a single tube. Therefore, reporter plasmids were constructed that express dicistronic mRNAs containing the Rluc and Fluc open reading frames, as upstream and downstream cistrons, respectively. The cloning strategy for the assembly of the plasmid pGL3R is shown in figure 3.5. The Rluc coding sequence was obtained from the plasmid pRLCMV by restriction digestion with *Nhe*I and *Pst*I. The protruding termini were converted to blunt ends using T4 DNA polymerase and the fragment was inserted into pSK+ at the *Hind*III site. Subsequently, a fragment containing the Rluc coding region was excised from pSK+Rluc by digesting the plasmid with *Eco*RV and *Xho*I. In effect, this step extends the sequence at the 3' end of the Rluc open reading frame and consequently increases the length of the intercistronic region in pGL3R. The recessed 3' end produced by *Xho*I digestion was filled in and the fragment was ligated into the *Eco*RV site of pGL3 generating pGL3R.

After transfecting HeLa cells with pGL3R, the expression of *Renilla* and firefly luciferase was monitored by assaying enzyme activity and correcting for transfection efficiency (fig. 3.6; -Splice). Surprisingly, the number of light units produced by *Renilla* luciferase was only approximately 2.5-fold greater than the value measured for firefly luciferase (compare RL to FL). Using the Dual-luciferase assay system (Promega), the light output/µg of enzyme is approximately 2-fold higher for firefly luciferase when compared to *Renilla* luciferase. Therefore, in cells transfected with pGL3R, the actual upstream cistron expression was only approximately 5-fold greater than that from the downstream cistron. There are two possible explanations for the apparently high level of expression from the downstream cistron: 1) 20 % of ribosomes were able to reinitiate at the downstream start codon or 2) nuclear processing events resulted in the expression of transcripts truncated at the 5' end. In support of the latter argument, it has been reported that cryptic 5'-donor splice sites may reside in the *Renilla* luciferase gene sequence (Huang and Gorman, 1990). Thus, to prevent the use of these putative splice sites a chimeric intron was inserted upstream of the Rluc coding sequence. A DNA fragment containing the intron was excised from pRLCMV by digesting the plasmid
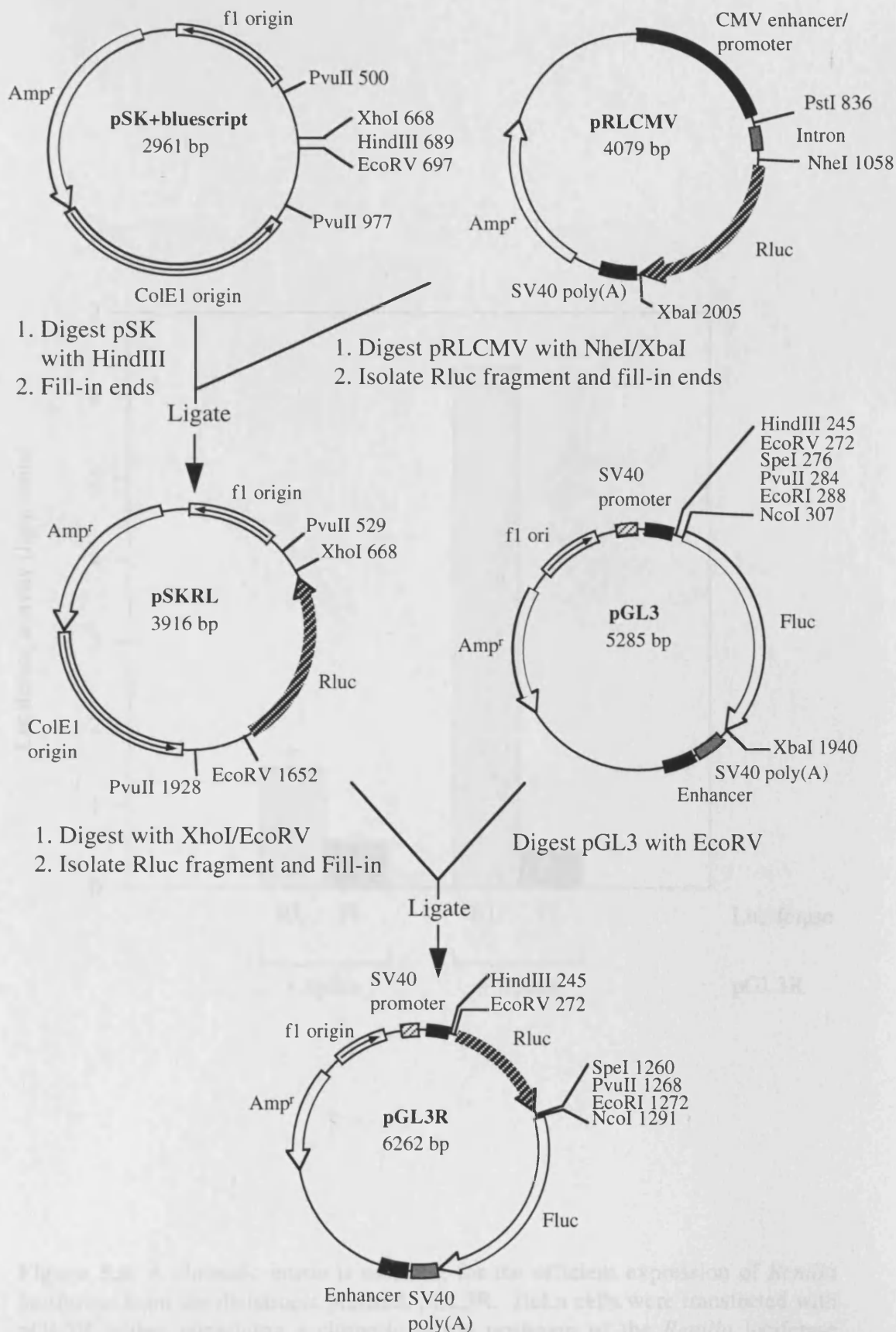
Figure 3.5: Construction of the dicistronic luciferase reporter plasmid pGL3R. The Rluc gene was obtained from the plasmid pRLCMV (Promega) and inserted into pSKbluescript. It was then excised from pSKRL, thus extending the 3' UTR, and inserted into pGL3 upstream of the Fluc open reading frame (see text). PGL3R expresses a dicistronic mRNA containing both Rluc and Fluc cistrons under the control of the SV40 promoter.
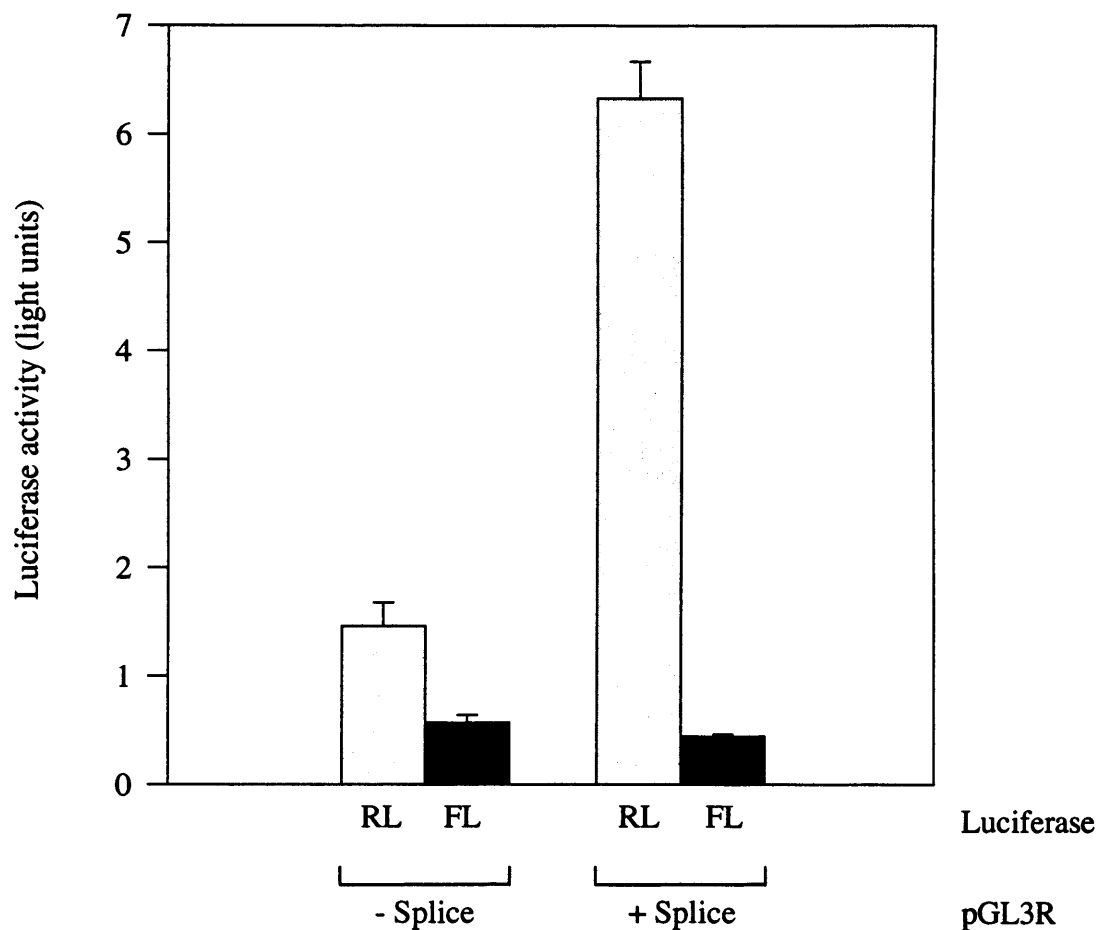
Figure 3.6: A chimeric intron is essential for the efficient expression of *Renilla* luciferase from the dicistronic plasmid, pGL3R. HeLa cells were transfected with pGL3R, either containing a chimeric intron upstream of the *Renilla* luciferase coding region (+Splice), or lacking this sequence (-Splice). *Renilla* luciferase (RL) and firefly luciferase (FL) activity was determined using the Dual-luciferase assay system (Promega).
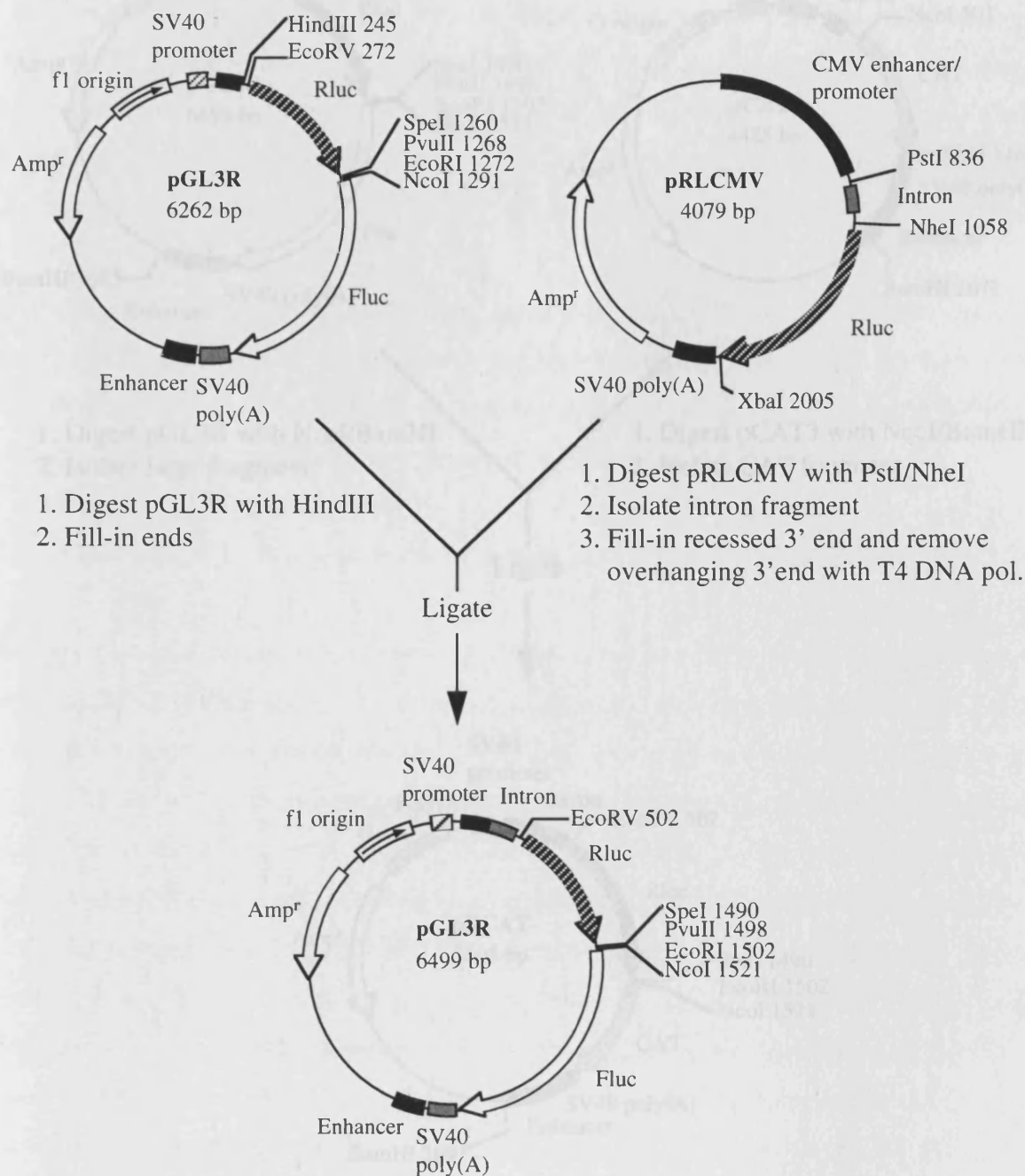
Figure 3.7: Modification of pGL3R by the inclusion of a chimeric intron. A chimeric intron was excised from pRLCMV (Promega) by digesting with *Nhe*I and *Pst*I. After the overhanging ends were converted to blunt termini using T4 DNA polymerase, the fragment was inserted into pGL3R at the *Eco*RV upstream of the Rluc open reading frame.

Figure 3.10: Construction of the dicistronic reporter plasmid pRCAT. The plasmid pGL3R was digested with *Nco*I and *Bam*HI and the larger fragment containing the Rluc cistron was isolated. A fragment containing the CAT open reading frame, the SV40 polyadenylation signal and enhancer was excised from pCAT3 (Promega) by digesting with *Nco*I and *Bam*HI. Ligation of the two fragments created pRCAT. This plasmid expresses an Rluc-CAT mRNA under the control of the SV40 promoter.

with the enzymes *Nhe*I and *Pst*I and was blunt-end ligated into pGL3R at the *Hind*III site (fig. 3.7).

Transfection of the modified pGL3R into HeLa cells revealed that the chimeric intron dramatically increased the expression of *Renilla* luciferase (fig. 3.6; +Splice). The number of light units produced by *Renilla* luciferase was 14.2-fold higher than that produced by firefly luciferase (compare RL to FL). Therefore, the *Renilla* luciferase expression in HeLa cells transfected with pGL3R was approximately 28-fold greater that firefly luciferase expression.

Having constructed the control dicistronic reporter plasmid, pGL3R, the sequence encoding the c-*myc* 5' UTR was inserted between the two cistrons. As described previously, the *Bam*HI/*Nco*I fragment from pSKutr2 was positioned directly upstream of the firefly luciferase coding region at the *Pvu*II/*Nco*I sites, thus creating pGL3Rutr (fig. 3.8).

3.3.2 The c-*myc* 5' UTR stimulates downstream cistron expression in cultured cells

The plasmids pGL3R and pGL3Rutr were co-transfected into HeLa, HepG2 and HK293 cells with pcDNA3.1/HisB/*lacZ*. The level of expression from both the *Renilla* and firefly luciferase cistrons was determined and normalised according to the transfection efficiency. Figure 3.9 shows the average activity of both the upstream and downstream gene products after three separate transfections with pGL3R and pGL3Rutr. In the cells transfected with pGL3R, the *Renilla* luciferase activity was significantly higher than that of firefly luciferase (pGL3R; compare RL to FL). In fact, the number of light units produced by *Renilla* luciferase was 14.39, 37.47, and 41.01-fold greater in HeLa, HepG2, and HK293 cells, respectively. Thus, the downstream cistron of this construct was translated inefficiently in these three cell lines. However, in the cells transfected with pGL3Rutr, expression from the downstream cistron was greatly enhanced (compare pGL3Rutr FL to pGL3R FL). The presence of the 5' UTR-encoding sequence in this construct increased the firefly luciferase activity by 48.77, 51.81, and 23.79-fold in HeLa, HepG2 and HK293 cells, respectively. Thus, the sequence encoding the 5' UTR promotes efficient translation of the downstream cistron when inserted into the intercistronic region of a dicistronic reporter plasmid in these cell lines.
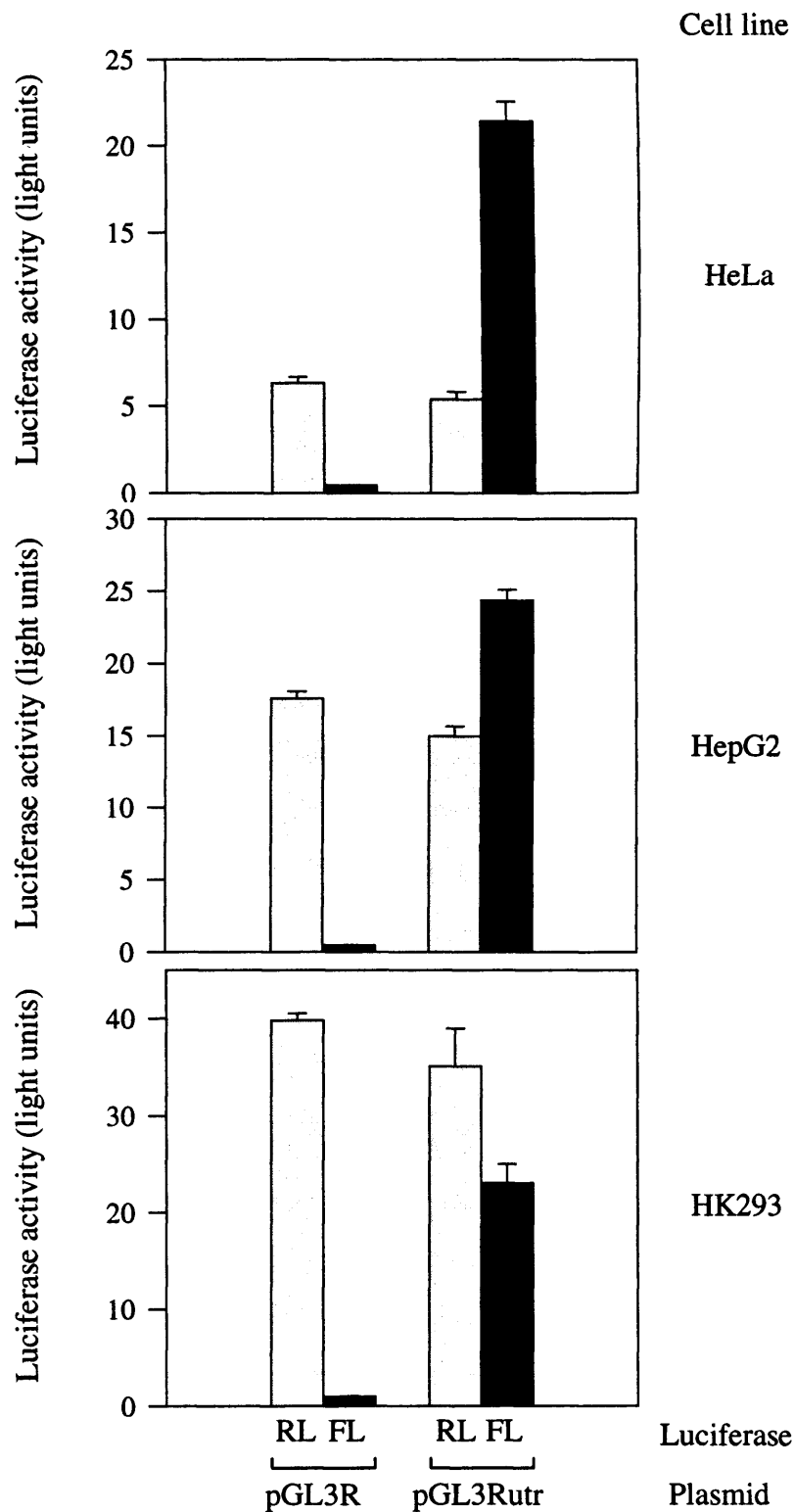
Figure 3.9: The c-*myc* 5' UTR stimulates downstream cistron expression from a dicistronic mRNA in human cell lines. HeLa, HepG2, and HK293 cells were transfected with the control dicistronic plasmid, pGL3R, and the 5' UTR containing plasmid, pGL3Rutr. *Renilla* luciferase (RL) and firefly luciferase (FL) activities were determined as described previously.

It is also noteworthy that expression from the *Renilla* luciferase cistron was decreased in cells transfected with pGL3Rutr by 15, 15, and 12% in HeLa, HepG2 and HK293 cells, respectively (fig. 3.9; compare pGL3Rutr RL to pGL3R RL). Although this decrease is relatively small, it was consistently observed. A similar reduction in the synthesis of the upstream gene product occurs when the eIF4G, BiP and poliovirus IRESes are inserted into the intercistronic region of a dicistronic mRNA (Macejak and Sarnow, 1991; Gan and Rhoads, 1995). This effect is believed to represent a competition between cap-dependent and IRES-directed mechanisms of translation initiation.

3.3.3 The effect of the 5' UTR on an alternative dicistronic reporter mRNA

Since the dicistronic reporter plasmids used in this study were novel, it seemed prudent to ensure that the c-*myc* 5' UTR-encoding sequence could enhance the expression of the downstream cistron using a different dicistronic reporter construct. Accordingly, the firefly luciferase cistron of pGL3R was replaced with the chloramphenicol acetyltransferase (CAT) coding region. Thus, the new plasmid retains the *Renilla* luciferase gene as the upstream cistron, and expression from the downstream cistron can be monitored by measuring CAT activity.

1. Construction of pRCAT and pRMCAT

The construction of pRCAT is detailed in figure 3.10. A DNA fragment of 1170 bp was excised from the plasmid pCAT3 using the restriction enzymes *Nco*I and *Bam*HI and subsequently purified. This sequence contains the CAT coding region, the SV40 late polyadenylation signal and the SV40 enhancer. The corresponding sequence was released from the plasmid pGL3R by digestion with *Nco*I and *Bam*HI and the 4335 bp fragment was purified. Finally, the 1170 bp fragment was ligated to the 4335 bp fragment, thus creating the control dicistronic reporter plasmid, pRCAT.

The sequence encoding the c-*myc* 5' UTR was then inserted between the *Renilla* luciferase and CAT coding regions to produce the plasmid pRMCAT (fig. 3.11). Restriction digestion of pGL3utr with the enzymes *Spe*I and *Nco*I released a DNA fragment containing the 5' UTR-encoding sequence. Following purification, this fragment was inserted into pRCAT between the *Spe*I and *Nco*I restriction sites.
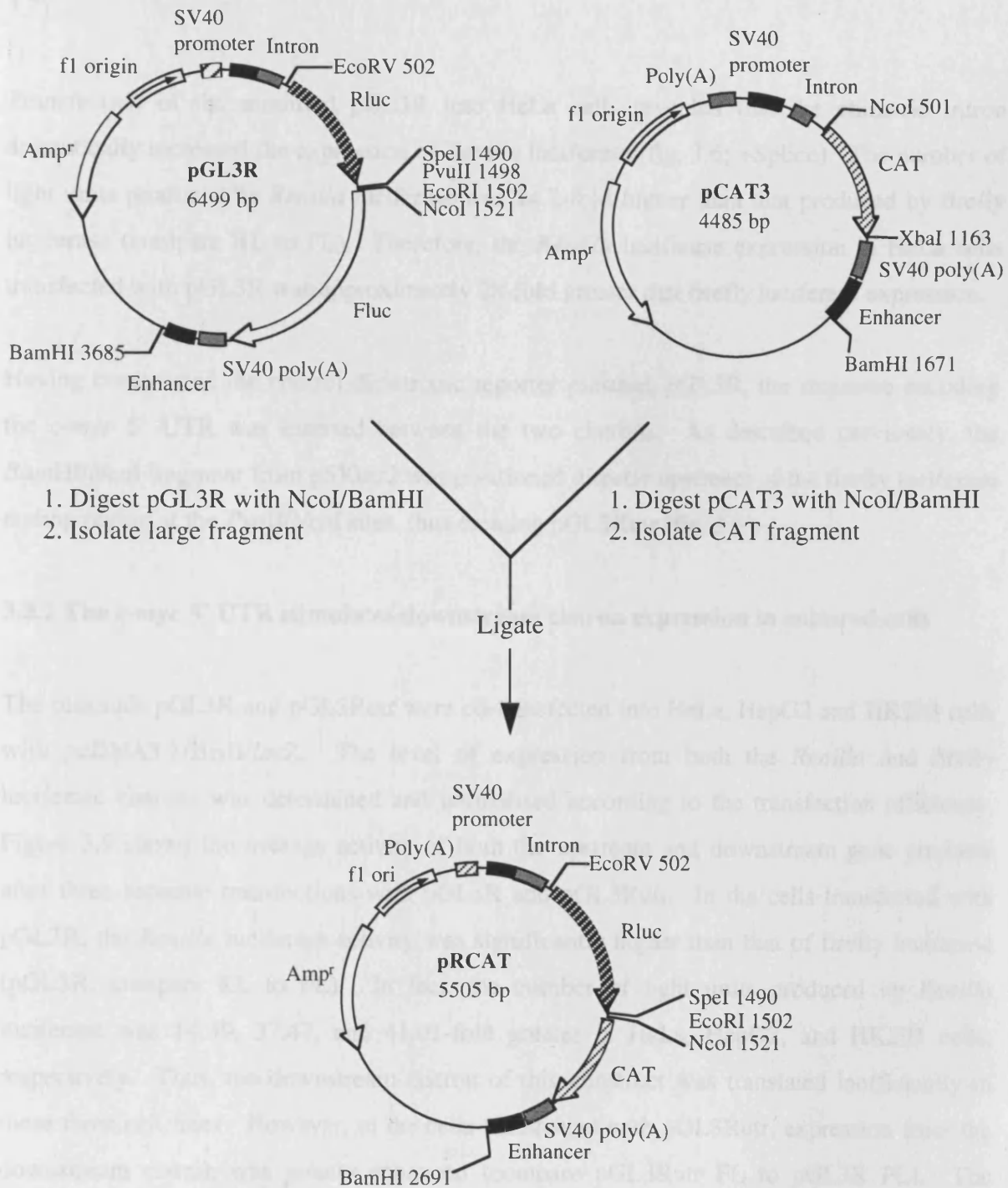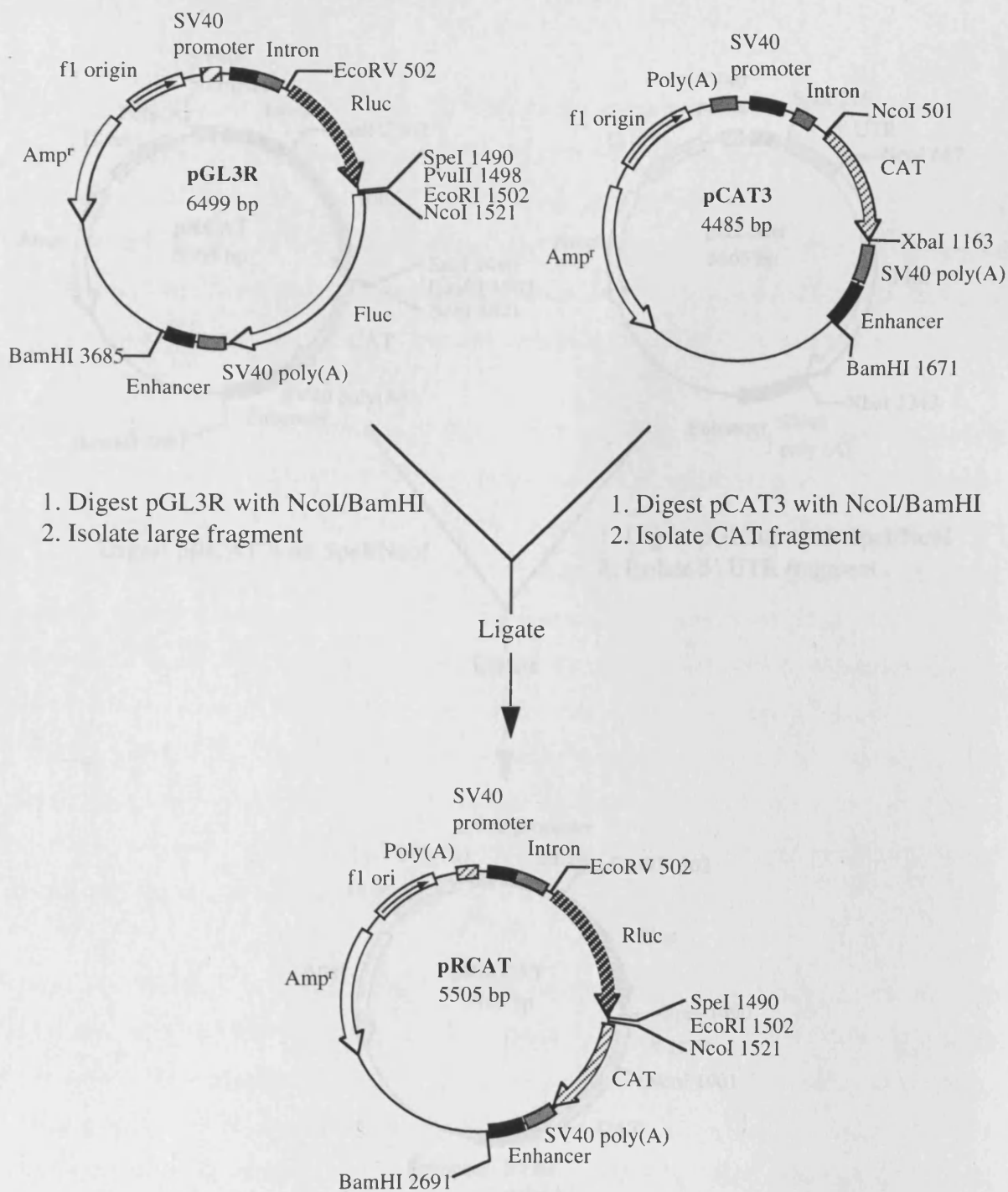
Figure 3.10: Construction of the dicistronic reporter plasmid pRCAT. The plasmid pGL3R was digested with *Nco*I and *Bam*HI and the larger fragment containing the Rluc cistron was isolated. A fragment containing the CAT open reading frame, the SV40 polyadenylation signal and enhancer was excised from pCAT3 (Promega) by digesting with *Nco*I and *Bam*HI. Ligation of the two fragments created pRCAT. This plasmid expresses an Rluc-CAT mRNA under the control of the SV40 promoter.

Figure 3.11: Construction of the c-*myc* 5' UTR-containing dicistronic reporter plasmid pRMCAT. The 5' UTR encoding sequence was excised from pGL3utr by digesting with *Spe*I and *Nco*I. This sequence was inserted into pRCAT between the Rluc and CAT cistrons. PRMCAT expresses an Rluc-CAT dicistronic mRNA with the 5' UTR in the intercistronic region.

2. Analysis of upstream and downstream cistron expression from pRCAT and pRMCAT

In order to determine whether the 5' UTR alters the expression of the reporter cistrons on *Renilla* luciferase-CAT dicistronic mRNAs, the plasmids pRCAT and pRMCAT were co-transfected into HeLa cells with pGL3. Expression from the upstream cistron was measured as before and normalised to firefly luciferase activity. Whilst, the CAT activity in transfected cell lysates was determined by measuring the quantity of butyrylated [^{14}C]-chloramphenicol produced from the enzyme substrates butyrl-Coenzyme A and [^{14}C]-chloramphenicol.

Figure 3.12a(i) shows that insertion of the 5' UTR-encoding sequence between the *Renilla* luciferase and CAT cistrons reduced *Renilla* luciferase expression by 27% (compare pRMCAT to pRCAT). Unfortunately, the level of CAT expressed from the control dicistronic plasmid, pRCAT, was outside the range of detection using liquid scintillation counting. However, this does suggest that reinitiation at the downstream initiation codon is inefficient (fig. 3.12a(ii); pRCAT). Nevertheless, the average number of counts measured in lysates made from pRMCAT-transfected cells was 1383 cpm above background (fig. 3.12a(ii); pRMCAT). Thus, the 5' UTR-encoding sequence enhanced downstream cistron expression when positioned between the *Renilla* luciferase and CAT cistrons. Nonetheless, the relative increase, when compared to the expression due to readthrough-reinitiation on the control mRNA, cannot be determined.

Visual confirmation of the enhanced expression from the downstream cistron in cells transfected with pRMCAT was provided by separating the products of the CAT assays using thin layer chromatography (TLC). This approach allows the butyrylated [^{14}C]-chloramphenicol to be detected using phosphorimager analysis (fig. 3.12b). HeLa cells were transfected with the monocistronic reporter construct, pCAT3, which expresses CAT under the control of the SV40 promoter/enhancer (fig. 3.10). Lysate from these cells was used as a positive control; indicating the distance that the butyrylated [^{14}C]-chloramphenicol migrated after TLC (fig. 3.12b; lane 4). The CAT activity in both mock-transfected HeLa lysate and lysate from cells transfected with pRCAT was almost undetectable and approximately equivalent. This demonstrates that CAT expression resulting from readthrough-reinitiation is indeed very low (fig. 3.12b; lanes 1 and 2). However, the CAT activity in lysates from pRMCAT-transfected cells produced considerably more butyrylated [^{14}C]-chloramphenicol

A.
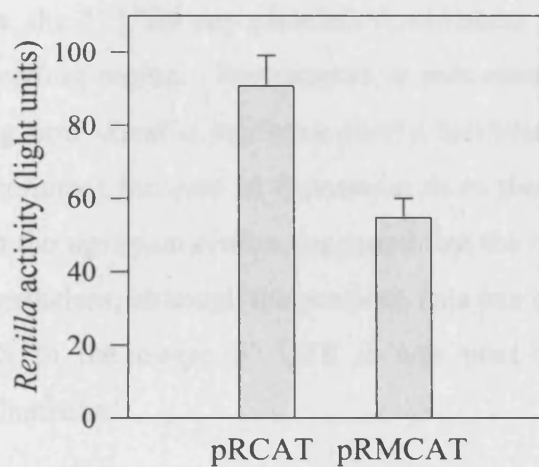
(i) Upstream cistron-*Renilla* luciferase   (ii) Downstream cistron-CAT
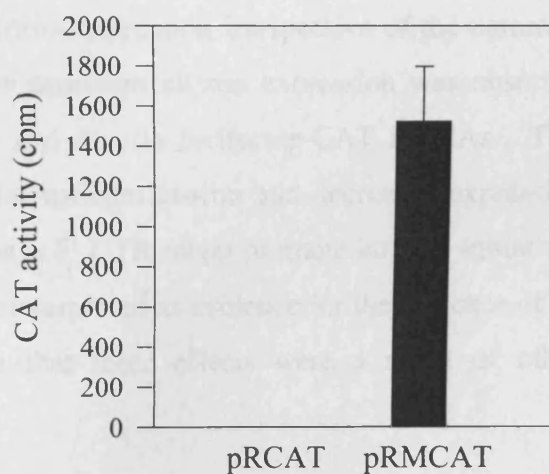
B.
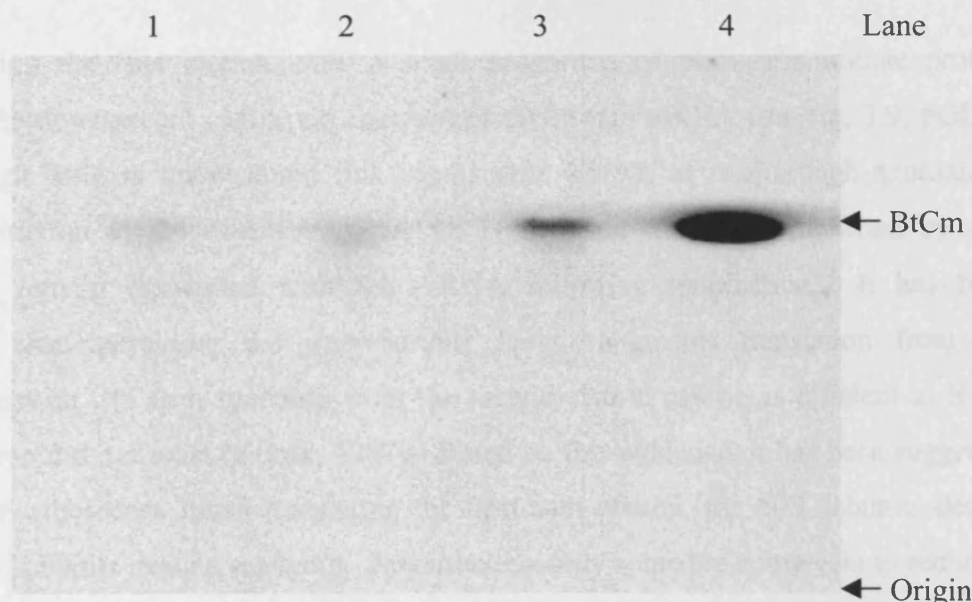
Figure 3.12: The c-*myc* 5' UTR stimulates expression from the downstream cistron on a *Renilla*-CAT dicistronic mRNA. A) HeLa cells were transfected with the plasmids pRCAT and pRMCAT. (i) Upstream cistron activity, *Renilla* luciferase, was measured using the Dual-luciferase assay system. (ii) Downstream cistron activity, CAT, was determined by measuring the production of butyryl-[^{14}C]chloramphenicol after 20 hours using liquid scintillation counting (see Materials and Methods). Both *Renilla* luciferase and CAT activities were normalised to the transfection control, firefly luciferase. (B) Visual conformation of the increased CAT activity in cells transfected with pRMCAT using TLC and phosphorimager analysis. Lane 1, mock transfected HeLa cells, lane 2, pRCAT-transfected cells, lane 3, pRMCAT-transfected cells, and lane 4, pCAT3-transfected cells. The position of butyryl-chloramphenicol (BtCm) is indicated.

(fig. 3.12b; lane 3) supporting the results achieved using liquid scintillation counting. Taken together, these data demonstrate that the presence of the 5' UTR between the *Renilla* luciferase and CAT cistrons results in increased expression from the downstream cistron. Thus, the 5' UTR can stimulate downstream cistron expression irrespective of the nature of the coding region. Furthermore, a reduction in upstream cistron expression was observed using both *Renilla* luciferase-firefly luciferase and *Renilla* luciferase-CAT mRNAs. This concomitant increase in expression from the downstream cistron and decreased expression from the upstream cistron suggested that the c-*myc* 5' UTR might promote internal initiation. Nevertheless, although the previous data can be interpreted as evidence for the presence of an IRES in the c-*myc* 5' UTR it was possible that these effects were a result of other mechanisms.

3.4 Ribosomal readthrough-reinitiation

After translating the first cistron, only a small proportion of ribosomes initiate protein synthesis at the downstream cistron on the control dicistronic mRNA (see fig. 3.9; pGL3R FL). Although little is know about this mechanism, known as readthrough-reinitiation, translation initiation at the downstream cistron is believed to be accomplished by 40S subunits that remain associated with the mRNA following termination. It has been demonstrated that increasing the intercistronic length augments translation from the downstream cistron. In fact, synthesis from the second cistron can be as efficient as if the upstream cistron did not exist (Kozak, 1987). Based on this evidence, it has been suggested that when 80S ribosomes finish translating the upstream cistron, the 60S subunits detach whilst all 40S subunits resume scanning. Nevertheless, only some are competent to reinitiate when they reach the downstream start site (Kozak, 1987). By increasing the intercistronic length, the 40S subunits are more likely to acquire a new ternary complex and consequently reinitiate translation (Kozak, 1987; Grant *et al.*, 1994).

Thus, one potential explanation for the increased synthesis of firefly luciferase from the dicistronic mRNA was that the 5' UTR increased the intercistronic length and consequently stimulated reinitiation at the downstream translation start site. Accordingly, to investigate the effect of the 5' UTR on ribosomal readthrough-reinitiation, an RNA hairpin structure with a calculated free energy of -55 kcal/mol was introduced into the 5' leader sequence of the mRNA transcribed from pGL3Rutr (fig. 3.13b). It has been demonstrated that a secondary

structure motif with a free energy of -50 kcal/mol is sufficient to inhibit the migration of the 40S ribosomal subunit (Kozak, 1989). Therefore, this stem-loop should reduce the rate of translation of the *Renilla* luciferase cistron. However, its effect on expression of the downstream cistron depends on the mechanism by which it is translated. Reinitiation at the downstream initiation codon is dependent on ribosome scanning. Hence, if the 5' UTR stimulates readthrough-reinitiation, the stem-loop motif will reduce expression from the upstream and downstream cistrons by an equivalent amount (fig 3.13a(i)). Alternatively, if the expression of the downstream cistron is due to internal initiation, the translation of the upstream and downstream cistrons are independent and the hairpin will have no effect on firefly luciferase expression (fig. 3. 13a(ii)).

3.4.1 Construction of pGL3RutrH

The plasmid pGL3RutrH was constructed as shown in figure 3.14. An oligonucleotide cassette of 33 bp was ligated into pGL3Rutr at the *Eco*RV site recreating this site at either the 5' or 3' end of the insert. The same oligonucleotide cassette was digested with the restriction enzyme *Pst*I, generating a 25 bp DNA fragment with an overhanging 3' terminus. This sequence was then introduced into the new plasmid between the *Pst*I and *Eco*RV sites. Consequently, the resulting plasmid, pGL3RutrH, has a 60 bp palindromic sequence upstream of the *Renilla* luciferase coding region.

3.4.2 The effect of an RNA hairpin on c-*myc* 5' UTR directed translation

HeLa and HK293 cells were co-transfected with either pGL3Rutr or pGL3RutrH and pcDNA3.1/HisB/*lacZ*. The average expression from the *Renilla* and firefly luciferase cistrons in these transfected cells is shown in figure 3.15. The hairpin structure in the mRNA transcribed from pGL3RutrH reduced *Renilla* luciferase expression by 3.45 and 4.23-fold in HeLa and HK293 cells, respectively (compare utr RL to utrH RL). Thus, the stem-loop was sufficiently stable to impede ribosome scanning. However, the expression of firefly luciferase in cells transfected with pGL3RutrH was comparable to that in cells transfected with pGL3Rutr (89 and 104 %) (compare utrH FL to utr FL). Therefore, the hairpin structure did not reduce the translational efficiency of the downstream cistron despite its ability to inhibit ribosome migration. Since the translation of the downstream cistron was clearly

A(i). Readthrough-re-initiation

+++   +++   Protein synthesis

+   +   Protein synthesis

A(ii). Internal initiation

+++   +++   Protein synthesis

+   +++   Protein synthesis

B. Predicted structure of the RNA hairpin

-55 kcal/mol

Figure 3. 13: Alternative models demonstrating the effect of an upstream hairpin on the expression of the downstream cistron of a dicistronic mRNA. (A(i)) In the readthrough-reinitiation model, the hairpin reduces translation from both upstream and downstream cistrons by an equivalent amount. (A(ii)) In the internal initiation model, the hairpin only reduces upstream cistron expression. The arrows represent the movement of ribosomes. (B) The predicted structure of the hairpin formed by the 60 bp palindromic sequence.

pGL3Rutr

EcoRV 502

SV40 promoter   Intron   Rluc

5' AGATCTGGTACCGAGCTCCCCGGGCTGCAGGAT 3'
3' TCTAGACCATGGCTCGAGGGGCCCGACGTCCTA 5'

Oligonucleotide cassette

1. Anneal oligonucleotides loop1 and loop2
2. Digest pGL3Rutr with EcoRV
3. Ligate oligonucleotide cassette and pGL3Rutr

PstI 531   EcoRV 535

SV40 promoter   Intron   oligo cassette   Rluc

5' AGATCTGGTACCGAGCTCCCCGGGCTGCA 3'
3' TCTAGACCATGGCTCGAGGGGCCCG 5'

Digested oligonucleotide cassette

1. Digest oligonucleotide cassette with PstI
2. Digest pGL3Rutr with EcoRV and PstI
3. Ligate oligonucleotide cassette and plasmid

PstI 531

SV40 promoter   Intron   60 bp palindrome   Rluc

Figure 3.14: Construction of the hairpin-containing dicistronic plasmid pGL3RutrH. An oligonucleotide cassette constructed from the oligonucleotides, loop1 and loop2, was inserted into pGL3Rutr upstream of the Rluc cistron at the *Eco*RV site. The same oligonucleotide cassette was digested with *Pst*I and inserted into the new plasmid between the *Pst*I and *Eco*RV sites. The resulting plasmid, pGL3RutrH, contains a 60 bp palidromic sequence upstream of the Rluc cistron.

Figure 3.15: The effect of an upstream RNA hairpin (-55 kcal/mol) on the expression of the upstream and downstream cistrons of a 5' UTR-containing dicistronic mRNA. HeLa and HK293 cells were transfected with the plasmids, pGL3Rutr (utr), and pGL3RutrH (utrH). The activity of *Renilla* luciferase (RL) and firefly luciferase (FL) was determined as described previously and normalised to that of β-galactosidase.

independent of the upstream cistron, the 5' UTR of c-*myc* does not contain an element capable of enhancing ribosomal readthrough-reinitiation.

3.5 Analysis of the mRNAs expressed by the dual-luciferase dicistronic plasmids

It was possible that the enhanced expression of the downstream cistron and its independent translation were due to the fragmentation of the dicistronic mRNAs. Figure 3.16 illustrates the potential mechanisms that could result in the production of functional monocistronic firefly luciferase mRNAs. A cryptic promoter in the 5' UTR could direct the transcription of truncated mRNAs encoding firefly luciferase (fig. 3.16a). Alternatively, the 5' UTR could contain a cryptic 3' acceptor splice site which together with a 5' donor splice site upstream of the *Renilla* luciferase coding region would remove the upstream cistron from the mature mRNA (fig. 3.16b). Finally, the insertion of the 5' UTR could introduce a specific RNA cleavage site into the sequence between the two cistrons (fig. 3.16c). This is the least likely mechanism as the resulting mRNA would be uncapped and therefore translated inefficiently.

3.5.1 Northern analysis of dicistronic luciferase mRNAs

In preliminary experiments, Northern analysis was performed on total cellular RNA isolated from HeLa cells transfected with pGL3R and pGL3Rutr. A region of the firefly luciferase coding sequence was used to generate a radiolabelled DNA probe and detect the dicistronic mRNAs. However, this probe failed to identify any complementary transcripts, either in mock-transfected cells or in cells transfected with the dicistronic plasmids. Since the same probe hybridised to the monocistronic mRNAs transcribed from pGL3 and pGL3utr (fig. 3.4), it was assumed that the dicistronic mRNAs accumulate to a considerably lower level. Indeed, the firefly luciferase activity produced by the dicistronic constructs is approximately an order of magnitude lower than the expression from the monocistronic plasmids. Accordingly, HeLa and HK293 c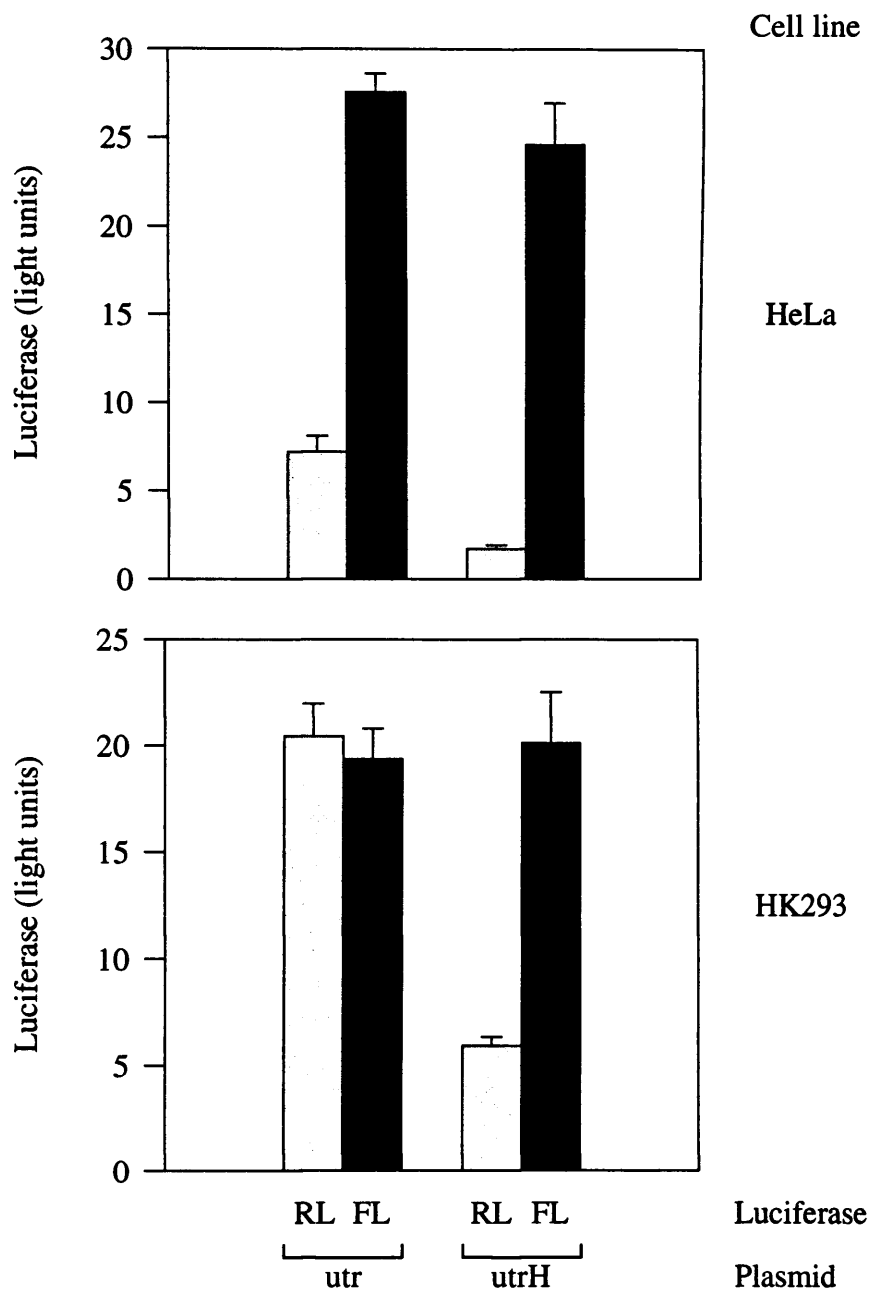ells were transfected with pGL3R and pGL3Rutr and Northern analysis was performed on polyadenylated mRNA purified from 50 µg of total RNA. The probe hybridised to species of approximately 3.1 kB or 3.5 kB in the RNA from cells transfected with pGL3R or pGL3Rutr, respectively (fig. 3.17a and b; lanes 3 and 4). Since the predicted sizes of the dicistronic transcripts (minus poly[A] tail) are 3 and 3.4 kB, the predominant mRNAs synthesised from both plasmids were of the correct size. In addition, all four constructs expressed a smaller mRNA of approximately 1.3 kB that may represent an aberrantly processed luciferase transcript. However, more importantly the construct

A. Transcriptional mechanism

Cryptic promoter

Rluc cistron

Fluc cistron

pGL3Rutr

5' UTR

A_n

m^7G

Fluc mRNA

A_n

B. Splicing mechanism

Intron

5' donor splice site

3' acceptor splice site

Rluc cistron

Fluc cistron

m^7G

5' UTR

A_n

Renilla-firefly pre-mRNA

m^7G

A_n

Fluc mRNA

C. RNA cleavage mechanism

RNA cleavage

Rluc cistron

Fluc cistron

m^7G

5' UTR

A_n

Renilla-firefly mRNA

A_n

Fluc mRNA
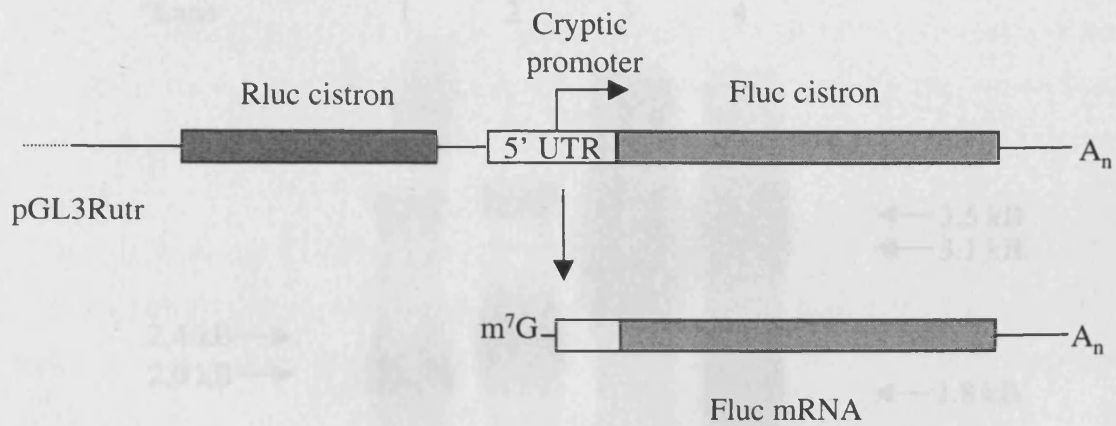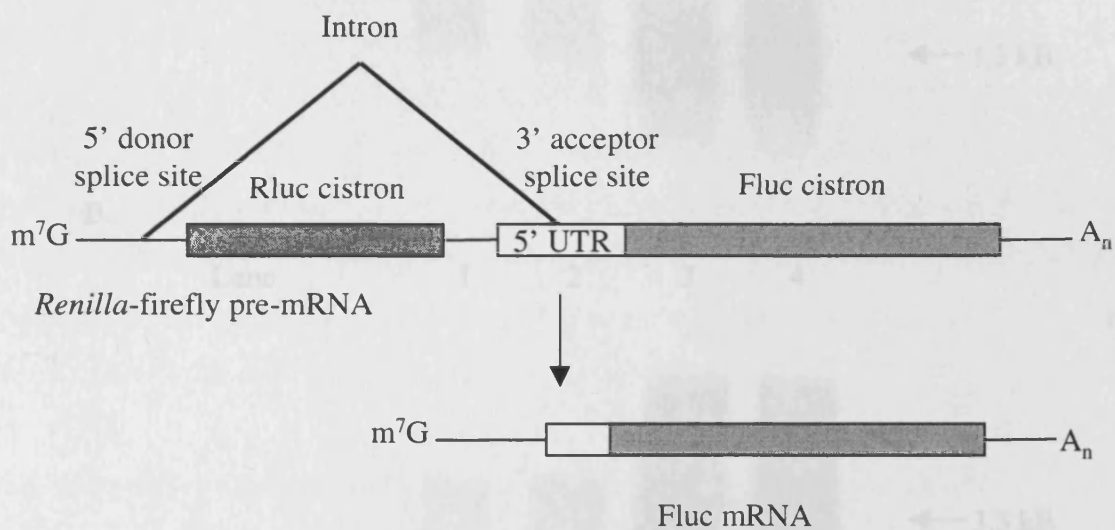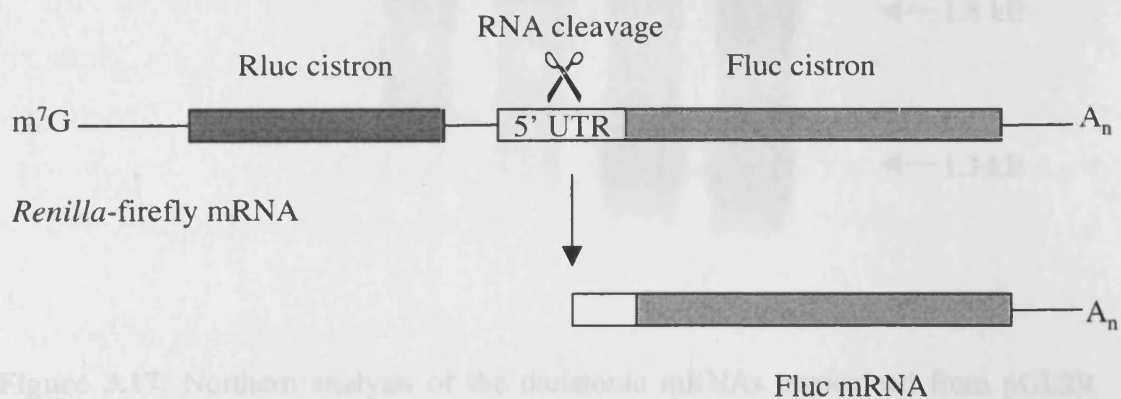
Figure 3.16: Potential mechanisms that could result in the production of functional monocistronic firefly luciferase transcripts. (A) A cryptic promoter is present in the 5' UTR. (B) An intron is formed from the 5' donor splice site in the leader sequence and a 3' acceptor splice site in the 5' UTR. (C) The dicistronic mRNA is cleaved at a specific site in the 5' UTR.

A.

Lane   1   2   3   4

←3.5 kB
←3.1 kB

2.4 kB→
2.0 kB→

←1.8 kB

←1.3 kB

B.

Lane   1   2   3   4

←3.5 kB
←3.1 kB

2.4 kB→
2.0 kB→

←1.8 kB
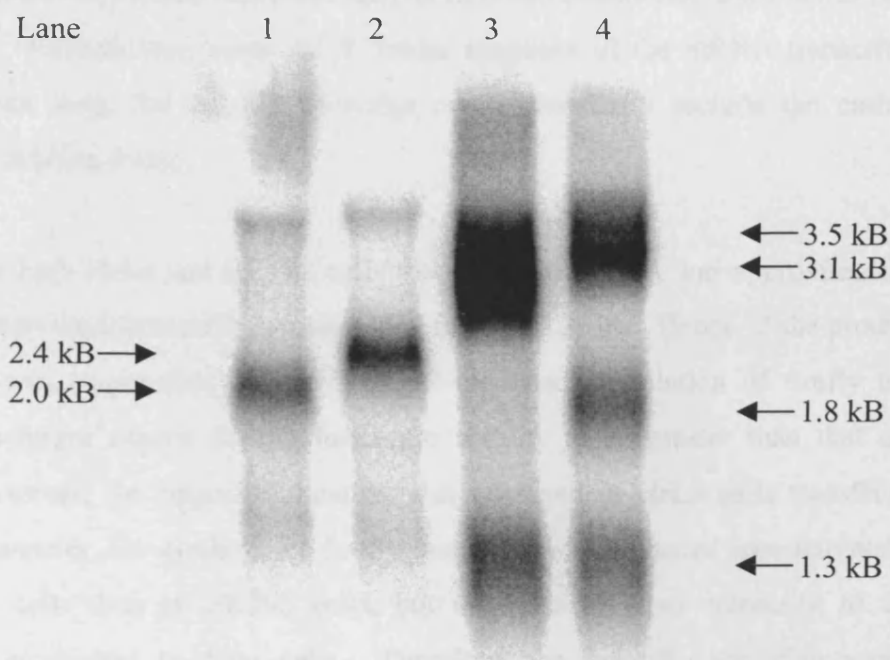
←1.3 kB
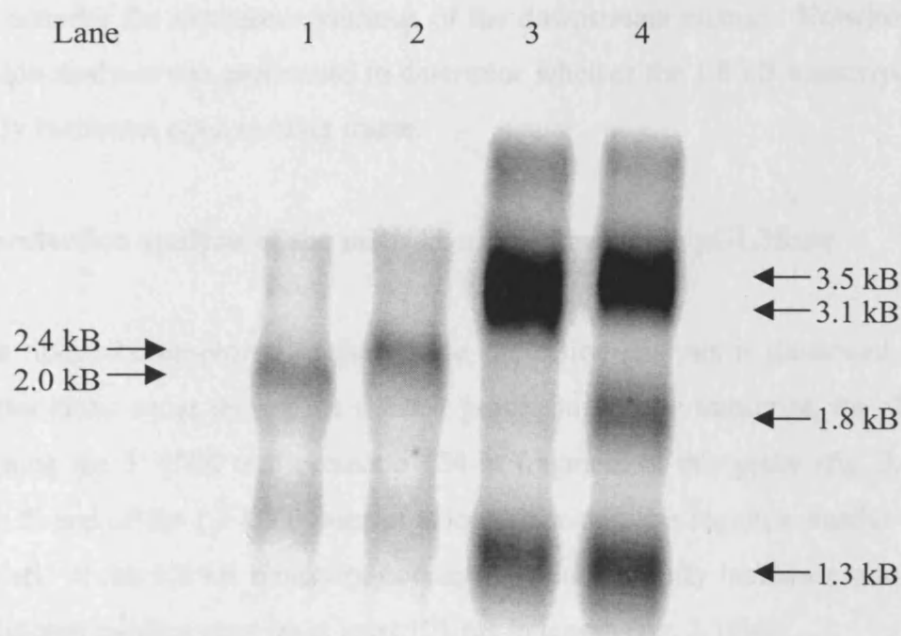
Figure 3.17: Northern analysis of the dicistonic mRNAs transcribed from pGL3R and pGL3Rutr. RNA was isolated from (a) HK293 and (b) HeLa cells transfected with pGL3 (lane1), pGL3utr (lane 2), pGL3R (lane 3) and pGL3Rutr (lane 4). 10 μg of total RNA (pGL3 and pGL3utr) or poly[A]$^+$ RNA isolated from 50μg of total RNA (pGL3R and pGL3Rutr) was subjected to denaturing agarose gel electrophoresis. Northern blots were probed with a randomly-primed radiolabelled probe generated from a 1058 bp firefly luciferase DNA fragment.

pGL3Rutr also expressed an mRNA of approximately 1.8 kB. This transcript is marginally smaller than the monocistronic luciferase mRNA (2.0 kB) transcribed from pGL3 (fig. 3.17a and b; lane 1). Nevertheless, since the 5' leader sequence of the mRNA transcribed from pGL3 is 120 nts long, the 1.8 kB transcript could potentially include the entire firefly luciferase open reading frame.

Interestingly, in both HeLa and HK293 cells the truncated mRNA was approximately 4-fold less abundant than the intact mRNA transcribed from pGL3Rutr. Hence, if the production of this transcript was responsible for the 5' UTR-mediated stimulation of firefly luciferase expression, we might expect *Renilla* luciferase activity to be greater than that of firefly luciferase. However, the opposite situation was observed in HeLa cells transfected with pGL3Rutr. Moreover, the synthesis of firefly luciferase was enhanced approximately 2-fold more in HeLa cells than in HK293 cells, but the ratio of intact transcript to truncated transcript was equivalent in these cells. Therefore, the lack of correlation between the abundance of this transcript and the expression of firefly luciferase implied that its production is unlikely to underlie the increased synthesis of the downstream cistron. Notwithstanding, RNase protection analysis was performed to determine whether the 1.8 kB transcript encodes the entire firefly luciferase open reading frame.

3.5.2 RNase protection analysis of the mRNAs transcribed from pGL3Rutr

The anti-sense riboprobe employed in the RNase protection analysis is illustrated in figure 3.18. If no alterations occur during the nuclear processing of the transcript, the dicistronic mRNA containing the 5' UTR will protect a 624 nt fragment of this probe (fig. 3.19a). In addition, if the 5' end of the 1.8 kB transcript is located within this region a smaller fragment will be protected. If the 1.8 kB transcript contains the entire firefly luciferase open reading frame this additional product must be at least 101 nts in length (fig. 3.19b).

1. Construction of pSKRNase

A DNA fragment of 624 nt, spanning the region from the 3' end of the *Renilla* luciferase cistron to the 5' end of the firefly luciferase cistron, was amplified from the plasmid pGL3Rutr using a polymerase chain reaction (fig. 3.19). The 3'-5' exonuclease activity of the Klenow fragment of *E. coli* DNA polymerase I was used to remove the single unpaired

A.
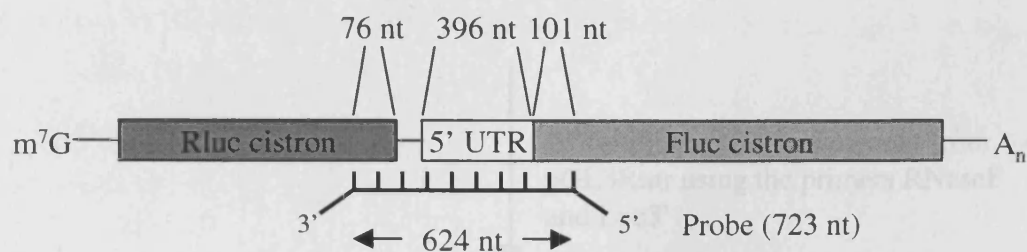
B.
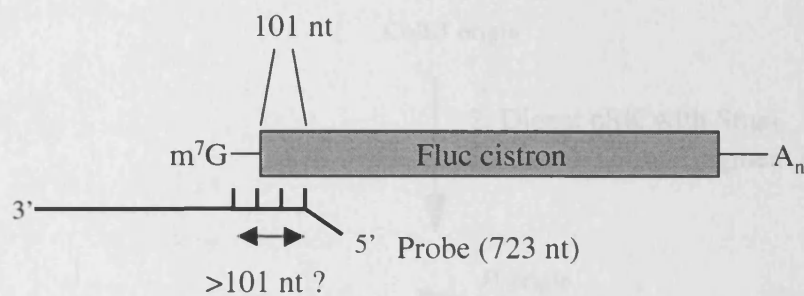
Figure 3.18: Diagrammatic representation of the 723 nt antisense RNA probe hybridised to the mRNAs transcribed from pGL3Rutr. (A) Hybridisation to the full length dicistronic transcript would result in a 624 nt product after RNase protection. (B) If the 1.8 kB firefly luciferase transcript contains the entire coding region a product of at least 101 nt will be detected after RNase protection.
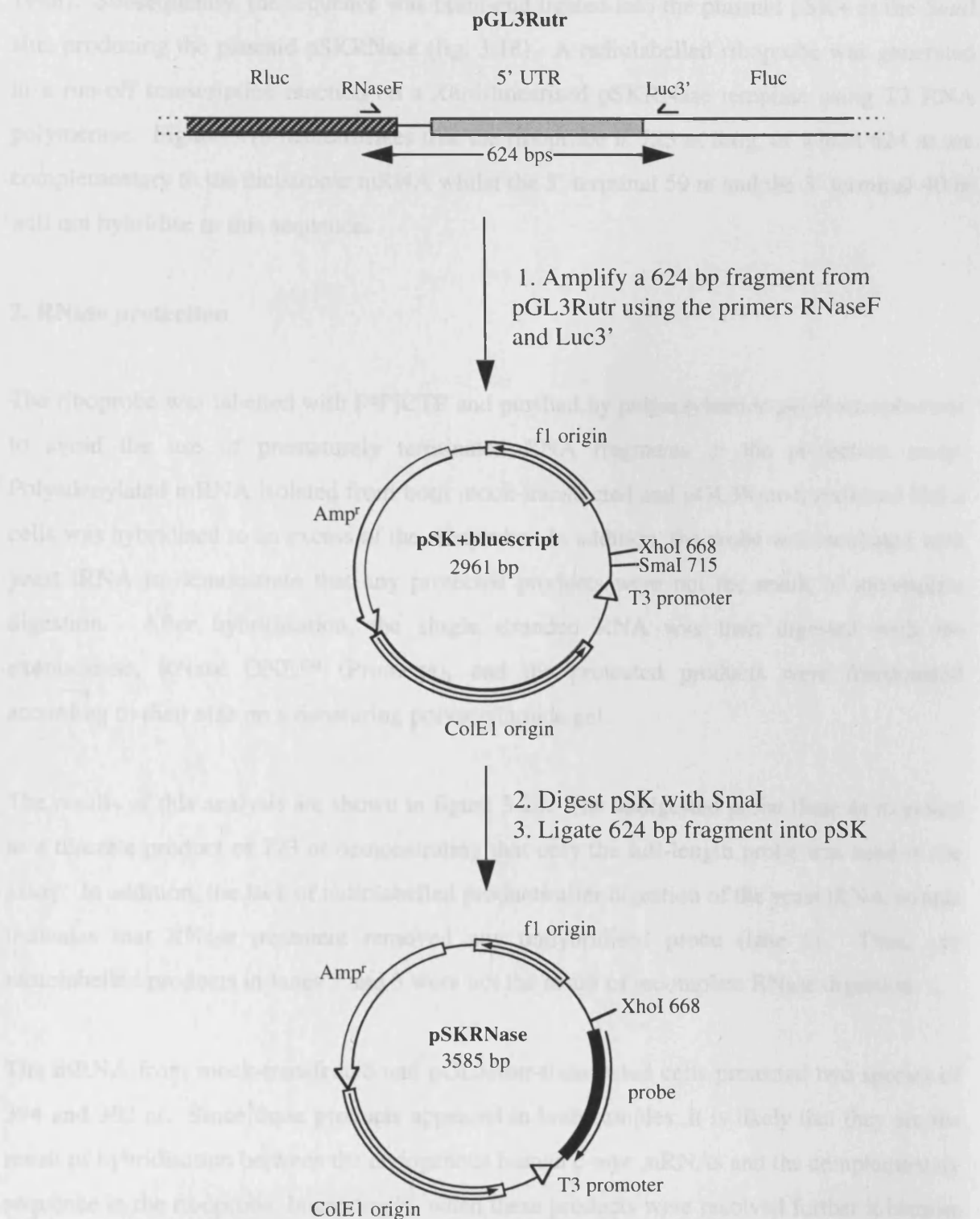
Figure 3.19: Construction of the plasmid pSKRNase. A 624 bp fragment was amplified from pGL3Rutr using the primers RNaseF and Luc3' (see Materials and Methods). The fragment was inserted into pSK+bluescript at the *Sma*I site creating pSKRNase. An antisense riboprobe was synthesised *in vitro* from the T3 promoter using *Xho*I-digested pSKRNase as a template.

nucleotide, added by *Taq* DNA polymerase, at the 3' termini of these fragments (Clarke, 1988). Subsequently, the sequence was blunt-end ligated into the plasmid pSK+ at the *Sma*I site, producing the plasmid pSKRNase (fig. 3.18). A radiolabelled riboprobe was generated in a run-off transcription reaction on a *Xho*I-linearised pSKRNase template using T3 RNA polymerase. Figure 3.18 demonstrates that the riboprobe is 723 nt long, of which 624 nt are complementary to the dicistronic mRNA whilst the 5' terminal 59 nt and the 3' terminal 40 nt will not hybridise to this sequence.

2. RNase protection

The riboprobe was labelled with [^{32}P]CTP and purified by polyacrylamide gel electrophoresis to avoid the use of prematurely terminated RNA fragments in the protection assay. Polyadenylated mRNA isolated from both mock-transfected and pGL3Rutr-transfected HeLa cells was hybridised to an excess of the riboprobe. In addition, the probe was incubated with yeast tRNA to demonstrate that any protected products were not the result of incomplete digestion. After hybridisation, the single stranded RNA was then digested with the exonuclease, RNase ONE™ (Promega), and the protected products were fractionated according to their size on a denaturing polyacrylamide gel.

The results of this analysis are shown in figure 3.20. The undigested probe (lane 4) migrated as a discrete product of 723 nt demonstrating that only the full-length probe was used in the assay. In addition, the lack of radiolabelled products after digestion of the yeast tRNA sample indicates that RNase treatment removed any unhybridised probe (lane 1). Thus, any radiolabelled products in lanes 2 and 3 were not the result of incomplete RNase digestion.

The mRNA from mock-transfected and pGL3Rutr-transfected cells protected two species of 394 and 362 nt. Since these products appeared in both samples, it is likely that they are the result of hybridisation between the endogenous human c-*myc* mRNAs and the complementary sequence in the riboprobe. Interestingly, when these products were resolved further it became clear that endogenous c-*myc* mRNAs protect three fragments of the riboprobe (fig. 3.20b). These data suggest that in addition to the previously defined transcription start sites there are minor initiation sites downstream of this site.
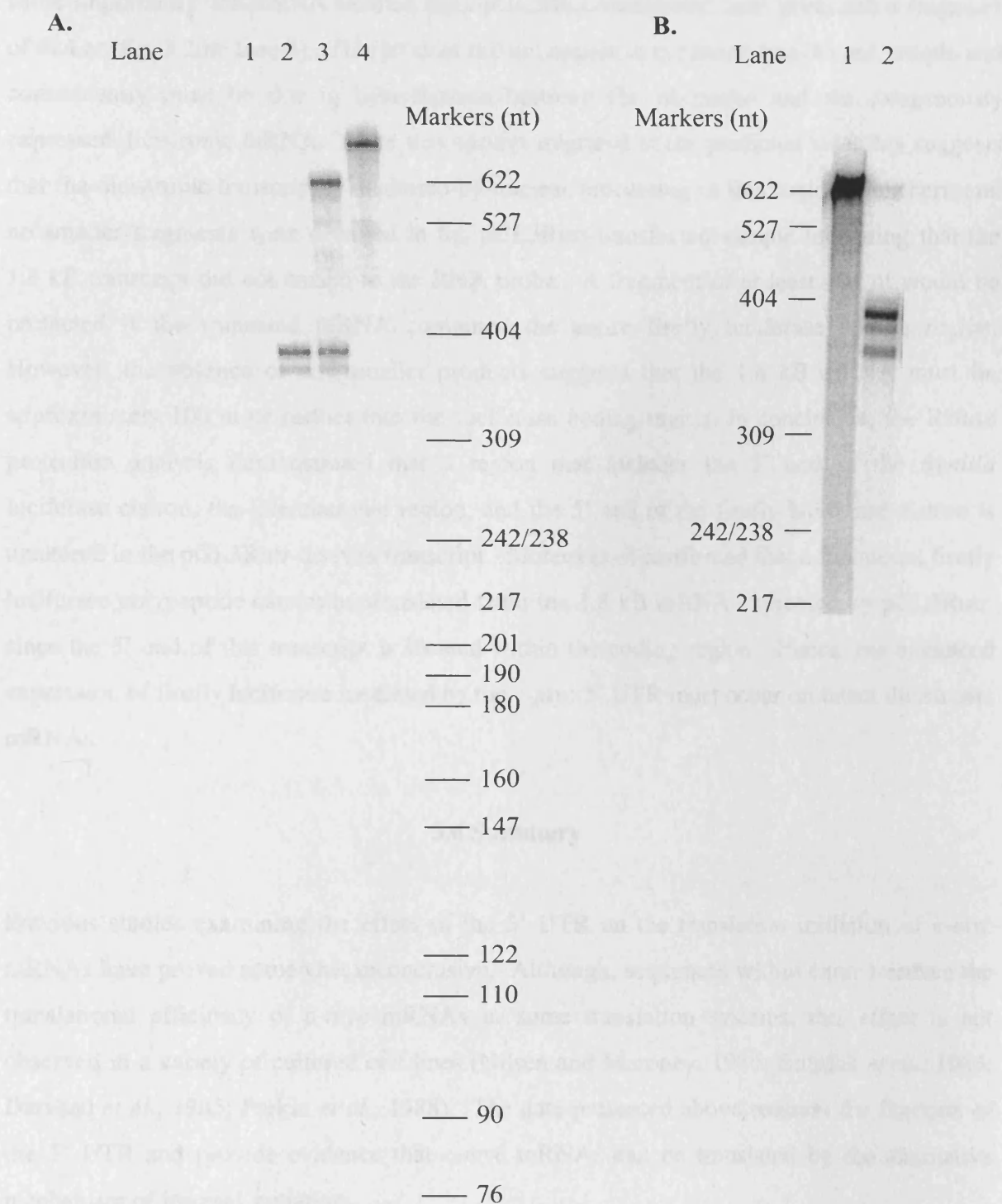
Figure 3.20: RNase protection analysis of the mRNAs transcribed from pGL3Rutr. (A) A 723 nt radiolabelled antisense riboprobe (lane 4) was hybridised with 10 μg of yeast tRNA (lane 1), poly[A]+ RNA isolated from mock-transfected HeLa cells (lane 2), and poly[A] + RNA isolated from pGL3Rutr-transfected HeLa cells (lane 3). After RNase treatment with RNase ONE™ (Promega), protected fragments were subjected to denaturing polyacrylamide gel electrophoresis and detected by phosphorimager analysis. Fragment sizes were determined using radiolabelled pBR322 HpaI fragments. (B) 10μg of total RNA isolated from HeLa cells was hybridised to a 624 nt riboprobe. Protected species were detected as described above. Lane 1, undigested probe and lane2, HeLa RNA.

More importantly, the mRNA isolated from pGL3Rutr-transfected cells protected a fragment of 624 nt (fig. 3.20a; lane 4). This product did not appear in the mock-transfected sample and consequently must be due to hybridisation between the riboprobe and the exogenously expressed dicistronic mRNA. Since this species migrated at the predicted size, this suggests that the dicistronic transcript is unaltered by nuclear processing in this region. Furthermore, no smaller fragments were detected in the pGL3Rutr-transfected sample indicating that the 1.8 kB transcript did not anneal to the RNA probe. A fragment of at least 101 nt would be protected if the truncated mRNA contained the entire firefly luciferase coding region. However, the absence of any smaller products suggests that the 1.8 kB mRNA must lie approximately 100 nt or further into the luciferase coding region. In conclusion, the RNase protection analysis demonstrated that a region that includes the 3' end of the *Renilla* luciferase cistron, the intercistronic region, and the 5' end of the firefly luciferase cistron is unaltered in the pGL3Rutr-derived transcript. Moreover, it confirmed that a functional firefly luciferase polypeptide cannot be translated from the 1.8 kB mRNA expressed by pGL3Rutr, since the 5' end of this transcript is located within the coding region. Hence, the enhanced expression of firefly luciferase mediated by the c-*myc* 5' UTR must occur on intact dicistronic mRNAs.

3.6 Summary

Previous studies examining the effect of the 5' UTR on the translation initiation of c-*myc* mRNAs have proved somewhat inconclusive. Although, sequences within exon 1 reduce the translational efficiency of c-*myc* mRNAs in some translation systems, this effect is not observed in a variety of cultured cell lines (Nilsen and Maroney, 1984; Butnick *et al.*, 1985; Darveau *et al.*, 1985; Parkin *et al.*, 1988). The data presented above reassess the function of the 5' UTR and provide evidence that c-*myc* mRNAs can be translated by the alternative mechanism of internal initiation.

3.6.1 The c-*myc* 5' UTR does not reduce the translational efficiency of a heterologous mRNA

The 5' UTR of the predominant c-*myc* mRNA did not reduce the translational efficiency of a heterologous reporter mRNA expressed in four cell lines of different origins (fig. 3.3). In fact, in HeLa cells the synthesis of luciferase was stimulated to a small extent by the 5' UTR.

Furthermore, Northern analysis demonstrated that this element had little effect on the steady-state levels of these heterologous mRNAs (fig. 3.4). Thus, the secondary structure motifs within the c-*myc* 5' UTR that inhibit translation initiation in RRL and *Xenopus* oocytes do not repress translation *in vivo* (Stoneley *et al.*, 1998; see chapter 5). The simplest explanation for this disparity is that translation initiation in cell lines is more refractory to inhibition by secondary structure. In this respect, it has been reported that structural elements located in the 5' UTR have a greater effect in RRL than in a translation extract derived from HeLa cells (Parkin *et al.*, 1988). Furthermore, a hairpin structure of -20 kcal/mol was reported to reduce the translational efficiency of an mRNA by approximately 10-fold in RRL, but the same structure had relatively little effect *in vivo* (Pelletier and Sonenberg, 1985). However, in similar study a hairpin structure of -30 kcal/mol had no effect on translation initiation, in either RRL or *in vivo*. In the light of these conflicting data, a more detailed analysis of the effects of secondary structure in both systems is necessary to support this contention. An alternative hypothesis suggests that the translation of c-*myc* mRNAs requires non-canonical *trans*-acting factors not present in either RRL or *Xenopus* oocytes (Parkin *et al.*, 1988). However, there is no direct evidence for the existence of such factors.

3.6.2 Evidence for an IRES in the c-*myc* 5' UTR

Recently, it has become clear that the structured 5' UTRs of some cellular mRNAs contain a specific RNA element capable of directing ribosomes to a site within the 5' leader sequence (Iizuka *et al.*, 1995). These internal ribosome entry segments, as they have become known, are able to efficiently drive the translation of the second cistron on a dicistronic mRNA (Pelletier and Sonenberg, 1988). Thus, to determine whether the c-*myc* 5' UTR contains an IRES, reporter plasmids were constructed that express dicistronic mRNAs in cultured cell lines. Insertion of the 5' UTR into the intercistronic region stimulated the synthesis of the downstream cistron and marginally reduced upstream cistron expression (fig. 3.9). Furthermore, the enhanced downstream cistron expression was not a peculiar feature of one dicistronic mRNA as it occurred using both *Renilla* luciferase-firefly luciferase and *Renilla* luciferase-CAT mRNAs (fig. 3.9 and 3.12).

Analysis of the mRNAs transcribed from the dicistronic reporter plasmids revealed that they were of the expected size (fig. 3.17). In addition, a small amount of a truncated mRNA was expressed by the 5' UTR-containing construct. However, RNase protection analysis

confirmed that the 5' end of this mRNA is located some distance within the firefly luciferase coding region and hence this mRNA is unlikely to encode a functional polypeptide (fig. 3.20). It is possible that the existence of this mRNA is due to the presence of transcription factor binding sites located within the 5' UTR that activate a cryptic promoter in the firefly luciferase coding region. Thus, the 5' UTR-mediated stimulation of firefly luciferase synthesis occurs only on intact dicistronic mRNAs.

An RNA hairpin structure (-55 kcal/mol) was inserted into the 5' leader sequence of the dicistronic mRNA containing the 5' UTR. Although this structure reduced the synthesis of the first cistron, it had no effect on the translation of the downstream cistron (fig. 3.15). Therefore, translation of second cistron is independent of initiation occurring at the upstream cistron start codon. Consequently, the stem-loop motif demonstrated that the 5' UTR does not stimulate downstream cistron expression by enhancing reinitiation at the downstream start codon. However, the autonomous translation of the downstream cistron is consistent with the presence of an IRES within the 5' UTR.

Taken together, these data suggest that the c-*myc* protein can be translated by the mechanism of internal initiation (this thesis; Stoneley *et al.*, 1998). Furthermore, a similar study performed by other workers using a CAT-based dicistronic reporter system also supports this hypothesis (Nanbru *et al.*, 1997). However, these studies do not discount the involvement of both cap-dependent and internal initiation mechanisms of translation in the synthesis of endogenous c-*myc* protein.

Chapter 4

Mechanistic analysis of the c-*myc* IRES

4.1 Introduction

The 5' UTRs of the Picornaviridae RNA genomes all contain IRES structures extending over approximately 450 nt (Jackson and Kaminski, 1995; Jackson *et al.*, 1996). Phylogenetic analysis and direct biochemical probing have demonstrated that these sequences form a complex secondary and presumably tertiary structure. The current model for internal initiation suggests that the IRES structure provides a three dimensional array of conserved sequence elements. Interactions between these elements and the translational apparatus are believed to result in the recruitment of the 40S ribosomal subunit to the 3' end of the IRES (Jackson *et al.*, 1995). In contrast, little is know about the mechanism of ribosome binding to eukaryotic IRESes. The few examples identified to date show no sequence homology and are of varied length. Furthermore, the analysis of these elements has been hampered by the lack of a suitable *in vitro* assay. Data from the previous chapter suggested that an IRES is located within the 5' UTR of the c-*myc* proto-oncogene. Thus, the function of this *cis*-acting element was analysed *in vivo* to gain some understanding of the underlying mechanism.

4.2 Deletion analysis of the c-*myc* 5' UTR

4.2.1 Construction of a 5' UTR deletion series in pGL3R

To define the element responsible for internal initiation within the c-*myc* 5' UTR, the 5' and 3' boundaries of the minimum sequence required for full activity were delimited by deletion analysis. A deletion series was created by inserting portions of the sequence encoding the c-*myc* 5' UTR into the intercistronic region of the dicistronic reporter plasmid, pGL3R. The construction of these plasmids is illustrated in figure 4.1. DNA fragments were excised from the plasmid pSKutr2 by digestion with *Nco*I and *Nci*I, *Acc*III, or *Ava*I. Insertion of these sequences into pGL3R between the *Pvu*II and *Nco*I sites generated the constructs pGL3R(-340/1), pGL3R(-298/1) and pGL3R(-162/1). In addition, a further 5' truncated sequence was amplified using the primers FP2760 and MS4519. This fragment was digested with *Nco*I and inserted into pGL3R at the same position to produce the plasmid, pGL3R(-226/1). The

sequences for 3' deletion series were generated by digesting pSKutr2 with *Bam*HI and *Pvu*II, *Eco*O901I, or *Ava*I and a larger deletion was created by amplifying the sequence from −396 to −276 using the primers FP2501 and JLQ1. These fragments were inserted into pGL3R at the *Pvu*II site generating the plasmids pGL3R(-396/-57), pGL3R(-396/-85), pGL3R(-396/-158), and pGL3R(-396/-277).

4.2.2 Analysis of the activity of truncated 5' UTR sequences

The dicistronic deletion constructs, along with the plasmids pGL3R and pGL3Rutr, were co-transfected into HeLa cells with pcDNA3.1/*His*B/*lac*Z. Lysates were prepared from the transiently transfected cells in the usual manner and the activity of *Renilla* luciferase, firefly luciferase and β-galactosidase was determined. After normalising the luciferase activities to that of β-galactosidase, the stimulation of the downstream cistron activity was calculated relative to the activity produced from the control, pGL3R, for each plasmid (fig. 4.2). Interestingly, in these experiments the presence of the whole 5' UTR upstream of firefly luciferase enhanced expression from this cistron by 104.5-fold. This value is approximately 2-fold greater than the value previously observed and further experiments revealed that the IRES-driven expression was consistently higher in these cells. One possibility is that the length of time that the cells were kept in culture is responsible for this increase in internal initiation. A deletion of 56 nt from the 5' end of the 5' UTR reduced the increase in downstream cistron activity to 70-fold (see fig. 4.2, (-340/1)). Furthermore, this trend continued since the removal of larger portions from the 5' end resulted in a corresponding decrease in the stimulation of firefly luciferase expression (fig. 4.2, (-298/1), (-226/1) and (-162/1)). At the 3' end of the 5' UTR, a deletion of 56 nt had little effect on the activity of the downstream gene product (fig. 4.2, compare (-396/-57) to UTR). However, a 5' UTR lacking 84 nt of the 3' end only enhanced the downstream cistron expression by 62.9-fold. Thus, deletion of the sequence between −57 and −85 nt decreased the downstream cistron activity by approximately 40%. Finally, deletions from the 3' end extending further into the 5' UTR resulted in an additional diminution of firefly luciferase activity (fig. 4.2, (-396/-158) and (-396/-277)).

In summary, deletions of 56 nt and 84 nt from the 5' end and 3' end, respectively, reduced the activity of the putative IRES. Thus, the minimum element required for maximum activity is located between nucleotides −396 and −57. Furthermore, at 340 nt in length the c-*myc* IRES is somewhat shorter than those of the picornaviruses. It is also noteworthy that

A. 5' deletion series
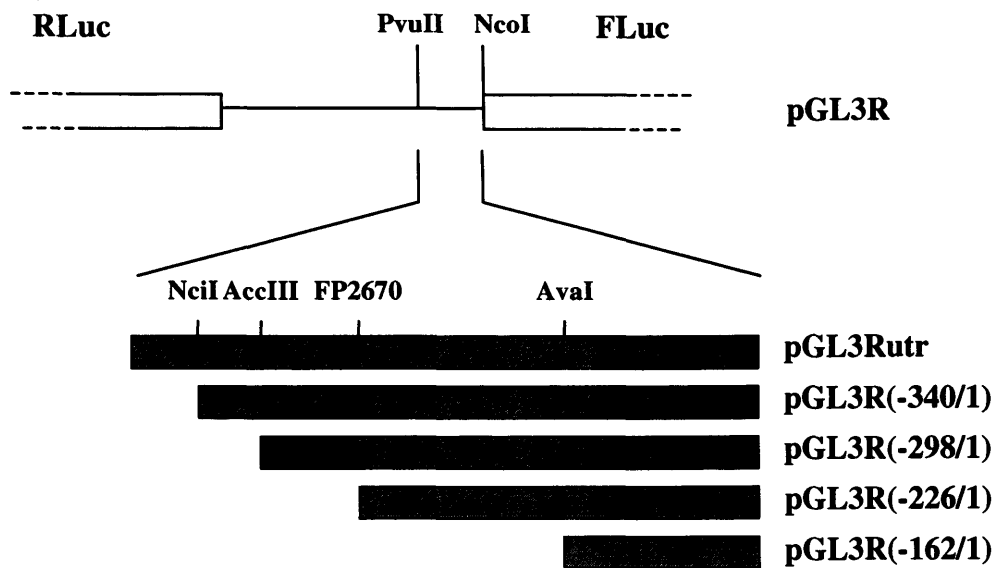
B. 3' deletion series
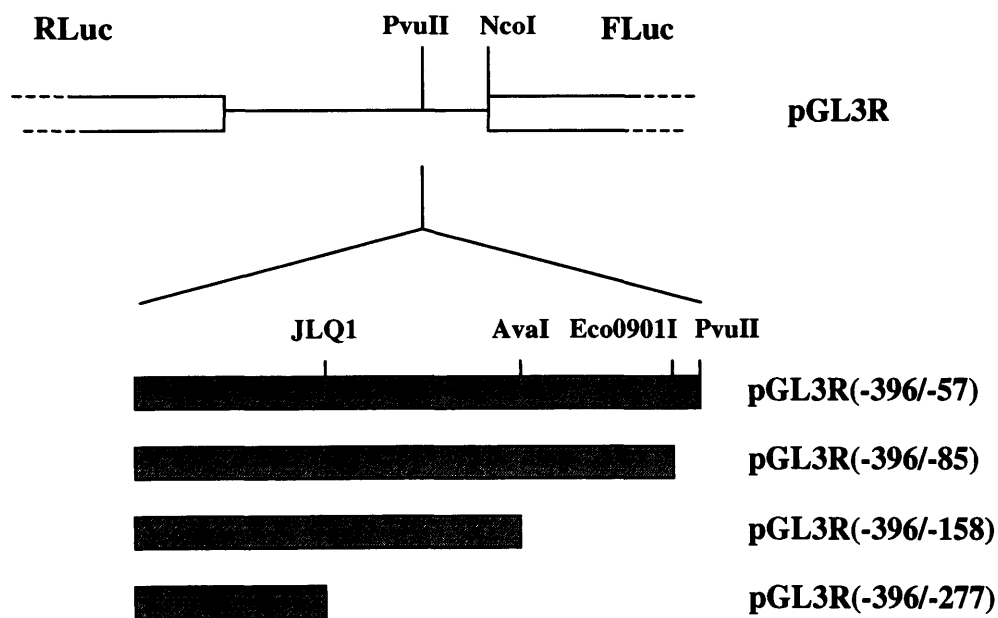
Figure 4.1: Construction of 5' UTR deletion series in the dicistronic reporter plasmid pGL3R. (A) To create the 5' deletion series, truncated sequences were inserted between the *Renilla* luciferase and firefly luciferase cistrons using the *Pvu*II and *Nco*I restriction sites. (B) To create the 3' deletion series, blunt-ended fragments were inserted into pGL3R at the *Pvu*II site.

A.
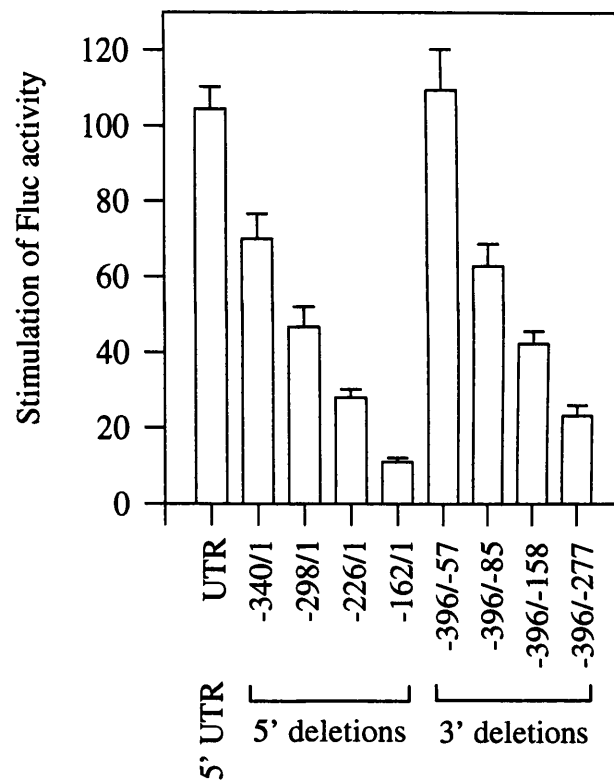
B.

Plasmid	% Activity
UTR	100
-340/1	67
-298/1	45
-226/1	27
-162/1	11
-396/-57	105
-396/-85	60
-396/-158	41
-396/-277	22

Figure 4.2: Analysis of the downstream cistron expression directed by truncated 5' UTR sequences. (A) HeLa cells were transfected with pGL3R, pGL3Rutr, pGL3R(x/-1) (5' deletions), and pGL3R(-396/x) (3' deletions) and the expression from the *Renilla* and firefly luciferase cistrons was determined. After normalising firefly luciferase activity to β-galactosidase activity, the stimulation of expression from the downstream cistron was calculated relative to the expression from the pGL3R. (B) Downstream cistron expression from the deletion constructs relative to pGL3Rutr.

deletions within the IRES did not completely ablate its activity. Similar deletions within the poliovirus and EMCV IRESes have a more dramatic effect on internal initiation (Pelletier and Sonenberg, 1988; Jang and Wimmer, 1990).

4.3 A potential role for a conserved non-AUG initiation codon

Translation initiation on the poliovirus IRES is dependent on the presence of a conserved AUG triplet that lies upstream of the authentic initiation codon. Mutation of this codon or the surrounding sequence resulted in a reduction in translational efficiency and adverse effects on the phenotype of the virus (Pelletier et al., 1988b; Pilipenko et al., 1992). It is believed that the 40S ribosomal subunit interacts with the RNA at or near this codon (Pestova et al., 1994). In comparison, mammalian c-myc genes have a CUG initiation codon at the 3' end of exon 1, in addition to the AUG start codon located within exon 2 (see fig. 4.15; boxed region). Thus, by analogy to the poliovirus IRES, it seemed possible that this CUG codon was involved in the interaction between the ribosome and the mRNA. In the human c-myc mRNA this translation start site is found 45 nt upstream of the major initiation codon and consequently lies outside of the putative IRES. However, since the 3' deletion fragments were inserted into the PvuII site of pGL3R, they are located immediately upstream of a CUG codon. Furthermore, the context of this initiation codon could be enhanced by G and A residues at positions +4 and +5, respectively (Grünert and Jackson, 1994; Boeck and Kolakofsky, 1994; Kozak, 1997). Therefore, in theory this sequence could substitute for the authentic CUG codon in the (-396/-340) deletion mutant and mask the effect produced by the loss of this element.

4.3.1 Construction of a dicistronic plasmid containing a mutant 5' UTR

To assess the potential contribution of the CUG codon towards the function of the c-myc IRES it was mutated to CUC, a triplet that is not recognised by the initiator-methionyl tRNA. Initially, a DNA fragment was amplified from pSKutr2 by asymmetric PCR using the mutagenic primer 5'CUG as the 5' primer and KS as the 3' primer. The product of this reaction is a 111 bp fragment that encodes 56 bp of the c-myc 5' UTR and contains the CUG to CUC mutation. A second amplification was then performed using the previous fragment as a 3' megaprimer and FP2501 as the 5' primer. The resulting fragment contains the sequence coding for the 5' UTR with a single base change at nucleotide –45. The mutant 5' UTR sequence was released from this fragment by digestion with NcoI and was subsequently

inserted into pGL3Rutr at the *Pvu*II and *Nco*I sites. The new plasmid, pGL3Rcuc, contains the mutant 5' UTR sequence between the two luciferase cistrons.

4.3.2 Analysis of the function of the conserved CUG codon

The plasmids pGL3R, pGL3Rutr and pGL3Rcuc were co-transfected into HeLa cells with the β-galactosidase expression construct. The activity of each enzyme in the transfected cells was determined as described previously and luciferase expression was normalised to that of β-galactosidase (fig. 4.3). Insertion of the 5' UTR in the intercistronic region of the dicistronic reporter mRNA stimulated firefly luciferase expression and marginally reduced *Renilla* luciferase expression (fig. 4.3, compare –UTR to +UTR). In addition, the mutant 5' UTR sequence had a similar effect on the expression of both luciferases (fig. 4.3, compare –UTR to +CUC). A comparison of the magnitude of these effects reveals that the wild-type and mutant sequences activated firefly luciferase expression by 89.3-fold and 98.5-fold, respectively, whilst *Renilla* luciferase expression was reduced by 0.85-fold and 0.83-fold, respectively. Thus, it appears that mutation of the CUG initiation codon to a CUC triplet has no effect on internal initiation.

The results of this experiment indicate that the conserved CUG initiation codon probably does not play a significant role in recruiting the ribosome to the c-*myc* mRNA. Thus, a model in which the ribosome interacts with the mRNA at or near this upstream initiation codon followed by scanning to the authentic start site, as suggested for the poliovirus IRES, is not supported by these data. Furthermore, since the loss of the CUG codon did not effect internal initiation it is likely that the 3' boundary of the IRES, as determined by deletion analysis, is correct.

4.4 A comparison of 5' UTR-mediated internal initiation in various cell lines

In the previous chapter, the ability of the c-*myc* 5' UTR to promote translation of the downstream cistron on a dicistronic mRNA was examined in three cell lines, HeLa, HepG2 and HK293. It was apparent that internal initiation mediated by the c-*myc* 5' UTR in HK293 cells was less efficient than in either of the other two cell lines. Consequently, it seemed conceivable that the activity of this element could vary in a cell-type specific manner. To test this hypothesis the efficiency of the c-*myc* IRES was examined in three more cell lines.
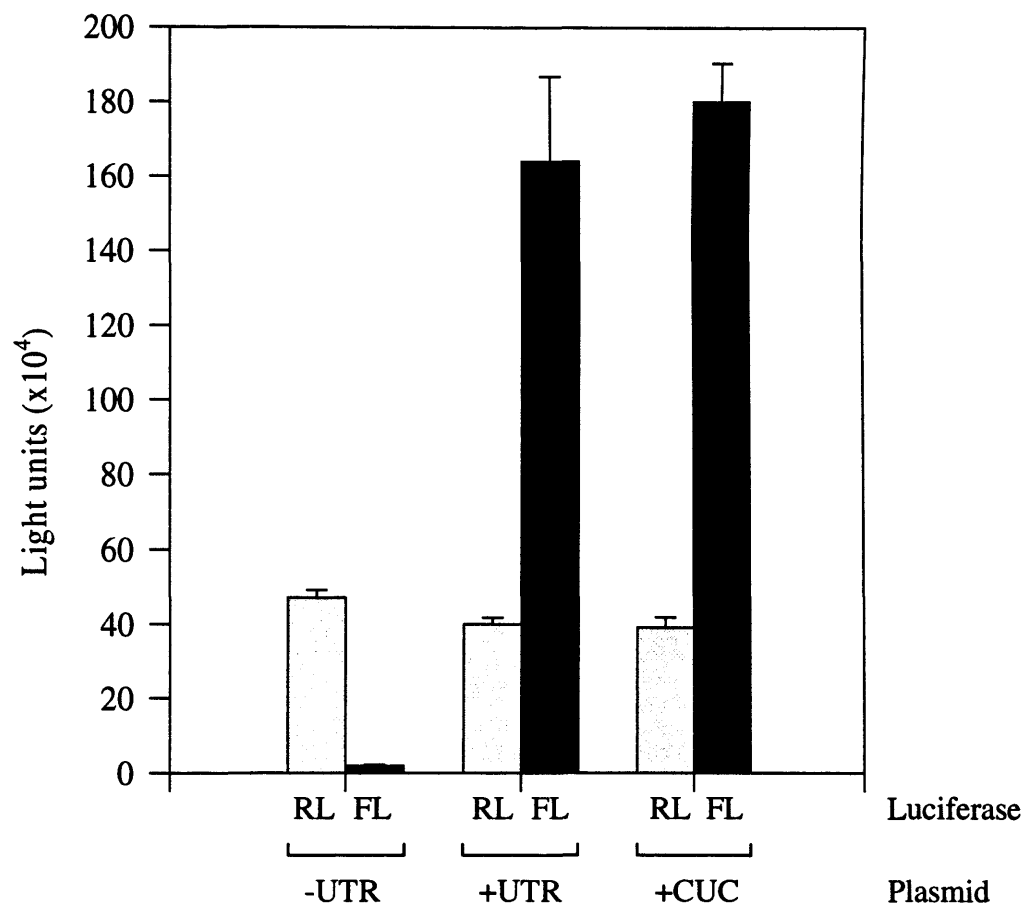
Figure 4.3: Analysis of the effect of the CUG initiation codon on 5' UTR-directed internal initiation. HeLa cells were transfected with the plasmids pGL3R (-UTR), pGL3Rutr (+UTR) and pGL3Rcuc (+CUC). Expression from the *Renilla* luciferase (RL) and firefly luciferase (FL) cistrons was determined as before.

4.4.1 Analysis of the IRES-driven translation in COS7, MCF7 and Balb/c-3T3 cells

Accordingly, the cell lines COS7, MCF7, Balb/c-3T3 and HeLa were co-transfected with either pGL3R or pGL3Rutr and pcDNA3.1/*His*B/*lac*Z. The expression from both *Renilla* and firefly luciferase cistrons was assayed and normalised to the transfection control, β-galactosidase. In each cell line, the presence of the 5' UTR in the mRNA did not significantly alter *Renilla* luciferase expression (fig. 4.4, compare −UTR RL to +UTR RL). Indeed, the largest difference was observed in HeLa cells, in which the 5' UTR reduced *Renilla* luciferase activity by approximately 11%. In contrast, analysis of the firefly luciferase activity revealed that it was consistently greater in those cells transfected with pGL3Rutr (fig. 4.4, compare −UTR FL to +UTR FL). However, the magnitude of the stimulation varied between the cell lines. In HeLa cells, the 5' UTR enhanced downstream cistron expression by approximately 85-fold. Whilst in MCF7, COS7 and Balb/c-3T3 cells, a lesser stimulation of 12-fold, 10-fold or 6-fold, respectively, was observed. Therefore, it appears that the efficiency of internal initiation driven by the c-*myc* IRES is dependent on the cell-type.

The 5' UTR appeared to enhance the translation of the downstream cistron in COS7 and MCF7 cells to a similar extent. However, in COS7 cells the level of readthrough-reinitiation that occurred on the control mRNA was 4.4-fold higher than in MCF7 cells (fig. 4.4). Consequently, the stimulation of downstream cistron expression does not represent an absolute measure of 5' UTR-directed internal initiation in each cell line. To eliminate the effect of variation in readthrough-reinitiation, the activity of the IRES can also be assessed by comparing the firefly and the *Renilla* luciferase expression from the dicistronic mRNA containing the 5' UTR (i. e. Fluc/Rluc). By interpreting the data in this manner, it is clear that the activity of the c-*myc* IRES was 3.6-fold higher in COS7 cells than in MCF7 cells (fig. 4.5). Furthermore, these data demonstrate that the efficiency of c-*myc* IRES-driven translation varies widely between cell lines (fig. 4.5).

4.4.2 The effect of the 5' UTR on heterologous gene expression in MCF7 and Balb/c-3T3 cells

Interestingly, in comparison to HeLa cells the c-*myc* IRES was 22 and 24-fold less active in the Balb/c-3T3 and MCF7 cell lines, respectively (fig. 4.5). Moreover, the 5' UTR did not significantly affect the translation of a heterologous mRNA in HeLa cells. Therefore, in
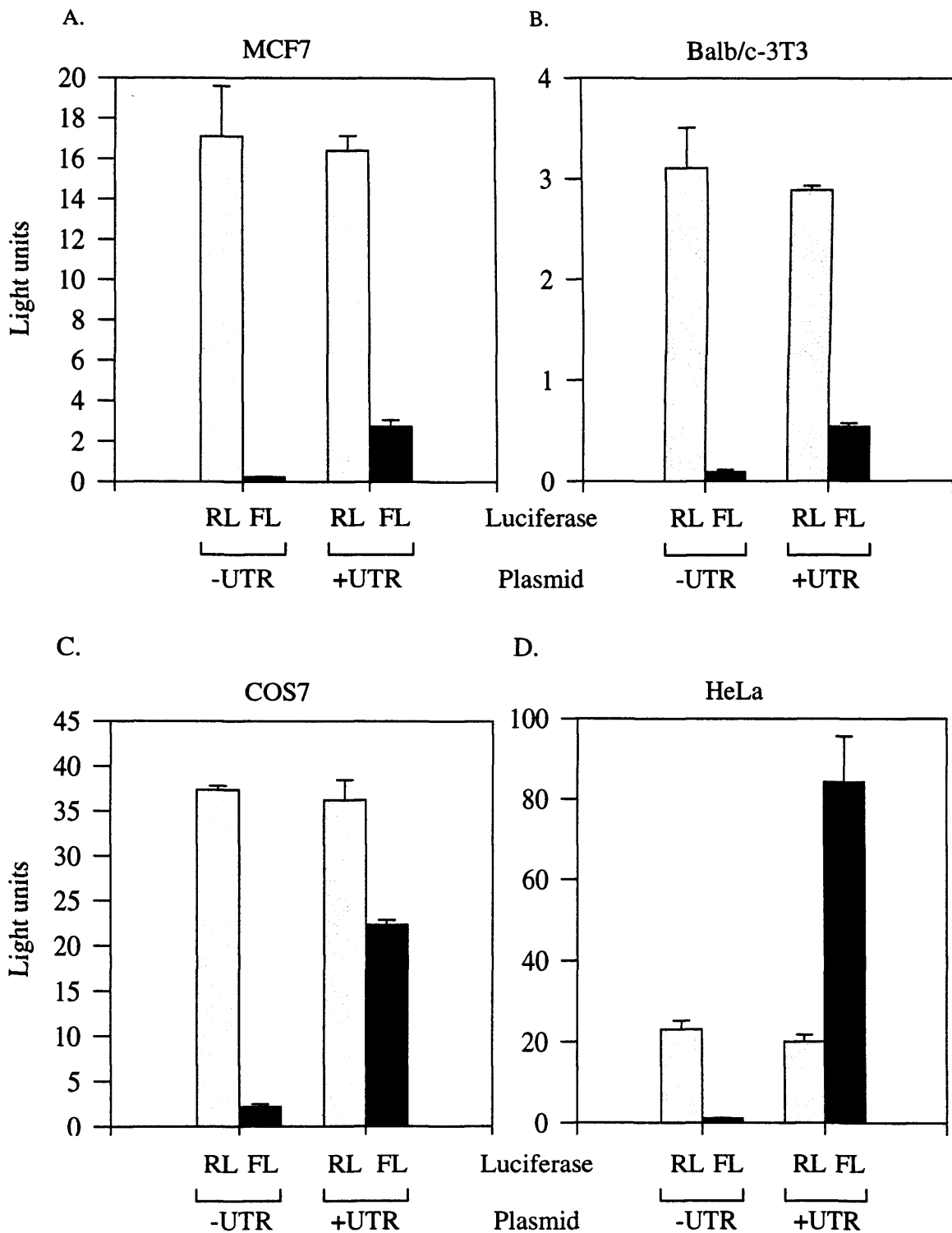
Figure 4.4: Analysis of the efficiency of 5' UTR-directed internal initiation in cell lines of different origin. (A) MCF7, (B) Balb/c-3T3, (C) COS7 and (D) HeLa cells were transfected with the plasmids pGL3R (-UTR) or pGL3Rutr (+UTR). Expression from the upstream cistron (RL) and downstream cistron (FL) was determined as described previously.
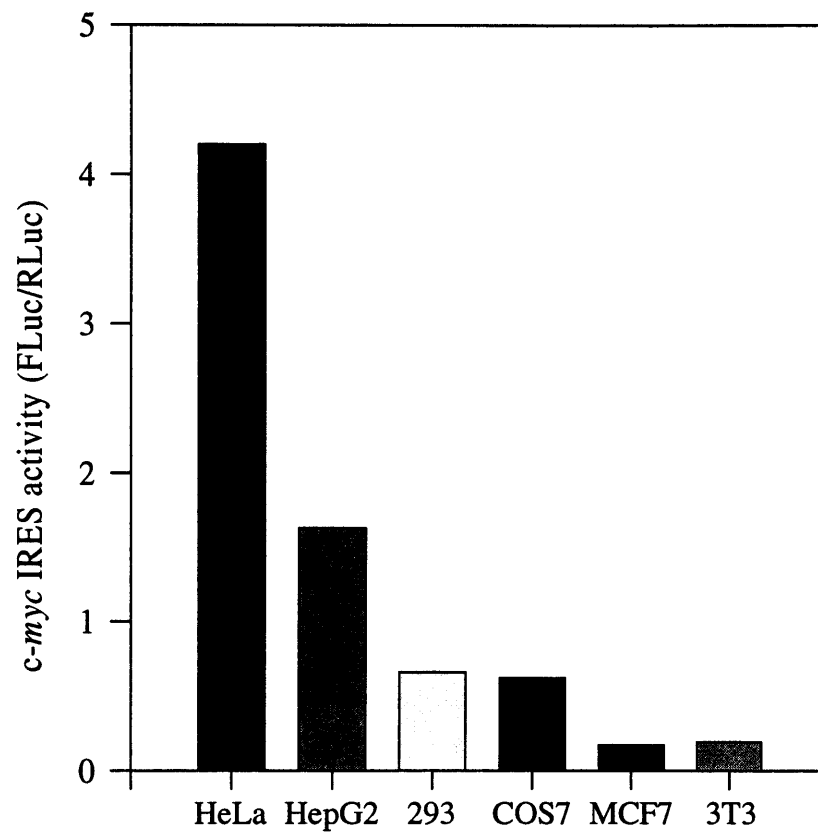
Figure 4.5: A comparison of the efficiency of c-*myc* 5' UTR-driven internal initiation in cell lines of different origins. IRES activity is expressed using the ratio of downstream cistron expression to upstream cistron expression (FLuc/RLuc).
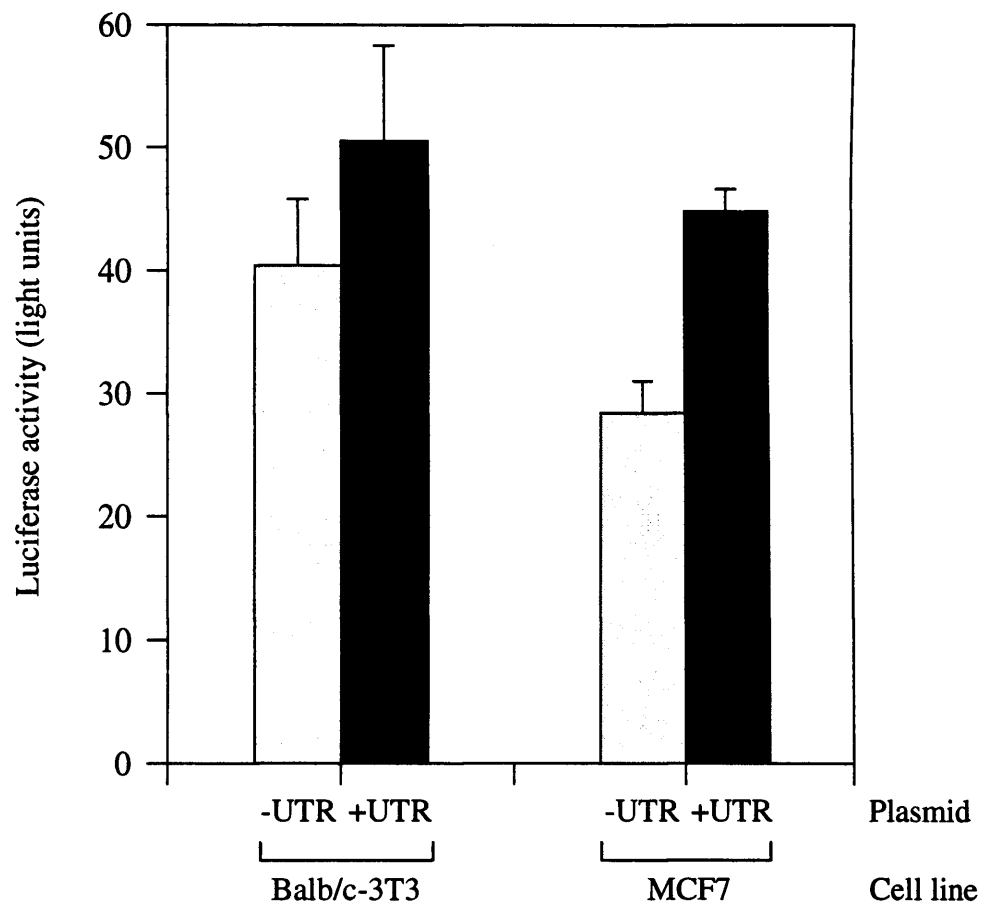
Figure 4.6: The effect of the 5' UTR on the expression of a heterologous mRNA in the MCF7 and Balb/c-3T3 cell lines. MCF7 and Balb/c-3T3 cells were transfected with the plasmids pGL3 (-UTR) or pGL3utr (+UTR) and firefly luciferase activity was measured as described previously.

MCF7 and Balb/c-3T3 cells the inefficient internal initiation could potentially reduce the translational efficiency of an mRNA bearing this element. Hence, the monocistronic reporter constructs pGL3 and pGL3utr (see chapter 3; fig. 3.1 and 3.2) were transfected into these cells along with the transfection control plasmid. The firefly luciferase activities produced from both the control luciferase mRNA (-UTR) and the mRNA bearing the c-myc 5' UTR (+UTR) are shown in figure 4.6. In both cell lines, higher luciferase expression was observed in the cells transfected with pGL3utr than with the control plasmid. However, the increase in expression was only 1.25 and 1.58-fold greater in Balb/c-3T3 and MCF7 cells, respectively. Thus, as previously observed in HeLa, HepG2, COS7, and HK293 cells the 5' UTR does not dramatically alter the expression of a heterologous mRNA. Furthermore, the translational efficiency of the chimeric monocistronic mRNA did not vary in the same cell-type specific manner as the efficiency of internal initiation. If internal initiation were the only mechanism involved in the translation of an mRNA bearing the c-myc 5' UTR, one would expect a direct correlation between these results. Thus, these data represent evidence that c-myc mRNAs could be translated by both cap-dependent and internal initiation mechanisms.

4.5 The effect of a strong viral promoter on the function of the c-myc IRES

One model that would explain the cell-type specific variation in the efficiency of c-myc IRES-driven translation posits that non-canonical trans-acting factors are required for the recruitment of the 40S ribosome to this element. In this scenario, the activity of one or more of these factors is considerably reduced in the Balb/c-3T3 and MCF7 cell lines. The expression of dicistronic mRNAs under the control of the very strong cytomegalovirus (CMV) promoter/enhancer region provided further circumstantial evidence in support of this model.

4.5.1 Construction of pRLuc and pRMLuc

Construction of the dicistronic dual-luciferase reporter plasmids, pRLuc and pRMLuc, is detailed in figure 4.7. Essentially, the plasmids pSKL and pSKLutr (see chapter 5, fig. 5.9) were digested with HindIII and XhoI and the luciferase coding region fragments were isolated. After purification, the overhanging 5' ends of these fragments were filled in using Klenow DNA polymerase. Subsequently, the plasmid pRLCMV was digested with XbaI and the ends were filled in with Klenow DNA polymerase, the luciferase coding region fragments were then inserted into this site. The new plasmids, pRLuc and pRMLuc, express dicistronic
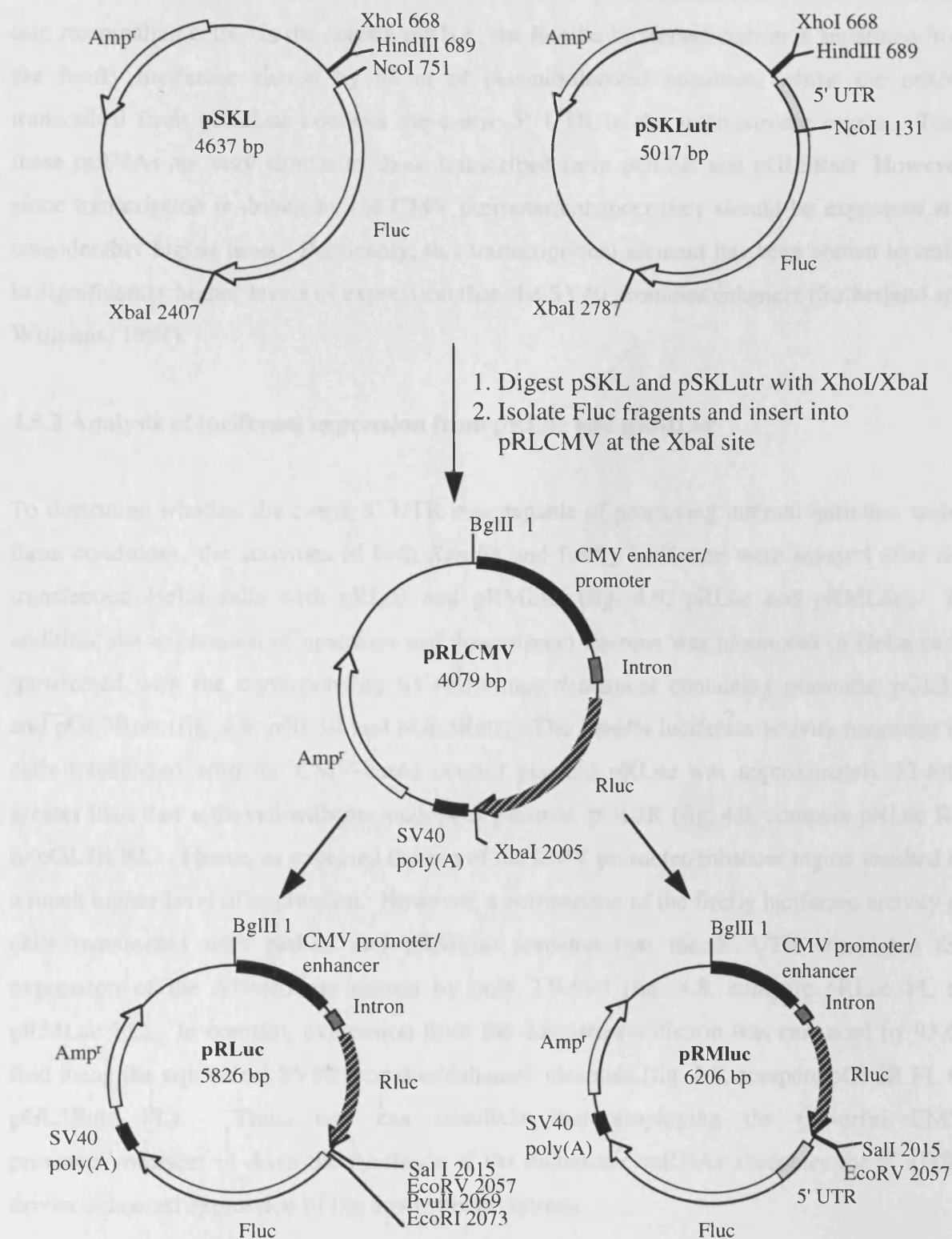
Figure 4.7: Construction of the CMV promoter/enhancer-based dicistronic plasmids pRLuc and pRMLuc. DNA fragments containing either the Fluc open reading frame or the c-*myc* 5' UTR fused to Fluc cistron were excised from pSKL or pSKLutr, respectively. After treatment with Klenow DNA polymerase, these fragments were inserted into pRLCMV at the blunt *Xba*I site. The resulting plasmids, pRLuc and pRMLuc express Rluc-Fluc or Rluc-5' UTR-Fluc dicistronic mRNAs, respectively, under the control of the CMV promoter/enhancer.

dual-luciferase mRNAs under the control of the CMV promoter/enhancer when transfected into mammalian cells. In the control mRNA, the *Renilla* luciferase cistron is separated from the firefly luciferase cistron by 88 nt of plasmid-derived sequence, whilst the mRNA transcribed from pRMLuc contains the c-*myc* 5' UTR in the intercistronic region. Thus, these mRNAs are very similar to those transcribed from pGL3R and pGL3Rutr. However, since transcription is driven by the CMV promoter/enhancer they should be expressed at a considerably higher level. Previously, this transcriptional element has been shown to result in significantly higher levels of expression than the SV40 promoter/enhancer (Sutherland and Williams, 1997).

4.5.2 Analysis of luciferase expression from pRLuc and pRMLuc

To determine whether the c-*myc* 5' UTR was capable of promoting internal initiation under these conditions, the activities of both *Renilla* and firefly luciferase were assayed after the transfection HeLa cells with pRLuc and pRMLuc (fig. 4.8; pRLuc and pRMLuc). In addition, the expression of upstream and downstream cistrons was monitored in HeLa cells transfected with the corresponding SV40 promoter/enhancer containing plasmids, pGL3R and pGL3Rutr (fig. 4.8; pGL3R and pGL3Rutr). The *Renilla* luciferase activity measured in cells transfected with the CMV-based control plasmid pRLuc was approximately 32-fold greater than that achieved with the analogous plasmid, pGL3R (fig. 4.8, compare pRLuc RL to pGL3R RL). Hence, as expected the use of the CMV promoter/enhancer region resulted in a much higher level of expression. However, a comparison of the firefly luciferase activity in cells transfected with pRLuc and pRMLuc revealed that the 5' UTR stimulated the expression of the downstream cistron by only 2.9-fold (fig. 4.8, compare pRLuc FL to pRMLuc FL). In contrast, expression from the downstream cistron was enhanced by 93.6-fold using the equivalent SV40 promoter/enhancer plasmids (fig. 4.8, compare pGL3R FL to pGL3Rutr FL). Thus, one can conclude that employing the powerful CMV promoter/enhancer to drive the synthesis of the dicistronic mRNAs abrogates the 5' UTR-driven enhanced expression of the downstream cistrons.

These data appear to contradict the previous evidence that an IRES is located within the c-*myc* 5' UTR. However, one possible explanation is that the high level of mRNA expressed from these constructs reduced the efficiency of internal initiation by interfering with the function of a *trans*-acting factor. Borman *et al.* have reported a similar observation for the entero- and rhinovirus IRESes. The efficiency of translation mediated by these IRESes was
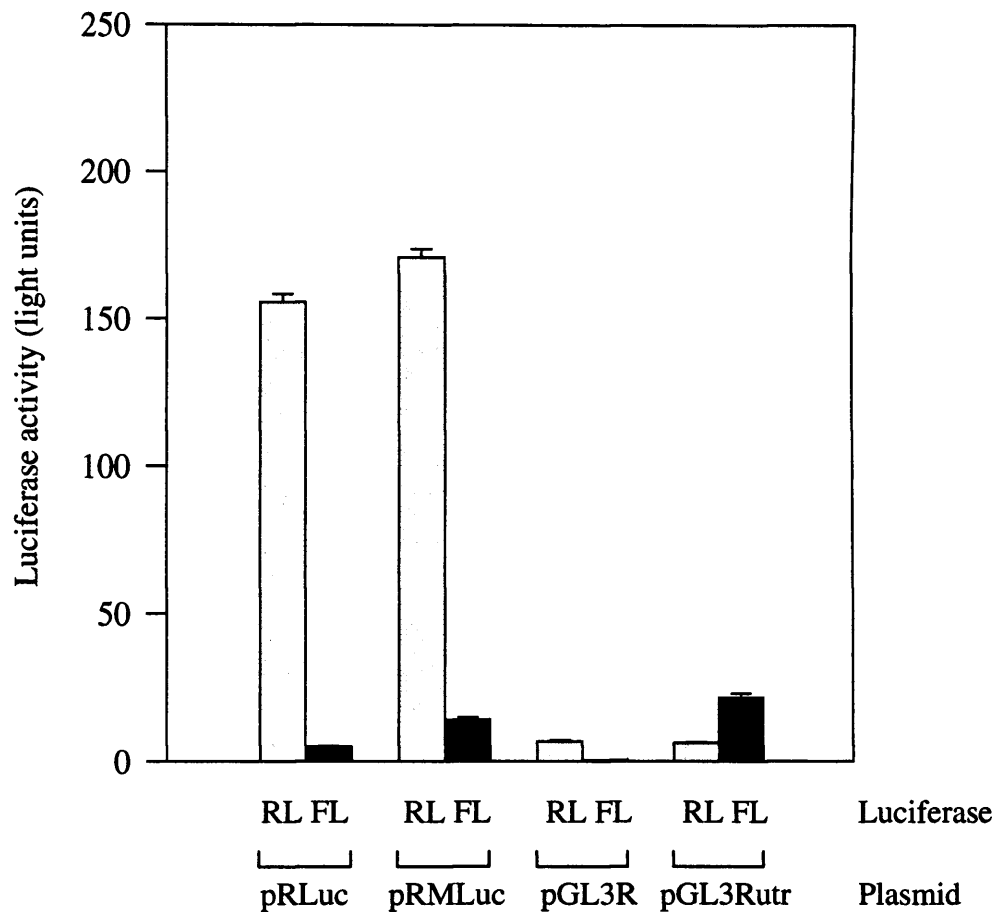
Figure 4.8: The effect of the CMV promoter/enhancer on c-*myc* 5' UTR-directed internal initiation. HeLa cells were transfected with the CMV promoter/enhancer-based plasmids, pRLuc and pRMLuc, or the SV40 promoter/enhancer-based plasmids, pGL3R and pGL3Rutr. *Renilla* luciferase (RL) and firefly luciferase (FL) activity was determined and normalised to that of the transfection control, β-galactosidase.

considerably reduced when dicistronic mRNAs were expressed at high levels *in vivo* (Borman *et al.*, 1997). This phenomenon correlates with a requirement for non-canonical factors, since it was not observed for either cap-dependent translation or translation driven by the cardio- and aphthovirus IRESes.

4.6 A comparison of the efficiency of the c-*myc* and the human rhinovirus IRESes

The previous data provided indirect evidence that the function of the c-*myc* IRES could depend on a non-canonical *trans*-acting factor. In this respect, it would be analogous to the IRESes of the entero- and rhinoviruses (see Belsham and Sonenberg, 1996). However, in studies performed in collaboration with Belsham and co-workers, the c-*myc* IRES was extremely inefficient at promoting downstream cistron expression on dicistronic mRNAs expressed in the cytoplasm. In these experiments, the plasmids pGL3R and pGL3Rutr were transfected into human TK143 cells previously infected with a recombinant vaccinia virus that expresses the T7 RNA polymerase (vTF7-3) (Fuerst *et al.*, 1986). The presence of a T7 RNA polymerase promoter upstream of the *Renilla* luciferase cistron in pGL3R and pGL3Rutr results in the transcription of dicistronic mRNAs in the cytoplasmic compartment. Furthermore, these RNAs are posttranscriptionally modified by the vaccinia encoded capping and polyadenylation enzymes. Whilst the *Renilla* luciferase cistron of both dicistronic mRNAs was translated efficiently, the activity of firefly luciferase in these cells was approximately 300-fold lower and independent of the presence of the c-*myc* 5' UTR sequence (data not shown). Thus, the c-*myc* 5' UTR did not promote internal initiation on mRNAs transcribed in the cytoplasm using the T7/vaccinia system. In contrast, the IRESes of the entero- and rhinoviruses have been shown to function efficiently using dicistronic mRNAs expressed in this manner (Borman *et al.*, 1997).

These data appeared to suggest a fundamental difference between the function of the entero- and rhinovirus IRESes and that of c-*myc*. Nevertheless, it was possible that these results were a consequence of the very high level of expression achieved using the T7/vaccinia system. Indeed, a previous study demonstrated that the expression of a heterologous reporter gene was approximately 650-fold higher when compared to that accomplished with the SV40 promoter/enhancer (Fuerst *et al.*, 1986). Furthermore, existing data implied that the function of the c-*myc* IRES could be compromised by the use of a strong promoter (fig. 4.8). Consequently, the efficiency of internal initiation driven by the c-*myc* and human rhinovirus

(HRV) IRESes was compared using dicistronic mRNAs either expressed in the nucleus or introduced directly into the cytoplasm by RNA transfection.

4.6.1 Construction of the plasmid pGL3Rhrv

The plasmid, pGL3Rhrv, was constructed to assess the efficiency of internal initiation mediated by the HRV IRES on transcripts synthesised in the nucleus by RNA polymerase II. A diagrammatic representation of the assembly of pGL3Rhrv is shown in figure 4.9. The plasmid pXLJ(10-605) (Borman and Jackson, 1992) was digested with *Sal*I and the overhanging 5' ends were filled in with Klenow DNA polymerase. A fragment containing the HRV2 IRES was released from the plasmid by digestion with *Nco*I. Subsequently, this DNA fragment was inserted into pGL3R at the *Pvu*II and *Nco*I sites creating the plasmid pGL3Rhrv. The mRNA expressed in cells transfected with this construct contains the sequence for the HRV2 IRES in the intercistronic region.

4.6.2 An analysis of the activity of the c-*myc* and HRV IRESes in transcripts with a nuclear origin

To compare the efficiency of the c-*myc* and HRV2 IRESes, HeLa cells were transfected with the plasmids pGL3R, pGL3Rutr and pGL3Rhrv. The activities of *Renilla* and firefly luciferase were determined and normalised to that of the transfection control, β-galactosidase (fig. 4.10). Expression of the upstream cistron, *Renilla* luciferase, was not greatly affected by the presence of the either the HRV or the c-*myc* IRES in the intercistronic region (fig. 4.10, compare Con RL to +HRV RL and +UTR RL). More importantly, a comparison of the downstream cistron activities revealed that both of these elements stimulated firefly luciferase expression (fig. 4.10, compare Con FL to +HRV FL and +UTR FL). However, the extent to which expression from the downstream cistron was enhanced differed widely between these IRESes. In fact, the c-*myc* IRES elevated firefly luciferase activity by 70.8-fold, whilst the HRV IRES caused a lesser stimulation of 9.6-fold. Thus, these data suggest that the HRV IRES is able to promote internal initiation on dicistronic transcripts synthesised in the nucleus, however it does so approximately 7-fold less efficiently than the c-*myc* IRES.

pXLJ (10-605)

1. Digest pXLJ (10-605) with SalI
2. Fill in recessed 3' ends
3. Release HRV 5' UTR with NcoI

pGL3R
6499 bp

SpeI 1490
PvuII 1498
EcoRI 1502
NcoI 1521

4. Digest pGL3R with PvuII/NcoI
5. Ligate HRV 5' UTR fragment into pGL3R

pGL3Rhrv
7070 bp

SpeI 1490
HRV 5' UTR
NcoI 2092
XbaI 3748
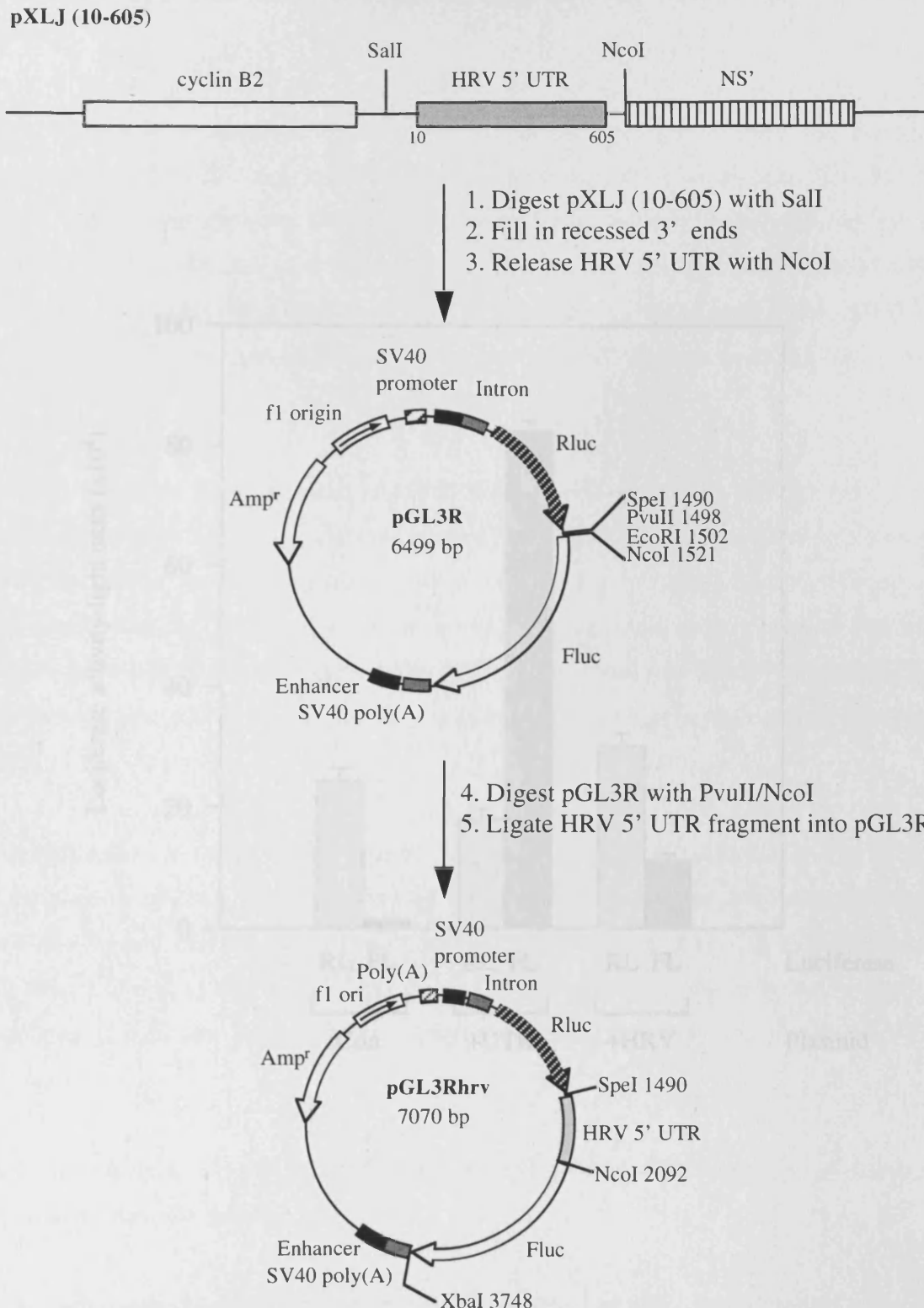
Figure 4.9: Construction of the dicistronic reporter plasmid, pGL3Rhrv, containing the HRV IRES. The plasmid pXLJ(10-605) was digested with *Sal*I and after filling in the recessed 3' ends, a fragment containing the HRV IRES was released by digesting with *Nco*I. This sequence was inserted into the multiple cloning site between the Rluc and Fluc cistrons of pGL3R at the *Pvu*II and *Nco*I sites. The resulting plasmid pGL3Rhrv expresses a dicistonic mRNA with the HRV IRES in the intercistronic region.
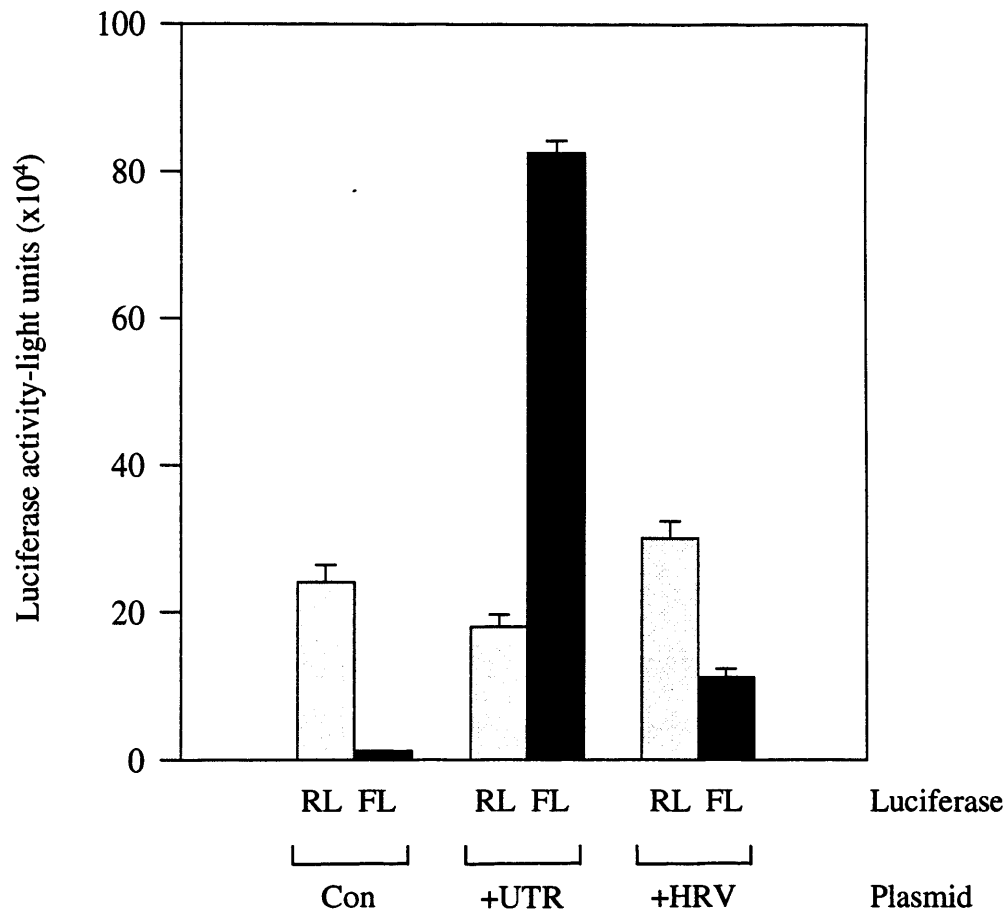
Figure 4.10: A comparison of the efficiency of HRV and c-*myc* 5' UTR-driven internal initiation on dicistronic mRNAs expressed in the nucleus. HeLa cells were transfected with the control dicistronic plasmid, pGL3R (Con), the c-*myc* 5' UTR containing plasmid, pGL3Rutr (+UTR), or the HRV IRES containing plasmid pGL3Rhrv (+HRV). Upstream cistron (RL) and downstream cistron (FL) activities were determined and normalised to that of the transfection control, β-galactosidase.

4.6.3 Construction of pSP64RL Poly(A), pSP64R(utr)L Poly(A) and pSP64R(hrv)L Poly(A)

RNA transcripts synthesised *in vitro* can be introduced directly into the cytoplasmic compartment of a cell using cationic liposome-mediated RNA transfection (Malone *et al.*, 1989). These transcripts are translated efficiently provided they are capped and have a 3' terminal polyadenylate tail (Dwarki *et al.*, 1993). Thus, in order to synthesise dual-luciferase dicistronic transcripts that can be used in RNA transfections, the plasmid series pSP64 R(x)L Poly(A) was generated (where x is either no insert or the sequence encoding the c-*myc* and HRV2 IRESes).

The polylinker region of the plasmid pSP64 Poly(A) is flanked by an SP6 RNA polymerase promoter sequence and a run of 30 consecutive A residues. Thus, capped and polyadenylated transcripts can be generated by run-off transcription using a template linearised by digestion with *Eco*RI (fig. 4.11). Initially, the sequence encoding the *Renilla* luciferase cistron was isolated from pRLCMV by digesting the plasmid with *Nhe*I and *Xba*I. This fragment was then inserted into pSP64 Poly(A) at the *Xba*I site, thus creating the plasmid pSP64R Poly(A) (fig. 4.11).

To generate the control dicistronic plasmid pSP64RL Poly(A), the sequence coding for firefly luciferase was excised from pGL3 using the enzymes *Eco*RI and *Xba*I and subsequently blunt-end ligated into the *Sma*I site of pSP64R Poly(A) (fig. 4.11). Whilst the plasmids pSP64RutrL Poly(A) and pSP64RhrvL Poly(A) were constructed by inserting the *Spe*I/*Xba*I fragments of pGL3utr and pGL3Rhrv, respectively, into the *Sma*I site of pSP64R Poly(A) (fig. 4.12).

4.6.4 An analysis of the efficiency of the c-*myc* and HRV IRESes in transcripts introduced directly into the cytoplasm

Dicistronic transcripts containing an m^7GpppG cap structure and a polyadenylate tail at the 5' and 3' termini, respectively, were synthesised from each of the plasmids in the pSP64 R(x)L Poly(A) series by *in vitro* run-off transcription on a DNA template linearised with *Eco*RI. The resulting mRNAs, denoted Rluc, RutrL and RhrvL are illustrated diagrammatically in figure 4.13a. Cationic liposomes were used to encapsulate equimolar quantities of each transcript and introduce them into the cytoplasm of HeLa cells. After a period of 8 hours, the
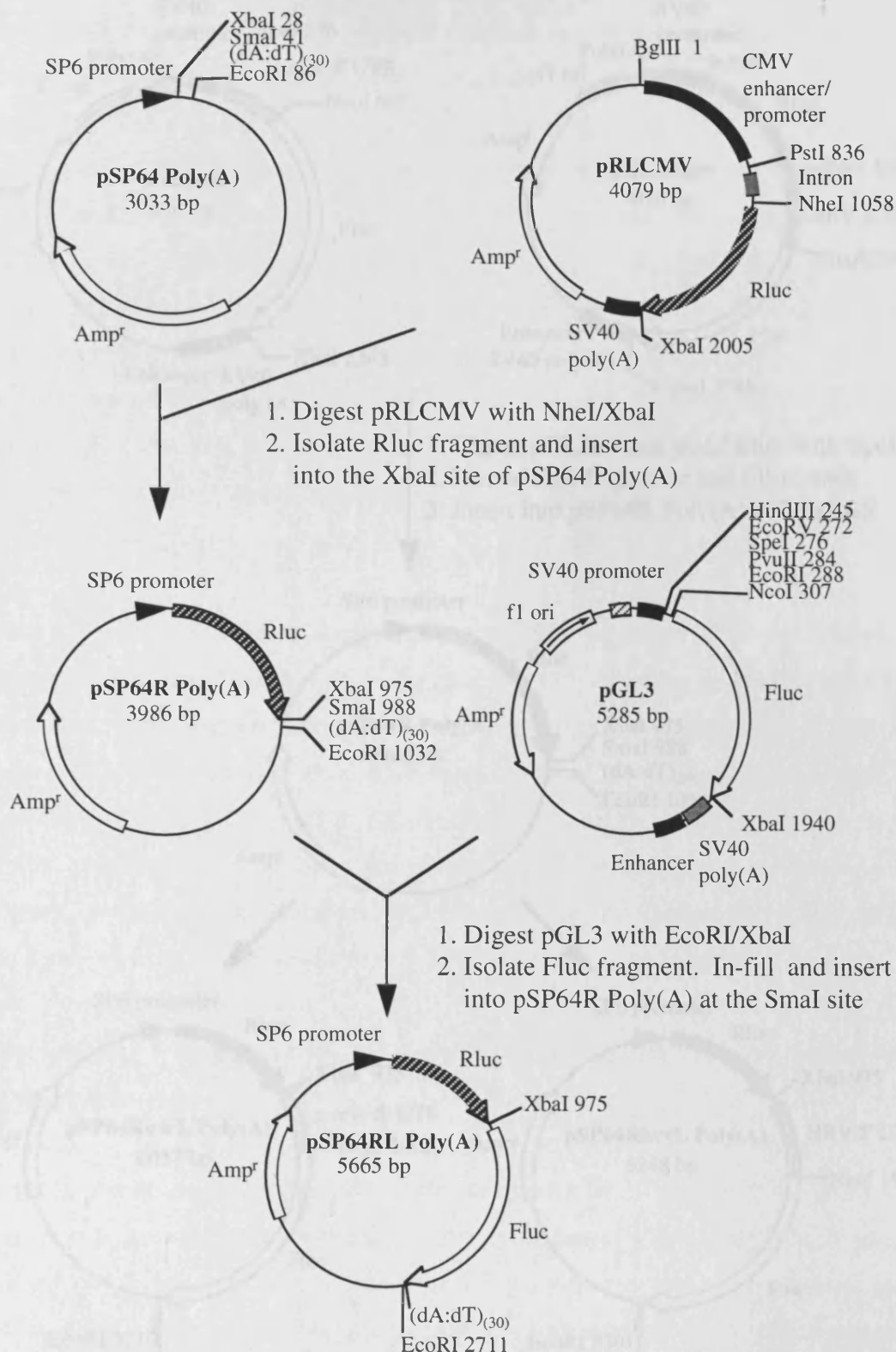
Figure 4.11: Construction of the control dicistronic plasmid pSP64RL Poly(A). Briefly, this plasmid was constructed using a two-stage protocol. In the first stage, a DNA fragment, containing the Rluc open reading frame (ORF), was excised from pRLCMV by digesting with *Nhe*I and *Xba*I. This fragment was then inserted into pSP64 Poly(A) at the *Xba*I site creating pSP64R Poly(A). Subsequently, pGL3 was digested with *Eco*RI and *Xba*I and the fragment containing the Fluc ORF was isolated. After treatment with Klenow DNA polymerase, this fragment was inserted into pSP64R Poly(A) at the *Sma*I site. PSP64RL Poly(A) was digested with *Eco*RI and used as a template to synthesise Rluc-Fluc dicistronic mRNAs terminating with a Poly(A) tail.

SV40 promoter
Poly(A)
fl ori
SpeI 276
c-myc 5' UTR
NcoI 687
Amp^r

pGL3utr
5665 bp

Fluc

Enhancer SV40 poly (A)
XbaI 2343

SV40 promoter
Poly(A)
fl ori
Intron
Rluc
Amp^r

pGL3Rhrv
7070 bp

SpeI 1490
HRV 5' UTR
NcoI 2092

Fluc

Enhancer
SV40 poly(A)
XbaI 3748

1. Digest pGL3utr and pGL3Rhrv with SpeI/XbaI
2. Isolate Fluc fragments and fill-in ends
3. Insert into pSP64R Poly(A) at SmaI site

SP6 promoter
Rluc

pSP64R Poly(A)
3986 bp

XbaI 975
SmaI 988
(dA:dT)(30)
EcoRI 1032

Amp^r

SP6 promoter
Rluc

XbaI 975
c-myc 5' UTR
NcoI 1405

Amp^r

pSP64RutrL Poly(A)
6057 bp

Fluc

EcoRI 3110
(dA:dT)(30)

SP6 promoter
Rluc

XbaI 975
HRV 5' UTR
NcoI 1596

Amp^r

pSP64RhrvL Poly(A)
6248 bp

Fluc

EcoRI 3301
(dA:dT)(30)

Figure 4.12: Construction of the c-*myc* 5' UTR- and HRV IRES-containing dicistronic plasmids, pSP64RutrL Poly(A) and pSP64RhrvL Poly(A). DNA fragments containing the Fluc gene, fused to either the sequence encoding the c-*myc* 5' UTR or HRV IRES, were excised from pGL3utr or pGL3Rhrv, respectively, by digesting with *Spe*I and *Xba*I. After filling in the recessed 3' ends, these fragments were inserted into pSP64R Poly(A) at the *Sma*I site creating the plasmids pSP64utrL Poly(A) or pSP64hrvL Poly(A). These plasmids were digested with *Eco*RI and used as templates to synthesise dicistronic mRNAs terminating in a Poly(A) tail. In vitro transcription reactions were performed using SP6 RNA polymerase.

expression from the upstream and downstream cistrons was monitored (fig. 4.13b and c). In cells transfected with the control dicistronic transcript, Rluc, the *Renilla* luciferase cistron was translated efficiently, whilst little expression of the downstream cistron was observed (fig. 4.13b and c, compare Rluc RL to Rluc FL). Insertion of the HRV2 IRES between the two cistrons resulted in a 52-fold stimulation of firefly luciferase activity when compared to the expression due to readthrough-reinitiation (fig. 4.13c, compare RhrvL FL to Rluc FL). This figure compares favourably with the 100-fold activation of downstream cistron expression observed in TK143 cells using the HRV14 IRES (Roberts *et al.*, 1998). In contrast, the expression of the downstream cistron was only enhanced by 1.4 fold on the RutrL transcript (fig. 4.13b, compare RutrL FL to Rluc FL). Thus, the c-*myc* 5' UTR cannot stimulate the translation of the downstream cistron on a dicistronic mRNA introduced directly into the cytoplasm.

In summary, both the HRV and c-*myc* IRESes are able to promote internal initiation on transcripts expressed in the nucleus, however only the HRV element is capable of performing this task on mRNAs that do not originate in this compartment. The high level of expression achieved with the T7/vaccinia system represented one possible reason why the c-*myc* IRES failed to stimulate downstream cistron activity in the cytoplasm. However, the use of RNA transfection, which results in the accumulation of considerably less RNA in this compartment, produced very similar results. Hence, these data suggest that a nuclear event could be a pre-requisite for efficient c-*myc* 5' UTR-driven internal initiation.

4.7 A preliminary investigation of the c-*myc* 5' UTR-binding proteins located in the nuclear compartment

One model that would satisfy the data accumulated thus far on the function of the c-*myc* IRES posits that a nuclear *trans*-acting factor may influence the activity of this element. Interestingly, using gel shift and ultraviolet crosslinking assays two predominantly nuclear proteins, La and PTB, have been identified as picornavirus RNA binding proteins (Meerovitch *et al.*, 1989; Borman *et al.*, 1993; Hellen *et al.*, 1993). Furthermore, these factors have been shown to alter the efficiency of certain IRESes (Meerovitch *et al.*, 1993; Kaminski *et al.*, 1995). However, neither of these proteins interacts specifically with the c-*myc* 5' UTR (Paulin, 1997). Therefore, an ultraviolet crosslinking assay was employed to identify nuclear proteins that could form specific complexes with the c-*myc* 5' UTR.
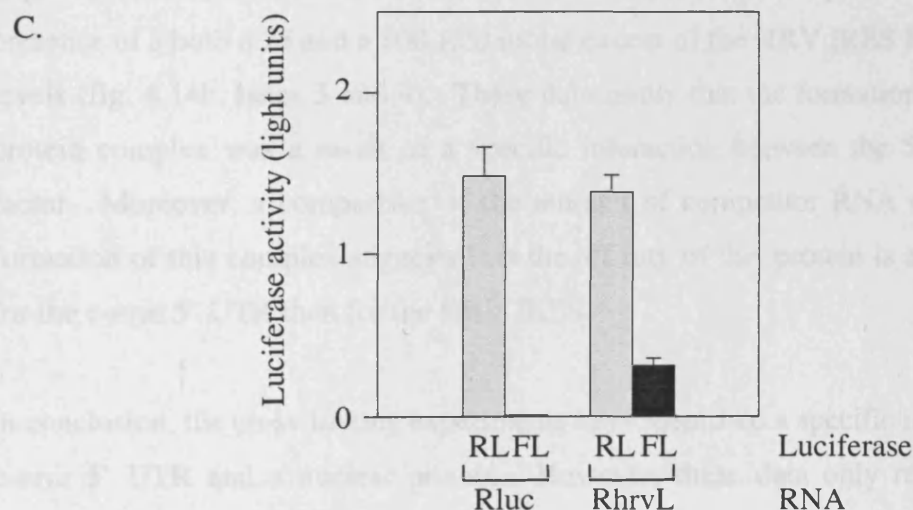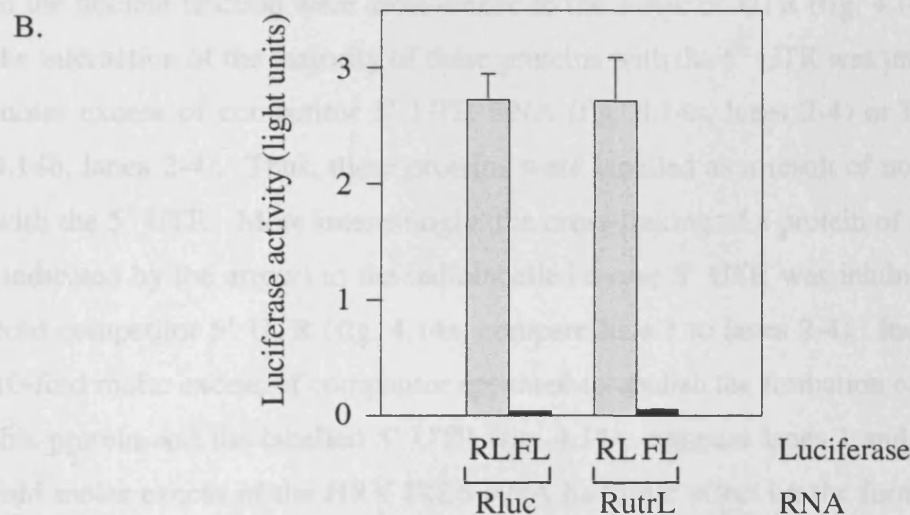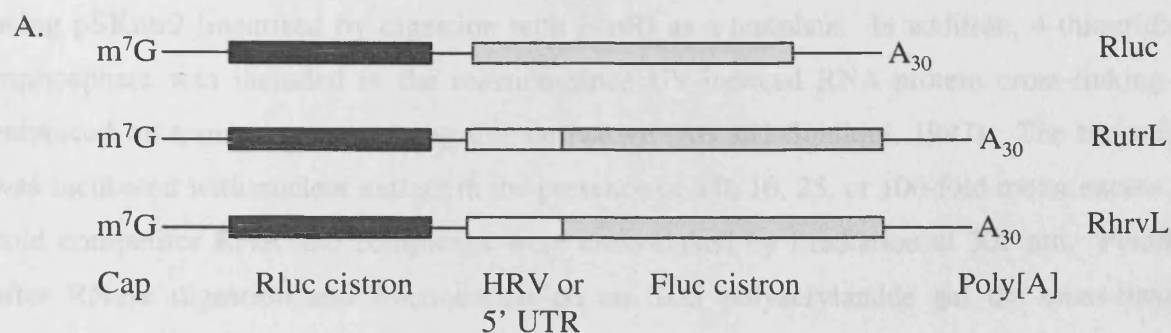
Figure 4.13: A comparison of the efficiency of c-*myc* 5' UTR and HRV IRES-directed internal initiation on mRNAs introduced directly into the cytoplasm. (A) A diagrammatic representation of the control dicistronic mRNA, Rluc, the c-*myc* 5' UTR-containing mRNA, RutrL, and the HRV IRES-containing mRNA, RhrvL. (B) HeLa cells were transfected with Rluc or RutrL by lipofection. After 8 hours *Renilla* and firefly luciferase expression was determined (RL and FL, respectively). (C) Similarly, HeLa cells were transfected with Rluc or RhrvL and luciferase activity was measured.

A radiolabelled transcript containing the entire c-*myc* P2 5' UTR was synthesised *in vitro* using pSKutr2 linearised by digestion with *Eco*RI as a template. In addition, 4-thiouridine triphosphate was included in the reaction since UV-induced RNA-protein cross-linking is enhanced on transcripts containing this derivative (Ali and Siddiqui, 1997). The transcript was incubated with nuclear extract in the presence of a 0, 10, 25, or 100-fold molar excess of cold competitor RNA and complexes were cross-linked by irradiation at 302 nm. Finally, after RNase digestion and fractionation on an SDS polyacrylamide gel the cross-linked proteins were visualised by phosphorimager analysis (fig. 4.14). Numerous proteins present in the nuclear fraction were cross-linked to the c-*myc* 5' UTR (fig. 4.14a, lane 1). However, the interaction of the majority of these proteins with the 5' UTR was unaffected by a 100-fold molar excess of competitor 5' UTR RNA (fig. 4.14a, lanes 2-4) or HRV IRES RNA (fig. 4.14b, lanes 2-4). Thus, these proteins were labelled as a result of non-specific interactions with the 5' UTR. More interestingly, the cross-linking of a protein of approximately 98 kDa (indicated by the arrow) to the radiolabelled c-*myc* 5' UTR was inhibited by the presence of cold competitor 5' UTR (fig. 4.14a, compare lane 1 to lanes 2-4). Indeed, the addition of a 10-fold molar excess of competitor appeared to abolish the formation of the complex between this protein and the labelled 5' UTR (fig. 4.14a, compare lanes 1 and 2). In contrast, a 10-fold molar excess of the HRV IRES RNA had little effect on the formation of this complex (fig. 4.14b, compare lanes 1 and 2). Furthermore, 98 kDa complex was also detected in the presence of a both a 25 and a 100-fold molar excess of the HRV IRES RNA, albeit at reduced levels (fig. 4.14b, lanes 3 and 4). These data imply that the formation of the 98 kDa RNA-protein complex was a result of a specific interaction between the 5' UTR and a nuclear factor. Moreover, a comparison of the amount of competitor RNA required to inhibit the formation of this complex suggests that the affinity of this protein is at least 10-fold greater for the c-*myc* 5' UTR than for the HRV IRES.

In conclusion, the cross-linking experiments have identified a specific interaction between the c-*myc* 5' UTR and a nuclear protein. However, these data only represent a preliminary investigation of potential 5' UTR-nuclear protein complexes. Therefore, further studies will be required to assess whether the formation of this complex influences the activity of the c-*myc* IRES.
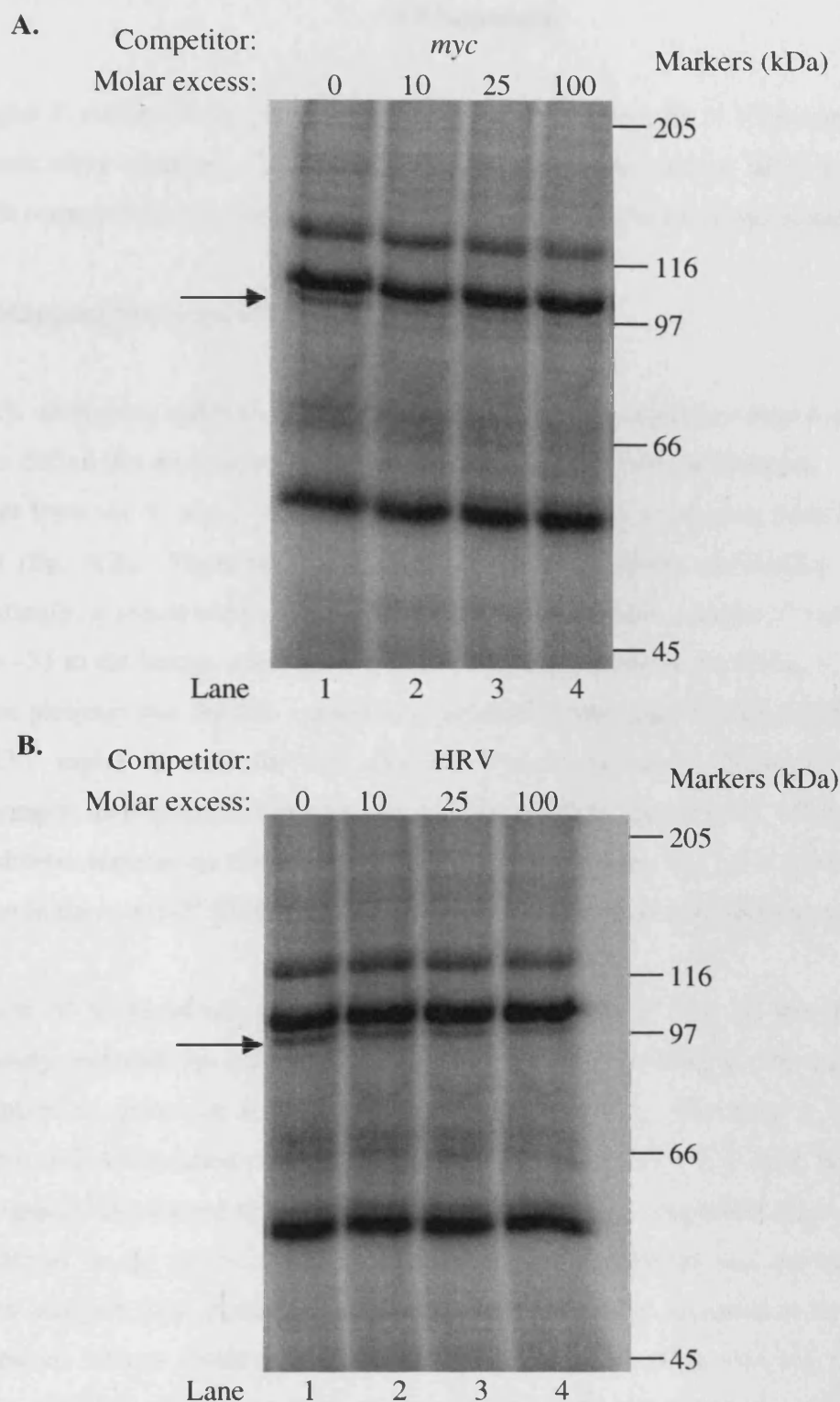
Figure 4.14: RNA-protein complexes formed between the c-*myc* 5' UTR and HeLa nuclear proteins. A radiolabelled 4-thioUTP-containing c-*myc* 5' UTR transcript was incubated with HeLa nuclear extract in the presence of increasing amounts of either (A) c-*myc* 5' UTR or (B) HRV IRES cold competitor RNA. Proteins were cross-linked by irradiation with UV light (302 nm). Following RNase treatment, labelled complexes were fractionated on SDS/polyacrylamide gels and detected using phosphorimager analysis. The position of the 98 kDa complex is indicated with an arrow.

4.8 Summary

In chapter 3, evidence was presented indicating that the c-*myc* P2 5' UTR contains an internal ribosome entry segment. Therefore, the function of this putative IRES was examined to provide some insight into the mechanism of translation mediated by this element.

4.8.1 Mapping the c-*myc* IRES

Initially, dicistronic mRNAs containing truncated 5' UTR sequences were expressed in HeLa cells to define the minimum element required to mediate internal initiation. Deletions of 56 or 84 nt from the 5' and 3' ends, respectively, reduced the expression from the downstream cistron (fig. 4.2). Thus, the c-*myc* IRES is located between nucleotides –396 and –57. Interestingly, a conserved polypyrimidine tract, situated at the extreme 3' end of the 5' UTR (-40 to –33 in the human sequence), does not form part of this element (fig. 4.15, underlined). In some picornavirus IRESes a conserved polypyrimidine tract located 20-25 nt upstream of an AUG triplet is essential for efficient internal initiation (Pilipenko *et al.*, 1992). Furthermore, an oligopyrimidine sequence at the 3' end of the eIF4G 5' UTR is necessary for IRES-driven translation (Gan *et al.*, 1998). Nevertheless, the tract present in a similar position in the c-*myc* 5' UTR does not appear to function in an analogous manner.

Mutation of a conserved upstream AUG codon at the 3' end of the poliovirus IRES profoundly reduced the efficiency of internal initiation leading to the suggestion that it participates in ribosome binding (Pilipenko *et al.*, 1992). Similarly, a conserved CUG initiation codon is located at the distal end of the c-*myc* 5' UTR (fig. 4.15, boxed region). It was originally considered that this element could perform a comparable function to that of the AUG triplet in the poliovirus IRES. However, this hypothesis was not supported by the deletion analysis data, since the removal of the CUG triplet appeared to have no effect on downstream cistron expression. Nevertheless, it was possible that the function of this element was replaced by a CUG codon derived from the polylinker region of pGL3R. Furthermore, this triplet was surrounded by a similar sequence context to the original CUG. Consequently, to resolve this issue the authentic CUG-initiation codon was mutated to CUC. This mutant 5' UTR was as effective as the wild-type sequence at promoting downstream cistron expression (fig. 4.3). Therefore, in conjunction with the deletion analysis this data indicates that the CUG-initiation codon is unlikely to play a significant role in c-*myc* 5' UTR-mediated internal initiation.

Figure 4.15: Alignment of the human *c-myc* 5'UTR encoding sequence with those of gibbon, marmoset, pig, cat, woodchuck, mouse, rat, and sheep performed using the program, clustalW (generated by J. P. C. le Quesne). Shaded areas represent conserved positions, whilst the position of the CUG initiation codon and polypyrimidine tract are indicated with a box and a line, respectively

In conclusion, the deletion and mutational analysis revealed that elements within the −396 to −57 region are responsible for the stimulation of downstream cistron expression. Furthermore, unlike the picornavirus IRESes deletions within the c-myc element did not completely abolish internal initiation. However, whether a mechanistic distinction between the c-myc IRES and those of the picornaviruses underlies this observation is disputable. An alternative hypothesis suggests that readthrough-reinitiation could be responsible for the residual activity observed once IRES function has been ablated. Thus, these experiments must be repeated under circumstances where cap-dependent translation is downmodulated to distinguish between these possibilities.

4.8.2 Evidence for a nuclear event

Two distinct methods, RNA transfection and the T7/vaccinia system, were used to introduce dicistronic mRNAs into the cytoplasmic compartment and consequently bypass the nucleus. The experiments demonstrated that the c-myc 5' UTR did not stimulate downstream cistron expression on mRNAs that lack a nuclear origin. In contrast, the ability of the HRV2 IRES to promote internal initiation appeared to be independent of the history of the mRNA (compare fig. 4.10 and 4.13). It is also interesting to note that in a cytoplasmic HeLa cell extract, the murine c-myc 5' UTR does not direct efficient translation from the downstream cistron of a dicistronic mRNA (Pelletier and Sonenberg, 1988). These data are consistent with a model in which the activity of the c-myc IRES is dependent on a prior nuclear event. The nature of this event is unknown, however two different models can be envisaged. Transcription in the nucleus could result in the recruitment of trans-acting factors to the IRES that are subsequently involved in cytoplasmic translation initiation (Iizuka et al., 1995). Alternatively, nuclear processes could be essential to achieve a functional IRES structure.

Thus, the requirement for a nuclear event represents a fundamental difference between the function of the c-myc IRES and those of the picornaviruses. In addition, a direct comparison between the c-myc and HRV IRESes revealed that downstream cistron expression is enhanced approximately 7-fold more by the former than the latter (fig. 4.10). Therefore, it is clear that under these conditions the c-myc IRES is an efficient translational element.

4.8.3 Evidence for *trans*-acting factors

The activity of the c-*myc* IRES has been analysed in a variety of cultured cells from different origins. These experiments demonstrated that the efficiency of downstream cistron translation mediated by the 5' UTR varies in a cell-type specific manner (fig. 4.5). Unfortunately, the range of cell lines investigated thus far limits the conclusions that can be drawn from these data. However, the fact that the IRES functioned inefficiently in both a human (MCF7) and a murine (Balb/c-3T3) cell line suggests that both the cell-type and/or the species from which the line was cultured could be determinants of IRES activity. In addition, the translational efficiency of a heterologous reporter mRNA bearing the 5' UTR was examined in both MCF7 and Balb/c-3T3 cells. Despite, the poor function of the IRES in these cells, the 5' UTR did not inhibit the translation of the transcript (fig. 4.6). These data support the contention that the c-*myc* P2 mRNA could be translated by both cap-dependent and internal initiation mechanisms.

The cell-type specific variation in IRES activity implied that a *trans*-acting factor could be a critical regulator of the function of this element. Indeed, the IRESes of the entero- and rhinoviruses, which are known to require non-canonical translation factors, also display a range of activity in cell lines from different origins (Borman *et al.*, 1997; Roberts *et al.*, 1998). In addition, the expression of dicistronic mRNAs under the control of the powerful CMV promoter/enhancer region abolished the function of the c-*myc* IRES (fig. 4.8). One possible interpretation is that overexpression of dicistronic 5' UTR-containing transcripts interfered with the activity of an essential factor. However, in order to confirm this hypothesis dicistronic mRNAs must be expressed using a range of promoters of increasing strength. These experiments will determine whether c-*myc* 5' UTR-mediated internal initiation can be saturated in a similar manner to entero- and rhinovirus IRES-driven translation (Borman *et al.*, 1997).

Finally, UV crosslinking experiments have identified a specific complex between a nuclear protein of approximately 98 kDa and the c-*myc* 5' UTR. Although, this protein also binds to the HRV IRES, its affinity for the 5' UTR is at least 10-fold greater. Clearly, these preliminary binding studies provide no information about the potential function of the complex. Therefore, it will be of great interest to determine whether this complex can be formed using nuclear extract derived from either MCF7 or Balb/c-3T3 cells. Furthermore,

these cross-linking studies must be combined with a functional assay to determine the relevance of this complex to c-*myc* 5' UTR-mediated internal initiation.

Chapter 5

In vitro studies on the c-_myc_ 5' leader sequences

5.1 Introduction

Micrococcal nuclease-treated reticulocyte lysates (RRL) have been used successfully to analyse the effect of the murine c-_myc_ 5' UTR on translation initiation (Darveau _et al._, 1985; Parkin _et al._, 1988). However, only limited studies have been performed with the human 5' leader sequences in this system (Parkin _et al._, 1988). Since evidence from the previous chapters suggested that c-_myc_ protein synthesis could potentially involve both the cap-dependent and internal initiation mechanisms, the role of the human 5' UTR was further investigated _in vitro_ using RRL.

5.2 Analysis of internal initiation mediated by the c-_myc_ 5' UTR _in vitro_

The RNA genomes of the picornavirus family are translated by the mechanism of internal initiation (Jackson, 1995). However, not all picornavirus IRESes function efficiently in rabbit reticulocyte lysate (Jackson _et al._, 1995; Belsham and Sonenberg, 1996). Consequently, since there is evidence suggesting that an IRES is present within the 5' UTR of the c-_myc_ mRNA, it was of interest to determine whether the element could mediate internal initiation in this translation system.

The dicistronic reporter plasmids, pGL3R and pGL3Rutr, (see chapter 3; fig. 3.5 and 3.7) have a T7 RNA polymerase recognition sequence upstream of the _Renilla_ luciferase cistron. These plasmids were digested with _Hpa_II and used to generate dicistronic RNAs by _in vitro_ run-off transcription. Figure 5.1a, shows a diagrammatic representation of these transcripts. The control RNA contains the _Renilla_ luciferase and firefly luciferase open reading frames as upstream and downstream cistrons, respectively. As in previous experiments, the c-_myc_ 5' UTR is positioned in the intercistronic region to investigate its ability to mediate internal initiation.

In vitro translation reactions were performed as described in Materials and Methods using 5, 10 and 20 ng/µl of these uncapped RNAs. The products of these reactions were separated by SDS/polyacrylamide gel electrophoresis and visualised using phosphorimager analysis.

Lanes 1-3 of figure 5.1b show the polypeptides synthesised from the control dicistronic transcript. The major translation product, *Renilla* luciferase, migrated at 38 kDa. Whilst, three polypeptides of 62, 64 and 65 kDa were synthesised from the downstream cistron. The most abundant of these, the 62 kDa protein is the correct mass for firefly luciferase, whilst the two larger products may be a result of spurious initiation events. Taking into account the number of labelled amino acids in each polypeptide, approximately 10% of ribosomes reinitiated protein synthesis at the downstream AUG start site. Insertion of the c-*myc* 5' UTR between the two cistrons had no effect on the synthesis of either the 38 kDa or 62 kDa polypeptide (figure 5.1b; lanes 4-6). Hence, translation of the downstream cistron was not stimulated by this element. This data suggests that the 5' UTR does not mediate internal initiation in rabbit reticulocyte lysate.

The transcripts used in the previous experiment did not resemble eukaryotic mRNAs as they lacked both a 7-methylguanylic acid cap structure and a polyadenylate tail. Thus, the ability of the c-*myc* 5' UTR to promote internal ribosome entry was determined on an RNA molecule with either a polyadenylate tail alone or both cap and polyadenylate tail. Control dicistronic transcripts and transcripts containing the 5' UTR in the intercistronic region were generated using the plasmids pSP64Rluc Poly(A) and pSP64RutrLuc Poly(A), respectively (see fig. 4.11 and 4.12). A schematic of the RNAs used is shown in figure 5.2a. Lanes 1 and 2 of figure 5.2b show the translation products synthesised using uncapped transcripts with a polyadenylate tail. On the control transcript, the upstream cistron was translated efficiently, whilst approximately 10% of ribosomes reinitiated at the firefly luciferase initiation codon (fig. 5.2, lane 1). However, the presence of the 5' UTR had no effect on the translation of the downstream cistron (Fluc) (fig. 5.2; compare lanes 1 and 2). A cap structure at the 5' end of the transcript stimulated synthesis of the *Renilla* luciferase by 2.1 fold (s. d. 0.4) (fig. 5.2b; compare lanes 1 and 2 to lanes 3 and 4). Furthermore, capping also resulted in reduced translation of the firefly luciferase cistron compared to the *Renilla* luciferase cistron, with only 3.4 % (s. d. 0.4 %) of ribosomes reinitiating at the downstream cistron (fig. 5.2b, lane 3). Nevertheless, the 5' UTR still did not enhance translation of the downstream cistron on the capped and polyadenylated transcript (fig. 5.2b, compare lane 4 to lane 3). In conclusion, the 5' UTR does not mediate internal initiation on dicistronic mRNAs in rabbit reticulocyte lysate.
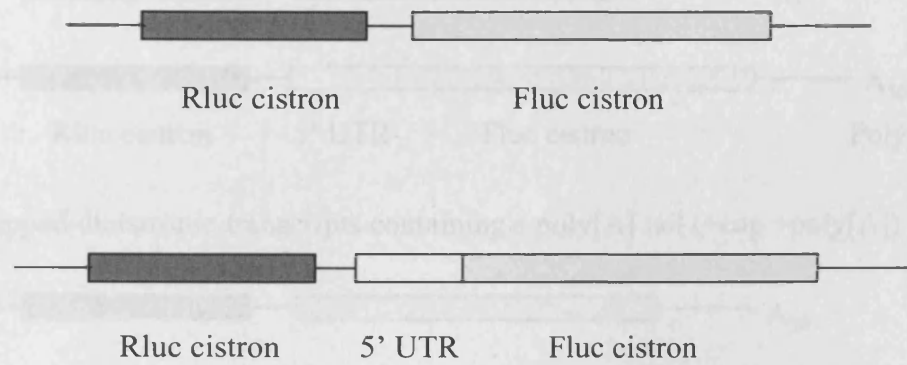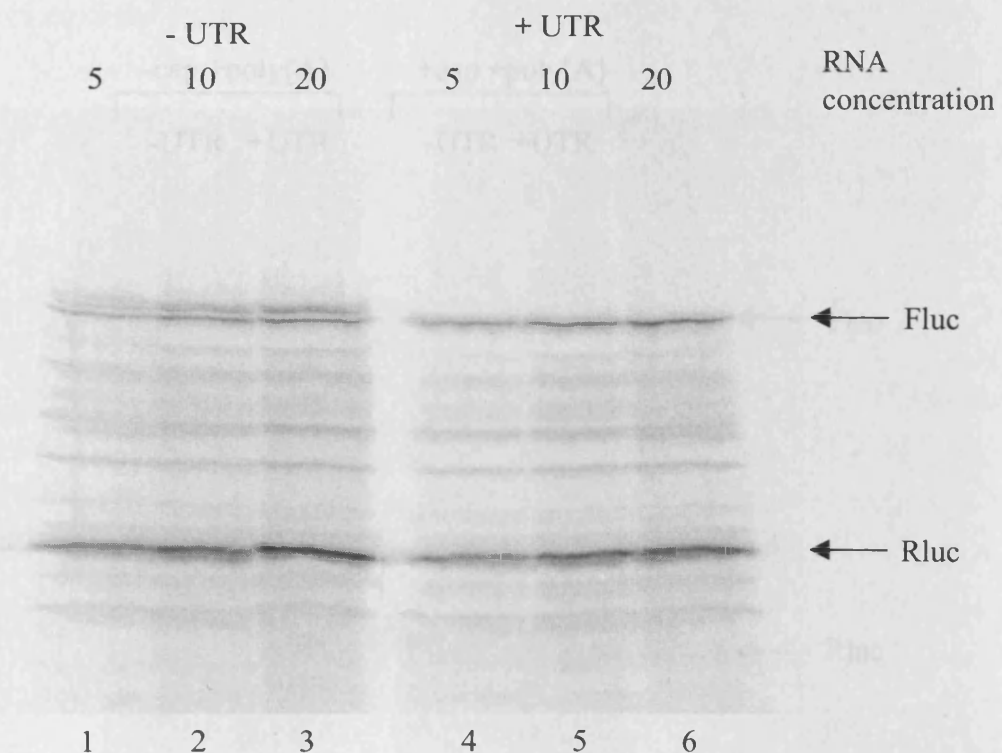
Figure 5.1: Analysis of c-*myc* 5' UTR-driven internal initiation in rabbit reticulocyte lysate (A) A diagrammatic representation of the control and 5' UTR-containing dicistronic transcripts. Transcripts were synthesised by *in vitro* transcription using pGL3R or pGL3Rutr linearised by digestion with *Hpa*I. (B) The radiolabelled polypeptides synthesised from uncapped control (-UTR, lanes 1-3) or 5' UTR-containing (+UTR, lanes 4-6) dicistronic RNAs were detected using phosphorimager analysis. The positions of the 38 kDa *Renilla* luciferase polypeptide (Rluc) and the 62 kDa firefly luciferase polypeptide (Fluc) are indicated.

A(i). Uncapped dicistronic transcripts containing a poly[A] tail (-cap +poly[A])

Rluc cistron   5' UTR   Fluc cistron   Poly[A]
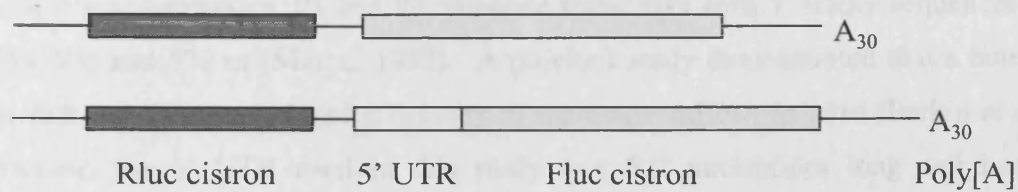
(ii) Capped dicistronic transcripts containing a poly[A] tail (+cap +poly[A])

Cap   Rluc cistron   5' UTR   Fluc cistron   Poly[A]

B.
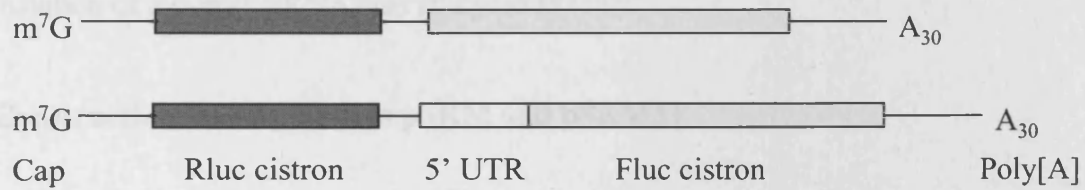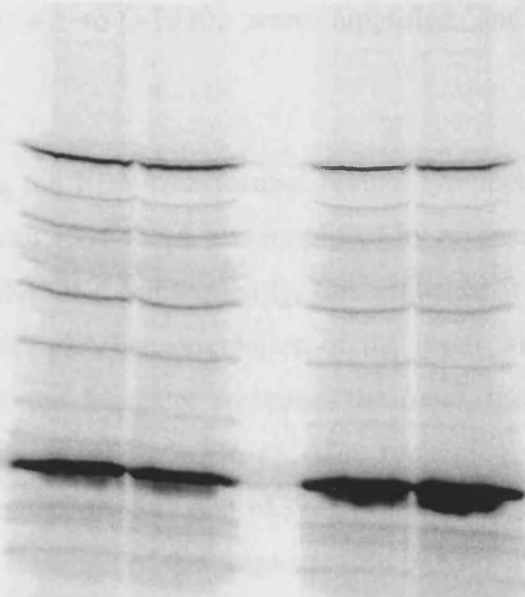
Figure 5.2: The effect of a 5' cap structure and a polyadenylate tail on c-*myc* 5' UTR directed internal initiation in rabbit reticulocyte lysate. (A) A diagrammatic representation of the control (-UTR) and 5' UTR-containing (+UTR) dicistronic transcripts either uncapped and with a poly[A] tail (-cap +poly[A]) or capped and with a poly[A] tail (+cap +poly[A]). Transcripts were synthesised *in vitro* using either pSP64RL Poly[A] or pSP64RutrL Poly[A] linearised with *Eco*RI. (B) Radiolabelled polypeptides synthesised in rabbit reticulocyte lysates programmed with 10 ng/µl of uncapped control or 5' UTR-containing transcripts (lane 1 and lane 2, respectively) or the equivalent capped transcripts (lane 3 and lane 4, respectively). The positions of the 38 kDa *Renilla* luciferase polypeptide (Rluc) and the 62 kDa firefly luciferase polypeptide (Fluc) are indicated.

5.3 The effect of the P2 5' UTR on the translational efficiency of a c-*myc* mRNA

The two major c-*myc* promoters, P1 and P2, generate transcripts with 5' leader sequences of approximately 400 and 570 nt (Marcu, 1992). A previous study demonstrated that a human c-*myc* leader reduces the translational efficiency of the c-*myc* mRNA *in vitro* (Parkin *et al.*, 1988). However, the 5' UTR used in this study was 502 nucleotides long and hence contained approximately 100 nucleotides of the P1 mRNA. Thus, since the P2 5' UTR did not appear to reduce the translational efficiency of a heterologous mRNA *in vivo*, its effect on the translation of a c-*myc* mRNA was analysed *in vitro*.

5.3.1 Construction of the plasmids pSKM and pSKMΔ1

The c-*myc* cDNA sequence from −396 to +1320 was amplified by PCR and inserted into pSK+bluescript. Initial attempts to amplify this sequence from single-stranded DNA failed, possibly due to the structured nature of the RNA template. Therefore, two fragments, from −396 to +6 and from +7 to +1320, were amplified and inserted sequentially into pSK+bluescript.

RNA was isolated from the EBV-transformed normal lymphoblastoid cell line, GM03201, and a DNA fragment from −396 to +6 was amplified by reverse-transcription PCR using the primers FP2501 and MS4526. Subsequently, this sequence was blunt-end ligated into the *Sma*I site of pSK+bluescript. The orientation of the insert was selected such that a CCC triplet at the 3' end of the fragment recreated the *Sma*I site. Figure 5.3 illustrates the construction of this plasmid, pSKM(-396-6). The remaining sequence, +7 to +1320, was amplified using the primers MS4527 and MS7216 from the plasmid pOTS*myc* (Watt *et al.*, 1983). To facilitate the insertion of this fragment into pSKM(-396-6), the recognition site for the enzyme *Eco*RI was included in the 3' primer sequence. Finally after digestion with *Eco*RI, the PCR product was inserted into the plasmid pSKM(-396-6) between the *Sma*I and *Eco*RI restriction sites, thus creating the plasmid pSKM (fig. 5.4)

The control plasmid, pSKMΔ1 contains the c-*myc* cDNA sequence from −56 to +1320 and consequently lacks the majority of exon 1. A 1381 bp DNA fragment was generated by partial digestion of pSKM with *Pvu*II followed by complete digestion with *Eco*RI. Insertion
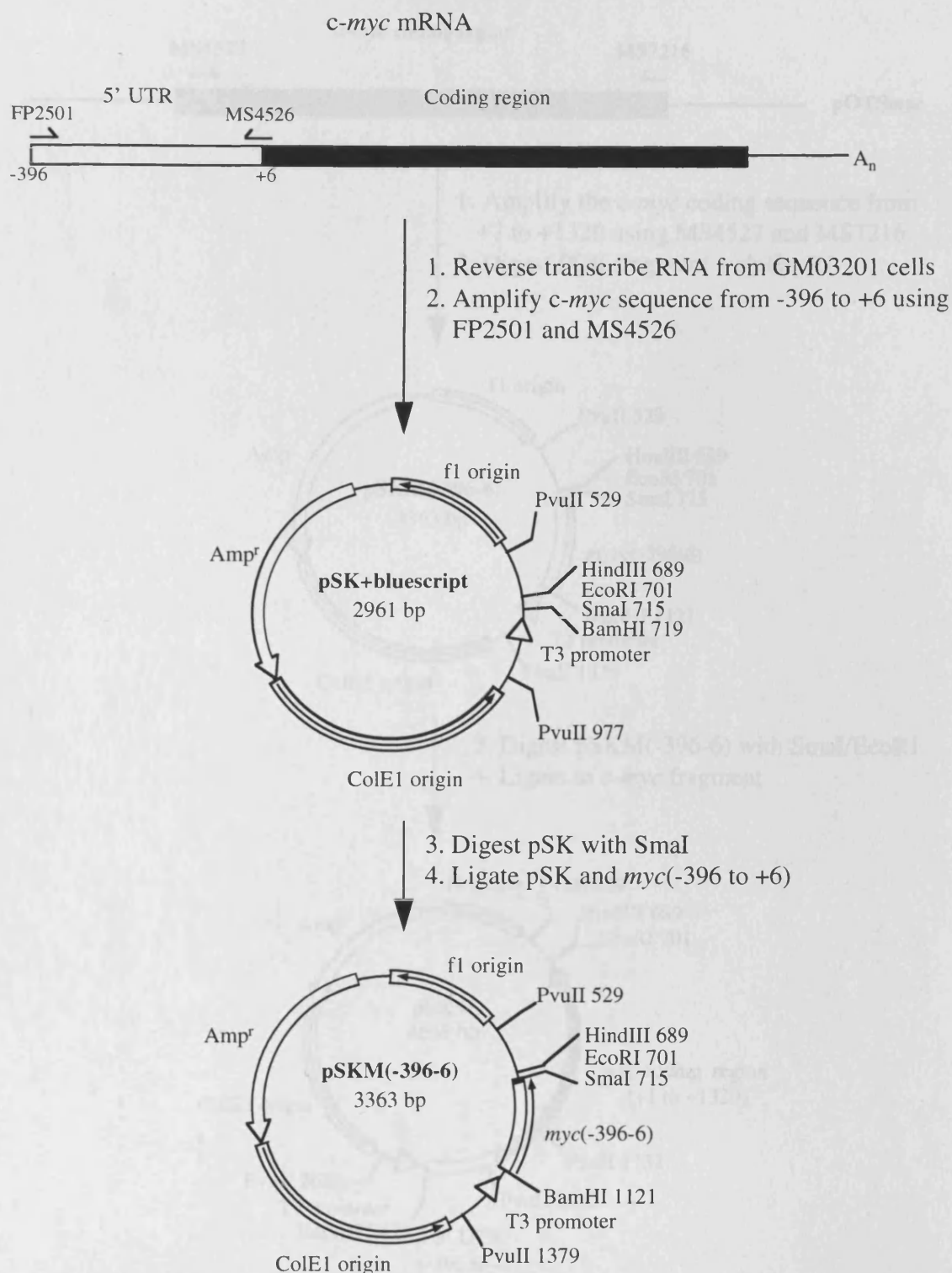
Figure 5.3: Construction of the plasmid pSKM(-396-6). Initially, single stranded DNA was synthesised from total cellular RNA using reverse transcriptase. A fragment encoding nucleotides -396 to +6 of the c-*myc* mRNA was amplified by PCR using the primers FP2501 and MS4526 (see Materials and Methods). This sequence was then inserted into pSK+bluescript at the *Sma*I site creating the plasmid pSKM(-396-6).
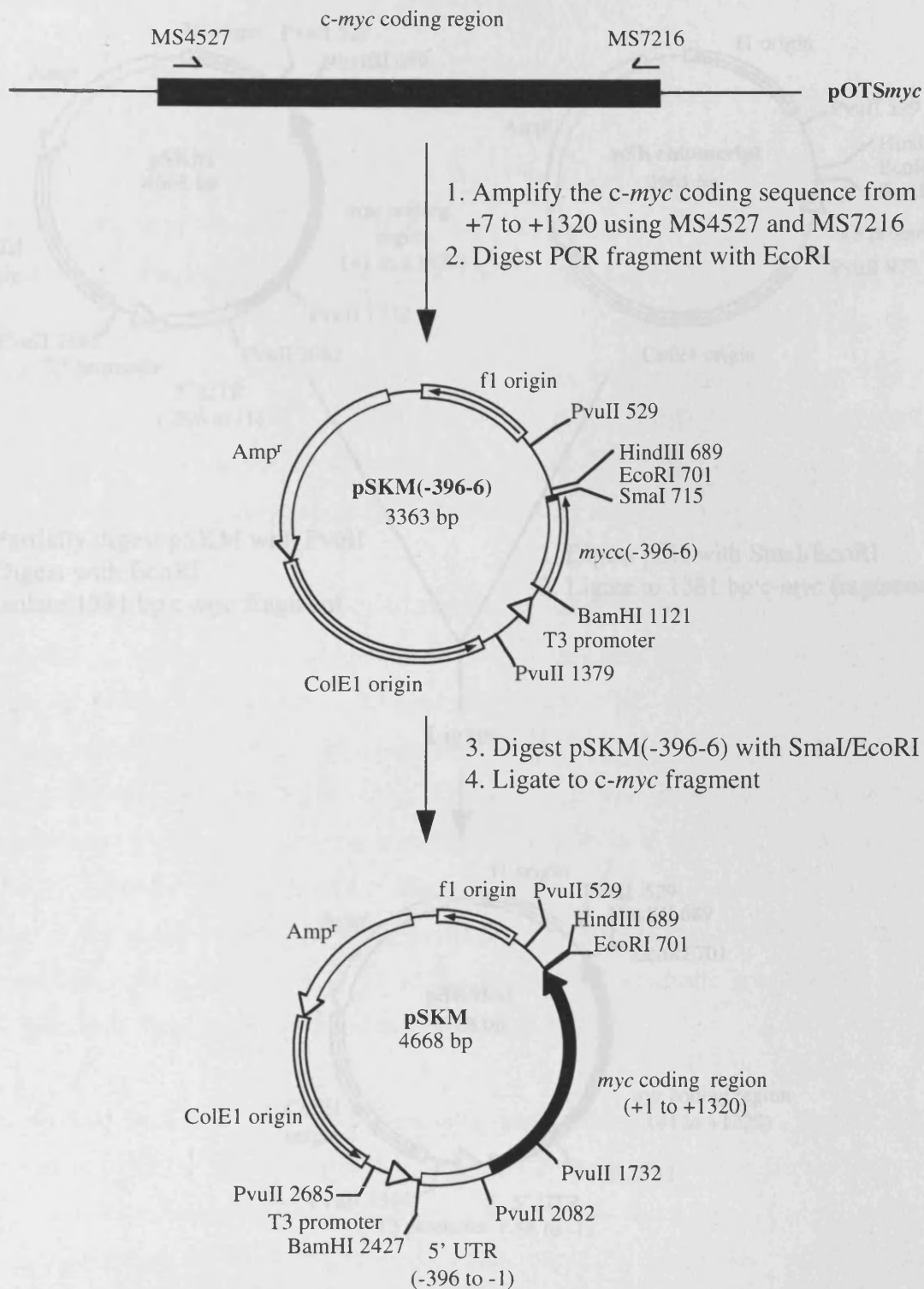
Figure 5.4: Construction of the plasmid, pSKM, containing the human c-*myc* cDNA sequence. A DNA fragment encoding nucleotides +7 to +1320 was amplified from the plasmid pOTS*myc* by PCR using the primers MS4527 and MS7216. After digestion with *Eco*RI, this fragment was inserted into the plasmid pSKM(-396-6) between the *Sma*I and *Eco*RI site. The resulting plasmid pSKM contains the human c-*myc* cDNA sequence from -396 to +1320. PSKM was digested with *Hind*III and used as a template to synthesise c-*myc* transcripts *in vitro* from the T3 promoter.

1. Partially digest pSKM with PvuII
2. Digest with EcoRI
3. Isolate 1381 bp c-*myc* fragment

1. Digest pSK with SmaI/EcoRI
2. Ligate to 1381 bp c-*myc* fragment

Ligate
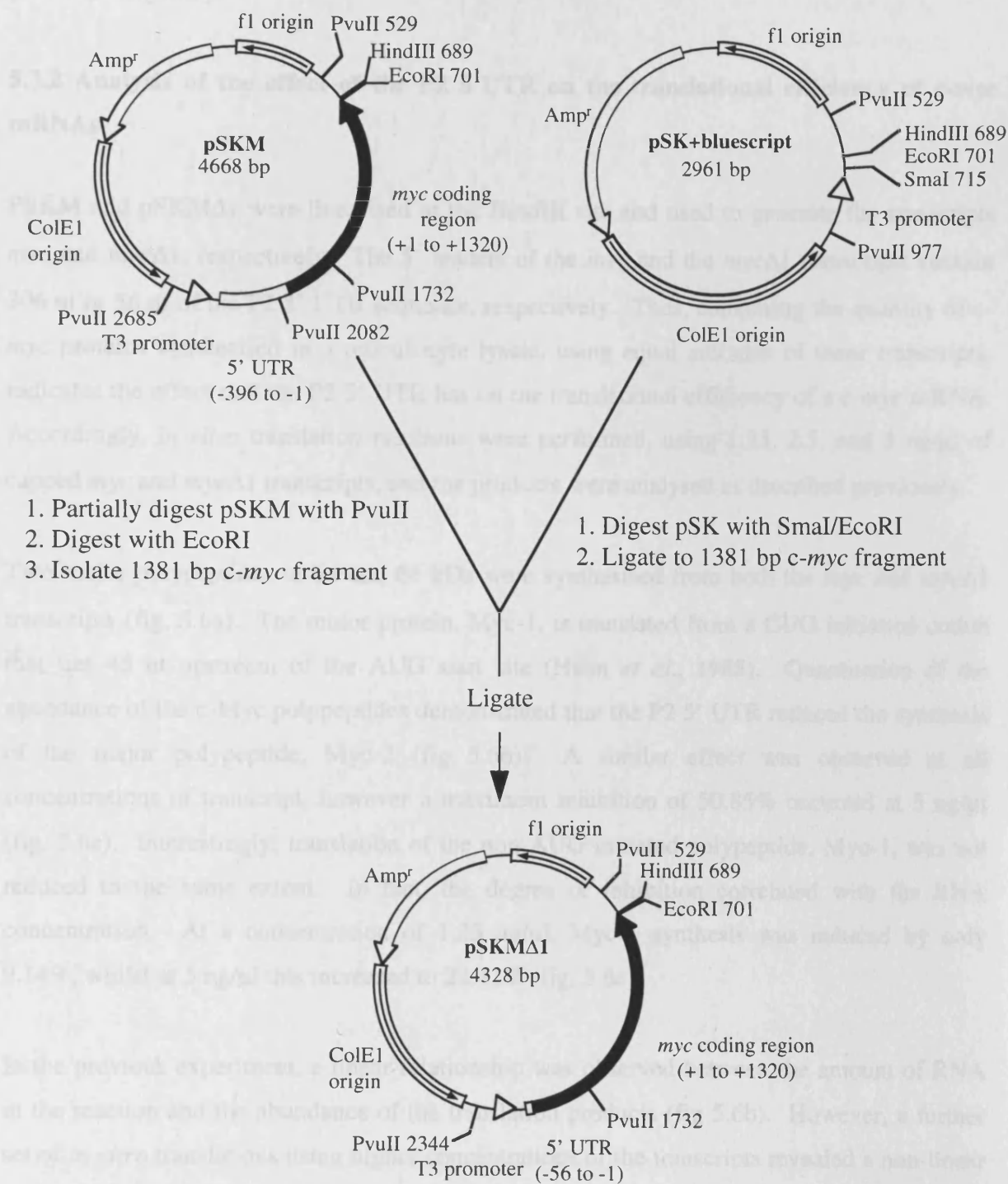
Figure 5.5: Construction of the plasmid pSKMΔ1 containing the human c-*myc* cDNA sequence from -56 to +1320. Initially, the plasmid pSKM was incompletely digested with *Pvu*II. After which it was digested with *Eco*RI and a 1381 bp fragment was isolated. This fragment was inserted into pSK+bluescript between the *Sma*I and *Eco*RI sites. The resulting plasmid, pSKMΔ1 contains the human c-*myc* cDNA sequence from -56 to +1320. PSKMΔ1 was digested with *Hind*III and used as a template to synthesise *myc*Δ1 transcripts from the T3 promoter.

of this sequence between the *SmaI* and *EcoRI* sites of pSK+bluescript produced the plasmid pSKMΔ1 (fig. 5.5).

5.3.2 Analysis of the effect of the P2 5'UTR on the translational efficiency of c-*myc* mRNAs

PSKM and pSKMΔ1 were linearised at the *HindIII* site and used to generate the transcripts *myc* and *mycΔ1*, respectively. The 5' leaders of the *myc* and the *mycΔ1* transcripts contain 396 nt or 56 nt of the P2 5' UTR sequence, respectively. Thus, comparing the quantity of c-*myc* proteins synthesised in a reticulocyte lysate, using equal amounts of these transcripts, indicates the effect that the P2 5' UTR has on the translational efficiency of a c-*myc* mRNA. Accordingly, *in vitro* translation reactions were performed, using 1.25, 2.5, and 5 ng/μl of capped *myc* and *mycΔ1* transcripts, and the products were analysed as described previously.

Two major polypeptides of 64 and 66 kDa were synthesised from both the *myc* and *mycΔ1* transcripts (fig. 5.6a). The minor protein, Myc-1, is translated from a CUG initiation codon that lies 45 nt upstream of the AUG start site (Hann *et al.*, 1988). Quantitation of the abundance of the c-Myc polypeptides demonstrated that the P2 5' UTR reduced the synthesis of the major polypeptide, Myc-2 (fig 5.6b). A similar effect was observed at all concentrations of transcript, however a maximum inhibition of 50.85% occurred at 5 ng/μl (fig. 5.6c). Interestingly, translation of the non-AUG initiated polypeptide, Myc-1, was not reduced to the same extent. In fact, the degree of inhibition correlated with the RNA concentration. At a concentration of 1.25 ng/μl, Myc-1 synthesis was reduced by only 9.14%, whilst at 5 ng/μl this increased to 22.41% (fig. 5.6c).

In the previous experiment, a linear relationship was observed between the amount of RNA in the reaction and the abundance of the translation products (fig 5.6b). However, a further set of *in vitro* translations using higher concentrations of the transcripts revealed a non-linear relationship for both the *myc* and the *mycΔ1* RNAs (fig. 5.7). Under these conditions one or more components of the translation reaction has become limiting. In addition, the effect on the two transcripts was not uniform, but was greater for the *myc* RNA. Thus, raising the *mycΔ1* RNA concentration from 10 to 20 ng/μl resulted in a 30% and 44% increase in Myc-2 and Myc-1 synthesis, respectively. However, no change in the abundance of either Myc-1 or Myc-2 was observed with a similar increase in *myc* RNA concentration (fig. 5.7b).
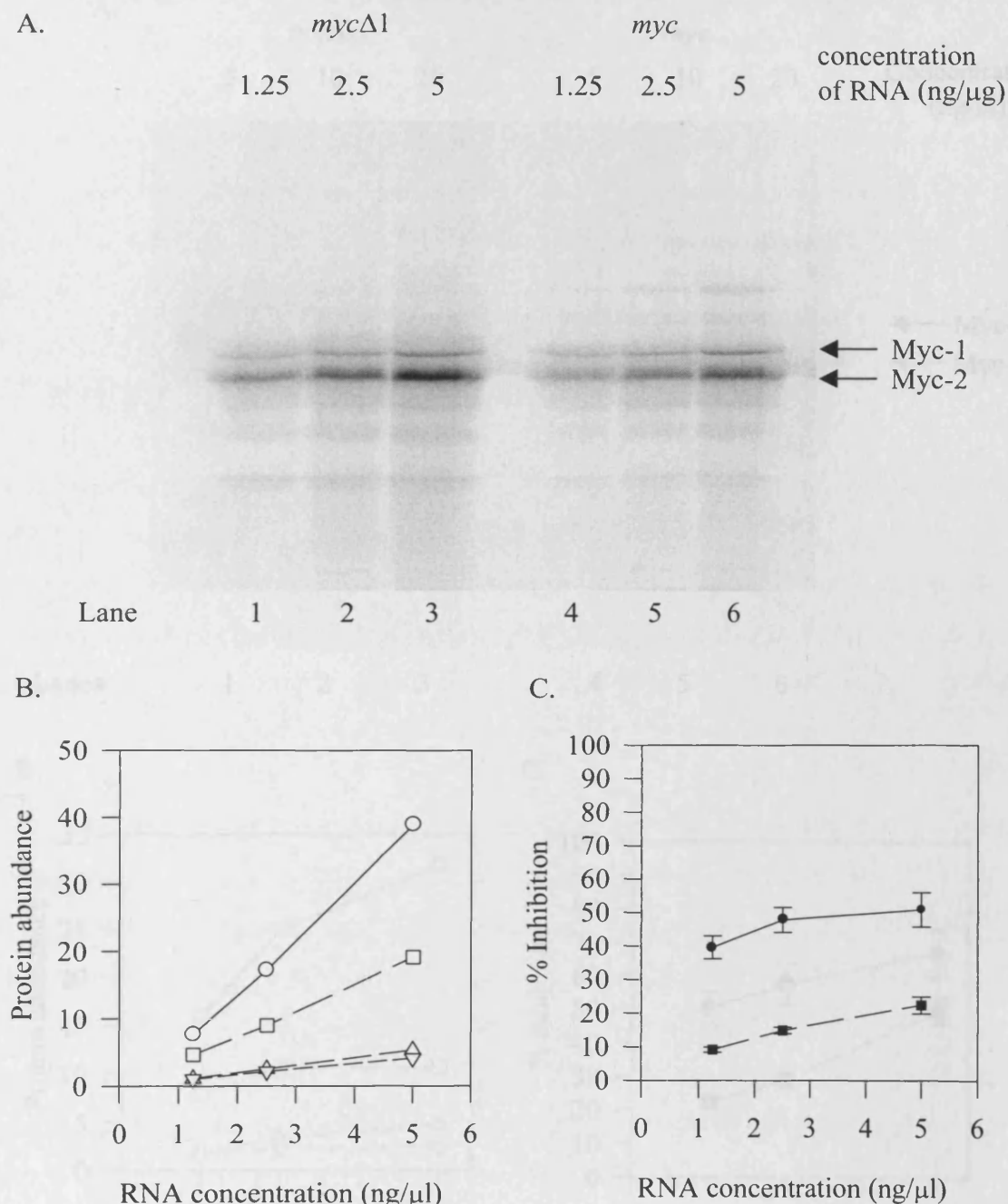
Figure 5.6: Analysis of the translational efficiency of the c-*myc* P2 mRNA *in vitro*. (A) The transcripts *myc* and *myc*Δ1 were synthesised *in vitro* using either *Hind*III digested pSKM or pSKMΔ1, respectively. Radiolabelled polypeptides were fractionated by SDS/PAGE and detected using phosphorimager analysis. Lanes 1-3 and lanes 4-6 show the products of *in vitro* translation reactions using increasing concentrations of *myc*Δ1 or *myc* RNAs, respectively. (B) Quantitation of the polypeptides in (A) using phosphorimager analysis. Myc-2 and Myc-1 synthesis from *myc*Δ1 RNA are represented by [A] and [B], respectively, whilst Myc-2 and Myc-1 synthesis from *myc* are represented by [Γ] and [X], respectively. (C) Average inhibition of Myc-2 (●) and Myc-1 (■) synthesis by the P2 5' UTR from three separate experiments.
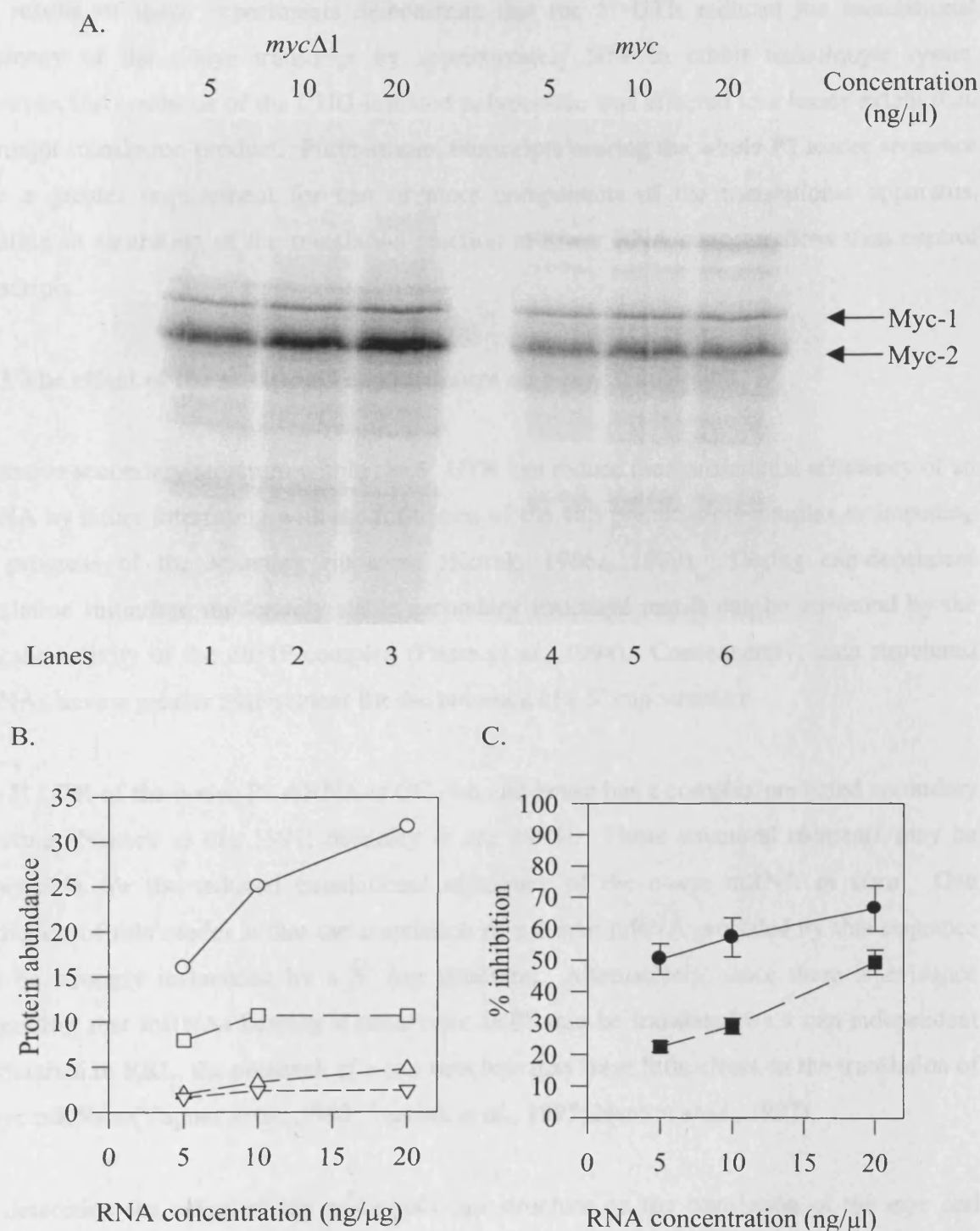
Figure 5.7: Analysis of the translational efficiency of the c-*myc* P2 mRNA at higher RNA concentrations. (A) This experiment was performed as in fig 5.6 except RNA concentrations of 5, 10 and 20 ng/μl were used. (B) Quantitation of the products in (A) using phosphorimager analysis. Myc-2 and Myc-1 synthesis from *myc*Δ1 RNA are represented by [A] and [B], respectively, whilst Myc-2 and Myc-1 synthesis from *myc* are represented [Γ] by and [X], respectively. (C) Average inhibition of Myc-2 (●) and Myc-1 (■) synthesis by the P2 5' UTR from three separate experiments.

The results of these experiments demonstrate that the 5' UTR reduced the translational efficiency of the c-*myc* transcript by approximately 50% in rabbit reticulocyte lysate. However, the synthesis of the CUG-initiated polypeptide was affected to a lesser extent than the major translation product. Furthermore, transcripts bearing the whole P2 leader sequence have a greater requirement for one or more components of the translational apparatus, resulting in saturation of the translation reaction at lower RNA concentrations than control transcripts.

5.3.3 The effect of the m^7GpppG cap structure on c-*myc* translation

Extensive secondary structure within the 5' UTR can reduce the translational efficiency of an mRNA by either interfering with the formation of the 48S preinitiation complex or impeding the progress of the scanning ribosome (Kozak, 1986a, 1989). During cap-dependent translation initiation, moderately stable secondary structural motifs can be unwound by the helicase activity of the eIF4F complex (Pause *et al.*, 1994). Consequently, such structured mRNAs have a greater requirement for the presence of a 5' cap structure.

The 5' UTR of the c-*myc* P2 mRNA is GC rich and hence has a complex predicted secondary structure (Nanbru *et al.*, 1997; Stoneley *et al.*, 1998). These structural elements may be responsible for the reduced translational efficiency of the c-*myc* mRNA *in vitro*. One prediction of this model is that the translation of a c-*myc* mRNA preceded by this sequence will be strongly influenced by a 5' cap structure. Alternatively, since there is evidence suggesting that mRNAs bearing a eukaryotic IRES can be translated by a cap-independent mechanism in RRL, the presence of a cap structure may have little effect on the translation of c-*myc* mRNAs (Vagner *et al.*, 1995; Teerink *et al.*, 1995; Nanbru *et al.*, 1997).

To determine the effect of the m^7GpppG cap structure on the translation of the *myc* and *myc*Δ1 RNAs, rabbit reticulocyte lysate was programmed with 5 ng/μl of uncapped or capped transcripts. The radiolabelled products of these reactions were analysed as described before (fig. 5.8a). As expected, capping the *myc*Δ1 RNA stimulated the synthesis of Myc-2 and Myc-1 by 2.4 and 2.1 fold (s. d. 0.31 and 0.25), respectively (fig. 5.8; compare lanes 1 and 2). This modest increase is consistent with the previously reported values for relatively unstructured mRNAs (Muthukrishnan *et al.*, 1976; Lodish and Rose, 1977; Svitkin *et al.*, 1996). The 5' UTR inhibited the synthesis of the AUG and CUG-initiated polypeptides by 91.7 and 87.4 % (s. d. 5.2 % and 4.7 %), respectively, on uncapped transcripts (compare lanes

A.

mycΔ1　　myc　　transcript

−　　+　　−　　+　　+/- cap

← Myc-1
← Myc-2

Lanes　　1　　2　　3　　4

B.
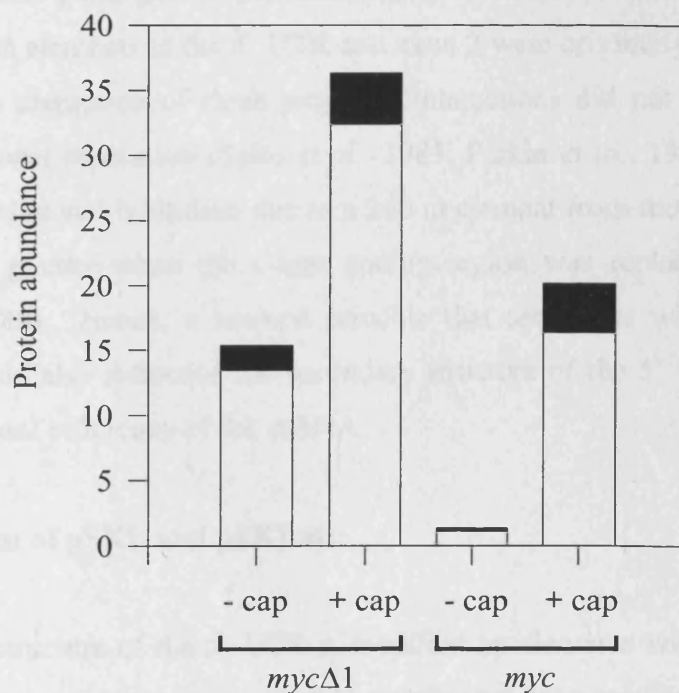
Figure 5.8: The effect of the 5' cap structure on the translation of the c-*myc* P2 transcript. (A) Uncapped (-) and capped (+) *myc*Δ1 and *myc* transcripts were synthesised as described previously. Reticulocyte lysates were programmed with 5 ng/µl of uncapped or capped   *myc*Δ1 or *myc* RNA. Radiolabelled polypeptides synthesised in these reactions were fractionated using SDS/PAGE and detected using phosphorimager analysis. (B) Quantitation of the polypeptides in (A) using phosphorimager analysis. Unshaded and shaded areas refer to the abundance of Myc-2 polypeptides and Myc-1 polypeptides, respectively.

1 and 3). However, the presence of a cap structure on the *myc* RNA enhanced the translation of both Myc-2 and Myc-1 by 14.6 and 16.1 fold, respectively (fig. 5.8; compare lanes 3 and 4). Thus compared to *myc*Δ1, the cap-dependent stimulation of translation on the *myc* RNA was significantly greater.

In summary, in the absence of a 5' cap the translational efficiency of the *myc* transcript was strongly attenuated by the structured P2 5' UTR. Nevertheless, much of this repression was relieved by the m^7GpppG cap structure. Hence, translation initiation on the P2 c-*myc* transcript is strongly dependent on the 5' cap.

5.4 The effect of the c-*myc* P2 5' UTR on the translation of a heterologous mRNA

Having established that sequences within the 5' UTR modulate the *in vitro* translational efficiency of the c-*myc* P2 transcript, it was of interest to determine whether elements within the coding region also participate in the formation of secondary structural motifs. Long range interaction between elements in the 5' UTR and exon 2 were originally postulated by Saito *et al*. However, the disruption of these proposed interactions did not alleviate the 5' UTR-mediated translational repression (Saito *et al.*, 1983; Parkin *et al.*, 1988). Nevertheless, the magnitude of translational inhibition due to a 240 nt element from the murine c-*myc* 5' UTR was significantly greater when the c-*myc* coding region was replaced with that of CAT (Parkin *et al.*, 1988). Hence, it seemed possible that sequences within the human c-*myc* coding region could also influence the secondary structure of the 5' UTR and consequently alter the translational efficiency of the mRNA.

5.4.1 Construction of pSKL and pSKLutr

If the secondary structure of the 5' UTR is modified by elements within exon 2 and 3 then substitution of the c-*myc* coding region for a heterologous open reading frame should alter the effect of this leader. Alternatively, the structure of the 5' UTR may be independent of the coding region and consequently it should downmodulate the translation of a chimeric RNA to the same extent as the endogenous RNA. Thus, the plasmids pSKL and pSKLutr were created to investigate the role of the c-*myc* coding region (fig. 5.9). Essentially, a DNA fragment containing the firefly luciferase coding region was excised from pGL3 using the restriction enzymes *Hind*III and *Xba*I. This sequence was inserted into pSK+bluescript at the *Hind*III and *Xba*I sites creating pSKL. Likewise, a DNA fragment containing the firefly
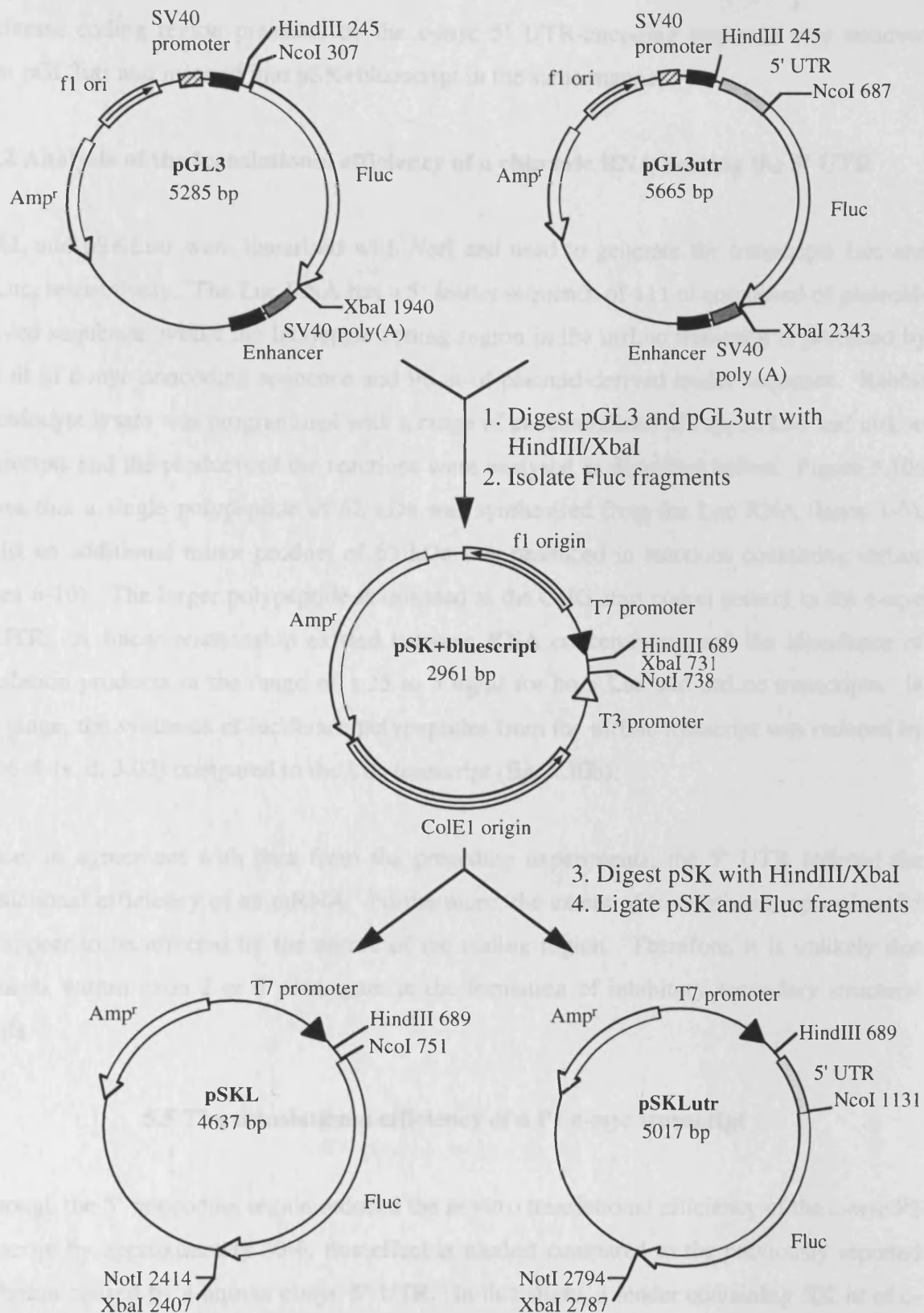
Figure 5.9: Construction of the plasmids pSKL and pSKLutr. DNA fragments containing either the Fluc open reading frame or the Fluc open reading frame fused to the c-*myc* 5' UTR, were excised from pGL3 or pGL3utr, respectively, by digesting with *Hind*III and *Xba* I. These fragments were inserted into pSK+bluescript between the *Hind*III and *Xba* I sites, creating pSKL and pSKLutr. Both plasmids were digested with *Not*I and used as templates to synthesise transcripts from the T7 promoter. In this manner luciferase transcripts or luciferase transcripts bearing the 5' UTR were generated.

luciferase coding region preceded by the c-*myc* 5' UTR-encoding sequence was removed from pGL3utr and inserted into pSK+bluescript in the same manner.

5.4.2 Analysis of the translational efficiency of a chimeric RNA bearing the 5' UTR

PSKL and pSKLutr were linearised with *Not*I and used to generate the transcripts Luc and utrLuc, respectively. The Luc RNA has a 5' leader sequence of 111 nt composed of plasmid-derived sequence, whilst the luciferase coding region in the utrLuc transcript is preceded by 396 nt of c-*myc* noncoding sequence and 96 nt of plasmid-derived leader sequence. Rabbit reticulocyte lysate was programmed with a range of concentrations of capped Luc and utrLuc transcripts and the products of the reactions were analysed as described before. Figure 5.10a shows that a single polypeptide of 62 kDa was synthesised from the Luc RNA (lanes 1-5), whilst an additional minor product of 63 kDa was produced in reactions containing utrLuc (lanes 6-10). The larger polypeptide is initiated at the CUG start codon present in the c-*myc* 5' UTR. A linear relationship existed between RNA concentration and the abundance of translation products in the range of 1.25 to 5 ng/μl for both Luc and utrLuc transcripts. In this range, the synthesis of luciferase polypeptides from the utrLuc transcript was reduced by 50.06 % (s. d. 3.02) compared to the Luc transcript (fig. 5.10b).

Hence, in agreement with data from the preceding experiments, the 5' UTR reduced the translational efficiency of an mRNA. Furthermore, the extent of translational repression did not appear to be affected by the nature of the coding region. Therefore, it is unlikely that elements within exon 2 or 3 participate in the formation of inhibitory secondary structural motifs.

5.5 The translational efficiency of a P1 c-*myc* transcript

Although the 5' noncoding region reduced the *in vitro* translational efficiency of the c-*myc* P2 transcript by approximately 50%, this effect is modest compared to the previously reported inhibition caused by a human c-*myc* 5' UTR. In this study, a leader containing 502 nt of c-*myc* upstream sequence inhibited translation by approximately 90% (Parkin *et al.*, 1988). The discrepancy between these data suggested that sequences upstream of the P2 transcription initiation site could further reduce the translational efficiency of the P1 transcript.

A.

	Luc					utrLuc					Transcript
	1.25	2.5	5	10	20	1.25	2.5	5	10	20	RNA concentration

CUG
AUG

	1	2	3	4	5	6	7	8	9	10	Lane
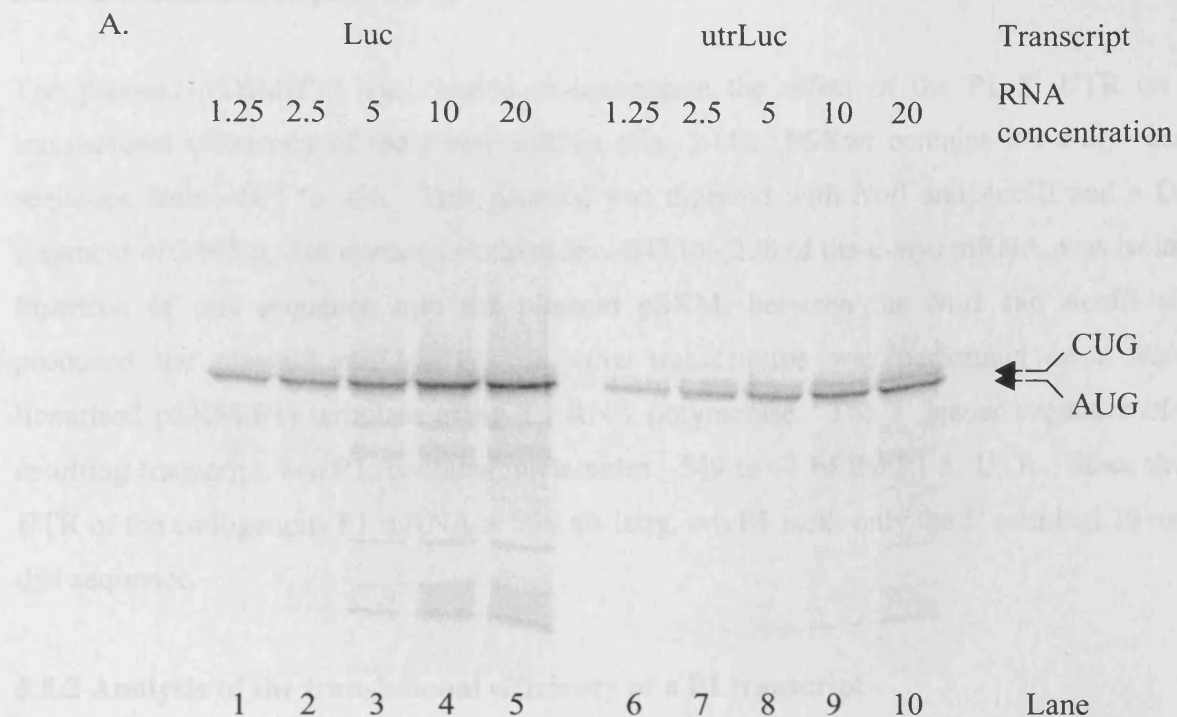
B.
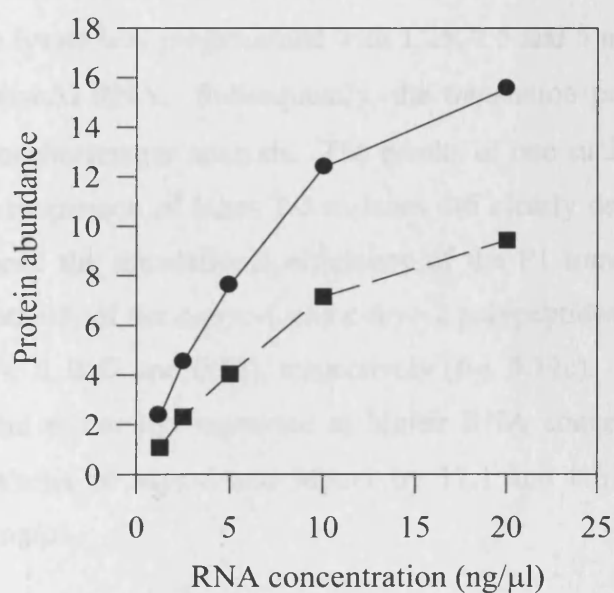
Figure 5.10: The effect of the c-*myc* P2 5' UTR on the translational efficiency of a heterologous mRNA *in vitro*. (A) Luciferase (Luc) and luciferase transcripts bearing the P2 5' UTR were synthesised *in vitro* using *Not*I-digested pSKL and pSKLutr, respectively. Radiolabelled polypeptides synthesised in translation reactions using increasing amounts (1.25-20 ng/μl) of either capped Luc (lanes 1-5) or utrLuc (lanes 6-10) were fractionated by SDS/PAGE and visualised using phosphorimager analysis. CUG and AUG-initiated polypeptides are indicated using arrows (B) Quantitation of the polypeptides shown in (A) using phosphorimager analysis. Closed circles (●) and closed squares (■) represent polypeptides synthesised using Luc and utrLuc transcripts, respectively.

5.5.1 Construction of pSKM(P1)

The plasmid pSKM(P1) was created to investigate the effect of the P1 5' UTR on the translational efficiency of the c-*myc* mRNA (fig. 5.11). PSKwt contains the c-*myc* exon1 sequence from –607 to –16. This plasmid was digested with *Not*I and *Acc*III and a DNA fragment of 249 bp, that encodes nucleotides –547 to –298 of the c-*myc* mRNA, was isolated. Insertion of this sequence into the plasmid pSKM, between the *Not*I and *Acc*III sites, produced the plasmid pSKM(P1). *In vitro* transcription was performed on a *Hind*III linearised pSKM(P1) template using T3 RNA polymerase. The 5' leader sequence of the resulting transcript, *myc*P1, contains nucleotides –549 to –1 of the P1 5' UTR. Since the 5' UTR of the endogenous P1 mRNA is 568 nts long, *myc*P1 lacks only the 5' terminal 19 nts of this sequence.

5.5.2 Analysis of the translational efficiency of a P1 transcript

To determine the effect of the P1 5' UTR on the translational efficiency of a c-*myc* mRNA, rabbit reticulocyte lysate was programmed with 1.25, 2.5 and 5 ng/μl of either capped *myc*P1 RNA or capped *myc*Δ1 RNA. Subsequently, the translation products were visualised and quantitated by phosphorimager analysis. The results of one such experiment can be seen in figure 5.12a. A comparison of lanes 1-3 to lanes 4-6 clearly demonstrates that the 5' UTR dramatically reduced the translational efficiency of the P1 transcript. At the lowest RNA concentration, synthesis of the c-*myc*-1 and c-*myc*-2 polypeptides was reduced on average by 6.5 and 7.1 fold (s. d. 0.47 and 0.32), respectively (fig. 5.12c). Furthermore, the magnitude of this translational repression increased at higher RNA concentrations. The P1 5' UTR inhibited the synthesis of Myc-2 and Myc-1 by 17.1 and 8.6 fold (s. d. 1.46 and 0.57), respectively, at 5 ng/μl.

Figure 5.12 also demonstrates that increasing the *myc*P1 RNA concentration from 2.5 to 5 ng/μl elevated the abundance of Myc-1 and Myc-2 by 1.44 and 1.05 fold, respectively. This observation suggests that a component of the translational apparatus was limiting at this concentration. In contrast, synthesis of the c-*myc* proteins from the control mRNA was directly proportional to the RNA concentration in this range (fig. 5.12a; lanes 1-3). Therefore, it follows that translation of the P1 mRNA requires a higher concentration of this factor than the control mRNA. Moreover, the increased inhibition of translation caused by
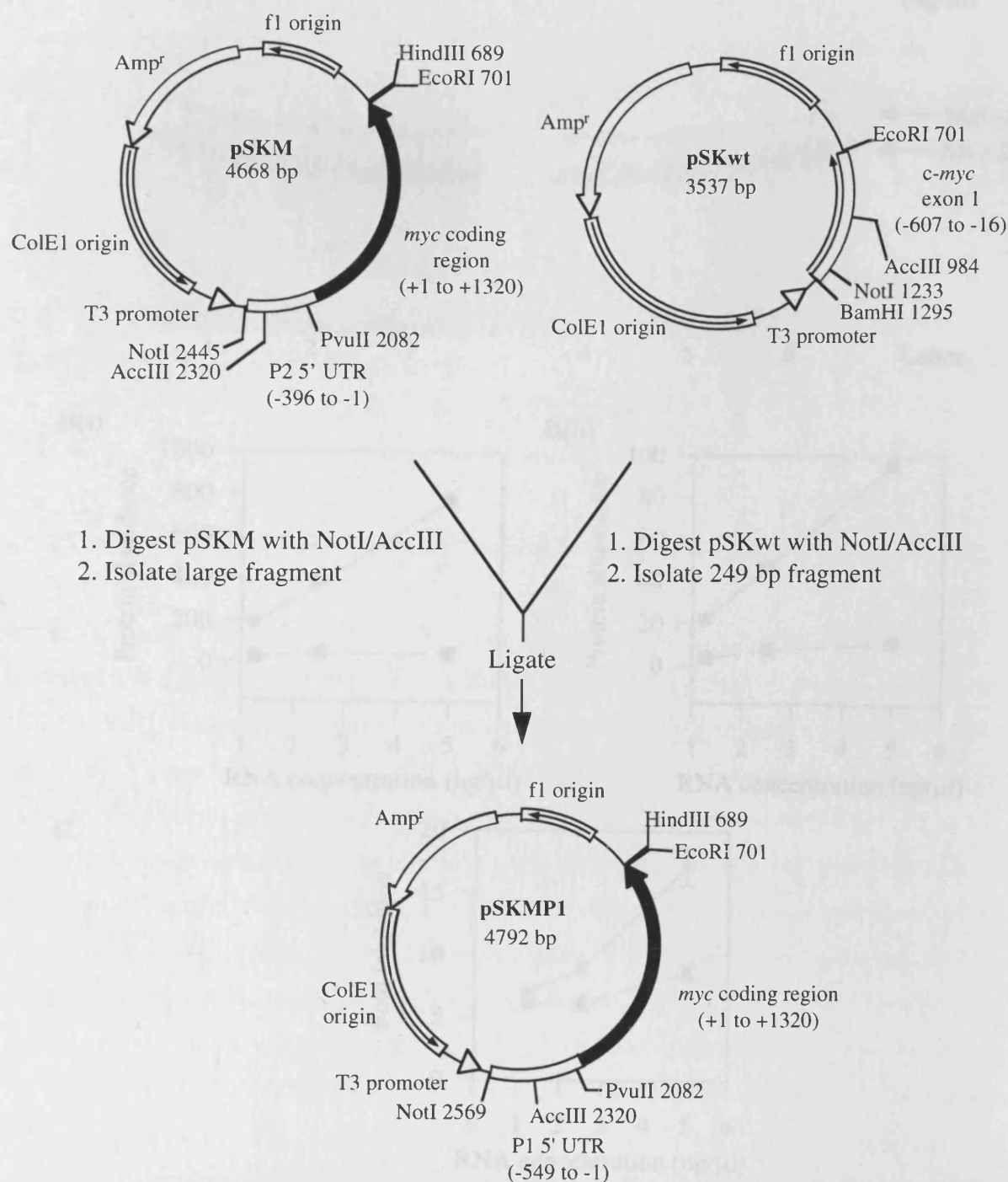
Figure 5.11: Construction of the plasmid, pSKMP1, containing the human c-*myc* cDNA sequence from -549 to +1320. Briefly, a plasmid containing c-*myc* exon 1 from -607 to -16 (pSKwt) was digested with *Not*I and *Acc*III. A 249 bp fragment was isolated and inserted into pSKM between the *Not*I and *Acc*III sites. The resulting plasmid, pSKMP1, contains the human c-*myc* cDNA sequence from -56 to +1320. PSKMP1 was digested with *Hind*III and used as a template to synthesise transcripts from the T3 promoter. The transcript generated, *myc*P1, contain the c-*myc* open reading frame fused to the P1 5' UTR.
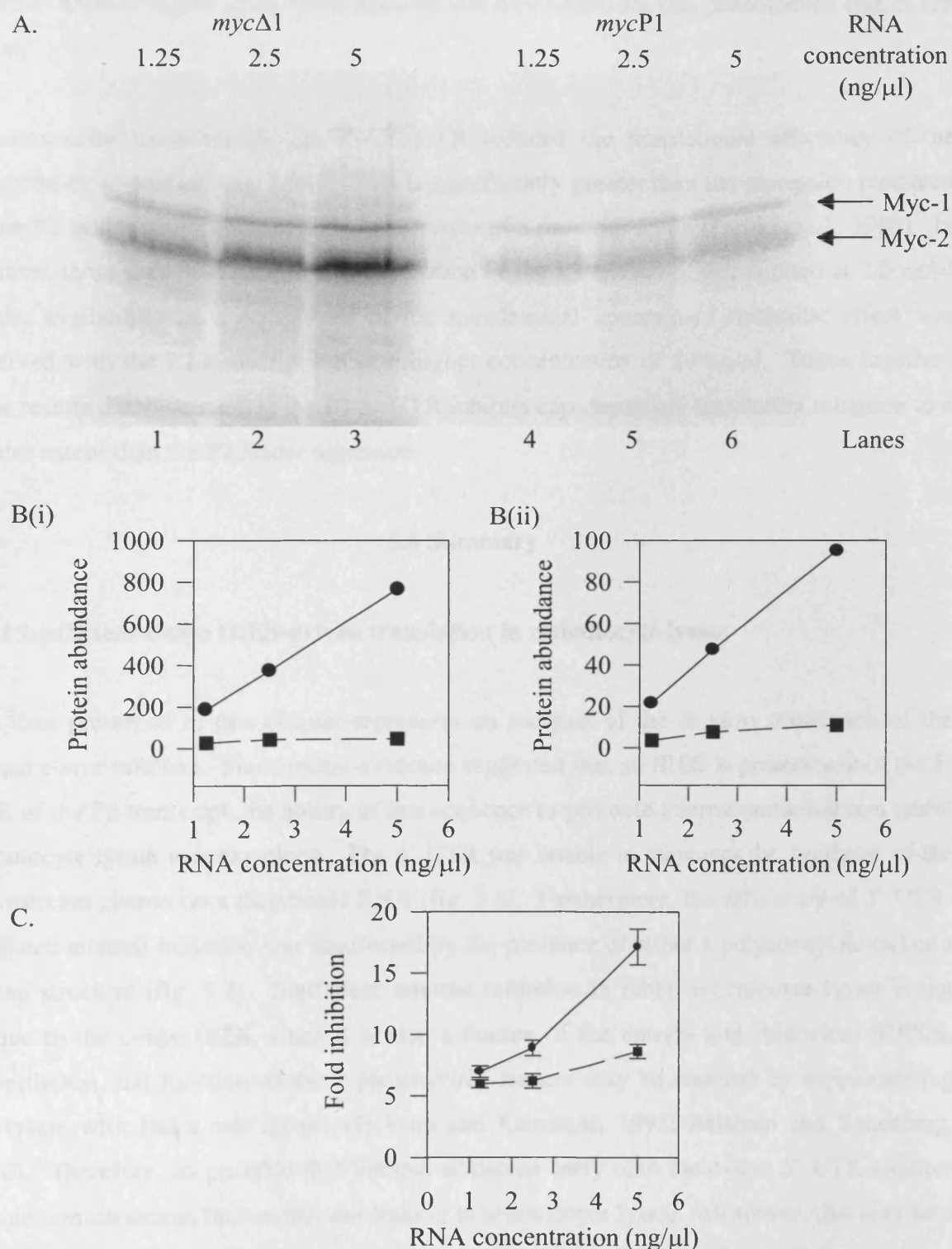
Figure 5.12: Analysis of the translational efficiency of the c-*myc* P1 transcript *in vitro*. (A) Capped *myc*P1 and *myc*Δ1 transcripts were synthesised *in vitro* using *Hind*III-digested pSKMP1 and pSKMΔ1, respectively. Reticulocyte lysates were programmed with increasing amounts (1.25-5 ng/µl) of either *myc*Δ1 (lanes 1-3) or *myc*P1 (lanes 4-6) transcripts. The radiolabelled polypeptides were visualised as described previously. (B) Quantitation of the polypeptides in (A) using phosphorimager analysis. (i) Myc-2 polypeptides and (ii) Myc-1 polypeptides synthesised from *myc*Δ1 (●) and *myc*P1 (■), respectively. (C) Average inhibition of translation initiation at the AUG (●) or CUG (■) codons caused by the P1 5' UTR in three separate experiments.

the P1 5' UTR at higher RNA concentrations was a consequence this phenomenon (fig. 5.12b and c).

To summarise these results, the P1 5' UTR reduced the translational efficiency of the transcript by approximately 7-fold. This is significantly greater than the repression mediated by the P2 leader and is comparable to the results of a previous study (Parkin *et al.*, 1988). In addition, these data demonstrate that translation of the P1 transcript was limited at 2.5 ng/μl by the availability of a component of the translational apparatus. A similar effect was observed with the P2 transcript but at a higher concentration of 10 ng/μl. Taken together, these results demonstrate that the P1 5' UTR inhibits cap-dependent translation initiation to a greater extent than the P2 leader sequence.

5.6 Summary

5.6.1 Inefficient c-*myc* IRES-driven translation in reticulocyte lysate

The data presented in this chapter represents an analysis of the *in vitro* translation of the human c-*myc* mRNAs. Since recent evidence suggested that an IRES is present within the 5' UTR of the P2 transcript, the ability of this sequence to promote internal initiation in a rabbit reticulocyte lysate was examined. The 5' UTR was unable to stimulate the synthesis of the downstream cistron on a dicistronic RNA (fig. 5.1). Furthermore, the efficiency of 5' UTR-mediated internal initiation was unaffected by the presence of either a polyadenylate tail or a 5' cap structure (fig. 5.2). Inefficient internal initiation in rabbit reticulocyte lysate is not unique to the c-*myc* IRES, since it is also a feature of the entero- and rhinovirus IRESes. Nevertheless, the function of these picornavirus leaders may be restored by supplementing the lysate with HeLa cell factors (Jackson and Kaminski, 1995; Belsham and Sonenberg, 1996). Therefore, its possible that internal ribosome entry onto the c-*myc* 5' UTR requires certain non-canonical factors that are lacking in reticulocyte lysate. Moreover, this may be a general feature of cellular IRESes, since none of the examples identified to date are able to function in this translation system.

5.6.2 The P2 and P1 c-*myc* transcripts show reduced translational efficiency

In addition, the translational efficiency of the human P1 and P2 c-*myc* transcripts was also determined in the reticulocyte lysate system. The P2 leader inhibited the translation of the c-

myc mRNA by approximately 50% (fig. 5.6). Furthermore, a similar effect was observed when a heterologous open reading frame was fused to the P2 5' UTR (fig. 5.10). Therefore, sequences within the 5' UTR can modulate the translation efficiency of the P2 transcript. It is well established that there is an inverse correlation between the degree of secondary structure in the 5' noncoding region and the translational efficiency of the mRNA (Pelletier and Sonenberg, 1985; Kozak, 1986; Koromilas *et al.*, 1992). Since, the *c-myc* 5' UTR is GC-rich and consequently is predicted to contain multiple secondary structural motifs, it seems likely that such structures reduce the rate of translation initiation on the mRNA. Interestingly, the equivalent murine 5' UTR inhibits c-*myc* translation by 8-10 fold, despite a high degree of sequence conservation between these two elements (Darveau *et al.*, 1985; Parkin *et al.*, 1988). One possible explanation for the greater magnitude of inhibition is the existence of more stable structural elements within the murine 5' UTR. Alternatively, the transcripts used in this study also differed at the 3' end, which may account for the discrepancy (Parkin *et al.*, 1988). A further distinction between the murine and human sequences was highlighted by their effect on the translational efficiency of heterologous mRNAs. Thus, the translational repression mediated by the murine 5' UTR was more pronounced on a chimeric mRNAs than on c-*myc* transcripts (Parkin *et al.*, 1988). A plausible interpretation of these observations is that the structure of the murine 5' UTR is modulated by elements in the coding region whilst the human P2 leader is not affected in the same manner.

The P1 promoter is located 160 bps upstream of the major promoter, P2. A transcript bearing sequences from the P1 5' UTR reduced the translational efficiency of the c-*myc* mRNA by approximately 7-fold (fig. 5.12). Thus, it follows that sequences upstream of the P2 transcription initiation site must contribute further to translational attenuation. An analysis of this region reveals an 82 bp sequence that is 78% GC rich. However, the Gibb's free energy of the most stable predicted structure formed from this element is only -33.6 kcal/mol. Since a synthetic RNA hairpin of -30 kcal/mol has no effect on translation initiation, this structure alone is unlikely to account for the reduced translational efficiency of the mRNA (Kozak, 1989). An alternative hypothesis suggests that translational inhibition is a result of base-pairing between sequences upstream and downstream of the P2 cap site. Furthermore, this result is comparable with the previously reported inhibition of 10-fold attributed to the c-*myc* 5' UTR. Since the 5' leader sequence used in this study was shorter by 48 nt, these data imply that the sequences involved lie between nucleotides -502 and -1 (Parkin *et al.*, 1988).

However, a more precise determination of the minimal element required to confer translational attenuation is required before further conclusions can be drawn.

5.6.3 c-*myc* translation is limited by the concentration of a factor in reticulocyte lysate

It is noteworthy that the translation of both the P1 and P2 transcripts was limited by the availability of a factor in reticulocyte lysate (fig. 5.7 and 5.12). Furthermore, there was an inverse correlation between the translational efficiency of the mRNA and the amount of RNA required to saturate the lysate (10 ng/μl for P2 and 2.5 ng/μl for P1). It has been demonstrated that a greater concentration of eIF4F is necessary for the efficient translation of mRNAs with highly structured 5' terminal regions when compared to those transcripts with less structured 5' UTRs (Sonenberg *et al.*, 1981; Fletcher *et al.*, 1990; Timmer *et al.*, 1993). Therefore, it is possible that the translation of both the P1 and P2 mRNAs is limited by the concentration of active eIF4F in reticulocyte lysate. An analysis of the effect of the m^{7}GpppG cap structure on c-*myc* translation provided further evidence that the P2 transcript has a strong requirement for eIF4F. In the absence of a cap, the 5' UTR inhibited the synthesis of the c-*myc* proteins by approximately 90%. Whilst on a capped transcript, this translational repression was largely relieved (fig. 5.8). Interaction of the eIF4F complex with the 5' cap structure could facilitate the unwinding of inhibitory secondary structures within the c-*myc* 5' UTR, thus promoting efficient translation initiation. Indeed, one can speculate that the availability of active eIF4F complexes could potentially modulate c-*myc* translation.

In direct contrast to the data presented herein, a recent study demonstrated that the translation of a heterologous transcript bearing the c-*myc* 5' UTR was only moderately cap-dependent (Nanbru *et al.*, 1997). Although these data are difficult to reconcile with the model presented above it is clear that certain differences exist between these studies. Firstly, the amount of RNA used in each study differs dramatically. Cap-independent translation was demonstrated at an RNA concentration of 0.03 ng/μl, whilst cap-dependent translation was observed at 5 ng/μl. Since the abundance of general RNA binding proteins is low in reticulocyte lysate (Svitkin *et al.*, 1996), it may be that the factors required for cap-independent translation are also underrepresented. Consequently, cap-independent translation can only proceed at low RNA concentrations. In addition, the nature of the transcripts used in these studies may have affected the results. Although the chimeric RNAs used to demonstrate cap-independent translation include 144 nt of c-*myc* coding sequence it remains possible that other sequences, not represented in these transcripts, influence the translation of c-*myc* mRNAs. Furthermore,

it is noteworthy that this study failed to equate the cap-independent translation of transcripts bearing the 5' UTR with efficient internal initiation mediated by this sequence. Nevertheless, these disparate results suggest that a more detailed analysis of the effects of the cap structure and the eIF4F complex on the translation of c-*myc* mRNAs is required before any conclusions can be drawn.

Chapter 6

Discussion

6.1 Evidence for the translation of c-*myc* mRNAs by internal initiation

Initial experiments demonstrated that the human c-*myc* P2 5' UTR did not reduce the translational efficiency of a heterologous mRNA when expressed in HeLa, HK293, HepG2 or COS7 cells. However, the c-*myc* 5' UTR is GC-rich and predicted to contain secondary structural motifs (Saito *et al.*, 1984; Parkin *et al.*, 1988; Nanbru *et al.*, 1997; Stoneley *et al.*, 1998). This property of the 5' UTR is believed to be responsible for the reduced translational efficiency of mRNAs bearing this element in rabbit reticulocyte lysate and *Xenopus* oocytes (Darveau *et al.*, 1985; Parkin *et al.*, 1988; Nanbru *et al.*, 1997; this thesis). Thus, the efficient translation of mRNAs bearing the c-*myc* 5' UTR *in vivo* suggested that either the capacity of these systems to relieve RNA structure differs or that the c-*myc* 5' UTR contains an internal ribosome entry segment.

6.1.1 The c-*myc* 5' UTR stimulates the expression of a downstream cistron on a dicistronic mRNA

Dicistronic reporter plasmids were constructed to determine whether the c-*myc* 5' UTR contains an internal ribosome entry segment (IRES). The downstream cistron of a control *Renilla* luciferase-firefly luciferase mRNA or a *Renilla* luciferase-CAT mRNA was translated inefficiently, as expected. However, insertion of the P2 5' UTR sequence into the intercistronic region of these mRNAs resulted in enhanced expression of the downstream cistron. In the case of the *Renilla*-CAT mRNAs, this stimulation could not be quantified since CAT expression from the control mRNA was outside the range of detection. Nevertheless, a clear increase in CAT activity was observed in HeLa cells transfected with the 5' UTR-containing plasmid, pRMCAT. In contrast, the sensitivity of the luciferase assay is approximately 30-1,000 times greater compared to the sensitivity of CAT assays (Pazzagli *et al.*, 1992). Thus in HeLa and HepG2 cell lines, the 5' UTR stimulated the expression of the downstream cistron on a *Renilla*-firefly dicistronic mRNA by approximately 50-fold. Whilst, a somewhat lesser stimulation of approximately 25-fold was observed in HK293 cells. Interestingly, in later studies using HeLa cells the magnitude of this stimulation

increased to 70-100-fold. It is possible that due to an extended period of growth in culture a more rapidly growing cell line was selected. Consequently, the efficiency of c-*myc* translation may have increased.

Eukaryotic IRESes have been reported to increase the expression from a downstream cistron by 20 to 240-fold (20 to 30-fold, 40-fold, 240-fold for BiP, eIF4G, and *antennapedia*, respectively) (Macejak and Sarnow, 1991; OH *et al.*, 1992; Gan and Rhoads, 1996). Furthermore, the well-characterised poliovirus IRES enhances second cistron expression by 20 to 30-fold (Macejak and Sarnow, 1991). Thus, the elevated expression obtained when the c-*myc* 5' UTR was inserted between two cistrons compares favourably with these values. In addition, the 5' UTR reduced the expression from the upstream cistron by approximately 15-30% on both types of dicistronic mRNA. This phenomenon has also been observed using the BiP, poliovirus, and eIF4G IRESes and is believed to be a consequence of competition between cap-dependent and IRES-driven translation (Macejak and Sarnow, 1991; Gan *et al.*, 1996). In combination, these results suggested that the c-*myc* P2 5' UTR could contain an IRES.

6.1.2 The mechanism responsible for enhanced downstream cistron translation

Although, internal initiation provides a satisfactory explanation for the 5' UTR-mediated increase in expression from a downstream cistron, it was possible that other mechanisms could be responsible for this effect. The production of functional monocistronic firefly luciferase transcripts by transcriptional, splicing, or RNA cleavage mechanisms was investigated. Northern analysis of the mRNAs transcribed from pGL3R and pGL3Rutr demonstrated that the majority of dicistronic transcripts were intact. However, a 1.8 kB mRNA that hybridised to the firefly luciferase probe was also produced from the 5' UTR-containing construct. This transcript was 4-fold less abundant than the full-length dicistronic mRNA in HeLa and HK293 cells and its abundance did not correlate with the observed increase in firefly luciferase expression. In addition, RNase protection analysis demonstrated that the 5' end of this mRNA lies within the luciferase coding region. Therefore, these data demonstrate that functional firefly luciferase can only be translated from the full-length dicistronic mRNAs.

An alternative mechanism that could account for the increased firefly luciferase expression is enhanced readthrough-reinitiation. It has been demonstrated that the translation of a cistron

118

downstream of a small open reading frame can be dramatically stimulated by increasing the distance between the two cistrons (Kozak, 1987). Thus, the increased interval between the luciferase cistrons, resulting from the inclusion of the 5' UTR in the dicistronic mRNA, could potentially stimulate reinitiation at the downstream start site. A hairpin structure of −55 kcal/mol was introduced into the 5' leader sequence of the 5'-UTR containing dicistronic mRNA to investigate this possibility. This structure reduced translation initiation at the upstream start codon by approximately 75%, whilst it had no effect of the synthesis of firefly luciferase. Hence, 5' UTR-directed translation of the downstream cistron does not depend on ribosome scanning from the upstream cistron and consequently readthrough-reinitiation.

The foregoing results demonstrate that the c-*myc* 5' UTR drives efficient translation of a downstream cistron on a dicistronic mRNA. Furthermore, this effect is not due to mRNA fragmentation and is independent of upstream cistron translation. In conclusion, these data represent strong evidence that the c-*myc* 5' UTR contains an IRES and suggest that the c-*myc* mRNA may be translated by the mechanism of internal initiation.

6.2 Further studies on c-*myc* mRNA translation by internal initiation

Although the data accumulated thus far indicate that c-*myc* mRNAs could be translated by the mechanism of internal initiation, further studies are necessary to confirm this hypothesis. A mechanism in which the 43S complex binds to the 5' end of the mRNA, and is then transferred to a site within the c-*myc* 5' UTR cannot be discounted using the current data. The argument for authentic internal initiation driven by the c-*myc* 5' UTR can be strengthened by demonstrating that the translation of mRNAs bearing this element is manifestly cap-independent.

Infection of mammalian cells with poliovirus results in the cleavage of eIF4G and the dephosphorylation of eIF4E-BP1, both of which contribute to the abrogation of cap-dependent translation (Etchison *et al.*, 1982; Gingras *et al.*, 1996). Thus, demonstration that c-*myc* 5' UTR-directed stimulation of downstream cistron expression occurs in poliovirus-infected cells would strongly support the internal initiation model. In addition, the constitutive over-expression of eIF4E-BP1 or BP2 has been demonstrated to downmodulate cap-dependent translation from the upstream cistron of dicistronic mRNAs, whilst having no effect on IRES-driven translation (Roberts *et al.*, 1998). Therefore, if c-*myc* 5'UTR-mediated translation of a downstream cistron is independent of a 5' cap structure, it should not be

attenuated by the eIF4E-BPs. Finally, whilst transcripts lacking a 5' cap structure are translated inefficiently in mammalian cells, an open reading frame preceded by an IRES is translated efficiently on an uncapped RNA (Hambridge and Sarnow, 1991). An uncapped transcript bearing the c-*myc* 5' UTR would be expected to be translated significantly more efficiency than a transcript lacking this element. Thus, the effect of the c-*myc* 5' UTR on translation initiation could be examined on uncapped mRNAs synthesised in the nucleus using RNA polymerase III (Gunnery and Matthews, 1995).

It is noteworthy that the majority of the evidence for internal initiation on eukaryotic mRNAs has been accumulated using heterologous mRNAs. However, support for a cap-independent mechanism of translation has been provided for the endogenous BiP mRNA (Sarnow, 1989). It would be of interest to determine whether translation of the endogenous c-*myc* mRNAs can also proceed by a cap-independent mechanism, *in vivo*. This can be achieved by investigating the synthesis of endogenous c-*myc* proteins in poliovirus-infected mammalian cell lines. In addition, the translation of c-*myc* proteins could be analysed in cells expressing antisense eIF4E transcripts (De Benedetti *et al.*, 1991) or overexpressing the eIF4E-BPs (Roberts *et al.*, 1998).

6.3 Mechanistic analysis of the c-*myc* IRES

The model for picornavirus internal initiation proposes that multiple sequence elements, arranged in a precise three-dimensional structure, recruit the ribosome to the 3' end of the IRES. This process is believed to involved RNA-RNA and RNA-protein interactions between the IRES and the 43S preinitiation complex or alternatively in some instances a *trans*-acting factor may mediate the interaction between these components (Jackson and Kaminski, 1995; Jackson, 1996). In contrast, comparatively little is known about the mechanism of internal initiation on eukaryotic cellular mRNAs (Iizuka *et al.*, 1995). Thus, the IRES in the c-*myc* P2 mRNA was characterised further.

6.3.1 Location of the c-*myc* IRES within the P2 5' UTR

To locate the IRES within the c-*myc* P2 5' UTR, truncated sequences were inserted into a dicistronic reporter plasmid, pGL3R. This deletion analysis demonstrated that maximum IRES-driven translation could be achieved using the sequence from –396 to –57. Hence, the c-*myc* IRES is approximately 340 nt in length and thus marginally shorter than those of the

picornaviruses (~450 nt long). Few eukaryotic IRESes have been mapped in this manner, but it is interesting to note that the BiP, eIF4G and VEGF sequences are considerably shorter than the c-myc IRES (92, 101, and 163 nt, respectively) (Yang and Sarnow, 1997; Gan et al., 1998; Stein et al., 1998). Thus, the c-myc IRES may represent a different class of this element. There is no striking sequence homology between the c-myc IRES and those derived from other eukaryotic mRNAs. However, a comparison of the c-myc and FGF2 elements has identified several conserved GC-rich stretches (Nanbru et al., 1997). It has been suggested that these sequences are involved in the formation of stem-loop structures in the predicted FGF2 and c-myc IRES structures. Nevertheless, the contribution of these stretches to IRES function remains to be determined experimentally.

The picornavirus paradigm has demonstrated that structure of the IRES is critical for the interaction of the ribosome with the RNA. The definition of the c-myc IRES is an essential pre-requisite for the construction of a structural model. Such a model is currently under investigation using a combination of direct biochemical probing, phylogenetic analysis and structure prediction algorithms (J. P. C. Le Quesne and A. E. Willis, pers. comm.). This model will permit an analysis of the role that structural motifs play in c-myc IRES-driven translation initiation and in addition may identify sequence elements essential for mRNA-ribosome interaction. Interestingly, the deletion analysis highlighted a potential difference between the c-myc IRES and those of the picornaviruses. Removal of sequences from the 3' end of the c-myc IRES did not completely preclude the stimulation of expression from a downstream cistron. Whilst, similar deletions made in picornavirus IRESes drastically reduce IRES-driven translation initiation (Pelletier and Sonenberg, 1988; Jang and Wimmer, 1990; Kaminski et al., 1990; Borman and Jackson, 1992). It is possible that a mechanistic distinction underlies these observations. However, an alternative explanation suggests that once the function of the c-myc IRES is compromised, the increased intercistronic distance can stimulate readthrough-reinitiation at the downstream start site. In order to distinguish between these models, the deletion analysis should be performed in poliovirus-infected cells.

Finally, in some picornavirus IRESes and in the eIF4G IRES a polypyrimidine tract positioned upstream of a conserved AUG codon can profoundly influence translational efficiency (Pilipenko et al., 1992; Gan et al., 1998). However, a similar element in the c-myc 5' UTR (-40 to –33 in the human sequence) lies outside of the c-myc IRES. Nevertheless, the removal of an 84 nt sequence from the 3' end of the 5' UTR reduced internal initiation by 40% and this region contains two further pyrimidine-rich elements (-85 to –75 and –61 to –

68). Thus, the contribution of these sequences to c-*myc* internal initiation must be assessed using mutational analysis.

6.3.2 The role of a conserved CUG-initiation codon

The human c-*myc* 5' UTR contains a conserved CUG triplet 45 nt upstream of the major start codon. In addition to its role as a minor translation initiation site (Hann *et al.*, 1988), it was envisaged that this element could potentially contribute to ribosome binding. In this respect, its function would be analogous to that of a conserved upstream AUG codon found at the 3' end of the poliovirus IRES. Studies have demonstrated that the ribosome lands at or very near to this triplet and that mutation of this codon profoundly reduces poliovirus translation initiation (Pelletier *et al.*, 1988b; Meerovitch *et al.*, 1991; Pilipenko *et al.*, 1992; Pestova *et al.*, 1994).

The location of this CUG codon outside of the c-*myc* IRES suggested that it does not participate directly in ribosome-mRNA complex formation. However, it remained possible that a CUG codon located in the intercistronic multiple cloning site of the dicistronic plasmid, pGL3R substituted for the deleted triplet. Thus, the authentic CUG triplet was mutated to CUC to analyse its contribution to c-*myc* IRES-driven translation initiation. The mutant 5' UTR sequence promoted translation from a downstream cistron as efficiently as the wild type sequence. Hence, coupled with the deletion analysis these data indicate that the conserved CUG initiation codon does not influence c-*myc* 5' UTR-mediated internal initiation.

Although the preceding data suggest that ribosome binding to the c-*myc* mRNA is independent of this CUG triplet they provide no information as to the actual location of the ribosome entry site. In picornaviruses, ribosome entry occurs at a conserved AUG codon at the 3' end of the IRES (Jackson and Kaminski, 1995). In contrast, the position from which a ribosome commences to migrate along the mRNA has not been studied in detail in the cellular examples. However, evidence has been presented for ribosome entry at the distal end of the eIF4G IRES (Gan *et al.*, 1998). Since there are two translation initiation sites in the c-*myc* mRNA, and the resulting polypeptides can perform opposing functions (Hann *et al.*, 1988; Hann *et al.*, 1992), it would be of great interest to determine the position of ribosome entry on the c-*myc* mRNA. This could be achieved by introducing AUG triplets into the 5' UTR out of frame with the authentic AUG codon. If the ribosome lands before such an AUG codon, initiation at the downstream reporter cistron will be abrogated. Whilst c-*myc* IRES-

driven translation should not affected by out-of-frame initiation codons positioned upstream of the ribosome entry site. These experiments will determine whether both c-*myc* proteins are synthesised by the mechanism of internal initiation.

6.4 Evidence for the involvement of *trans*-acting factors in c-*myc* IRES-directed translation initiation

Several observations suggest that entero/rhinovirus IRES-driven translation initiation is dependent on host-derived *trans*-acting factors. The addition of HeLa cytoplasmic extract to reticulocyte lysate dramatically enhances the efficiency of entero/rhinovirus internal initiation. Furthermore, a few *trans*-acting factors have been identified that are able to perform this function, including PTB, La, PCBP2 and p97/p38 (Borman *et al.*, 1993; Hellen *et al.*, 1993; Meerovitch *et al.*, 1993; Jackson, 1996; Blyn *et al.*, 1997). Finally, the ability of these IRESes to promote internal initiation varies widely in cell lines from different origins (Borman *et al.*, 1997; Roberts *et al.*, 1998). In comparison, although no direct evidence exists demonstrating that c-*myc* IRES-directed translation requires non-canonical *trans*-acting factors, much circumstantial evidence has accumulated supporting this hypothesis.

Firstly, expression from a downstream cistron directed by the c-*myc* IRES was found to vary in a cell-type specific manner. For example in HeLa cells an 85-fold stimulation of expression was observed, whilst only a moderate increase of 6-fold occurred in Balb/c-3T3 cells. Moreover, inefficient c-*myc* IRES-driven translation was not restricted to murine cells, since it was also manifest in the human cell line MCF7 (a 12-fold increase). Several different reasons could account for the cell-type specific variation in c-*myc* IRES function. These include: the tissue or species from which the cell line originates, and the transformation status of the cell. However, since c-*myc* IRES activity has only been investigated in only a small sample of cell lines it is difficult to distinguish between these possibilities. Therefore, the activity of the c-*myc* IRES should be determined in a wider range of cell lines.

The variation in c-*myc* IRES function can be explained if the activity of a factor essential for c-*myc* internal initiation is much reduced in the Balb/c-3T3 and MCF7 cells. Such a factor may be present at a reduced concentration in these cell lines or alternatively, its activity may be mitigated by an inhibitor. The latter model has been suggested to account for the stimulatory effect of the Foot and mouth disease virus Lb and the poliovirus 2A protease on entero/rhinovirus IRES function. In cell lines in which these IRESes promote internal

initiation inefficiently, the co-expression of either protease dramatically enhances IRES-directed protein synthesis (Borman *et al.*, 1997; Roberts *et al.*, 1998). It has been proposed that proteolysis may result in the loss of an inhibitor of IRES function. Thus, the effects of the Lb and 2A proteases on c-*myc* internal initiation of translation in Balb/c-3T3 and MCF7 cells should be examined. These experiments may provide further insight into the potential role of *trans*-acting factors.

The expression of dicistronic mRNAs under the control of the powerful CMV promoter/enhancer provided further indirect evidence that c-*myc* IRES-mediated translation initiation may require non-canonical *trans*-acting factors. Compared to similar SV40 promoter/enhancer-based dicistronic constructs, expression from the upstream cistron was increased by 32-fold after transfection of HeLa cells with the CMV promoter/enhancer-based plasmids. Nevertheless, since the c-*myc* 5' UTR only enhanced expression from the downstream cistron by 2.9-fold, IRES-driven translation initiation was substantially reduced. One possible interpretation of these results is that the high level of dicistronic mRNAs expressed from these constructs interferes with the function of a *trans*-acting factor. Indeed, similar observations have been reported using entero/rhinovirus IRESes. In this case, it was found that IRES-driven translation can be saturated in HeLa cells, whilst higher levels of expression actually inhibited entero/rhinovirus translation initiation. It was concluded that the IRES-containing RNAs were in excess with respect to essential non-canonical factors (Borman *et al.*, 1997). Thus, such a limiting factor may also be necessary for the function of the c-*myc* IRES. However, to provide support for this contention it must be shown that c-*myc* IRES-driven translation can be saturated.

Finally, it has been demonstrated that reticulocyte lysate does not support c-*myc* IRES-directed translation initiation. Hence, in this respect the c-*myc* IRES resembles those of the entero/rhinoviruses. However, unlike the picornavirus IRESes it has yet to be demonstrated that supplementing this translation system with cytoplasmic factors stimulates internal initiation. In fact, given that the activity of the c-*myc* IRES is very low when introduced directly into the cytoplasm of HeLa cells, it seems unlikely that this approach will result in the restoration of IRES function. In addition, it is noteworthy that the reticulocyte system has never been shown to support internal initiation using an IRES derived from a cellular mRNA. Thus, one can speculate that the requirement for non-canonical *trans*-acting factors is a feature common to many of these eukaryotic IRESes

6.5 Evidence for an essential nuclear event

The introduction of dicistronic mRNAs directly into the cytoplasm, thus avoiding nuclear processing of the transcript, has provided evidence that a prior nuclear event is essential for efficient c-*myc* IRES activity. Preliminary experiments, performed in collaboration with Belsham and co-workers, demonstrated that the c-*myc* 5' UTR did not stimulate downstream cistron expression on mRNAs synthesised in the cytoplasm using T7 RNA polymerase. However, since there was some concern over the high level of expression achieved with the vaccinia/T7 expression system, the activity of the IRES was assessed on transcripts introduced into the cytoplasm using RNA transfection (Fuerst *et al.*, 1986; Malone *et al.*, 1989). Whilst, the HRV IRES stimulated downstream cistron expression by 52-fold under these conditions, translation initiation directed by the c-*myc* 5' UTR was negligible. In comparison, the c-*myc* IRES was approximately 7-fold more efficient than the HRV IRES on mRNAs synthesised in the nucleus by RNA polymerase II. These data imply that a prior nucleus process is required for the efficient translation of c-*myc* 5' UTR-bearing mRNAs by the mechanism of internal initiation. Furthermore, this phenomenon is not unique to the c-*myc* IRES since BiP IRES-directed translation initiation is also inefficient on mRNAs lacking a nuclear history (Iizuka *et al.*, 1995). These data also indicate that the c-*myc* IRES is a more efficient translational element when compared to the HRV IRES. The HRV IRES has previously been shown to be one of the least efficient picornavirus IRESes in some cell lines (Borman *et al.*, 1997; Roberts *et al.*, 1998). In fact, the HRV14 IRES promotes internal initiation 4-5 times less efficiently that the EMCV or FMDV IRESes in HTK143 cells (Roberts *et al.*, 1998). Thus, the efficiency of the c-*myc* IRES may be more comparable to those of the cardio/aphthoviruses. However, a direct comparison of relative stimulation of downstream cistron expression would be necessary to confirm this supposition.

It is not a novel concept that the translational efficiency of a transcript can be influenced by the processes involved in synthesis and maturation of the pre-mRNA. Indeed, it has recently been demonstrated that the presence of an intron at the 5' end of a transcript can strongly enhance the translation of the mRNA (Matsumoto *et al.*, 1998). One model that would account for the effects of nuclear history on c-*myc* IRES activity suggests that an essential *trans*-acting factor could be recruited to the IRES during the synthesis/processing of the pre-mRNA. Alternatively, the attainment of a functional c-*myc* IRES structure may depend on these nuclear processes.

The predominantly nuclear proteins PTB, La and PCBP2 have all been shown to influence picornavirus IRES activity (Borman *et al.*, 1993; Hellen *et al.*, 1993; Meerovitch *et al.*, 1993; Blynn *et al.*, 1997). However, neither La nor PTB interacts specifically with the c-*myc* 5' UTR (Paulin, 1997). Since nuclear processing appears to be essential for c-*myc* IRES function, the formation of complexes involving the 5' UTR and nuclear proteins was investigated. Ultraviolet cross-linking studies identified a complex of approximately 98 kDa between a nuclear protein and a radiolabelled 4-thioUTP-containing c-*myc* 5' UTR probe. The formation of this complex was prevented by the addition of a 10-fold molar excess of cold competitor 5' UTR RNA. In contrast, the c-*myc* 5' UTR-p98 complex could still be detected in the presence of a 100-fold molar excess of HRV IRES RNA. Thus, p98 appears to interact specifically with the c-*myc* 5' UTR. This protein is an obvious candidate for a *trans*-acting factor involved in c-*myc* translational regulation. However, these preliminary studies provide no information about the function of this complex. Thus, the formation of the p98 complex should be assessed using cytoplasmic extracts and reticulocyte lysate since the c-*myc* IRES cannot function in either of these systems (Pelletier and Sonenberg, 1988; this thesis). In addition, two nuclear proteins of 60 and 95 kDa have been shown to bind to the BiP IRES (Yang and Sarnow, 1997). However, both proteins also interact with the HCV and EMCV IRESes. Since, these IRESes function efficiently in reticulocyte lysate and have different mechanisms it seems unlikely that p60 and p95 are the essential factors required for BiP internal initiation. Thus, the interaction of the c-*myc* 5' UTR-binding protein, p98, with cardio/aphthovirus and HCV-like IRESes should also be investigated. Most importantly, nuclear fractions containing p98 should be tested for their ability to stimulate c-*myc* IRES activity in reticulocyte lysate.

6.6 Evidence for the translation of c-*myc* mRNAs by a cap-dependent mechanism

Although much of the data accumulated in this study suggests that c-*myc* mRNAs can be translated by the mechanism of internal initiation, evidence has also emerged implicating the involvement of a cap-dependent mechanism. In previous studies the c-*myc* 5' UTR was shown to reduce the translation efficiency of an mRNA in rabbit reticulocyte lysate and *Xenopus* oocytes, but not in cultured cell lines (Butnick *et al.*, 1985; Darveau *et al.*, 1985; Parkin *et al.*, 1988). One potential explanation for this discrepancy is that c-*myc* mRNAs are translated by internal initiation *in vivo*, but a cap-dependent mechanism operates in *Xenopus* oocytes and RRL. If internal initiation were the only mechanism involved in the translation of c-*myc* mRNAs in cultured cells, one would expect a direct correlation between c-*myc*

IRES activity and the translational efficiency of an mRNA bearing the c-*myc* 5' UTR. However, despite a significant variation in the efficiency of c-*myc* IRES-driven translation in cell lines from different origins, the c-*myc* 5' UTR had little effect on the translation of heterologous monocistronic mRNAs in the same cells. Thus, it is likely that these 5' UTR-containing mRNAs can be efficiently translated by a cap-dependent mechanism.

Since the c-*myc* IRES is not able to promote internal initiation in rabbit reticulocyte lysate, this system has been used to analyse the effects of the 5' UTR on cap-dependent translation initiation. Both the P1 and P2 5' leader sequences reduced the translational efficiency of a c-*myc* mRNA, by approximately 7-fold and 2-fold, respectively. In addition, the synthesis of c-*myc* polypeptides from 5' UTR-bearing c-*myc* mRNAs was saturated at lower RNA concentrations than the control transcript. Moreover, translation of the P2 c-*myc* mRNA demonstrated a strong dependence on the presence of a 5' cap structure. In the absence of a cap the 5' UTR reduced the translational efficiency of a c-*myc* mRNA by approximately 90%. In contrast, this translational repression was largely relieved on a capped transcript. Taken together, these data suggest that c-*myc* mRNA translation can be modulated by the structured 5' leader sequences and that the activity of translation initiation factors, such as eIF4F, may have a profound effect on c-*myc* mRNA translation. Indeed, it has been demonstrated that translation initiation occurring on mRNAs with more structured 5' leader sequences has a greater requirement for eIF4F (Sonenberg *et al.*, 1981; Fletcher *et al.*, 1990; Timmer *et al.*, 1993). Thus, a more detailed analysis of the effect of eIF4F activity on the translation of c-*myc* mRNAs is merited. In particular, since the murine c-*myc* P2 5' UTR does not inhibit translation initiation in HeLa cell extracts the activity of eIF4F could be reduced in this system to determine the effect of this complex on c-*myc* translation. Additionally, reticulocyte lysate could be supplemented with eIF4F to determine whether this complex can overcome the translational inhibition mediated by the c-*myc* 5' UTRs.

In some circumstances, c-*myc* protein synthesis may be regulated through alterations in the activity of translation initiation factors *in vivo*. For example, a reduction in eIF4F activity has been observed during heat shock and in serum starved cells (Duncan and Hershey, 1985; Duncan *et al.*, 1987). Under these conditions, the c-*myc* mRNAs would compete poorly for eIF4F due to their structured leader sequences and consequently cap-dependent translation of these mRNAs may be effected by a greater extent than global protein synthesis. Furthermore, during *Xenopus* oogenesis the c-*myc* protein accumulates without a corresponding increase in mRNA. Thus, it has been suggested that a translational mechanism is responsible for the

dissociation of protein and mRNA levels (Godeau *et al.*, 1986; Taylor *et al.*, 1986). Interestingly, hormone-induced meiotic maturation of *Xenopus* oocytes is associated with a general increase in translation initiation and enhanced phosphorylation of the eIF4F components, eIF4E and eIF4G (Morley and Pain, 1995). Therefore, the increased activity of eIF4F may relieve the translational repression caused by the structured 5' UTR sequences. To provide support for this hypothesis, the translational efficiency of a heterologous mRNA bearing the c-*myc* 5' UTR could be analysed under these conditions to determine whether this sequence modulates cap-dependent translation initiation of c-*myc* mRNAs *in vivo*. Finally, it has been demonstrated that c-*myc* protein synthesis is stimulated in Chinese Hamster ovary cells that overexpress eIF4E (De Benedetti *et al.*, 1994). However, since the c-*myc* 5' UTR does not repress translation initiation in cultured cell lines (Butnick *et al.*, 1985; Parkin *et al.*, 1985; Stoneley *et al.*, 1998) it is unlikely that this observation can be accounted for by the relief of structural inhibition. Nevertheless, since increased expression of eIF4E and eIF4G causes malignant transformation and has been associated with some tumour types, the effect of these factors on both cap-dependent and internal initiation mechanisms of c-*myc* translation may be critical to the attainment of a tumorigenic phenotype (Lazaris-Karatzas *et al.*, 1990; Antony *et al.*, 1996; Fukuchi-Shimogori *et al.*, 1997).

In summary, there is evidence suggesting that c-*myc* mRNAs can be translated by a cap-dependent mechanism *in vivo*. Furthermore, *in vitro* analysis of the c-*myc* mRNAs indicates that the 5' UTR may modulate the translational efficiency of the transcripts. However, the disparate effects observed in different translation systems suggest that this may only occur under some circumstances.

6.7 The evolution of two alternative mechanisms of c-*myc* translation initiation

If the mechanism of ribosome recruitment mediated by the c-*myc* IRES is comparable to that of the picornavirus IRESes, then structural motifs within the c-*myc* 5' UTR will perform an essential role in c-*myc* IRES-driven internal initiation. In contrast, a ribosome scanning from the 5' end of a c-*myc* mRNA would traverse the IRES and unwind any RNA structure. Thus, the cap-dependent and internal initiation mechanisms of translation on the c-*myc* mRNA would be mutually exclusive. This leads to the hypothesis that internal initiation can only occur on a c-*myc* transcript when cap-dependent translation initiation is blocked. Thus, a subset of c-*myc* mRNAs may exist on which cap-dependent translation initiation is extremely inefficient. Alternatively, c-*myc* IRES-mediated internal initiation could occur when the

activity of eIF4F is compromised. However, at present nothing is known about the cellular circumstances when the c-*myc* IRES operates. Nevertheless, one can speculate about the potential involvement of this mechanism in certain cellular processes.

6.7.1 c-*myc* protein synthesis and mitosis

Previous studies have demonstrated that the levels of c-*myc* mRNA and protein are invariant throughout the cell cycle (Hann *et al.*, 1985; Thompson *et al.*, 1985). Both c-*myc* proteins and mRNAs are very unstable with half-lives of 15-30 minutes and 10-20 minutes, respectively (Dani *et al.*, 1984; Hann and Eisenman, 1984). Therefore, since c-*myc* expression does not vary in a cell cycle dependent manner, the mRNAs and proteins must be synthesised continuously in all phases of the cell cycle. However, during mitosis the activity of eIF4F is reduced as a consequence of the dephosphorylation of eIF4E (Bonneau and Sonenberg, 1987). Thus, since cap-dependent translation is diminished in M-phase, c-*myc* proteins may be synthesised by the mechanism of internal initiation during this period.

Although this hypothesis provides a function for the c-*myc* IRES it has recently been challenged by a study demonstrating that c-*myc* mRNA levels do fluctuate in a cell cycle dependent manner. A synchronous population of Swiss 3T3 cells exiting M-phase contained considerably lower levels of c-*myc* mRNA and transcripts accumulated rapidly during early G_1-phase (Cosenza *et al.*, 1991). In the original studies, steady-state levels of c-*myc* mRNA and protein were analysed in the G_1, S, and G_2/M-phases but the abundance of either species was not investigated specifically in M-phase. Therefore, it seems likely that c-*myc* mRNA levels do fall throughout mitosis. Nevertheless, it remains possible that c-*myc* protein synthesis occurs by a cap-independent mechanism during this period. In order to resolve this issue, the synthesis of the c-*myc* proteins and the association of c-*myc* mRNAs with the polysome fraction should be analysed in M-phase. Furthermore, the ability of the 5' UTR to direct internal initiation in the different phases of the cell cycle should be investigated.

6.7.2 c-*myc* protein synthesis and heat shock

Heat shock results in a reduction in global protein synthesis in many cell types, but the synthesis of heat shock proteins is either unaltered or enhanced (see Rhoads and Lamphear, 1995). This effect is achieved in part by a reduction in both the phosphorylation and activity of the eIF4 initiation factors (Duncan and Hershey, 1984; Duncan *et al.*, 1989). In spite of

this decrease in cap-dependent translation initiation, the synthesis of c-*myc* proteins was found to increase between 1.5 to 2-fold in a lymphoma cell line following heat shock. Furthermore, no alteration in the abundance of c-*myc* mRNAs was detected during the same period suggesting that heat shock is able to enhance c-*myc* translation (Lüscher and Eisenman, 1988). These observations may be explained if heat shock promotes the translation of c-*myc* mRNAs by the mechanism of internal initiation. However, c-*myc* 5' UTR-driven internal initiation must be analysed during heat shock to support this hypothesis.

The continued synthesis of c-*myc* proteins after heat shock was accompanied by a delay in cell proliferation (Lüscher and Eisenman, 1988). Therefore, under these conditions cell cycle progression is uncoupled from c-*myc* protein levels. Thus, it is possible that c-*myc* expression is essential for cell growth during the recovery from heat shock or alternatively for the reinitiation of cell proliferation.

6.7.3 Internal initiation and development

The expression of c-*myc* is essential for development of the early embryo and a c-*myc* null mutation causes lethality in homozygous murine embryos after 9.5 to 10.5 days (Davies *et al.*, 1993). At the later stages of embryogenesis c-*myc* mRNA expression correlates with cell proliferation (Schmid *et al.*, 1989). In contrast, only a limited set of dividing embryonic cells express c-*myc* mRNA during early human and murine development and high levels of c-*myc* mRNA can also be detected in some post-mitotic cells (Downs *et al.*, 1989; Hirvonen *et al.*, 1990). However, little is know about c-*myc* protein synthesis during mammalian development. Given the variation in c-*myc* IRES-activity observed in cell lines from different origins, it is possible that c-*myc* internal initiation could be subject to tissue-specific and temporal regulation throughout development. In order to test this hypothesis, dicistronic mRNAs could be expressed in transgenic mice and the efficiency of c-*myc* IRES-driven internal initiation could be monitored during embryonic development. A similar study performed in *Drosophila* demonstrated that the activity of both the *antennapedia* and *ultrabithorax* IRESes is regulated in the developing embryo. Furthermore, in many cases the efficiency of IRES-driven translation in various tissues correlated with the levels of endogenous gene expression (Ye *et al.*, 1997). These observations imply that internal initiation can contribute to the temporal and spatial regulation of gene expression during development.

6.7.4 Internal initiation and tumorigenesis

In cell lines derived from patients with Bloom's syndrome and multiple myeloma, the synthesis of c-*myc* proteins is de-regulated. In both cases an increased association of the c-*myc* mRNAs with the polysomes was observed suggesting that a translational mechanism is involved (West *et al.*, 1995; Paulin *et al.*, 1995). Thus, a model has been proposed in which c-*myc* protein synthesis contributes to de-regulated cell proliferation and consequently tumorigenesis. Furthermore, a single point mutation was identified in the 5' UTR of the c-*myc* mRNAs isolated from the multiple myeloma cell lines (Paulin *et al.*, 1995). This mutation lies within the c-*myc* IRES and consequently it is conceivable that it alters the efficiency of internal initiation. Interestingly, a number of cellular factors have been shown to interact with the c-*myc* 5' UTR. The affinity of these factors appears to be greater for the mutant sequence and in addition, certain myeloma cell type-specific factors have been identified (Paulin *et al.*, 1997, 1998). It has been suggested that the altered spectrum of binding proteins may be directly related to the increased c-*myc* protein synthesis in these cell lines. One mechanism that would account for these observations suggests that in multiple myeloma cells both the enhanced binding of *trans*-acting factors and the higher concentration of certain factors may stimulate the activity of the c-*myc* IRES. However, so far no function has been assigned to any of these RNA-protein complexes. The activity of the c-*myc* IRES, both mutant and wild type sequences, is currently under investigation in multiple myeloma cell lines to determine whether internal initiation is responsible for the increased synthesis of c-*myc* proteins. If this is the case, then the translation of c-*myc* mRNAs will be analysed in cell lines derived from various tumour-types, since it may represent a common mechanism involved in the development of neoplasia.

6.8 Concluding Remarks

The c-*myc* proto-oncogene is a critical regulator of many cellular processes including, cell growth, cell proliferation, differentiation and apoptosis. Consequently, c-*myc* gene expression is controlled at multiple levels, including both transcriptional and post-transcriptional (see Henriksson and Lüscher, 1996). Previous evidence suggested that the 5' UTR could reduce the translational efficiency of c-*myc* mRNAs and consequently contribute to the complex modulation of c-*myc* gene expression (Darveau *et al.*, 1985; Lazarus *et al.*, 1988; Parkin *et al.*, 1988). However, this study has increased our understanding of c-*myc* protein synthesis by providing evidence that the translation of c-*myc* mRNAs may occur by

both the conventional scanning mechanism and the internal entry of ribosomes. Potentially, c-*myc* protein synthesis could be regulated using both of these mechanisms. In the cap-dependent mechanism, c-*myc* protein synthesis would be dependent on the activity of canonical translation initiation factors, most notably eIF4F. In addition, the IRES within the c-*myc* 5' UTR may allow the translation of c-*myc* mRNAs to occur in a cap-independent manner. By employing both mechanisms, c-*myc* gene expression can be regulated at the level of translation under diverse conditions, such as during development and after heat shock or the withdrawal of growth factors. Moreover, c-*myc* protein synthesis may be de-regulated through either mechanism, thus contributing to a transformed phenotype. Given the significant position that this protein occupies in the determination of cellular fate and its role in tumorigenesis, it is of vital importance that we gain an understanding of the influence of both the cap-dependent and internal initiation mechanisms of translation on the regulation of c-*myc* gene expression.

Abrahamsen, M. S. and Morris, D. R. (1990). Cell-type specific mechanisms of regulating expression of the ornithine decarboxylase gene after growth stimulation. *Mol. Cell. Biol.*, **10**, 5525-5528.

Alexander, W. S., Bernard, O., Cory, S., and Adams, J. M. (1989). Lymphomagenesis in E-mu-*myc* transgenic mice can involve Ras mutations. *Oncogene*, **4**, 575-581.

Ali and Siddiqui, 1997. The La autoantigen binds the 5' noncoding region of the hepatitis C virus RNA in the context of the initiator AUG codon and stimulates internal ribosome entry site-mediated translation. *Proc. Natl. Acad. Sci. USA.*, **94**, 2249-2254.

Altmann, M., Muller, P. P., Wittmer, B., Ruchti, F., Lanker, S., and Trachsel, H. (1993). A *Saccharomyces cerevisiae* homologue of mammalian translation initiation factor-4B contributes to RNA helicase activity. *EMBO J.*, **12**, 3997-4003.

Amati, B., Dalton, S., Brooks, M. W., Littlewood, T. D., Evan, G. I., and Land, H. (1992). Transcriptional activation by the human c-Myc oncoprotein in yeast requires interaction with Max. *Nature (London)*, **359**, 423-426.

Amati, B., Brooks, M. W., Levy, N., Littlewood, T. D., Evan, G. I., and Land, H. (1993a). Oncogenic activity of the c-Myc protein requires dimerisation with Max. *Cell*, **72**, 233-245.

Amati, B., Littlewood, T. D., Evan, G. I., and Land, H. (1993b). The c-Myc protein induces cell cycle progression and apoptosis through dimerisation with Max. *EMBO J.*, **12**, 5083-5087.

Anthony, B., Carter, P., and DeBenedetti, A. (1996). Overexpression of the proto-oncogene translation factor 4E in breast-carcinoma cell lines. *Int. J. Cancer*, **65**, 858-863.

Anthony, D. D., and Merrick, W. C. (1991). Eukaryotic initiation factor (eIF)-4F. Implications for a role in internal initiation of translation. *J. Biol. Chem.*, **266**, 10218-10226.

Armelin, H. A., Armelin, M. C. S., Kelly, K., Stewart, T., Leder, P., Cochran, B. H., and Stiles, C. D. (1984). Functional role for c-*myc* in the mitogenic response to platelet-derived growth-factor. *Nature (London)*, **310**, 655-660.

Arsura, M., Wu, M., and Sonenshein, G. E. (1996). TGFβ1 inhibits NF-κB/Rel activity inducing apoptosis of B-cells: transcriptional activation of IκBα. *Immunity*, **5**, 31-40.

Askew, D., Ashum, R., Simmons, B., and Cleveland, J. (1991). Constitutive c-*myc* expression in an IL-3-dependent myeloid cell-line suppresses cell cycle arrest and accelerates apoptosis. *Oncogene*, **6**, 1915-1922.

Auviven, M., Paasinen, A., Andersson, L. C., and Holtta, E. (1992). Ornithine decarboxylase activity is critical for cell transformation. *Nature (London)*, **360**, 355-358.

Barnes, W. M. (1994). PCR amplification of up to 35 kB DNA with high fidelity and high yield from lambda-bacteriophage templates. *Proc. Natl. Acad. Sci. USA.*, **91**, 2216-2220.

Belsham, G. J., and Sonenberg, N. (1996). RNA-protein interactions in regulation of picornavirus RNA translation. *Microbiological Rev.*, **60**, 499-511.

Benne, R., and Hershey, J. W. B. (1978). The mechanism of action of protein synthesis initiation factors in rabbit reticulocyte lysate. *J. Biol. Chem.*, **253**, 3078-3087.

Bentley, D. L., and Groudine, M. (1986a). A block to elongation is largely responsible for decreased transcription of c-*myc* in differentiated HL60 cells. *Nature (London)*, **321**, 702-706.

Bentley, D. L., and Groudine, M. (1986b). A novel promoter upstream of the human c-*myc* gene and regulation of c-*myc* expression in B-cell lymphomas. *Mol. Cell. Biol.*, **6**, 3481-3489.

Benvenisty, N., Leder, A., Kuo, A., and Leder, P. (1992). An embryonically expressed gene is a target for c-*myc* regulation via the c-Myc binding sequence. *Genes and Dev.*, **6**, 2513-2523.

Berberich, S., Hyde-DeRuyscher, N., Espenshade, P., and Cole, M. (1992). Max encodes a sequence-specific DNA binding protein and is not regulated by serum growth factors. *Oncogene*, **7**, 775-779

Bernstein, J., Shefler, I., and Elroy-Stein, O. (1995). The translational repression mediated by the platelet-derived growth factor 2/c-sis mRNA leader is relieved during megakaryocyte differentiation. *J. Biol. Chem.*, **270**, 10559-10565.

Bernstein, J., Sella, O., Le, S.-Y., and Elroy-Stein, O. (1997). PGDF2/c-sis mRNA leader contains a differentiation-linked internal ribosome entry site (D-IRES). *J. Biol. Chem.*, **272**, 9356-9362.

Blackwell, T. K., Kretzner, L., Blackwood, E. M., Eisenman, R. N. and Weintraub, H. (1990). Sequence-specific DNA binding by the c-Myc protein. *Science*, **250**, 1149-1151.

Blackwell, T. K., Huang, J., Ma, A., Kretzner, L., Alt, F. W., Eisenman, R. N., and Weintraub, H. (1993). Binding of Myc proteins to canonical and non-canonical DNA sequences. *Mol. Cell. Biol.*, **13**, 5216-5224.

Blackwood, E. M., and Eisenman R. N. (1991). Max: a helix-loop-helix zipper protein that forms a sequence-specific DNA-binding complex with Myc. *Science*, **51**, 1211-1217.

Blackwood, E. M., Luscher, B., and Eisenman, R. N. (1992). Myc and Max associate *in vivo*. *Genes and Dev.*, **6**, 71-80.

Blanchard, J.-M., Piechaczyk, M., Dani, C., Chambard, J.-C., Franchi, A., Pouyssegur, J., and Jeanteur, P. (1985). c-*myc* gene is transcribed at high rate in G_0-arrested fibroblasts and is post-transcriptionally regulated in response to growth factors. *Nature (London)*, **317**, 443-445.

Blyn, L. B., Swiderek, K. M., Richards, O., Stahl, D. C., Semler, B. L., and Ehrenfeld, E. (1996). Poly(rC) binding protein 2 binds to stem-loop IV of the poliovirus RNA 5' noncoding region: identification by automated liquid chromatography-tandem mass spectroscopy. *Proc. Natl. Acad. Sci. USA.*, **93**, 11115-11120.

Blyn, L. B., Towner, J. S., Semler, B. L., and Ehrenfeld, E. (1997). Requirement of poly(rC) binding protein 2 for translation of poliovirus RNA. *J. Virol.*, **71**, 6243-6246.

Boeck, R., and Kolakofsky, D. (1994). Position +5 and +6 can be major determinants of the efficiency of non-AUG initiation codons for protein synthesis. *EMBO J.*, **15**, 3608-3617.

Bommer, U. A., Lutsch, G., Stahl, J., and Bielka, H. (1991). Eukaryotic initiation factors eIF2 and eIF3: interactions, structure, and localisation in ribosomal initiation complexes. *Biochimie*, **73**, 1007-1019.

Bonneau, A.-M., and Sonenberg, N. (1987). Involvement of the 24 kDa cap-binding protein in the regulation of protein synthesis in mitosis. *J. Biol. Chem*, **262**, 11134-11139.

Borman, A., and Jackson, R. (1992). Initiation of translation of human Rhinovirus RNA: Mapping the internal ribosome entry site. *Virology*, **188**, 685-696.

Borman, A., and Kean, K. M. (1997). Intact eukaryotic initiation factor 4G is required for hepatitis A virus internal initiation of translation. *Virology*, **237**, 129-136.

Borman, A., Howell, M. T., Patton, J. G., and Jackson, R. J. (1993). The involvement of a spliceosome component in internal initiation of human rhinovirus RNA translation. *J. Gen. Virology*, **74**, 1775-1788.

Borman, A. M., Kirchwegwer, R., Ziegler, E., Rhoads, R. E., Skern, T., and Kean, K. M. (1997). eIF4G and its proteolytic cleavage products: Effect on initiation of protein synthesis from capped, uncapped and IRES-containing mRNAs. *RNA*, **3**, 186-196.

Borman, A., Le Mercier, P., Girard, M., and Kean, K. M. (1997). Comparison of picornaviral IRES-driven internal initiation of translation in cultured cells of different origins. *Nucleic Acids Res.*, **25**, 925-932.

Bowlin, T. L., McKnown, B. J., and Sunkara, P. S. (1986). Ornithine decarboxylase and polyamine biosynthesis are required for the growth of interleukin-2 and interleukin-3 dependent cell lines. *Cell. Immunol.*, **98**, 341-350.

Butnick, N. Z., Miyamoto, C., Chizzonite, R., Cullen, B. R., Ju, G., and Skalka, A. M. (1985). Regulation of the human c-*myc* gene: 5' noncoding sequences do not affect translation. *Mol. Cell. Biol.*, **5**, 3009-3016.

Campisi, J., Gray, H. E., Pardee, A. B., Dean, M and Sonenshein, G. E. (1984). Cell cycle control of c-*myc* but not c-*ras* is lost following chemical transformation. *Cell*, **36**, 241-247.

Carmeliet, P., Ferreira, V., Breier, G., Pollefeyt, S., Kieckens, L., Gertsenstein, M., Fahrig, M., Vandenhoeck, A., Harpal, K., Eberhardt, C., Declercq, C., Pawling, J., Moons, L., Collen, D., Risau, W., and Nagy, A. (1996). Abnormal blood vessel development and lethality in embryos lacking a single VEGF allele. *Nature (London)*, **380**, 435-439.

Chang, Y., Spicer, D. B., and Sonenshein, G. E. (1991). Effect of IL-3 on promoter usage, attenuation and antisense transcription of the c-*myc* oncogene in the IL-3 dependent Ba/F3 early pre-B cell line. *Oncogene*, **6**, 1979-1982.

Chang, C.-C., Ye, B. H., Changanti, R. S. K., and Dalla-Favera, R. (1996). BCL-6, a POZ/zinc-finger protein is a sequence-specific transcriptional repressor. *Proc. Natl. Acad. Sci. USA.*, **93**, 6947-6952.

Chaudhuri, J., Das, K., and Maitra, U. (1994). Purification and characterisation of bacterially expressed mammalian translation initiation factor-5 (eIF-5). Demonstration that eIF-5 forms a complex with eIF-2. *Biochemistry*, **33**, 4794-4799.

Chaudhuri, J., Si, K., and Maitra, U. (1997). Function of eukaryotic translation initiation factor 1A (eIF 1A) (formerly call eIF 4C) in initiation of protein synthesis. *J. Biol. Chem.*, **272**, 7883-7891.

Chomczynski, P., and Sacchi, N. (1987). Single-step method of RNA isolation by acid guanidium thiocyanate phenol-chloroform extraction. *Anal. Biochem.*, **162**, 156-159.

Chu, E., Voeller, D., Koeller, D. M., Drake, J. C., Takimoto, C. H., Maley, G. F., Maley, F., and Allegra, C. J. (1993). Identification of an RNA-binding site for thymidylate synthase. *Proc. Natl. Acad. Sci. USA.*, **90**, 517-521.

Cigan, A. M., Feng, L., and Donahue, T. F. (1988). tRNAi-met functions in directing the scanning ribosome to the start site of translation. *Science*, **242**, 93-97.

Cigan, A. M., Pabich, E. K., Feng, L., and Donahue, T. F. (1989). Yeast translation initiation suppressor SUI2 encodes the alpha-subunit of eukaryotic initiation factor-II and shares sequence identity with the human alpha-subunit. *Proc. Natl. Acad. Sci. USA.*, **86**, 2784-2788.

Clark, J. M. (1988). Novel non-template nucleotide addition-reactions catalysed by procaryotic and eukaryotic DNA-polymerases. *Nucleic Acids Res.*, **16**, 9677-9686.

Coppola, J. A., and Cole, M. D. (1986). Constitutive c-*myc* oncogene expression blocks mouse erythroleukemia cell differentiation but not commitment. *Nature (London)*, **320**, 760-763.

Cosenza, S. C., Carter, R., Pena, A., Donigan, A., Borrelli, M., Soprano, D. R., and Soprano, K. J. (1991). Growth-associated gene expression is not constant in cells traversing G1 after exiting mitosis. *J. Cell. Physiology*, **147**, 231-241.

Dalla-Favera, R., Bregni, M., Ericson, J., Patterson, D., Gallo, R. C., and Croce, C. M. (1982). Human c-*myc* oncogene is located on the region of chromosone 8 that is translocated in Burkitt's lymphoma cells. *Proc. Natl. Acad. Sci. USA.*, **79**, 7824-7827.

Dang, C. V., Dam, H. V., Buckmire, M., Lee, W. M. F. (1989). DNA binding domain of the human c-Myc produced in *Escherichia coli. Mol. Cell. Biol.*, **9**, 2477-2486.

Dani, C., Blanchard, J. M., Piechaczyk, M., El Sabouty, S., Marty, L., and Jeanteur, P. (1984). Extreme instability of c-*myc* mRNAs in normal and transformed human cells. *Proc. Natl. Acad. Sci. USA.*, **81**, 7046-7050.

Darveau, A., Pelletier, J., and Sonenberg, N. (1985). Differential efficiencies of *in vitro* translation of mouse c-*myc* transcripts differing in the 5' untranslated region. *Proc. Natl. Acad. Sci. USA.*, **82**, 2315-2319.

Das, K., Chevesich, J., and Maitra, U. (1993). Molecular cloning and expression of a cDNA for mammalian translation initiation factor-5. *Proc. Natl. Acad. Sci. USA.*, **90**, 3058-3062.

Davies, A. C., Wims, M., Spotts, G. D., Hann, S. R., and Bradley, A. (1993). A null c-*myc* mutation causes lethality before 10.5 days of gestation in homozygotes and reduced fertility in heterozygotes. *Genes and Dev.*, **7**, 671-682.

Dean, M., Levine, R. A., Ran, W., Kindy, M. S., Sonenshein, G. E., and Campisi, J. (1986). Regulation of c-*myc* transcription and mRNA abundance by serum growth factors and cell contact. *J. Biol. Chem.*, **261**, 9161-9166.

Dean, M., Cleveland, J. L., Rapp, U. R., and Ihle, J. N. (1987). Role of MYC in the abrogation of IL-3 dependence of myeloid FDC-P1 cells. *Oncogene Res.*, **1**, 279-296.

De Benedetti, A., Joshi-Barve, S., Rinker-Schaeffer, C., and Rhoads, R. E. (1991). Expression of antisense RNA against initiation factor eIF4E mRNA in HeLa cells results in lengthened cell division times, diminished translation rates, and reduced levels of both eIF4E and the p220 component of eIF4F. *Mol. Cell. Biol.*, **11**, 5435-5445.

De Benedetti, A., Joshi, B., Graff, J. R., and Zimmer, S. G. (1994). CHO cells transformed by the translation factor eIF-4E display increased c-*myc* expression, but require overexpression of Max for tumorigenicity. *Mol. Cell. Diff.*, **2**, 347-371.

Delgardo, M. D., Lerga, A., Canelles, M., Gómez-Casares, M. T., and León, J. (1995). Differential regulation of Max and the role of c-Myc during erythroid and myelomonocytic differentiation of K562 cells. *Oncogene*, **10**, 1659-1665.

DeMelo Neto, O. P., Standart, N., and Martins de Sa, C. (1995). Autoregulation of poly[A]-binding protein synthesis *in vitro*. *Nucleic Acids Res.*, **23**, 2198-2205.

Dignam, J. D., Lebovitz, R. M., and Roeder, R. G. (1983). Eukaryotic gene expression with purified components. *Nucleic Acids Res.*, **11**, 1475-1489.

Dmitrovsky, E., Kuehl, W. M., Hollis, G. F., Kirsh, I. R., Bender, T. P., and Segal, S. (1986). Expression of a transfected human c-*myc* oncogene inhibits differentiation of a mouse erythroleukemia cell line. *Nature (London)*, **322**, 748-750.

Donahue, T. F., Cigan, A. M., Pabich, E. K., and Valavicius, B. C. (1988). Mutations at a Zn(II) finger motif in the yeast eIF-2β gene alter ribosome start site selection during ribosome scanning. *Cell*, **54**, 633-639.

Dorner, A. J., Semler, B. L., Jackson, R. J., Hanecak, R., Duprey, E., and Wimmer, E. (1984). *In vitro* translation of poliovirus RNA-utilisation of internal initiation sites in reticulocyte lysate. *J. Virol.*, **50**, 507-514.

Dorris, D. R., Erickson, F. L., and Hannig, E. M. (1995). Mutations in GCD11, the structural gene for eIF-2γ in yeast, alter translational regulation of GCN4 and the selection of the start site for protein synthesis. *EMBO J.*, **14**, 2239-2249.

Dosil, M., Alvarez-Fernandez, L., and Gomez-Marquez, J. (1993). Differentiation-linked expression of α-prothymosin in human myeloid leukemic cells. *Exp. Cell. Res.*, **204**, 94-101.

Dou, Q. P., Levin, A. H., Zhao, S., and Pardee, A. B. (1993). Cyclin E and cyclin A as candidates for the restriction point protein. *Cancer Res.*, **53**, 1493-1497.

Downs, K. M., Martin, G. R., and Bishop, J. M. (1989). Contrasting patterns of c-Myc and N-Myc expression during gastrulation of the mouse embryo. *Genes and Dev.*, **3**, 860-869.

Drummond, D. R., Armstrong, J., and Colman, A. (1985). The effect of capping and polyadenylation on the stability, movement and translation os synthetic messenger RNAs in *Xenopus* oocytes. *Nucleic acids Res.*, **13**, 7375-7394.

Duncan, R., and Hershey, J. W. B. (1984). Heat shock-induced translational alterations in HeLa cells. Initiation factor modifications and the inhibition of translation. *J. Biol. Chem.*, **259**, 11882-11889.

Duncan, R., and Hershey, J. W. B. (1985). Regulation of initiation factors during translational repression caused by serum depletion-Covalent modification. *J. Biol. Chem.*, **260**, 5493-5497.

Duncan, R., Milburn, S. C., and Hershey, J. W. B. (1987). Regulated phosphorlyation and low abundance of HeLa cell initiation factor eIF-4F suggests a role in translational control. *J. Biol. Chem.*, **262**, 380-388.

Dunn, B. K., Cogliati, T., Cultaro, C. M., Bar-Ner, M., and Segal, S. (1994). Regulation of murine Max (Myn) parallels the regulation of c-Myc in differentiating murine erythroleukemia cells. *Cell Growth Diff.*, **5**, 847-854.

Dwarki, V. J., Malone, R. W., and Verma, I. M. (1993). Cationic liposome-mediated RNA transfection. *Meth. in Enzymology*, **217**, 644-654.

Eick, D., Berger, R., Polack, A. and Bornkamm, G. W. (1987). Transcription of c-*myc* in human mononuclear cells is regulated by an elongation block. *Oncogene*, **2**, 61-65.

Eilers, M., Schirm, S., and Bishop, J. M. (1991). The MYC protein activates transcription of the α-prothymosin gene. *EMBO J.*, **10**, 133-141.

Ekici, A. B., Park, O. S., Fuchs, C., and Rautenstrauss, B. (1997). One-tube two-stage PCR-directed mutagenesis using megaprimers. *Elsvier Trends Journals Technical Tips Online*, **T01122**.

El-Deiry, W. S., Tokino, T., Velculescu, V. E., Levy, D. B., Parsons, R., Trent, J. M., Lin, D., Mercer, W. E., Kinzler, K. W., and Vogelstein, B. (1993). WAF1, a potential mediator of p53 tumour suppression. *Cell*, **75**, 817-825.

Etchison, D., and Smith, K. (1990). Variations in cap-binding complexes from uninfected and poliovirus-infected HeLa cells. *J. Biol. Chem.*, **265**, 7492-7500.

Etchison D., Milburn, S. C., Edery, I., Sonenberg, N., and Hershey, J. W. B. (1982). Inhibition of HeLa cell protein synthesis following poliovirus infection correlates with the proteolysis of a 220,000-dalton polypeptide associated with eukaryotic initiation factor 3 and a cap binding protein complex. *J. Biol. Chem.*, **257**, 14806-14810.

Evan, G. I., Wyllie, A. H., Gilbert, C. S., Littlewood, T. D., Land, H., Brooks, M., Waters, C. M., Penn, L. Z., and Hancock, D. C. (1992). Induction of apoptosis in fibroblasts by c-*myc* protein. *Cell*, **69**, 119-128.

Evan, G., Harrington, E., Fanidi, A., Land, H., Amati, B., and Bennett, M. (1994). Integrated control of cell proliferation and cell death by the c-*myc* oncogene. *Phil. Trans. R. Soc. Lond. B*, **345**, 269-275.

Evan, G. I., Kauffmann-Zeh, A., McCarthy, N., Ulrich, E., and Whyte, M. (1996). Interplay between cytokine signalling and oncogene expression in the control of cell viability. *Mol. Biol. of the Cell*, **7**, 2938.

Evans, D. R. (1986). CAD, a chimeric protein that initiates de novo pyrimidine biosynthesis in higher eukaryotes. *In Multidomain proteins-structure and evolution*. Elsvier Biochemical Press, Amsterdam. p. 283-331.

Fletcher, L., Corbin, S. D., Browning, K. S., and Ravel., J. M. (1990). The absence of a m^7G cap on beta-globin mRNA and alfalfa mosaic virus RNA 4 increases the amount of initiation factor 4F required for translation. *J. Biol. Chem.*, **265**, 19582-19587.

Fraser, S. D., Wilkes-Johnston, J., and Browder, L. W. (1996). Effects of c-*myc* first exons and 5' synthetic hairpins on RNA translation in oocytes and early embryos of *Xenopus laevis*. *Oncogene*, **12**, 1223-1230.

Freytag, S. O., Dang, C. V., and Lee, W. M. F. (1990). Definition of the activities and properties of c-Myc required to inhibit cell differentiation. *Cell Growth Diff.*, **1**, 339-343.

Fu, L., Ye, R., Browder, L. W., and Johnston, R. N. (1991). Translational potentiation of messenger RNA with secondary structure in *Xenopus*. *Science*, **251**, 807-810.

Fuerst, T. R., Niles, E. G., Studier, F. W., and Moss, B. (1986). Eukaryotic transient-expression system based on recombinant vaccinia virus that synthesises bacteriophage-T7 RNA-polymerase. *Proc. Natl. Acad. Sci. USA.*, **83**, 8122-8126.

Fukuchi-Shimogori, T., Ishii, I., Kashiwagi, K., Mashiba, H., Ekimoto, H., and Igarashi, K. (1997). Malignant transformation by overproduction of translation initiation factor eIF4G. *Cancer Res.*, **57**, 5041-5044.

Galaktionov, K., Chen, X., and Beach, D. (1996). Cdc25 cell-cycle phosphatase as a target of c-*myc*. *Nature (London)*, **382**, 511-517.

Gamarnik, A. V., and Andino, R. (1996). Replication of poliovirus in *Xenopus* oocytes requires two human factors. *EMBO J.*, *15*, 5988-5998.

Gan, W., and Rhoads, R. E. (1996). Internal initiation of translation directed by the 5'-untranslated region of the mRNA for eIF4G, a factor involved in the picornavirus induced switch from cap-dependent to internal initiation. *J. Biol. Chem.*, **271**, 623-626.

Gan, W., La Celle, M., and Rhoads, R. E. (1998). Functional characterisation of the internal ribosome entry site of eIF4G mRNA. *J. Biol. Chem.*, **273**, 5006-5012.

Gaubatz, S., Miechle, A., and Eilers, M. (1994). An E-box element localized in the first intron mediates regulation of the prothymosin-α gene by c-*myc*. *Mol. Cell. Biol.*, **14**, 3853-3862.

Geballe, A. P., and Morris, D. R. (1994). Initiation codons within 5' leaders of messenger-RNAs as regulators of translation. *Trends Biochem. Sci.*, **19**, 159-164.

Gingras, A. C., Svitkin, Y., Belsham, G. J., Pause, A., and Sonenberg, N. (1996). Activation of the translational suppressor 4E-BP1 following infection with encephalomyocarditis and poliovirus. *Proc. Natl. Acad. Sci. USA.*, **93**, 5578-5583.

Godeau, F., Persson, H., Gray, H. E., and Pardee, A. B. (1986). c-*myc* expression is dissociated from DNA synthesis and cell proliferation in *Xenopus* oocyte and early embryonic development. *EMBO J.*, **5**, 3571-3577.

Godefrey-Colburn, T., and Thatch, R. E. (1981). The role of mRNA competition in regulating translation. *J. Biol. Chem.*, **256**, 11762-11773.

Goumans, H., Thomas, A., Verhoeven, A., Voorma, H. O., and Benne, R. (1980). The role of eIF-4C in protein synthesis initiation complex formation. *Biochim. Biophys. Acta.*, **608**, 39-46.

Goyer, C., Altmann, M., Lee, H. S., Blanc, A., Deshmukh, M., Woolford, J. L. Jr., Trachsel, H., and Sonenberg, N. (1983). TIF4631 and TIF4632: Two yeast genes encoding the high-molecular-weight subunits of the cap-binding protein (eIF 4F) contain an RNA recognition motif-like sequence and carry out an essential function. *Mol. Cell. Biol.*, **13**, 4860-4874.

Grandori, C., Mac, J., Siebelt, F., Ayer, D. E., and Eisenman R. N., (1996). Myc-Max heterodimers activate a DEAD box gene and interact with multiple E box related sites *in vivo*. *EMBO J.*, **15**, 4344-4357.

Grant, C. M., Miller, P. F., and Hinnebusch, A. G. (1994). Requirements for intercistronic distance and level of eukaryotic initiation factor-II activity in reinitiation on GCN4 mRNA vary with the downstream cistron. *Mol. Cell. Biol.*, **14**, 2616-2628.

Gray, N. K., and Hentze, M. W. (1994). Regulation of protein synthesis by mRNA secondary structure. *Mol. Biol. Reports*, **19**, 195-200.

Grens, A., and Scheffler, I. E. (1990). The 5' and 3' untranslated regions of ornithine decarboxylase mRNA affect the translational efficiency. *J. Biol. Chem.*, **265**, 11810-11816.

Griep, A. E., and Westphal, H. (1988). Antisense Myc sequences induce differentiation of F9 cells. *Proc. Natl. Acad. Sci. USA.*, **85**, 6806-6810.

Grifo, J. A., Tahara, S. M., Morgan, M. A., Shatkin, A. J., and Merrick, W. C. (1983). New initiation factor activity required for globin messenger RNA translation. *J. Biol. Chem.*, **258**, 5804-5810.

Grifo, J. A., Abramson, R. D., Satler, C. A., and Merrick, W. C. (1984). RNA-stimulated ATPase activity of eukaryotic initiation factors. *J. Biol. Chem.*, **259**, 8648-8654.

Grignani, F., Lombardi, L., Inghirami, G., Sternas, L., Cechova, K., and Dalla-Favera, R. (1990). Negative autoregulation of c-*myc* gene expression is inactivated in transformed cells. *EMBO J.*, **9**, 3913-3922.

Grünert, S., and Jackson, R. J. (1994). The immediate downstream codon strongly influences the efficiency of eukaryotic translation initiation codons. *EMBO J.*, **13**, 3618-3630.

Gunnery, S., and Mathews, M. B. (1995). Functional mRNA can be generated by RNA polymerase III. *Mol. Cell. Biol.*, **15**, 3597-3607.

Haas, I. G. (1991). BiP-a heat shock protein involved in immunoglobulin chain assembly. *Current topics in microbiology and immunology*, **167**, 71-82.

Haghighat, A., and Sonenberg, N. (1997). eIF4G dramatically enhances binding of eIF4E to the mRNA 5'-cap structure. *J. Biol. Chem.*, **272**, 21677-21680.

Haller, A. A., and Semler, B. L. (1992). Linker scanning mutagenesis of the internal ribosome entry site of poliovirus RNA. *J. Virol.*, **66**, 5075-5086.

Hambridge, S. J., and Sarnow, P. (1991). Terminal 7-methyl-guanosine cap structure on the normally uncapped 5' noncoding region of poliovirus mRNA inhibits its translation in mammalian cells. *J. Virol.*, **65**, 6312-6315.

Hambridge, S. J., and Sarnow, P. (1992). Translational enhancement of the poliovirus 5' noncoding region mediated by virus-encoded polypeptide 2A. *Proc. Natl. Acad. Sci. USA*, **89**, 10272-10276.

Hann, S. R., and Eisenman, R. N. (1984). Proteins encoded by the human c-*myc* oncogene: differential expression in neoplastic cells. *Mol. Cell. Biol.*, **4**, 2486-2497.

Hann, S. R., Thompson, C. B., and Eisenman, R. N. (1985). c-*myc* oncogene protein synthesis is independent of the cell cycle in human and avian cells. *Nature (London)*, **314**, 366-369.

Hann, S. R., King, M. W., Bentley, D. L., Anderson, C. W., and Eisenman, R. N. (1988). A non-AUG translational initiation codon in c-*myc* exon 1 generates an N-terminally distinct protein whose synthesis is disrupted in Burkitt's lymphoma. *Cell*, **52**, 185-195.

Hann, S. R., Sloan-Brown, K., and Spotts, G. (1992). Translational activation of the non-AUG-initiated c-*myc* 1 protein at high cell densities due to methionine deprivation. *Genes and Dev.*, **6**, 1229-1240.

Hann, S. R., Dixit, M., Sears, R. C., and Sealy, L. (1994). The alternatively initiated c-Myc proteins differentially regulate transcription through a noncanonical DNA-binding site. *Genes and Dev.*, **8**, 2441-2452.

Hatakeyama, M., Brill, J. A., Fink, G. R., and Weinberg, R. A. (1994). Collaboration of G(1) cyclins in the functional inactivation of the retinoblastoma protein. *Genes and Dev.*, **8**, 1759-1771.

Heikkila, R., Schwab, G., Wickstrom, E., Loke, S. L., Pluznik., D. H., Watt, R., and Neckers, L. M. (1987). A c-*myc* antisense oligodeoxynucleotide inhibits entry into S-phase but not progression from G_0 to G_1. *Nature (London)*, **328**, 445-449.

Hellen, C. U. T., Witherell, G. W., Schmid, M., Shin, S. H., Pestova, T. V., Gil, A., and Wimmer, E. (1993). A cytoplasmic 57 kDa protein that is required for translation of picornavirus RNAs by internal ribosome entry is identical to the nuclear pyrimidine tract binding protein. *Proc. Natl. Acad. Sci. USA.*, **90**, 7642-7646.

Henriksson, M., and Lüscher, B. (1996). Proteins of the Myc network: Essential regulators of cell growth and differentiation. *Advances in Cancer Res.*, **68**, 109-182.

Hermeking, H., and Eick, D. (1994). Mediation of c-Myc-induced apoptosis by p53. *Science*, **265**, 2091-2093.

Hershey, J. W. B. (1991). Translational control in mammalian cells. *Ann. Rev. Biochem.*, **60**, 717-755.

Hinnebusch, A. G. (1996). Translational control of GCN4: gene-specific regulation by phosphorylation of eIF2. *In Translational control* (Hershey, J. W. B., Matthews, M. B., and Sonenberg, N., eds) pp. 199-244, Cold Spring Harbour Laboratory Press.

Hiremath, L. S., Webb, R. N., and Rhoads, R. E. (1985). Immunological detection of the messenger RNA cap binding protein. *J. Biol. Chem.*, **260**, 7843-7849.

Hirvonen, H., Makela, T. P., Sandberg, M., Kalimo, H., Vuorio, E., and Alitalo, K. (1990). Expression of the *myc* proto-oncogenes in developing human fetal brain. *Oncogene*, **5**, 1787-1797.

Holt, J. T., Redner, R. L., and Nienhuis, A. W. (1988). An oligomer complementary to c-*myc* mRNA inhibits proliferation of HL60 cells and induces differentiation. *Mol. Cell. Biol.*, **8**, 963-973.

Hoover, D. S., Wingett, D. G., Zhang, J., Reeves, R., and Magnuson, N. S. (1997). Pim-1 protein expression is regulated by its 5'-untranslated region and translation initiation factor eIF-4E. *Cell Growth and Diff.*, **8**, 1371-1380.

Huang, J., and Schneider, R. J. (1991). Adenovirus inhibition of cellular protein synthesis involves inactivation of the cap binding protein. *Cell*, **65**, 271-280.

Huang, M. T. F., and Gorman, C. M. (1990). The simian virus-40 small T-intron, present in many common expression vectors, leads to abberant splicing. *Mol. Cell. Biol.*, **10**, 1805-1810.

Hurlin, P. J., Queva, C., Koskinen, P. J., Steingrimsson, E., Ayer, D. E., Copeland, N. G., Jenkins, N. A., and Eisenman, R. N. (1995). Mad3 and Mad4: novel Max-interacting transcriptional repressors that suppress c-*myc* dependent transformation and are expressed during neural and epidermal differentiation. *EMBO J.*, **14**, 5646-5659.

Iizuka, N., Najita, L., Franzusoff, A., Sarnow, P. (1994). Cap-dependent and cap-independent translation by internal initiation of mRNAs in cell extracts prepared from *Saccharomyces cerevisiae*. *Mol. Cell. Biol.*, **14**, 7322-7330.

Iizuka, N., Chen, C., Yang, G., Johannes, G., and Sarnow, P. (1995). Cap-independent translation and internal initiation of translation in eukaryotic cellular mRNA molecules. *Current topic in microbiology and immunology*, **203**, 155-177.

Imataka, H., and Sonenberg, N. (1997). Human eukaryotic initiation factor 4G (eIF4G) possesses two separate and independent binding sites for eIF4A. *Mol. Cell. Biol.*, **17**, 6940-6947.

Ingvarsson, S., Asker, C., Axelson, H., Klein, G., and Sumegi, J (1988). Structure and expression of B-Myc, a new member of the Myc gene family. *Mol. Cell. Biol.*, **8**, 3168-3174.

Jackson, R. J., Howell, M. T., and Kaminski, A. (1990). The novel mechanism of internal initiation of picornavirus RNAs. *Trends in Biochem. Sci.*, **15**, 477-483.

Jackson, R. J., Hunt, S. L., Gibbs, C. L., and Kaminski, A. (1994). Internal initiation of translation of picornavirus RNAs. *Molecular Biology Reports*, **19**, 147-159.

Jackson, R. J., and Kaminski, A. (1995). Internal initiation of translation in eukaryotes: The picornavirus paradigm and beyond. *RNA*, **1**, 985-1000.

Jackson, R. J., Hunt, S. L., Reynolds, J. E., and Kaminski, A. (1995). Cap-dependent and cap-independent translation: operational distinctions and mechanistic interpretations. *Current topic in microbiology and immunology*, **203**, 1-29.

Jackson, R. J. (1996). A comparative view of initiation site selection mechanisms. In *Translational Control*, 1996. Cold Spring Harbour Laboratory Press, p71-111.

Jagus, R., Anderson, W. F., and Safer, B. (1981). The regulation of initiation of mammalian protein synthesis. *Prog. Nucleic Acids Res. Mol. Biol.*, **25**, 127-185.

Jang, S. K., Davies, M. V., Kaufman, R. J., and Wimmer, E. (1989). Initiation of protein synthesis by internal entry of ribosomes into the 5' nontranslated region of encephalomyocarditis virus RNA *in vivo*. *J. Virol.*, **63**, 1651-1660.

Jang, S. K., and Wimmer, E. (1990). Cap-independent translation of encephalomyocarditis virus RNA: structural elements in the internal ribosome entry site and the involvement of a 57 kDa RNA binding protein. *Genes and Dev.*, **4**, 1560-1572.

Jansen-Dürr, P., Meichle, A., Steiner, P., Pagano, M., Finke, K., Botz, J., Wessbecher, J., Draetta, G., and Eilers, M. (1993). Differential modulation of cyclin gene expression by MYC. *Proc. Natl. Acad. Sci. USA.*, **90**, 3685-3689.

Jefferies, H. B. J., Reinhard, C., Kozma, S. C., and Thomas, G. (1994). Rapamycin selectively represses translation of the "polypyrimidine tract" mRNA family. *Proc. Natl. Acad. Sci. USA.*, **91**, 4441-4445.

Jinno, S., Suto, K., Nagata, A., Igarashi, M., Kanaoka, Y., Nojima, H., and Okayama, H. (1994). Cdc25A is a novel phosphatase functioning early in the cell cycle. *EMBO J.*, **13**, 1549-1556.

Jones, R. J., Branda, J., Johnston, K. A., Polymenis, M., Gadd, M., Rustgi, A., Callanan, L., and Schmidt, E. V. (1996). An essential E-box in the promoter of the gene encoding the mRNA cap binding protein (eukaryotic initiation factor 4E) is a target for activation by c-myc. *Mol. Cell. Biol.*, **16**, 4754-4764.

Jordan, M., Schallhorn, A., and Wurm, F. M. (1996). Transfecting mammalian cells: optimization of critical parameters affecting calcium-phosphate precipitate formation. *Nucleic Acids Res.*, **24**, 596-601.

Joshi, B., Yan, R., and Rhoads, R. E. (1994). *In vitro* synthesis of human protein synthesis initiation factor eIF-4γ and its location on 43S and 48S initiation complexes. *J. Biol. Chem.*, **269**, 2048-2055.

Joshi-Barve, S., De Benedetti, A., and Rhoads, R. E. (1992). Preferential translation of heat shock mRNAs in HeLa cells deficient in protein synthesis initiation factors eIF4E and eIF4γ. *J. Biol. Chem.*, **267**, 21038-21043.

Kaminski, A., Howell, M. T., and Jackson, R. J. (1990). Initiation of encephalomyocarditis virus RNA translation: the authentic initiation site is not selected by a scanning mechanism. *EMBO J.*, **9**, 3753-3759.

Kaminski, A., Belsham, G. J., and Jackson, R. J. (1994). Translation of encephalomyocarditis virus RNA; parameters influencing the selection of the internal initiation site. *EMBO J.*, **13**, 1673-1681.

Kaminski, A., Hunt, S. L., Patton, J. G., and Jackson, R. J. (1995). Direct evidence that polypyrimidine tract binding protein (PTB) is essential for internal initiation of translation of encephalomyocarditis virus RNA. *RNA*, **1**, 924-938.

Kaptein, K. S., Lin, C. K., Wang, C. L., Nguyen, T. T., Kalunta, C., Park, E., Chen, F. S., and Lad, P. M. (1996). Anti-IgM-mediated regulation of c-*myc* and its possible relationship to apoptosis. *J. Biol. Chem.*, **271**, 18875-18884.

Kato, G. J., Barret, J., Villa-Garcia, M., and Dang, C. V. (1990). An amino-terminal c-Myc domain required for neoplastic transformation activates transcription. *Mol. Cell. Biol.*, **10**, 5914-5920.

Kelly, K., Cochran, B. H., Stiles, C. D., and Leder, P. (1983). Cell-specific regulation of the c-*myc* gene by lymphocyte mitogens and platelet-derived growth factor. *Cell*, **35**, 603-610.

Kevil, C., Carter, P., Hu, B., and De Benedetti, A. (1995). Translational enhancement of FGF-2 by eIF-4 factors and alternate utilisation of CUG and AUG codons for translation initiation. *Oncogene*, **11**, 2339-2348.

Koromilas, A. E., Lazaris-Karatzas, A., and Sonenberg, N. (1992). mRNAs containing extensive secondary structure in their 5' non-coding region translate efficiently in cells overexpressing initiation factor eIF-4E. *EMBO J.*, **11**, 4153-4158.

Kozak, M. (1986a). Influences of mRNA secondary structure on initiation by eukaryotic ribosomes. *Proc. Natl. Acad. Sci. USA.*, **83**, 2850-2854.

Kozak, M (1986b). Point mutations define a sequence flanking the initiator codon that modulates translation by eukaryotic ribosomes. *Cell*, **44**, 283-292.

Kozak, M (1987). An analysis of the 5' noncoding sequences upstream from 699 vetebrate messenger RNAs. *Nucleic Acids Res.*, **15**, 8125-8148.

Kozak, M. (1989). Circumstances and mechanisms of inhibition of translation by secondary structure in eukaryotic mRNAs. *Mol. Cell. Biol.*, **9**, 5134-5142.

Kozak, M. (1991a). An analysis of vertebrate mRNA sequences: Intimations of translational control. *J. Cell. Biol.*, **115**, 887-903.

Kozak, M. (1991b). Structural features in eukaryotic messenger-RNAs that modulate the initiation of translation. *J. Biol. Chem.*, **266**, 19867-19870.

Kozak, M. (1997). Recognition of AUG and alternative initiator codons is augmented by a G in position +4 but is not generally affected by the nucleotides in positions +5 and +6. *EMBO J.*, **16**, 2482-2492.

Kretzner, L., Blackwood, E. M., and Eisenman, R. N. (1992). Myc and Max proteins possess distinct transcriptional activities. *Nature (London)*, **359**, 426-429.

Kuge, S., Kawamura, N., and Nomoto, A. (1989). Genetic variation occurring on the genome of an *in vitro* insertion mutant of poliovirus type 1. *J. Virol.*, **63**, 1069-1075.

Laemelli, U. K. (1970). Cleavage of structural proteins during the assembly of the head of bacteriophage T4. *Nature (London)*, **227**, 680-685.

Lamphear, B. J., and Panniers, R. (1990). Cap-binding complex that restores protein synthesis in heat-shocked Ehrlich cell lysate contains highly phosphorylated eIF-4E. *J. Biol. Chem.*, **265**, 5333-5336.

Lamphear, B. J., and Panniers, R. (1991). Heat shock impairs the interaction of cap binding protein complex with the 5' mRNA cap. *J. Biol. Chem.*, **266**, 2789-2794.

Lamphear, B. J., Kirchweger, R., Skern, T., and Rhoads, R. (1995). Mapping of functional domains in the eukaryotic protein synthesis initiation factor 4G (eIF 4G) with picornaviral proteases. *J. Biol. Chem.*, **270**, 21975-21983.

Landschulz, W. H., Johnson, P. F., and McKnight, S. L. (1988). The leucine zipper-a hypothetical structure common to a new class of DNA-binding proteins. *Science*, **240**, 1759-1764.

Lawson, T. G., Ray, B. K., Dodds, J. T., Grifo, J. A., Abramson, R. D., Merrick, W. C., Betsch, D. F., Weith, H. L., and Thatch, R. E. (1986). Influence of 5' proximal secondary structure on the translational efficiency of eukaryotic messenger-RNAs and on their interaction with initiation factors. *J. Biol. Chem.*, **261**, 13979-13989.

Lazaris-Karatzas, A., Montine, K. S., and Sonenberg, N. (1990). Malignant transformation by a eukaryotic initiation factor that binds to the 5' cap. *Nature (London)*, **345**, 544-547.

Lazarus, P., Parkin, N., and Sonenberg, N. (1988). Developmental regulation of translation by the 5' noncoding region of murine c-*myc* mRNA in *Xenopus laevis*. *Oncogene*, **3**, 517-521.

Le, S.-Y., and Maizel, Jnr. J. V (1997). A common RNA structural motif involved in the internal initiation of translation of cellular mRNAs. *Nucleic Acids Res.*, **25**, 362-369.

Le, S.-Y., Siddiqui, A., and Maizel, Jnr. J. V. (1996). A common structural core in the internal ribosome entry sites of picornavirus, hepatitis C, and pestivirus. *Virus Gene*, **12**, 135-147.

Lee, K. A., Edery, I., and Sonenberg, N. (1985). Isolation and characterisation of cap-binding proteins from poliovirus-infected HeLa cells. *J. Virol.*, **54**, 515-524.

Lee, L. A., and Dang, C. V. (1997). c-Myc transrepression and cell transformation. *Current topics in microbiology and immunology*, **224**, 131-135.

Leffers, H., Dejgaard, K., and Celis, J. E. (1995). Characterisation of 2 major cellular poly(rC)-binding human proteins, each containing 3 K-homolous (KH) domains. *Eur. J. Biochem.*, **230**, 447-453.

Li, L.-H., Nerlov, C., Prendergast, G., MacGregor, D., and Ziff, E. B. (1994). c-Myc represses transcription *in vivo* by a novel mechanism dependent on the initiator element and Myc box II. *EMBO J.*, **13**, 4070-4079.

Lin, T.-A., Kong, X., Haystead, T. A. J., Pause, A., Belsham, G., Sonenberg, N., and Lawrence, J. C. Jr. (1994). PHAS-I as a link between mitogen-activated protein kinase and translation initiation. *Science*, **266**, 653-656.

Linquist, S. (1981). Regulation of protein synthesis during heat shock. *Nature (London)*, **293**, 311-314.

Linquist, S., and Petersen, R. (1991). Selective translation and degradation of heat-shock messenger RNAs in *Drosophila*. *Enzyme*, **44**, 147-166.

Lodish, H. F. (1974). Model for the regulation of mRNA translation applied to haemoglobin synthesis. *Nature (London)*, **251**, 385-388.

Lodish, H. F., and Rose, J. K., (1977). Relative importance of the 7-methylguanosine in ribosome binding and translation of vesicular stomatitis virus mRNA in wheat germ extract and reticulocyte cell-free systems. *J. Biol. Chem.*, **252**, 1181-1188.

Lüscher, B, and Eisenman, R. N. (1988). c-*myc* and c-*myb* protein degradation: effect of metabolic inhibitors and heat shock. *Mol. and Cell. Biol.*, **8**, 2504-2512.

Lüscher, B., and Eisenman, R. N. (1990). New light on Myc and Myb: 1. Myc. *Genes and Dev.*, **4**, 2025-2035.

Macejak, D. G., and Sarnow, P. (1991). Internal initiation of translation mediated by the 5' leader of a cellular mRNA. *Nature (London)*, **353**, 90-94.

Macejak, D. G., Hambridge, S. J., Najita, L. M., and Sarnow, P. (1990). EIF-4F-independent translation of poliovirus RNA and cellular mRNA encoding glucose regulated protein 78/immunoglobulin heavy-chain binding protein. In *New aspects of positive-stranded RNA viruses*. (Brinton, M. A., and Heinz, F. X., eds), pp 152-157, American society for microbiology.

Malone, R. W., Felgner, P. L., and Verma, I. M. (1989). Cationic liposome-mediated RNA transfection. *Proc. Natl. Acad. Sci. USA.*, **86**, 6077-6081.

Manzella, J. M., Rychlik, W., Rhoads, R. E., Hershey, J. W. B., and Blackshear, P. J. (1991). Insulin induction of ornithine decarboxylase. *J. Biol. Chem.*, **266**, 2383-2389.

Marcu, K. B., Bossone, S. A., and Patel, A. J. (1992). *myc* function and regulation. *Ann. Rev. Biochem.*, **61**, 809-860.

Martel, C., Lallemand, D., and Crémisi, C. (1995). Specific c-Myc and Max regulation in epithelial cells. *Oncogene*, **10**, 2195-2205.

Matsumoto, K., Wassarman, K. M., and Wolffe, A. P. (1998). Nuclear history of a pre-mRNA determines the translation activity of the cytoplasmic mRNA. *EMBO J.*, **17**, 2107.

McBratney, S., and Sarnow, P. (1996). Evidence for involvement of *trans*-acting factors in selection of the AUG start codon during eukaryotic translation initiation. *Mol. Cell. Biol.*, **16**, 3523-3534.

McGarry, T. J., and Lindquist, S. (1985). The preferential translation of *Drosophila* HSP70 messenger-RNA requires sequences in the untranslated leader. *Cell*, **42**, 903-911.

Meerovitch, K., Pelletier, J., and Sonenberg, N. (1989). A cellular protein that binds to the 5' non-coding region of poliovirus RNA: implications for internal translation initiation. *Genes and Dev.*, **3**, 1026-1034.

Meerovitch, K., Nicholson, R., and Sonenberg, N. (1991). *In vitro* mutational analysis of *cis*-acting RNA translational elements within the poliovirus type 2 5' untranslated region. *J. Virol.*, **65**, 5895-5901.

Meerovitch, K., Lee, H. S., Svitkin, Y., Kenan, D. J., Chan, E. K. L., Agol, V. I., Keene, J. D., and Sonenberg, N. (1993). La autoantigen enhances and corrects translation of poliovirus RNA in reticulocyte lysate. *J. Virol.*, **67**, 3798-3807.

Melefors, O., Goossen, B., Johansson, H. E., Stripecke, R., Gray, N. K., and Hentze, M. W. (1993). Translational control of the 5-aminolevulinate synthase messenger-RNA by the iron-response elements in erythroid cells. *J. Biol. Chem.*, **268**, 5974-5978.

Meyer, K., Petersen, A., Niepmann, M., and Beck, E. (1995). Interaction of the eukaryotic initiation factor-4B with a picornavirus internal translation initiation site. *J. Virol.*, **69**, 2819-2824.

Meyuhas, O., Avni, D., and Shama, S. (1996). In *Translational control* (Hershey, J. W. B., Mattews, M. B., and Sonenberg, N., eds) pp. 363-388, Cold Spring Harbour Laboratory Press.

Miltenberger, R. J., Sukow, K. A., and Farnham, P. J. (1995). An E-box-mediated increase in cad transcription at the G1/S-phase boundary is suppressed by inhibitory c-*Myc* mutants. *Mol. and Cell. Biol.*, **15**, 2527-2535.

Mink, S., Mutschler, B., Weiskirchen, R., Bister, K., and Klempnauer, K.-H. (1996). A novel function for Myc: Inhibition of C/EBP-dependent gene activation. *Proc. Natl. Acad. Sci. USA.*, **93**, 6635-6640.

Minnich, W. B., Balasta, M. L., Goss, D. J., and Rhoads, R. E. (1994). Chromatographic resolution of *in vivo* phosphorylated and nonphosphorylated eukaryotic translation initiation factor eIF-4E: increased cap affinity of the phosphorylated form. *Proc. Natl. Acad. Sci. USA.*, **91**, 7668-7672.

Mol, P. C., Wang, R.-H., Batey, D. W., Lee, L. A., Dang, C. V., and Berger, S. L. (1994). Do products of the c-*myc* proto-oncogene play a role in transcriptional regulation of the prothymosin α gene? *Mol. Cell. Biol.*, **15**, 6999-7009.

Morgan, M. A., and Shatkin, A. J. (1980). Initiation of Reovirus transcription by inosine 5'-triphosphate and properties of 7-methylinosine-capped, inosine substituted messenger ribonucleic acids. *Biochemistry*, **19**, 5960-5966.

Mori, M., Barnard, G. F., Staniumus, R. J., Jessup, J. M., Steel, G. D., Jnr., and Chen, L. B. (1993). Prothymosin-alpha messenger-RNA expression correlates with that of c-*myc* in human colon cancer. *Oncogene*, **8**, 2821-2826.

Morley, S. J., Rau, M., Kay, J. E., and Pain, V. M. (1993). Increased phosphorylation of eukaryotic initiation factor-4α during the activation of T-lymphocytes correlates with increase initiation factor-4F complex formation. *Eur. J. Biochem.*, **218**, 39-48.

Morley, S. J., and Pain, V. M. (1995). Translational regulation during activation of porcine peripheral blood lymphocytes: association and activation of the alpha and gamma subunits of the initiation factor complex eIF-4F. *Biochem. J.*, **312**, 627-635.

Morley, S. J., Curtis, P. S., and Pain, V. M. (1997). eIF4G: Translation's mystery factor begins to yield its secrets. *RNA*, **3**, 1085-1104.

Murre, C., McCaw, P. S., Baltimore, D. (1989). A new DNA-binding and dimerisation motif in the immunoglobulin enhancer binding, daughterless, MyoD and Myc proteins. *Cell*, **56**, 777-783.

Muthukrishnan, S., Morgan, M., Banerjee, A. K., and Shatkin, A. J. (1976). Influence of the 5' terminal m^{7}G and 2'-*O*-methylated residues on messenger ribonucleic acid binding to ribosomes. *Biochemistry*, **272**, 32061-32066.

Nanbru, C., Lafon, I., Audigier, S., Gensac, M.-C., Vagner, S., Huez, G., and Prats, A.-C. (1997). Alternative translation of the proto-oncogene c-*myc* by an internal ribosome entry site. *J. Biol. Chem.*, **272**, 32061-32066.

Nau, M. M., Brooks, B. J., Battey, J., Sausville, E., Gazdar, A. F., Kirsch, I. R., McBride, O. W., Bertness, V., Hollis, G. F., and Minna, J. D. (1985). L-Myc, a new Myc-related gene amplified and expressed in human small cell lung cancer. *Nature (London)*, **318**, 69-73.

Nepveu, A., and Marcu, K. B. (1986). Intragenic pausing and anti-sense transcription within the murine c-*myc* locus. *EMBO J.*, **5**, 2859-2866.

Nepveu, A., Levine, R. A., Campisi, J., Greenberg, M. E., Ziff, E. B., and Marcu, K. B. (1987). Alternative modes of c-*myc* regulation in growth factor-stimulated and differentiating cells. *Oncogene*, **1**, 243-250.

Nilsen, T. W., and Maroney, P. A. (1984). Translational efficiency of c-*myc* mRNA in Burkitt lymphoma cells. *Mol. Cell. Biol.*, **4**, 2235-2238.

Öberg, F., Larsson, L.-G., Anton, R., and Nilsson, K. (1991). Interferon-γ abrogates the differentiation block in v-*myc* expressing U-937 cells. *Proc. Natl. Acad. Sci. USA.*, **88**, 5567-5571.

Oh, S. K., Scott, M. P., and Sarnow, P. (1992). Homeotic gene *antennapedia* mRNA contains 5'-noncoding sequences that confer translational initiation by internal ribosome binding. *Genes and Dev.*, **6**, 1643-1653.

Ohlmann, T., Rau, M., Morley, S. J., and Pain, V. M. (1995). Proteolytic cleavage of the initiation factor eIF4 gamma in the reticulocyte lysate inhibits the translation of capped mRNAs but enhances that of uncapped mRNAs. *Nucleic Acids Res.*, **23**, 334-340.

Onclercq, R., Babinet, C., and Crémisi, C. (1989). Exogenous c-*myc* overexpression interferes with early events in F-9 cell differentiation. *Oncogene Res.*, **4**, 293-302.

Packham, G., and Cleveland, J. L. (1994). Ornithine decarboxylase is a mediator of c-Myc induced apoptosis. *Mol. and Cell. Biol.*, **14**, 5741-5747.

Pain, V. M. (1986). Initiation of protein synthesis in mammalian cells. *Biochem. J.*, **235**, 625-637.

Pain, V. M. (1996). Initiation of protein synthesis in eukaryotic cells. *Eur. J. Biochem.*, **236**, 747-771.

Parkin, N., Darveau, A., Nicholson, R., and Sonenberg, N. (1988). cis-Acting translational effects of the 5' noncoding region of c-myc mRNA. Mol. Cell. Biol., 8, 2875-2883.

Paulin, F. E. M., West, M. J., Sullivan, N. F., Whitney, R. L., Lyne, L., and Willis, A. E. (1996). Aberrant translational control of the c-myc gene in multiple myeloma. Oncogene, 13, 505-513.

Paulin, F. E. M., (1997). c-myc translational regulation in multiple myeloma. A thesis submitted for the degree of doctorate. Leicester University.

Paulin, F. E. M., Chappell, S. A., and Willis, A. E. (1998). A single nucleotide change in the c-myc IRES leads to enhanced binding of a group of protein factors. Nucleic Acids Res., 26, 3097-3103.

Pause, A., and Sonenberg, N. (1992). Mutational analysis of a DEAD box RNA helicase-the mammalian translation initiation factor eIF-4A. EMBO J., 11, 2643-2654.

Pause, A., Methot, N., Svitkin, Y., Merrick, W. C., and Sonenberg, N. (1994). Dominant negative mutants of mammalian translation initiation factor eIF-4A define a critical role for eIF-4F in cap-dependent and cap-independent initiation of translation. EMBO J., 13, 1205-1215.

Pazzagli, M., Devine, J. H., Peterson, D. O., and Baldwin, T. O. (1992). Use of bacterial and firefly luciferases as reporter genes in DEAE-dextran-mediated transfection of mammalian cells. Anal. Biochem., 204, 315-323.

Pelletier, J., and Sonenberg, N. (1985a). Insertion mutagenesis to increase secondary structure within the 5' noncoding region of a eukaryotic mRNA reduces translational efficiency. Cell, 40, 515-526.

Pelletier, J., and Sonenberg, N. (1985b). Photochemical cross-linking of cap binding proteins to eukaryotic messenger-RNAs: Effect of mRNA 5' secondary structure. Mol. Cell. Biol., 5, 3222-3230.

Pelletier, J., and Sonenberg, N. (1988a). Internal initiation of translation of eukaryotic messenger-RNA directed by a sequence derived from poliovirus RNA. *Nature (London)*, **334**, 320-325.

Pelletier, J., Flynn M. E., Kaplan, G., Racaniello, V and Sonenberg, N. (1988b). Mutational analysis of upstream poliovirus AUG codons of poliovirus RNA. *J. Virol.*, **62**, 4486-4492.

Peña, A., Reddy, C. D., Wu, S., Hickok, N. J., Reddy, E. P., Yumet, G., Soprano, D. R., and Soprano, K. J. (1993). Regulation of human ornithine decarboxylase expression by the c-Myc.Max protein complex. *J. Biol. Chem.*, **268**, 27277-27285.

Penn, L. J. Z., Brooks, M. W., Laufer, E. M., and Land, H. (1990). Negative autoregulation of c-*myc* transcription. *EMBO J.*, **9**, 1113-1121.

Pestova, T. V., Hellen, C. U. T., and Wimmer, E. (1994). A conserved AUG triplet in the 5' nontranslated region of poliovirus can function as an initiation codon *in vitro* and *in vivo*. *Virology*, **204**, 729-737.

Pestova, T. V., Hellen, C. U. T., and Shatsky, I. N. (1996a). Canonical eukaryotic initiation factors determine initiation of translation by internal ribosome entry. *Mol. Cell. Biol.*, **16**, 6859-6869.

Pestova, T. V., Shatsky, I. N., and Hellen, C. U. T (1996b). Functional dissection of eukaryotic initiation factor 4F: the 4A subunit and the central domain of the 4G subunit are sufficient to mediate internal entry of 43S preinitiation complexes. *Mol. Cell. Biol.*, **16**, 6870-6878.

Pestova, T. V., Shatsky, I. N., Fletcher, S. P., Jackson, R. J., and Hellen, C. U. T. (1998). A prokaryotic-like mode of cytoplasmic eukaryotic ribosome binding to the initiation codon during internal translation initiation of hepatitis C and classical swine fever virus RNAs. *Genes and Dev.*, **12**, 67-83.

Peukert, K., Staller, P., Schneider, A., Carmichael, G., Hänel, F., and Eilers, M. (1997). An alternative pathway for gene regulation by Myc. *EMBO J.*, **16**, 5672-5686.

Philipp, A., Schneider, A., Väsrik, I., Finke, K., Xiong, Y., Beach, D., Alitalo, K., and Eilers, M. (1994). Repression of cyclin D1: A novel function of MYC. *Mol. Cell. Biol.*, **14**, 4032-4043.

Pilipenko, E. V., Gmyl, A. P., Maslova, S. V., Svitkin, Y. V., Sinyakov, A. N., and Agol, V. I. (1992). Procaryotic-like *cis*-elements in the cap-independent internal initiation of translation on picornavirus RNA. *Cell*, **68**, 119-131.

Pilipenko, E. V., Gmyl, A. P., Maslova, S. V., Belov, G. A., Sinyakov, A. N., Huang, M., Brown, T. D. K., and Agol, V. I. (1994). Starting window, a distinct element in the cap-independent internal initiation of translation on picornaviral RNA. *J. Mol. Biol.*, **241**, 398-414.

Poole, T. L., Wang, R. A., Popp, L. N. D., Potgieter, A., Siddiqui, A., and Collet, M. S. (1995). Pestivirus translation initiation occurs by internal ribosome entry. *Virology*, **206**, 750-754.

Prats, A.-C., Vagner, S., Prats, H., and Amalric, F. (1992). *Cis*-acting elements in the alternative translation initiation process of human basic fibroblast growth factor mRNA. *Mol. Cell. Biol.*, **12**, 4796-4805.

Prendergast, G. C., and Ziff, E. B. (1991). Methylation-sensitive sequence-specific DNA binding by the c-Myc basic region. *Science*, **251**, 186-189.

Prendergast, G. C., Lawe, D., and Ziff, E. B. (1991). Association of Myn, the murine homologue of Max, with c-Myc stimulates methylation-sensitive DNA binding and Ras cotransformation. *Cell*, **65**, 395-407.

Price, N., and Proud, C. (1994). The guanine nucleotide exchange factor, eIF-2B. *Biochimie*, **76**, 748-760.

Prochownik, E. W., Kokuwska, J., and Rogers, C. (1988). c-*myc* antisense transcripts accelerate differentiation and inhibit G1-progression in murine erythroleukemia cell. *Mol. Cell. Biol.*, **8**, 3683-3695.

Quèva, C., Hurlin, P. J., Foley, K. P., and Eisenman, R. N. (1998). Sequential expression of the MAD family of transcriptional repressors during differentiation and development. *Oncogene*, **16**, 967-977.

Rao, C. D., Pech, M., Robbins, K. C., Aaronson, S. A. (1988). The 5' untranslated sequence of the c-*sis*/platelet-derived growth factor-II transcript is a potent translational inhibitor. *Mol. Cell. Biol.*, **8**, 284-292.

Rau, M., Ohlmann, T., Morley, S. J., and Pain, V. M. (1996). A re-evaluation of the cap-binding protein, eIF4E, as a rate-limiting factor for initiation of translation in reticulocyte lysate. *J. Biol. Chem.*, **271**, 8983-8990.

Ray, B. K., Brendler, T. G., Adya, S., Daniels-Mcqueen, S., Kelvin-Miller, J., Hershey, J. W. B., Grifo, J. A., Merrick, W. C., and Thatch, R. E. (1983). Role of messenger-RNA competition in regulating translation: further characterisation of messenger-RNA discriminatory initiation-factors. *Proc. Natl. Acad. Sci. USA.*, **80**, 663-667.

Ray, D., and Robert-Lezenges, J. (1989). Coexistence of a c-*myc* messenger-RNA initiated in intron-I with the normal c-*myc* messenger-RNA and similar regulation of both transcripts in mammalian cells. *Oncogene Res.*, **5**, 73-78.

Ray, R., Thomas, S., and Miller, D. M. (1989). Mouse fibroblasts transformed with the human c-*myc* gene express a high level of mRNA but a low level of c-*myc* protein and are non-tumorigenic in nude mice. *Oncogene*, **4**, 593-600.

Rhoads, R. E., and Lamphear, B. J. (1995). Cap-independent translation of heat shock messenger RNAs. *Current Topics in Microbiology and Immunology*, **203**, 131-153.

Rifkin, D. B., and Moscatelli, D. (1989). Recent developments in the cell biology of fibroblast growth factor. *J. Cell. Biol.*, **109**, 1-6.

Roberts, L. O., Seamons, R. A., and Belsham, G. J. (1998). Recognition of picornavirus internal ribosome entry sites within cells; influence of cellular and viral proteins. *RNA*, **4**, 520-529.

Rosen, H. G., Segni, D., and Kaempfer, R. (1982). Translational control by messenger-RNA competition for eukaryotic initiation factor-2. *J. Biol. Chem.*, **257**, 946-952.

Rosenwald, I. B., Rhoads, D. B., Callanan, L. D., Isselbacher, K. J., and Schmidt, E. (1993). Increased expression of eukaryotic initiation factors eIF 4E and eIF2α in response to growth induction by c-*myc*. *Proc. Natl. Acad. Sci. USA.*, **90**, 6175-6178.

Rousseau, D., Kaspar, R., Rosenwald, I., Gehrke, L., and Sonenberg, N. (1996). Translation initiation of ornithine decarboxylase and nucleocytoplasmic transport of cyclin D1 mRNA are increased in cells overexpressing eukaryotic initiation factor 4E. *Proc. Natl. Acad. Sci. USA.*, **93**, 1065-1070.

Roy, A. L., Malik, S., Meisterernst, M., and Roeder, R. G. (1993). An alternative pathway for transcription initiation involving TFII-I. *Nature (London)*, **365**, 355-361.

Roy, B., Beamon, J., Balint, E., and Reisman, D. (1994). Transactivation of the human p53 tumour suppressor gene by Myc/Max contributes to elevated mutant p53 expression in some tumours. *Mol. Cell. Biol.*, **14**, 7805-7815.

Rozen, F., Edery, I., Meerovitch, K., Dever, T. E., Merrick, W. C., and Sonenberg, N. (1990). Bidirectional RNA-helicase activity of eukaryotic translation initiation factor-4A and factor-4F. *Mol. Cell. Biol.*, **10**, 1134-1144.

Rudolf, B., Saffrich, R., Zwicker, J., Henglein, B., Muller, R., Ansorge, W., and Eilers, M. (1996). Acitivation of cyclin-dependent kinases by Myc mediates induction of cyclin A, but not apoptosis. *EMBO J.*, **15**, 3065-3076.

Saito, H., Hayday, A. C., Wiman, K., Hayward, W. S., Tonegawa, S. (1983). Activation of the c-*myc* gene by translocation: A model for translational control. *Proc. Natl. Acad. Sci. USA.*, **80**, 7476-7480.

Saporito-Irwin, S. M., Geist, R. T., and Gutmann, D. H. (1997). Ammonium acetate protocol for the preparation of plasmid DNA suitable for mammalian cell transfections. *Biotechniques*, **23**, 424-427.

Sarkar, G., Edery, I., Gallo, R., and Sonenberg, N. (1984). Preferential stimulation of rabbit α-globin messenger-RNA translation by a cap-binding protein complex. *Biochim. Biophys. Acta.*, **783**, 122-129.

Sarnow, P. (1989). Translation of glucose regulated protein 78/immunoglobulin heavy-chain binding protein mRNA is increased in poliovirus-infected cells at a time when cap-dependent translation of cellular mRNAs is inhibited. *Proc. Natl. Acad. Sci. USA.*, **86**, 5795-5799.

Scheper, G. C., Voorma, H. O., Thomas, A. A. M. (1992). Eukaryotic initiation factors-4E and -4F stimulate 5' cap-dependent as well as internal initiation of protein synthesis. *J. Biol. Chem.*, **267**, 7269-7274.

Schmid, P., Schulz, W. A., and Hameister, H. (1989). Dynamic expression pattern of the Myc proto-oncogene in midgestation mouse embryos. *Science*, **243**, 226-229.

Schwab, M., Alitalo, K., Klempnauer, K. H., Varmus, H. E., Bishop, J. M., Gilbert, G., Brodeur, M., Goldstein, M., and Trent, J. (1983). Amplified DNA with limited homology to Myc cellular oncogene is shared by human neuroblastoma cell lines and a neuroblastoma tumour. *Nature (London)*, **305**, 245-248.

Seth, A., Gupta, S., and Davies, R. J. (1993). Cell cycle regulation of the c-Myc transcriptional activation domain. *Mol. Cell. Biol.*, **13**, 4125-4136.

Shantz, L. M., and Pegg, A. E. (1994). Overproduction of ornithine decarboxylase caused by relief of translational repression is associated with neoplastic transformation. *Cancer Res.*, **54**, 2313-2316.

Shantz, L. M., Hu, R. H., and Pegg, A. E. (1996). Regulation of ornithine decarboxylase in a transformed cell line that overexpresses translation initiation factor eIF-4E. *Cancer Res.*, **56**, 3265-3269.

Shichiri, M., Hanson, K. D., and Sedivy, J. M. (1993). The effects of c-*myc* expression on proliferation, quiescence and the G_0 to G_1 transition in nontransformed cells. *Cell Growth Differ.*, **4**, 93-104.

Shindo, H., Tani, E., Matsumoto, T., Hashimoto, T., and Furuyama, J. (1993). Stabilisation of c-*myc* protein in human glioma-cells. *Acta Neuropathol.*, **86**, 345-352.

Shrivastava, A., Saleque, S., Kalpana, G. V., Artandi, S., Goff, S. P., and Calame, K. (1993). Inhibition of transcriptional regulator Ying-Yang-1 by association with c-Myc. *Science*, **262**, 1889-1891.

Sizova, D. V., Kolupaeva, V. G., Pestova, T. V., Shatsky, I. N., and Hellen, C. U. T. (1998). Specific interaction of the eukaryotic translation initiation factor 3 with the 5' nontranslated regions of hepatitis C virus and classical swine fever virus RNAs. *J. Virol.*, **72**, 4775-4782.

Smith, M. R., Al-Katib, A., Mohammad, R., Silverman, A., Szabo, P., Khilnani, S., Kohler, W., Nath, R., and Mutchnik, M. G. (1993). α-prothymosin gene expression correlates with proliferation, not differentiation of HL60 cells. *Blood*, **82**, 1127-1132.

Solomon, D. L. C., Amati, B., and Land, H. (1993). Distinct DNA-binding preferences for the c-Myc-Max and Max-Max dimers. *Nucleic Acids Res.*, **21**, 5372-5376.

Sonenberg, N., Merrick, W. C., Morgan, M. A., and Shatkin, A. J. (1978). A polypeptide in eukaryotic initiation factors that cross-links specifically to the 5'-terminal cap in mRNA. *Proc. Natl. Acad. Sci. USA.*, **75**, 4843-4847.

Sonenberg, N., Guertin, D., Cleveland, D., and Trachsel, H. (1981). Probing the function of the eukaryotic 5' cap structure using a monoclonal antibody directed against cap-binding proteins. *Cell*, **27**, 563-572.

Sonenberg, N., Guertin, D., and Lee, K. A. W. (1982). Capped mRNAs with reduced secondary structure can function in extracts from poliovirus-infected cells. *Mol. Cell. Biol.*, **2**, 1633-1638.

Spencer, C. A., and Groudine, M. (1991). Control of c-*myc* regulation in normal and neoplastic cells. *Adv. Cancer Res.*, **56**, 1-48.

Standaert, M. L., and Pollet, R. J. (1988). Insulin-glycolipid mediators and gene expression. *FASEB J.*, **2**, 2453-2461.

Stanton, B. R., Perkins, A. S., Tessarollo, L., Sassoon, D. A., and Parada, L. F. (1992). Loss of N-*myc* function results in embryonic lethality and failure of the epithelial component of the embryo to develop. *Genes and Dev.*, **6**, 2235-2247.

Stein, I., Itin, A., Einat, P., Skaliter, R., Grossman, Z., and Keshet, E. (1998). Translation of vascular endothelial growth factor mRNA by internal ribosome entry: implications for translation under hypoxia. *Mol. Cell. Biol.*, **18**, 3112-3119.

Steiner, P., Philipp, A., Lukas, J., Godden-Kent, D., Pagano, M., Mittnacht, S., Bartek, J., and Eilers, M. (1995). Identification of a Myc-dependent step during the formation of active G1 cyclin-cdk complexes. *EMBO J.*, **14**, 4814-4826.

Stoneley, M., Paulin, F. E. M., Le Quesne, J. P. C., Chappell, S. A., and Willis, A. E. (1998). C-*myc* 5' untranslated region contains an internal ribosome entry segment. *Oncogene*, **16**, 423-428.

Stripecke, R., and Hentze, M. W. (1992). Bacteriophage and spliceosomal proteins function as position-dependent *cis* repressors of mRNA translation *in vitro*. *Nucleic Acids Res.*, **20**, 5555-5564.

Stripecke, R., Oliveira, C. C., McCarthy, J. E. G., and Hentze, M. W. (1994). Proteins binding to the 5' untranslated region sites: a general mechanism for translational regulation of mRNAs in human and yeast cells. *Mol. Cell. Biol.*, **14**, 5898-5909.

Sugiyama, A., Kume, A., Nemoto, F., Nishimura, S., and Kuchino, Y. (1989). Isolation and characterisation of S-*myc*, a member of the Rat Myc gene family. *Proc. Natl. Acad. Sci. USA.*, **86**, 9144-9148.

Sutherland, L. C., and Williams, G. T. (1997). Viral promoter expression in CEM-C7 and Jurkat human T-lymphoid cell lines. *J. Immunol. Meths.*, **207**, 179-183.

Svitkin, Y. V., Meerovitch, K., Lee, H. S., Dholakia, J. N., Kenan, D. J., Agol, V. I., and Sonenberg, N. (1994). Internal translation initiation on poliovirus RNA: Further characterisation of La function in poliovirus translation *in vitro*. *J. Virol.*, **68**, 1544-1550.

Svitkin, Y. V., Ovchinnikov, L. P., Dreyfuss, G., and Sonenberg, N. (1996). General RNA binding proteins render translation cap dependent. *EMBO J.*, **15**, 7147-7155.

Tahara, S. M., Morgan, M. A., and Shatkin, A. J. (1981). Two forms of purified m^{7}G-cap binding protein with different effects on capped mRNA translation in extracts of uninfected and poliovirus-infected HeLa cells. *J. Biol. Chem.*, **256**, 7691-7694.

Taub, R., Moulding, C., Battey, J., Latt, S., Lenoir, G. M., and Leder, P. (1984). Activation and somatic mutation of the translocated c-*myc* gene in Burkitt-lymphoma cells. *Cell*, **36**, 339-348.

Taylor, M. V., Gusse, M., Evan, G. I., Dathan, N., and Mechali, M. (1986). *Xenopus myc* proto-oncogene during development: expression as a stable maternal mRNA uncoupled from cell division. *EMBO J.*, **5**, 3563-3570.

Teerink, H., Kasperaitis, M. A. M., De Moor, C. H., Voorma, H. O., and Thomas, A. A. M. (1994). Translation initiation on the insulin-like growth factor II leader 1 is developmentally regulated. *Biochem. J.*, **303**, 547-553.

Teerink, H., Voorma, H. O., and Thomas, A. A. M. (1995). The human insulin-like growth factor leader 1 contains an internal ribosome entry site. *Biochim. Biophys. Acta*, **1264**, 403-408.

Thomas, A. A. M., Scheper, G. C., Kleijn, M., DeBoer, M., and Voorma, H. O. (1992). Dependence of the adenovirus tripartite leader on the p220 subunit of eukaryotic initiation factor 4F during *in vitro* translation. *Eur. J. Biochem.*, **207**, 471-477.

Thompson, C. B., Challoner, P. B., Neiman, P. E., and Groudine, M. (1985). Levels of c-*myc* Oncogene mRNA are invariant throughout the cell cycle. *Nature (London)*, **314**, 363-366.

Timmer, R. T., Lax, S. R., Hughes, D. L., Merrick, W. C., Ravel, J. M., Browning, K. M. (1993). Characterisation of wheat germ protein synthesis initiation factor eIF-4C and comparison of eIF-4C from wheat germ and rabbit reticulocytes. *J. Biol. Chem.*, **268**, 24863-24867.

Trachsel, H., Erni, B., Schreier, M. H., and Staehelin, T. (1977). Initiation of mammalian protein synthesis. II. The assembly of the initiation complex with purified initiation factors. *J. Mol. Biol.*, **116**, 755-767.

Trachsel, H., and Staehelin, T. (1979). Initiation of mammalian protein synthesis. The multiple functions of the initiation factor eIF-3. *Biochim. Biophys. Acta.*, **565**, 305-314.

Tsukiyama-Kohara, Iizuka, K. N., Kohara, M., and Nomoto, A. (1992). Internal ribosome entry site within hepatitis C virus RNA. *J. Virol.*, **66**, 1476-1483.

Vagner, S., Gensac, M.-C., Maret, A., Bayard, F., Amalric, F., Prats, H., and Prats, A.-C. (1995). Alternative translation of human fibroblast growth factor 2 mRNA occurs by internal entry of ribosomes. *Mol. Cell. Biol.*, **15**, 35-44.

Vagner, S., Touriol, C., Galy, B., Audigier, S., Gensac, M.-C., Amalric, F., Bayard, F., Prats, H., and Prats, A.-C. (1996). Translation of CUG- but not AUG-initiated forms of human fibroblast growth factor is activated in transformed and stressed cells. *J. Cell. Biol.*, **135**, 1391-1402.

Vennström, B., Sheiness, D., Zabielski, J., and Bishop, J. M. (1982). Isolation and characterisation of c-*myc*, a cellular homologue of the oncogene (v-*myc*) of avian myelocytomatosis virus strain-29. *J. Virol.*, **42**, 773-779.

Vlach, J., Hennecke, S., Konstantinos, A., Conti, D., and Amati, B. (1996). Growth arrest by the cyclin-dependent kinase inhibitor p27^{Kip1} is abrogated by c-Myc. *EMBO J.*, **15**, 6595-6604.

Vogelstein, B. and Kinzer, K. W. (1992). P53 function and dysfunction. *Cell*, **70**, 523-526.

Vries, R. G. J., Flynn, A., Patel, J. C., Wang, X. M., Denton, R. M., and Proud, C. G. (1997). Heat shock increases the association of binding protein-1 with initiation factor 4E. *J. Biol. Chem.*, **272**, 32779-32784.

Wagner, A. J., Meyers, C., Laimins, L. A., and Hay, N. (1993). c-Myc induces expression and activity of ornithine decarboxylase. *Cell Growth Differ.*, **4**, 879-883.

Wagner, A. J., Kokontis, J. M., and Hay, N. (1994). Myc-mediated apoptosis requires wild-type p53 in a manner independent of cell cycle arrest and the ability of p53 to induce p21(WAF1/CIP1). *Genes and Dev.*, **8**, 2817-2830.

Wang, C., and Siddiqui, A. (1995). Structure and function of the Hepatitis C virus internal ribosome entry site. *Current topics in microbiology and immunology*, **203**, 99-115.

Warner, G. L., Ludlow, J., Nelson, D. O., Gaur, A., and Scott, D. (1992). Anti-immunoglobulin treatment of B-cell lyphomas induces active TGF-beta but pRb hyperphosphorylation is TGF-beta independent. *Cell Growth and Diff.*, **3**, 175-181.

Water, C. M., Littlewood, T. D., Hancock, D. C., Moore, J. P., and Evan, G. I., 1991. c-Myc protein expression in untransformed fibroblasts. *Oncogene*, **11**, 2515-2524.

Watson, R. J., 1988. Expression of the c-*myb* and c-*myc* genes is regulated independently in differentiating mouse erythroleukemia cells by common processes of premature transcription arrest and increased mRNA turnover. *Mol. Cell. Biol.*, **8**, 3938-3942.

Watt, R., Nishikura, K., Sorrentino, J., ar-Rushdir, A., Croce, C. M., and Rovera, G. (1983). The structure and nucleotide sequence of the 5' end of the human c-*myc* oncogene. *Proc. Natl. Acad. Sci. USA.*, **80**, 6307-6311.

Weinberg, R. A. (1995). The retinoblastoma protein and cell-cycle control. *Cell*, **81**, 323-330.

West, M. J., Sullivan, N. F., and Willis, A. E. (1995). Translational upregulation of the c-*myc* oncogene in Bloom's syndrome cell lines. *Oncogene*, **11**, 2515-2524.

Wolin, S. L., and Walter, P. (1988). Ribosome pausing and stacking during translation of a eukaryotic mRNA. *EMBO J.*, **7**, 3559-3569.

Wu, M., Arsura, M., Bellas, R. E., Fitzgerald, M. J., Lee, H., Schauer, S. L., Sherr, D. H., and Sonenshein, G. E. (1996). Inhibition of c-*myc* expression induces apoptosis of WEHI 231 Murine B cells. *Mol. Cell. Biol.*, **16**, 5015-5025.

Wurm, F., Gwinn, K., and Kingston, R. (1986). Inducible overexpression of the mouse c-myc protein in mammalian cells. *Proc. Natl. Acad. Sci. USA.*, **83**, 5414-5418.

Wyllie, A. H., Rose, K. A., Morris, R. G., Steel, C. M., Foster, E., and Spandidos, D. A. (1987). Rodent fibroblast tumours expressing human c-myc and Ras genes: growth, metastasis and endogenous oncogene expression. *Brit. J. Cancer*, **56**, 251-259.

Wyllie, A. H. (1997). Apoptosis and carcinogenesis. *Eur. J. Cell. Biol.*, **73**, 189-197.

Yang, B.-S., Geddes, T. J., Pogulis, R. J., Decrombrugghe, B., and Freytag, S. O. (1991). Transcriptional suppression of cellular gene expression by c-Myc. *Mol. Cell. Biol.*, **11**, 2291-2295.

Yang, Q., and Sarnow, P. (1997). Location of the internal ribosome entry site in the 5' non-coding region of the immunoglobulin heavy-chain binding protein (BiP) mRNA: evidence for specific RNA-protein interactions. *Nucleic Acids Res.*, **25**, 2800-2807.

Ye, X., Fong, P., Iizuka, N., Choate, D., and Cavener, D. R. (1997). *Ultrabithorax* and *Antennapedia* 5' untranslated regions promote developmentally regulated internal translation initiation. *Mol. Cell. Biol.*, **17**, 1714-1721.

Ziegler, E., Borman, A. M., Deliat, F. G., Liebig, H. G., Jugovic, D., Kean, K. M., Skern, T., Kuechler, E. (1995a). Picornavirus 2A protease-mediated stimulation of internal initiation is dependent on enzyme activity and the cleavage products of cellular proteins. *Virology*, **213**, 549-557.

Ziegler, E., Borman, A. M., Kirchweger, R., Skern, T., and Kean, K. M. (1995b). Foot-and-mouth disease Lb proteinase can stimulate rhinovirus and enterovirus IRES-driven translation and cleave several proteins of cellular and viral origin. *J. Virol.*, **69**, 3465-3474.

Zimmerman, K. A., Yankopoulos, G. D., Collum, R. G., Smith, R. K., Kohl, N. E., Denis, K. A., Nau, M. M., Witte, O. N., Toran-Allerand, D., Gee, C. E., Minna, J. D., and Alt, F. W. (1986). Differential expression of Myc family genes during murine development. *Nature (London)*, **319**, 780-783.

Publications

Mark Stoneley, Fiona EM Paulin, John PC Le Quesne, Stephen A Chappell, and Anne E Willis (1998). C-Myc 5' untranslated region contains an internal ribosome entry segment. Oncogene 16, 423-428.

Michelle J West, Mark Stoneley, and Anne E Willis (1998). Translational induction of the c-*myc* oncogene via activation of the FRAP/TOR signalling pathway. Oncogene 17, 769-780.

SHORT REPORT

C-Myc 5' untranslated region contains an internal ribosome entry segment

Mark Stoneley, Fiona EM Paulin, John PC Le Quesne, Stephen A Chappell and Anne E Willis

Department of Biochemistry University of Leicester, University Road, Leicester LE1 7RH, UK

Translation in eukaryotic cells is generally initiated by ribosome scanning from the 5' end of the capped mRNA. However, initiation of translation may also occur by a mechanism which is independent of the cap structure and in this case ribosomes are directed to the start codon by an internal ribosome entry segment (IRES). Picornaviruses represent the paradigm for this mechanism, but only a few examples exist which show that this mechanism is used by eukaryotic cells. In this report we show data which demonstrate that the 5' UTR of the proto-oncogene c-myc contains an IRES. When a dicistronic reporter vector, with c-myc 5' UTR inserted between the two cistrons, was transfected into both HepG2 and HeLa cells, the translation of the downstream cistron was increased by 50-fold, demonstrating that translational regulation of c-myc is mediated through cap-independent mechanisms. This is the first example of a proto-oncogene regulated in this manner and suggests that aberrant translational regulation of c-myc is likely to play a role in tumorigenesis.

Keywords: internal ribosome entry segment (IRES); c-myc 5' UTR; internal initiation; translation

The 5' untranslated region (UTR) of c-myc (which is well conserved amongst species) plays a significant role in modulating the steady state levels of the c-myc protein. A translational control mechanism residing in the first exon was originally postulated by Saito et al. arising from differential hypothetical secondary structures as a result of chromosomal translocations (Saito et al., 1983). In addition, c-myc mRNAs lacking exon 1 were found to be translated more efficiently in vitro when compared to full length transcripts (Darveau et al., 1985). Furthermore, a 240 nt restrictive element within exon 1 of murine c-myc was isolated and shown to inhibit translation of heterologous mRNAs in rabbit reticulocyte lysate and wheat germ extract (Parkin et al., 1988) demonstrating that the 5' UTR is highly structured and inhibitory to the scanning mechanism of translation. However, early studies in vivo examining translational efficiencies of c-myc mRNA in Burkitt's lymphoma cell lines suggested that both truncated and full length transcripts were translated with equal efficiencies (Nilsen and Maroney, 1984). Moreover, when expressed in numerous cell lines or translated in HeLa cell extracts the 5' UTR does not inhibit translation of either c-myc or reporter genes (Butnick et al., 1985; Parkin et al., 1988). This disparity suggests that non-canonical factors, which are lacking in rabbit

reticulolysate and wheat germ extract, facilitate c-myc translation through the 5' UTR in vivo (Parkin et al., 1988).

Translational regulation mediated through the 5' UTR is not unique to c-myc. Many cellular mRNAs encoding proto-oncogenes, growth factors, receptors and transcription factors possess long, highly structured 5' UTRs which affect their regulation (Gray and Hentze, 1994). For the overwhelming majority of eukaryotic mRNAs, where initiation of protein synthesis occurs via a cap-dependent mechanism (involving binding of the eukaryotic initiation factor (eIF) 4E, to the 7methyl G cap of the mRNA, for review see Hershey, 1991), such elements influence translation of the mRNA by repressing this cap-dependent mechanism. Alternatively, structured 5' UTRs may contain an internal ribosome entry segment (IRES) which allows cap-independent translation. These IRESes are capable of directing ribosomes to an internal start codon which may be some considerable distance (600–1000 nts) from the 5' end of the message (for reviews see Jackson et al., 1994, 1995; Jackson and Kaminski, 1995). The eukaryotic mRNAs which have so far been demonstrated to contain IRESes include the human immunoglobulin heavy chain binding protein (Macejak and Sarnow, 1991), basic fibroblast growth factor (Vagner et al., 1995) and eukaryotic initiation factor 4G (Gan and Rhoads, 1996). These may exemplify a group of mRNAs whose translation is required even when cap-dependent activity is compromised. However, to date no mechanisms have been elucidated for these eukaryotic IRESes and the cellular circumstances under which internal ribosome entry is required have yet to be fully defined (Sarnow, 1989; Vagner et al., 1995).

In cell lines derived from patients with Bloom's syndrome and Multiple Myeloma we have shown that de-regulated c-myc expression occurred by a translational mechanism (West et al., 1995; Paulin et al., 1996) and in the latter case a specific mutation was found in the 5' UTR of c-myc. In this paper we demonstrate that the 5' UTR of c-myc contains an IRES. This is the first example of a proto-oncogene which can utilise such a method to initiate protein synthesis and deregulation of c-myc via such a mechanism would have profound implications for tumorigenesis.
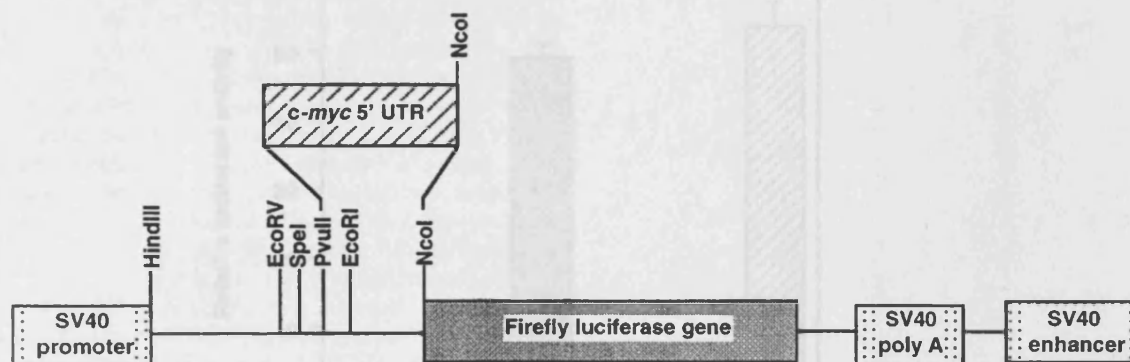
c-myc 5' UTR does not inhibit translation in cultured cells

Four promoters have been identified in the c-myc proto-oncogene; P1, P2, P3 and P0 which give rise to transcripts of approximately 2.4 kb, 2.25 kb, 2.0 kb

and 3.1 kb respectively (Battey et al., 1983; Bentley and Groudine, 1986; Yang et al., 1985). P2 is the major promoter from which 75–90% of cellular transcripts originate, with P1 producing only 10–25% (Stewart et al., 1984). Transcripts initiated at P0, P1 and P2 give rise to 5' untranslated regions of approximately 1000, 600 and 400 nucleotides respectively. In vitro studies on the 5' UTR of the P2 transcript have demonstrated that this region is highly structured and inhibitory to ribosome scanning (Darveau et al., 1985; Parkin et al., 1988). To

determine the effect of 5' UTR in vivo, we inserted a 396 bp segment into the plasmid pGL3 (Promega) directly upstream of the coding region for firefly luciferase to create the plasmid construct pGL3utr (Figure 1a). The pGL3utr construct and the control vector pGL3 were transfected into HeLa and HepG2 cells. The 5' UTR was not found to inhibit the downstream luciferase expression (Figure 1b) hence the activity of luciferase produced from pGL3utr was 1.2–1.6-fold higher than that produced from the control vector pGL3 (Figure 1b).
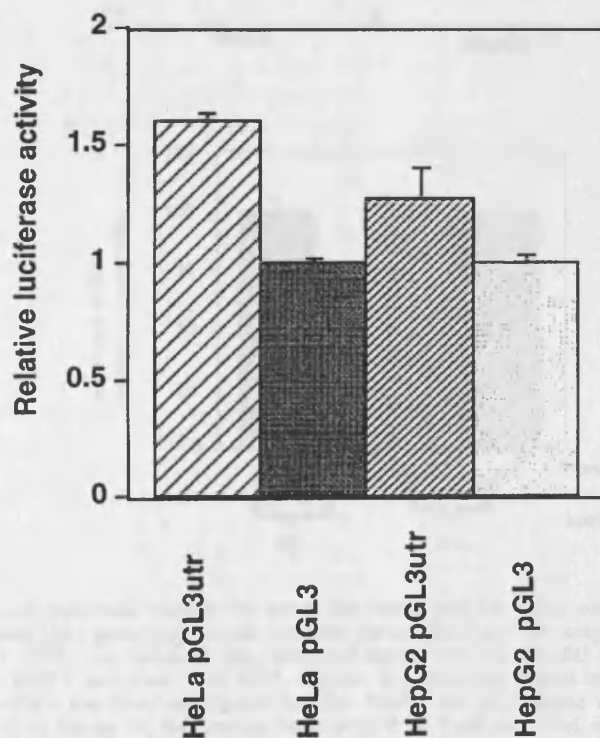
Figure 1 (a) Construction of monocistronic vectors. The c-myc 5' UTR was amplified using the primers FP2501. 5'-TAATTCCAGCGAGAGGCAGA-3' and MS4519 5'-ATACCATGGTCGCGGGAGGCTGCT-3'. Amplification resulted in a fragment of 396 bp which is contained within the region from 2501–4519 in the genomic sequence (Watt et al., 1983). This sequence was inserted into the control vector pGL3 (Promega) proximal to the firefly luciferase (FL) gene, using the PvuII and NcoI sites creating the vector pGL3utr. (b) The effect of the c-myc 5' UTR on a downstream cistron. HeLa and HepG2 cells were transfected with 20 µg of the luciferase constructs (pGL3 or pGL3utr) and 5 µg of the β-galactosidase construct pcDNA3.1/HisB/Lacz (Invitrogen) by the calcium phosphate method (Ausubel et al., 1987). Cells were harvested after 48 h and luciferase expression was determined using a luciferase assay system (Promega) and β-galactosidase expression was determined using a Galactolight plus system (Tropix). Both activities were measured in a 1253 Luminometer (BioOrbit). Variations in transfection efficiency were corrected by normalising luciferase activity to β-galactosidase activity. The results presented are an average of three independent experiments
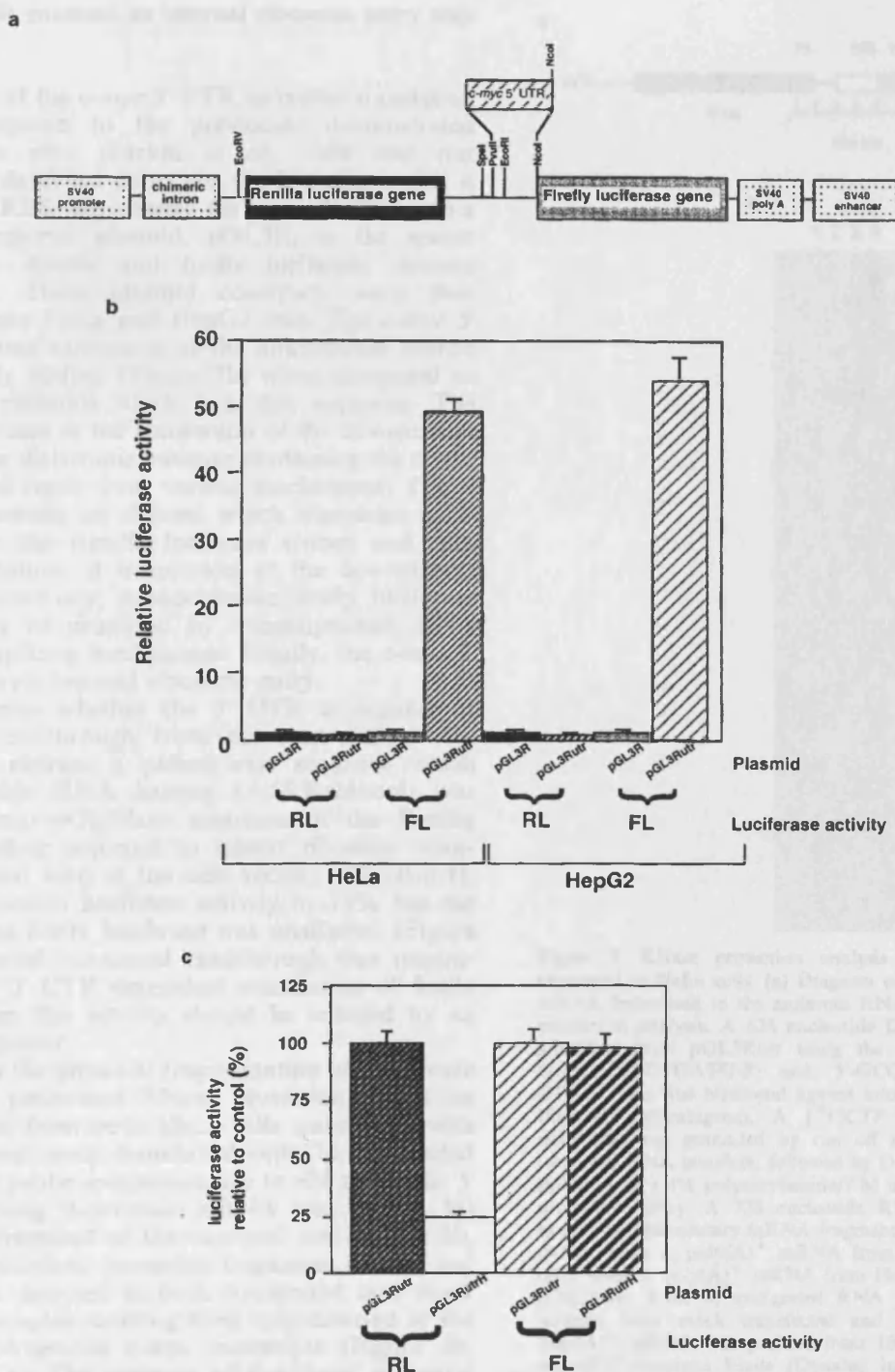
Figure 2 (a) Construction of dicistronic vectors. To create the vector pGL3R which contains two luciferase genes, the coding region of the *Renilla* luciferase (RL) gene was obtained from the vector pRL-CMV (Promega) by digestion with *Nhe*I and *Xba*I. To extend the length of the 3′ UTR, this fragment was blunt end ligated into the *Hind*III site of pSKBluescript (Stratagene) and subsequently excised using *Eco*RV and *Xho*I. This DNA segment was blunt-end ligated into the *Eco*RV site of pGL3. Finally, a chimeric intron from pRL-CMV was blunt-end ligated into the *Hind*III site to minimise utilisation of cryptic splice sites. The 5′ UTR of c-*myc* (generated as in Figure 1a) was inserted into pGL3R at *Pvu*II and *Nco*I sites to create the vector pGL3Rutr. (b) Expression of Renilla and firefly luciferase from dicistronic mRNAs in HeLa and HepG2 cells. The dicistronic constructs were transfected into HeLa and HepG2 cells as before. Both luciferase activities were measured using the Dual-Luciferase reporter assay system (Promega). The values were normalised to β-galactosidase activity as in Figure 1 and luciferase activities obtained are expressed relative to those obtained for pGL3R. The results presented are an average from three independent experiments. (c) An oligonucleotide cassette 5′-AGATCTGGTACCGAGCTCCCCGGGCTGCAGGAT-3′ and 5′-ATCCTGCAGCCCGGGGACC-TCGGTACCAGATCT-3′ containing an internal *Pst*I site was inserted into the *Eco*RV site of pGL3Rutr. This vector was digested with *Pst*I and *Eco*RV and the same oligonucleotide cassette was excised with *Pst*I and ligated into these sites creating a 60 bp palindronic sequence upstream of the Renilla coding sequence. This results in the production of a hairpin structure with an energy of −55 Kcal/mol. The vector was transfected into HeLa cells sand luciferase activity measured as before. The luciferase activities were normalised to β-galactosidase and expressed relative to those obtained from vector pGL3Rutr. The results presented are an average of three independent experiments

c-myc 5′ UTR contains an internal ribosome entry segment

The inability of the c-*myc* 5′ UTR to inhibit translation *in vivo* compared to the previously demonstrated inhibition *in vitro* (Parkin *et al.*, 1988 and our unpublished data) led us to test the hypothesis that it contains an IRES. We inserted the c-*myc* 5′ UTR into a dicistronic reporter plasmid, pGL3R, in the spacer between the *Renilla* and firefly luciferase cistrons (Figure 2a). These plasmid constructs were then transfected into HeLa and HepG2 cells. The c-*myc* 5′ UTR stimulated expression of the downstream cistron approximately 50-fold (Figure 2b) when compared to the control plasmids which lack this sequence. The apparent increase in the translation of the downstream cistron on the dicistronic message containing the c-*myc* 5′ UTR could result from various mechanisms. The 5′ UTR may contain an element which stimulates read-through past the Renilla luciferase cistron and thus causes reinitiation of translation at the downstream cistron. Alternatively, monocistronic firefly luciferase mRNAs may be produced by transcriptional, RNA cleavage or splicing mechanisms. Finally, the c-*myc* 5′ UTR may direct internal ribosome entry.

To determine whether the 5′ UTR is capable of stimulating readthrough from the upstream to the downstream cistron, a palindromic sequence which forms a stable RNA hairpin (-55 Kcal/mol) was introduced into pGL3Rutr upstream of the Renilla luciferase coding sequence to inhibit ribosome scanning. The stem loop in the new vector, pGL3RutrH, reduced the renilla luciferase activity by 75% but the activity of the firefly luciferase was unaffected (Figure 2c). If enhanced ribosomal readthrough was responsible for the 5′ UTR dependent stimulation of firefly luciferase then this activity should be reduced by an equivalent amount.

To address the potential fragmentation of dicistronic mRNAs we performed RNase protection assays on RNA isolated from both HeLa cells transfected with pGL3Rutr and mock transfected cells. In transfected cells a 725 nt probe complementary to 624 nts of the 5′ UTR containing dicistronic mRNA (see Figure 3a) protected a fragment of the expected size (Figure 3b, lane 3). In addition, protected fragments of 395 and 382 nts were detected in both transfected and mock transfected samples resulting from hybridisation of the probe to endogenous c-*myc* transcripts (Figure 3b, lanes 2 and 3). The presence of functional monocistronic transcripts would result in smaller protected fragments of at least 101 nts in length, and since no products of this size were detected the increased expression of firefly luciferase must occur on intact discistronic mRNAs.

Thus we conclude that c-*myc* 5′ UTR contains an IRES. The small, but reproducible, reduction in the expression of luciferase from the upstream cistron of between 15–20% in the cells which contain the plasmid pGL3Rutr, is also consistent with this hypothesis (Figure 2b). This probably reflects a competition between cap-dependent and IRES-dependent translation on the dicistronic mRNA and this phenomenon has also been observed for Bip, picornovirus and eIF4G IRESes (Macejak and Sarnow, 1991; Borman and Jackson, 1992; Gan and Rhodes, 1996).
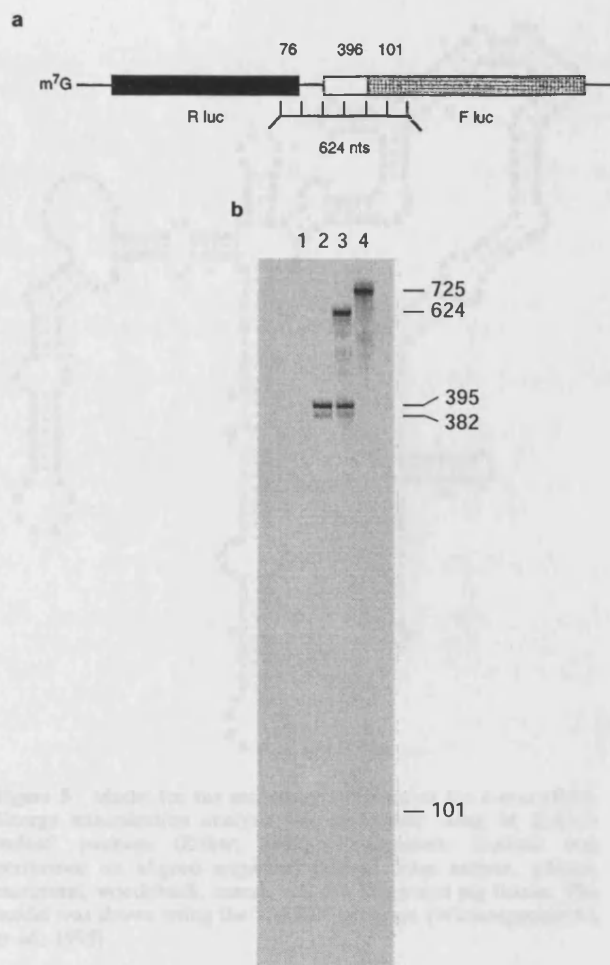

Figure 3 RNase protection analysis of dicistronic mRNAs expressed in HeLa cells. (a) Diagram of the 5′ UTR containing mRNA hybridised to the antisense RNA probe used for RNase protection analysis. A 624 nucleotide DNA fragment was PCR amplified from pGL3Rutr using the primers 5′-GCAAGAA-GATGCACCTGATG-3′ and 5′-GCGTATCTCTTCAGAGC-CTT-3′. This was blunt-end ligated into the *Sma*I site of pSK⁺ Bluescript (Stratagene). A [^{32}P]CTP (800 Ci/mmol) labelled riboprobe was generated by run off transcription on a *Xho*I restricted DNA template, followed by DNAse I digestion and gel isolation on a 4% polyacrylamide/7 M urea gel. (b) Ribonuclease protection assay. A 725 nucleotide RNA probe was used to protect complementary mRNA fragments. Lane 1, 10 μg of yeast tRNA. Lane 2, poly(A)⁺ mRNA from mock transfected HeLa cells. Lane 3, poly(A)⁺ mRNA from HeLa cells transfected with pGL3Rutr. Lane 4, undigested RNA probe. Total RNA was isolated from mock transfected and transfected HeLa cells. Poly(A)⁺ mRNA was purified from 10 μg of total RNA using oligo(dT) magnetic beads (Dynatec Inc). RNA samples were hybridised with 5×10^5 c.p.m. of riboprobe at 45°C for 16 h in hybridisation buffer (40 mM PIPES pH 6.4, 400 mM NaCl, 1 mM EDTA, 80% deionised formamide). Single stranded RNA was digested using RNase ONE (Promega). The products were size fractionated on a 4% polyacrylamide/7 M urea gel and visualised by phosphorimage analysis (Molecular Dynamics). Product sizes were determined using ^{32}P-dCTP labelled pBR322 *Hpa*II restriction fragments

Mapping the c-*myc* IRES

To define the boundaries of the c-*myc* IRES a series of plasmid constructs was generated containing decreasing lengths of the sequence coding for the 5′ UTR. The ability of these truncated sequences to promote internal ribosome entry on a dicistronic mRNA was compared
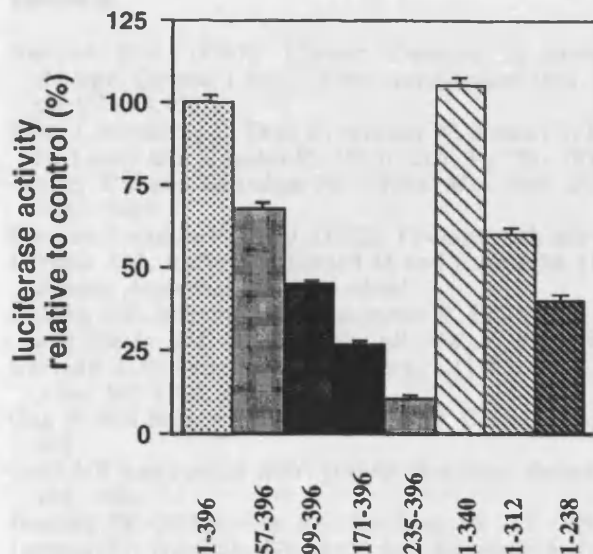
Figure 4 Downstream cistron activity from dicistronic mRNAs containing fragments of the c-myc 5′ UTR in HeLa cells. The 5′ deletion series was generated by restricting the c-myc 5′ UTR with NciI, AccIII and AvaI giving fragments of 340, 298 and 162 respectively. A fragment of 226 bp was amplified using the oligonucleotides FP 2670 5′-TGCCATCCACGAAACTTT-3′ and MS4519 (see Figure 1). These sequences were inserted into pGL3R at the PvuII and NcoI sites. Deletions from the 3′ end were produced by digesting the c-myc 5′ UTR with PvuII, EcoRO9011 and AvaI, generating fragments of 340, 312 and 238 bp. Fragments were inserted by blunt-end ligation into the PvuII site of pGL3R. The resulting constructs were then transfected into HeLa cells and luciferase activity measured and calculated as before. The reduction in luciferase activity from the downstream cistron is expressed as percentage of the values obtained with pGL3Rutr

Figure 5 Model for the secondary structure of the c-myc IRES. Energy minimization analysis was performed using M Zuker's 'mfold' package (Zuker, 1989). Phylogenetic analysis was performed on aligned sequences derived from human, gibbon, marmoset, woodchuck, mouse, rat, cat, sheep and pig tissues. The model was drawn using the 'CARD' program (Winnenpenninckx et al., 1995)

to the full length 5′ UTR. Removal of 56 nts from the 5′ end decreased the activity of the downstream cistron by 33% and larger deletions of 98, 170 and 234 nts resulted in a corresponding reduction in internal ribosome entry of 56, 74 and 91% respectively (Figure 4). Thus the 5′ border of this translational element lies within 56 nts of the 5′ end of exon 1.

At the 3′ end, deletion of 56 nts had no effect on the activity of the downstream cistron. However, deletions further upstream removing 84 and 158 nts reduced the efficiency of the internal ribosome entry by 40 and 60% respectively (Figure 4). Hence the 3′ end of the optimally effective IRES lies between 312 and 340 nts from the 5′ end. Furthermore, this analysis suggests a mechanistic distinction between viral IRESes and the c-myc IRES. In various viral IRESes 3′ end deletions that lie within the IRES completely ablate internal ribosome entry (Pelletier and Sonenberg, 1988; Borman and Jackson, 1992; Borman et al., 1995; Reynolds et al., 1995), whereas c-myc IRES 3′ end deletions result in a gradual loss of activity. This may reflect a structural difference between cellular and viral IRESes. We have performed phylogenetic and energy minimization analyses on the c-myc 5′ UTR and obtained a model for the secondary structure (Figure 5). Noteworthy features include the high degree of foldback in the structure when compared to those predicted for viral IRESes, and the absence of cryptic AUGs in all sequences examined.
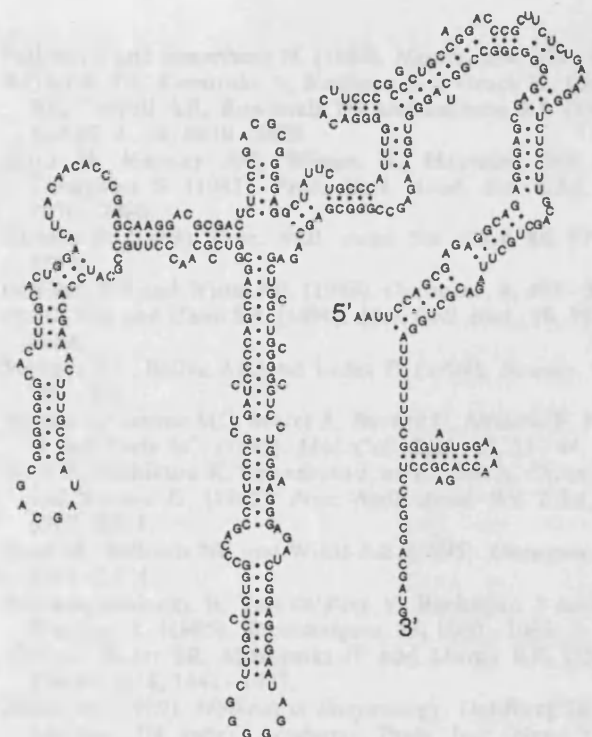
The preceding data demonstrate that the c-myc 5′ UTR contains a translational element capable of directing internal ribosome entry and we propose that c-myc protein synthesis may therefore be initiated by such a mechanism. This suggests that the c-myc protein can be translated under situations where initiation from the 5′ cap structure and ribosome scanning is reduced. There are a number of situations where modulation in the levels of c-myc protein via internal ribosome entry may be required including the onset of proliferation, during mitosis where cap-dependent translation is reduced (Jackson et al., 1995) and following DNA damage (Sullivan and Willis, 1989).

Deregulation of the c-myc proto-oncogene through enhanced internal ribosome entry could play a pivotal role in tumour development. We have described previously two cases where deregulation of c-myc by translational mechanisms occurs in cell lines derived from patients with Bloom's syndrome (West et al., 1995) and in multiple myeloma (Paulin et al., 1996).

Further work is merited to investigate the mechanism of action of this IRES, the pathophysiological circumstances under which it is used and the effects that the mutation in this region has on the aberrant translational regulation of c-myc in multiple myeloma.

References

Ausubel RM. (1987). *Current Protocols in Molecular Biology*. Greene J (ed.). Wiley-Interscience: New York, pp. 9.11–9.17.

Batty J, Moulding C, Taub R, Murphy W, Stewart T, Potter H, Lenoir G and Leder P. (1983). *Cell*, **34**, 779–797.

Bentley DL and Groudine M. (1986). *Mol. Cell. Biol.*, **6**, 3481–3489.

Borman A and Jackson RJ. (1992). *Virology*, **188**, 685–696.

Borman AM, Bailly J-L, Girard M and Kean KM. (1995). *Nucleic Acids Res.*, **23**, 3656–3663.

Butnick NZ, Miyamoto C, Chizzonite R, Cullen BR, Ju G and Skalka AM. (1985). *Mol. Cell. Biol.*, **5**, 3009–3016.

Darveau A, Pelletier J and Sonenberg N. (1985). *Proc. Natl. Acad. Sci. USA*, **82**, 2315–2319.

Gan W and Rhoads RE. (1996). *J. Biol. Chem.*, **271**, 623–626.

Gray NK and Hentze MW. (1994). *Mol. Biol. Reports*, **19**, 195–200.

Hershey JW. (1991). *Ann. Rev. Biochem.*, **60**, 717–755.

Jackson RJ, Hunt SL, Gibbs CL and Kaminski A. (1994). *Mol. Biol. Reports*, **9**, 147–159.

Jackson RJ, Hunt SL, Reynolds JE and Kaminski A. (1995). *Curr. Top. Microbiol. Immunol.*, **203**, 1–29.

Jackson RJ and Kaminski A. (1995). *RNA*, **1**, 985–1000.

Macejak DG and Sarnow P. (1991). *Nature*, **353**, 90–94.

Nilsen TW and Maroney PA. (1984). *Mol. Cell. Biol.*, **4**, 2235–2238.

Parkin N, Darveau A, Nicholson R and Sonenberg N. (1988). *Mol. Cell. Biol.*, **8**, 2875–2883.

Paulin FEMP, West MJ, Sullivan NF and Willis AE. (1996). *Oncogene*, **13**, 505–513.

Pelletier J and Sonenberg N. (1988). *Nature*, **334**, 320–325.

Reynolds JE, Kaminski A, Kettinen KJ, Grace K, Clarke BE, Carroll AR, Rowlands DJ and Jackson RJ. (1995). *EMBO J.*, **14**, 6010–6020.

Saito H, Hayday AC, Wiman K, Hayward WS and Tonegawa S. (1983). *Proc. Natl. Acad. Sci. USA*, **80**, 7476–7480.

Sarnow P. (1989). *Proc. Natl. Acad. Sci. USA*, **86**, 5795–5799.

Sullivan NF and Willis AE. (1989). *Oncogene*, **4**, 497–502.

Spotts GD and Hann SR. (1990). *Mol. Cell. Biol.*, **10**, 3952–3964.

Stewart TA, Bellve AR and Leder P. (1984). *Science*, **226**, 707–710.

Vagner S, Gensac MC, Maret A, Bayard F, Amalric F, Prats H and Prats AC. (1995). *Mol. Cell. Biol.*, **15**, 35–44.

Watt R, Nishikura K, Sorrentino J, ar-Rushdi A, Croce CM and Rovera G. (1983). *Proc. Natl. Acad. Sci. USA*, **80**, 6307–6311.

West M, Sullivan NF and Willis AE. (1995). *Oncogene*, **11**, 2515–2524.

Winnenpenninckx B, Van de Peer Y, Backeljau T and De Wachter R. (1995). *Biotechniques*, **18**, 1060–1063.

Yang J, Bauer SR, Mushinski JF and Marcu KB. (1985). *EMBO J.*, **4**, 1441–1447.

Zuker M. (1989). *Methods in Enzymology*, Dahlberg JE and Abelson JN (eds). Academic Press Inc: New York, pp. 262–288.

Translational induction of the c-myc oncogene via activation of the FRAP/TOR signalling pathway

Michelle J West[1,2], Mark Stoneley[1] and Anne E Willis[1]

[1]Department of Biochemistry, University of Leicester, Leicester, LE1 7RH, UK

Previous studies on the regulation of c-myc have focused on the transcriptional control of this proto-oncogene. We have investigated the signalling pathways involved under circumstances in which there is a translational up-regulation in the levels of c-myc protein. We have demonstrated an up to tenfold serum-dependent increase of c-myc protein levels in Epstein-Barr virus immortalized B-cell lines 2–4 h after disruption of cellular aggregates, which is not accompanied by an equivalent increase in mRNA. Overall protein synthesis rates only increased threefold suggesting that the c-myc message was being selectively translated. We observed increases in the phosphorylation of p70 and p85 S6 kinases and of initiation factor eIF-4E binding protein 1 (4E-BP1) 1–2 h after stimulation, suggesting activation of the FRAP/TOR signalling pathway. The increased phosphorylation of 4E-BP1 led to a decrease in its association with eIF-4E and an increase in its association with the eIF-4G component of the eIF-4F initiation complex. The signalling inhibitors rapamycin and wortmannin blocked the phosphorylation of 4E-BP1 and abolished the translational component of the c-myc response. Our data suggest that dissociation of eIF-4E from 4E-BP1, leading to an increase in the formation of the eIF-4F initiation complex, relieves the translation repression imposed on the c-myc mRNA by its structured 5'UTR.

Keywords: c-myc; eIF-4G; rapamycin; S6 kinase; TOR; translation

Introduction

The c-myc proto-oncogene belongs to a family of immediate-early genes, other members of which include c-fos, c-jun and egr-1, which are rapidly induced on exposure of quiescent cells to mitogens. Lipopolysaccharide-stimulated B-cells, Concanavalin A-treated T-cells and serum-starved fibroblasts exposed to EGF, PDGF, or serum, all induce c-myc mRNA levels up to 40-fold 2–9 h after stimulation (Dean et al., 1986, Kelly et al., 1983, Nepveu et al., 1987, Waters et al., 1991). There are data to suggest that these increases in c-myc mRNA levels cannot be completely accounted for by an increased transcription rate, and that post-transcriptional regulation, may also play a part (Blanchard et al., 1985).

There is evidence from other systems which demonstrates that c-myc protein expression can be modulated by translational control and that the 5' untranslated region of c-myc (encoded by exon 1), which is well conserved amongst species, has functional relevance in this process. Full length c-myc messages are translated less efficiently than those which lack the 5' UTR (Darveau et al., 1985) and this negative regulation has been mapped to a 240 nt element (Parkin et al., 1988). Similarly, Xenopus c-myc 5'UTR contains a region, between the promoters P0 and P1, which is important in regulating translation (Lazarus, 1992). Data from our own laboratory have provided evidence for the translational regulation of c-myc protein expression in cell lines established from patients with the chromosome breakage disorder Bloom's syndrome (West et al., 1995) and from individuals suffering from the B-cell neoplasia Multiple Myeloma (Paulin et al., 1996). In the latter case the 5'UTR was shown to contain a specific mutation.

Translational regulation mediated through the 5'UTR is not unique to c-myc, and indeed many cellular mRNAs encoding proto-oncogenes, growth factors and their receptors, and transcription factors, possess long highly structured 5'UTRs which affect their regulation (for review see Gray and Hentze, 1994). For example, on mitogenic stimulation of a number of cellular systems, which causes a 2–3-fold increase in the general rate of protein synthesis, there is an additional selective increase in the translation of a subset of mRNAs which are normally found in a translationally repressed state, including those messages with a high degree of secondary structure in their 5'UTRs and those with polypyrimidine tracts at their 5' termini (for reviews see Brown and Schreiber, 1996; Proud, 1994). Both general and specific increases in translation are mediated by changes in the activities and phosphorylation states of components of the translational apparatus. Messages with structured 5'UTRs e.g. ornithine decarboxylase, are particularly dependent on the RNA helicase activity of the eIF-4A component of the eIF-4F initiation complex (which also comprises eIF-4E and eIF-4G), for their efficient translation and it has been shown that over-expression of the limiting component of this complex, eIF-4E, can specifically activate the translation of this class of mRNA (Koromilas et al., 1991). Increased activity of eIF-4F can also be achieved by the phosphorylation of eIF-4G and eIF-4E (Manzella et al., 1991; Morley et al., 1991; Morley and Traugh, 1989; Morley and Traugh, 1990) and the release of eIF-4E from a binding partner, typically 4E-BP1, with which it is normally associated (Lin et al., 1994; Pause et al., 1994), thus increasing the amount of free eIF-4E that is available for 4F complex formation. The interaction of

eIF-4E with 4E-BP1 is regulated by phosphorylation, with phosphorylation of 4E-BP1 leading to a dissociation of this protein from eIF-4E (Lin *et al.*, 1994; Pause *et al.*, 1994). Specific increases in the translation of messages containing polypyrimidine tracts, e.g. mRNAs encoding translation factors and ribosomal proteins, are thought to be mediated through phosphorylation of the ribosomal protein S6 by p70 S6 kinase (Jefferies *et al.*, 1994; Terada *et al.*, 1994).

The external signals which lead to mitogenic stimulation of cells have been extensively studied. The polypeptide growth factors which cause such a stimulation have been shown to activate two protein kinase cascades: the mitogen activated protein (MAP) kinase and FRAP/TOR pathways. The former appears to be mostly involved with up-regulation of transcription (for reviews see Jones, 1996; Marshall, 1996) whilst the latter is associated with an increase in translational activity (Lin *et al.*, 1995; Mendez *et al.*, 1996; Von Manteuffel *et al.*, 1996). Activation of the FRAP/TOR pathway results in the phosphorylation of both p70 S6 kinase and 4E-BP1 and specific inhibition of this pathway by rapamycin blocks both of these events (Beretta *et al.*, 1996; Chung *et al.*, 1992; Lin *et al.*, 1995; Price *et al.*, 1992).

On observation of a serum-dependent induction of c-*myc* protein in disaggregated B-cells, we assessed the contribution of translational mechanisms to this induction by quantifying RNA and protein levels in parallel during the time course of this response. We show that c-*myc* protein levels are induced more rapidly and to a greater extent than c-*myc* mRNA levels, and that this is not the result of increased protein stability. On investigation of the mechanisms involved in this process we demonstrate a selective translation of c-*myc* caused by liberation of eIF-4E from 4E-BP1 which is mediated via the FRAP/TOR pathway. This is the first demonstration that translational regulation of c-*myc* in B-cells occurs through FRAP/TOR. The results presented herein differ from those where other genes e.g. ODC (Brown and Schreiber, 1996) have been shown to be regulated by translation, as c-*myc* translation regulation does not seem to involve an alteration in either the amount or the phosphorylation state of the cap binding protein eIF4E.

Results

c-myc *protein levels are translationally induced in B-cells*

Epstein–Barr virus immortalized B-cells form multicellular aggregates during their growth as a result of heterotypic interactions between the adhesion molecules LFA-1 and ICAM-1 on the cell surface (Gallie and Traugh, 1994; Gregory *et al.*, 1988, 1990). We observed a large induction of c-*myc* protein levels in these B-cell lines following disruption of cellular clusters in existing cell cultures or by resuspension of cells in total fresh medium. To assess the mechanisms involved in this induction, we performed parallel Western and Northern blot analysis of protein and RNA samples taken over 48 h following resuspension of a population of exponentially growing cells in fresh medium (Figure 1a and b). The experiments were

performed on a minimum of three independent occasions and the representative Western blot shows that c-*myc* protein levels began to rise as early as 2 h after resuspension, increased to a peak approximately eightfold higher than original expression levels by 8 h and began to decline by 24–48 h (Figure 1a). In contrast to the induction of c-*myc* protein levels, the c-*myc* RNA levels did not start to increase until 4 h after the stimulus and reached a peak of only 1.8-fold after 8 h (when compared to the control messages analysed, GAPDH, Figure 1b and tubulin, data not shown), clearly showing that the majority of the increase in the level of the c-*myc* protein is occurring by a post-transcriptional mechanism. Hence, on comparison of c-*myc* protein and mRNA levels during the response (Figure 1c) it can be seen that the small induction of c-*myc* mRNA levels observed is insufficient to account for the large increase in c-*myc* protein expression. Comparisons of the induction of c-*myc* protein and
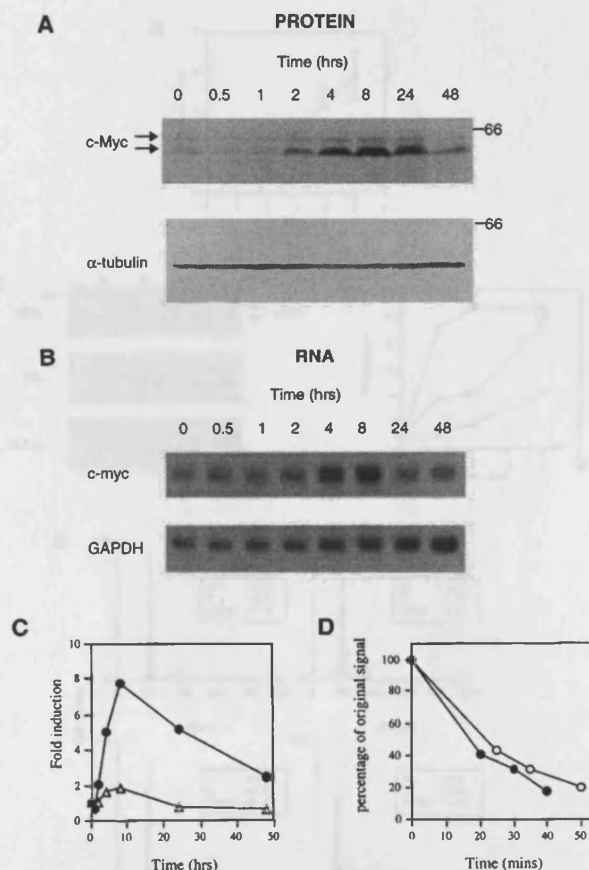

Figure 1 A comparison of c-*myc* protein and mRNA levels during the induction of c-*myc* expression in the EBV-LCL 0892A. (a) Cell extracts from 10^6 and 7×10^5 cells were separated by SDS–PAGE, Western blotted, and analysed for c-*myc* and α-tubulin protein expression, respectively. (b) Total cellular RNA was prepared from samples taken in parallel and then analysed by Northern blotting for levels of c-*myc* mRNA, and levels of the control message GAPDH with specific probes. (c) The Western blot shown in (a) was analysed by laser densitometry and the level of induction in c-*myc* protein (closed circles) compared to the increase in c-*myc* mRNA (triangles) following analysis of the Northern blot by phosphorimagery and normalization of c-*myc* mRNA levels to those of GAPDH. (d) Determination of the rate of degradation of the c-*myc* protein in cells treated at time 0 (closed circles) and at 6 h post-stimulation (open circles) with cycloheximide, and samples removed at time points up to 50 min for analysis by Western blotting and densitometry

mRNA in two other EBV-immortalized B-cell lines demonstrated a similar and reproducible dissociation between protein and mRNA inductions, with in every case, the induction in c-*myc* protein being far greater than the induction in c-*myc* mRNA (data not shown).

Consistent with the intimate role of the c-*myc* gene product in the regulation of cellular proliferation and differentiation, the expression of this proto-oncogene is controlled at multiple levels (for review see Marcu *et al.*, 1992). In the absence of a large induction of mRNA expression, it is evident that increased transcription rates and/or increased mRNA stability are not the key mechanisms involved in the induction of c-*myc* protein described here. Since c-*myc* protein expression has been shown to be subject to regulation at the level of both protein stability and translation (Lüscher and Eisenmann, 1988; Shindo *et al.*, 1993; Spotts and Hann, 1990) it was then necessary to distinguish between these two possibilities. Studies of the rate of degradation of the c-*myc* protein using the protein synthesis inhibitor cycloheximide revealed that there was no change in the stability of the protein during the peak of expression at 6 h (Figure 1d). The rates of degradation of the c-*myc* protein prior to (time 0) and 6 h post-stimulation were very similar; the time taken for the protein level to reach half of its original level in the presence of cycloheximide being 20–30 min at both time points, a value consistent with published data on the half-life of this protein (Hann and Eisenman, 1984).

Further experiments performed were aimed at determining the stimulus for the induction in c-*myc* translation.

The induction of c-myc protein is serum dependent

The time course in which we observed an increase in the levels of the c-*myc* protein (Figure 1a) is similar to that seen for c-*myc* mRNA induction in other systems (Kelly *et al.*, 1983), in particular on serum stimulation of resting fibroblasts. However, in all the cases described previously, this up-regulation only occurred on stimulation of resting cells or cells made quiescent as a result of serum deprivation (Dean *et al.*, 1986; Kelly *et al.*, 1983; Nepveu *et al.*, 1987; Waters *et al.*, 1991). In contrast, we observed an induction in c-*myc* protein when growing cultures of EBV-immortalized B-cells, 3 days after the addition of fresh medium (Figure 2a), were pelleted and resuspended in either fresh or conditioned media. The level of c-*myc* induction was dependent on the concentration of serum to which the cells were exposed (Figure 2b and c), suggesting that this response occurs as a result of increased exposure of B-cells to serum due to disruption of the cellular aggregates.

The cell cycle distribution of cells during a serum induction was analysed by FACS using propidium iodide stained cells. The cell cycle distribution of cells taken at Day 4 (prior to disruption of cellular aggregates, see Figure 2a) from actively growing cultures showed 72% of cells in the G_0/G_1 phase of the cycle (Figure 2d). Cell cycle arrest induced by serum deprivation in fibroblasts for example is characterized by the presence of >90% of cells in the G_0 phase of the cell cycle and consequently a negligible number of cells in S phase, a profile which is

not evident in the cultures analysed here. It has however been reported (Allday and Farrell, 1994) that on reaching saturation density in culture, EBV-LCLs can become growth arrested in early G_1. In our experiments (Figure 2a), it is possible that the cells in the centre of cellular aggregates may be beginning to arrest in G_1. This would explain the relatively high proportion of cells in G_0/G_1, and the ability of these cells to respond to increased serum exposure, following the disruption of cellular aggregates, by the induction of c-*myc*. The relatively slow shift of cells into S phase during the time course of the c-*myc* induction, evident by 24 h (Figure 2d) is consistent with previously published data which suggests that the G_1 phase of the cell cycle in LCLs exceeds 12 h (Allday and Farrell, 1994). These data suggest that this response differs from the response of G_0-arrested fibroblasts to serum exposure as the LCLs under study are not completely
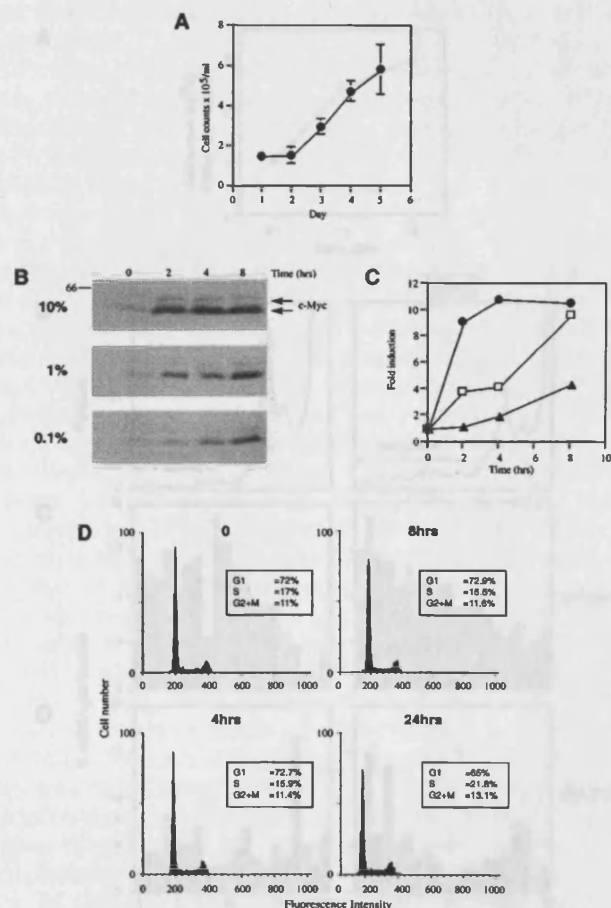

Figure 2 The c-*myc* induction occurs in exponentially growing cell cultures in response to serum exposure. (a) Growth curve of the GM0892A EBV-LCL. Viable cell counts were determined in the presence of trypan blue stain for up to 5 days after addition of fresh medium. Counts were performed in triplicate and the mean ±standard deviation is indicated. (b) Western blot showing the c-*myc* induction following culture of cells in 10%, 1%, or 0.1% FCS. Samples were removed at the times indicated. (c) Laser densitometric analysis of the blot shown in (b). Fold inductions in the presence of 10% FCS (closed circles), 1% FCS (squares), and 0.1% FCS (triangles) are shown. (d) Propidium iodide staining and fluorescence analysis of cells taken at the indicated time points following culture in 15% FCS to determine cell cycle distributions. The proportion of cells in G1, S and G2+M is indicated

quiescent. Importantly, there is evidence to suggest that EBV-LCLs cannot in fact leave the cell cycle and re-enter G_0 in the same manner as fibroblasts since, on the complete withdrawal of serum, LCLs do not growth arrest and apoptose, as is the case for fibroblasts, but continue to proliferate and die at various stages of the cell cycle as a result of the constitutive expression of c-myc (Cherney et al., 1994). We conclude that the c-myc induction in EBV-LCLs observed here results from the increased exposure of cells to serum following the disruption of cellular aggregates.

General protein synthesis rates increase only 2–3-fold

To assess the translational component of the c-myc induction described here, we investigated the response of the translational machinery to the increased exposure to serum. Polysomally and monosomally associated mRNA species were isolated by sucrose gradient density centrifugation. The relative distribution of specific messages was determined by fractionation of the gradients, extraction of RNA, and hybridization to specific probes. On comparison of the total mRNA from the absorbance profiles recorded during fractionation of the gradients (before and after treatment of cells), it is apparent that there is a shift in the relative distribution of a large number of messages by 8 h with an approximate 50% decrease in monosomally-associated mRNAs and a corresponding increase in the mRNAs associated with polysomes (Figure 3b). This is consistent with the 2–3-fold increase in the general rate of protein synthesis which occurs 3–8 h after stimulation (Figure 3a) and is similar to the response of starved rat epididymal fat cells to insulin (Lyons et al., 1980) and quiescent fibroblasts to serum (Jefferies et al., 1994). The distribution of c-myc mRNA (Figure 3c), and that of the control mRNA species GAPDH (Figure 3d) also followed this general shift in message re-distribution, with the peak of monosomally-associated message observed at time 0 for c-myc being greatly diminished. Analysis of a large number of polysome profiles from three different cell lines demonstrated that the c-myc message consistently showed this pattern of re-distribution to polysomes as did all individual messages examined (data not shown). Interestingly, not all of the gene products examined, e.g. eIF-4E and α-tubulin, showed increased expression at the protein level (Figures 1a, 4b and 7a). It is therefore possible that an increased association with polysomes does not result in increased expression levels of proteins such as eIF-4E and α-tubulin since the translation of these messages is proceeding at a maximum level or is under further control at the level of translational elongation or protein degradation. Since the initiation of translation of the c-myc mRNA is repressed by the presence of its structured 5'UTR, under normal circumstances, it follows that the expression of c-myc protein will be particularly affected by the general increases in translation initiation observed after the stimulation of cells (Figure 3a and b). In addition, specific changes to the activity of the translation initiation complex, eIF-4F, would be required to facilitate the increased polysomal association of the c-myc mRNA observed in these experiments by 8 h. However, as a result of the general re-distribution of

messages to polysomes observed (Figure 3b), any component of the response which results from selective translation of the c-myc message, mediated through changes in initiation complex formation, can not be further defined using this technique. It is clear, however, that the 2–3-fold increase in general protein synthesis observed here (Figure 3a) cannot account for the 5.5–10-fold increase in c-myc protein expression observed in this cell line (Figure 1), and that the remaining translational component of the c-myc response must be the result of just such a selective translation mechanism.

Regulation of translation initiation factors 4E and 2α

There is evidence which suggests that the translation initiation factors 4E and 2α are downstream target genes of the c-myc protein (Jones et al., 1996; Rosenwald et al., 1993), yet despite the high level
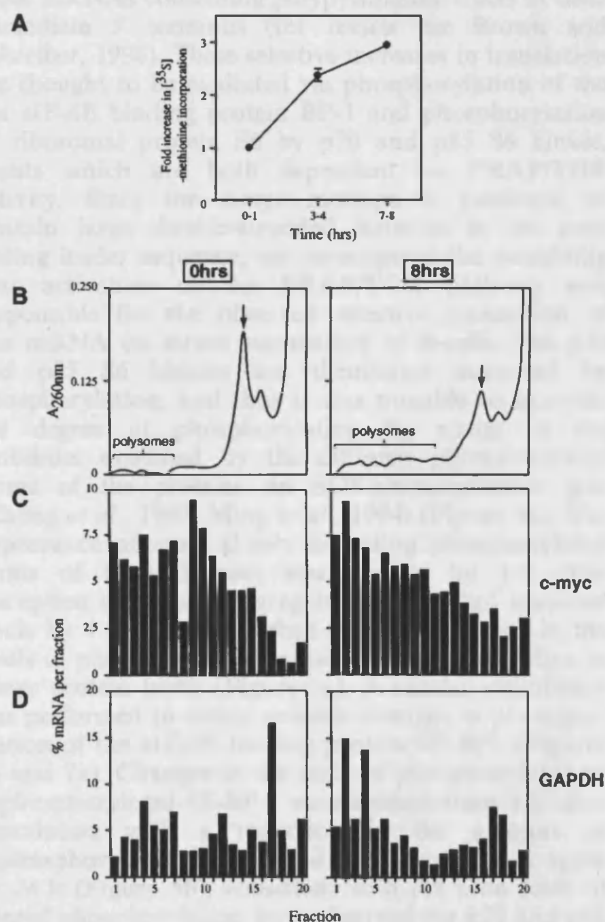
Figure 3 Increases in overall protein synthesis rates and the association of messages with polysomes after serum stimulation. (a) The incorporation of [^{35}S]-methionine into protein was determined by labelling cells for 1 h periods at time 0–1 h, 3–4 h and 7–8 h after serum stimulation. Samples were analysed in triplicate by scintillation counting and the fold-induction in protein synthesis is shown ± standard deviation. (b) Sucrose gradient density centrifugation performed prior to (time 0) and 8 h following stimulation and fractions collected with continuous monitoring at 260 nm. Arrows indicate the position of the 80S monosome peak. RNA was extracted from each fraction and analysed using slot-blot hybridization with specific probes to detect levels of c-myc (c) and GAPDH (d) mRNAs across the gradient

induction in c-*myc* protein levels evident during this time course (Figure 1a), we observed no increase in levels of either eIF-4E or 2α (Figure 4a and b). It does not appear therefore that the increased expression of c-*myc* in this system results in the transactivation of these genes. It has been shown that the expression of eIF-4E and 2α does not always correlate with the expression level of c-*myc* in certain transformed cell lines, and it has been suggested that in EBV-immortalized cell lines, increased expression of eIF-4E can occur in the absence of increased c-*myc* expression (Rosenwald, 1995). The lack of increased expression of these factors on higher level expression of c-*myc* protein observed in our previous studies with EBV-immortalized Bloom's Syndrome lines (West *et al.*, 1995), and in the present study is consistent with these findings.

Conversely, these results also suggest that the selective translation of the c-*myc* protein does not result from an increase in the levels of these initiation factors. Since limited expression of the eIF-4E protein is believed to restrict levels of the eIF-4F initiation complex, increased expression of eIF-4E in particular can lead to the selective translation of messages with secondary structure in their leader sequences (Rousseau *et al.*, 1996) which are particularly dependent on the helicase activity of eIF-4F. In addition, although increased expression of eIF-4E and 2α has been implicated in the translational response of cells to mitogens (Cohen *et al.*, 1990; Mao *et al.*, 1992) the general increases in translation observed here (Figure 3a) do not seem to result from the increased expression of these proteins.

Since increases in the level of phosphorylation of eIF-4E and other components of the eIF-4F complex have been correlated with increases in the rate of translation initiation (Morley *et al.*, 1991) we also examined the steady state phosphorylation level of eIF-

Figure 4 Analysis of the initiation factors eIF-4E and eIF-2α. Cell extracts (10^6 cells) were separated by SDS–PAGE, Western blotted and probed with antibodies to eIF-2α (a). The blot was then stripped and probed with antibodies to eIF-4E (b). The phosphorylated and dephosphorylated forms of eIF-4E, in extracts prepared in the presence of phosphatase inhibitors, were separated by isoelectric focusing and then Western blotted and detected as for SDS–PAGE (c)

4E during the time course of the c-*myc* induction, using isoelectric focusing techniques. Although increases in the phosphorylation of eIF-4E have been reported to occur in a number of systems in response to mitogens (Bu and Hagedorn, 1991; Flynn and Proud, 1996; Morley and Pain, 1995b; Morley and Traugh, 1990) we consistently observed no increase in the level of the phosphorylated form of the protein over the time course (Figure 4c). It appears therefore that the positive effects on translation, both at a general level (Figure 3a) and at a selective level (Figure 1a) are not mediated through increased phosphorylation of eIF-4E.

Activation of the FRAP/TOR pathway

The FRAP/TOR pathway has been identified as a signalling pathway which on activation by growth factors can lead to the increased translation of specific subclasses of mRNAs. These include messages with extensive secondary structure in their 5'UTRs and those mRNAs containing polypyrimidine tracts at their immediate 5' terminus (for review see Brown and Schreiber, 1996). These selective increases in translation are thought to be mediated via phosphorylation of the the eIF-4E binding protein BP-1 and phosphorylation of ribosomal protein S6 by p70 and p85 S6 kinase, events which are both dependent on FRAP/TOR activity. Since the c-*myc* message is predicted to contain large double-stranded hairpins in its non-coding leader sequence, we investigated the possibility that activation of the FRAP/TOR pathway was responsible for the observed selective translation of this mRNA on serum stimulation of B-cells. The p70 and p85 S6 kinases are themselves activated by phosphorylation, and thus it was possible to examine the degree of phosphorylation by virtue of the mobilities exhibited by the different phosphorylated forms of the proteins on SDS-polyacrylamide gels (Chung *et al.*, 1992; Ming *et al.*, 1994) (Figure 5a). The appearance of more slowly migrating phosphorylated forms of these kinases was evident by 1 h after disruption of cellular aggregates and reached maximal levels by 4 h. There was then a gradual decline in the levels of phosphorylation consistent with the decline in c-*myc* protein levels (Figure 1a). A similar experiment was performed to detect possible changes in phosphorylation of the eIF-4E binding protein 4E-BP1 (Figures 5b and 7a). Changes in the ratio of phosphorylated to dephosphorylated 4E-BP-1 were evident from 1 h after stimulation with a reduction in the amount of dephosphorylated protein and then an increase again by 24 h (Figure 5b), consistent with the time scale of altered phosphorylation state observed for p70 and p85 S6 kinases. These increases in the phosphorylation of p70 and p85 S6 kinases and 4E-BP1 are in accordance with activation of the FRAP/TOR pathway and both occur on a time scale suggestive of involvement of this pathway in the translational induction of c-*myc* protein expression.

Increases in the phosphorylation of 4E-BP1 have been shown to cause the dissociation of this protein from eIF-4E (Lin *et al.*, 1994; Pause *et al.*, 1994) a process which is postulated to affect the translation of growth-related translationally repressed messages, such as c-*myc*, by increasing the amount of active 4F
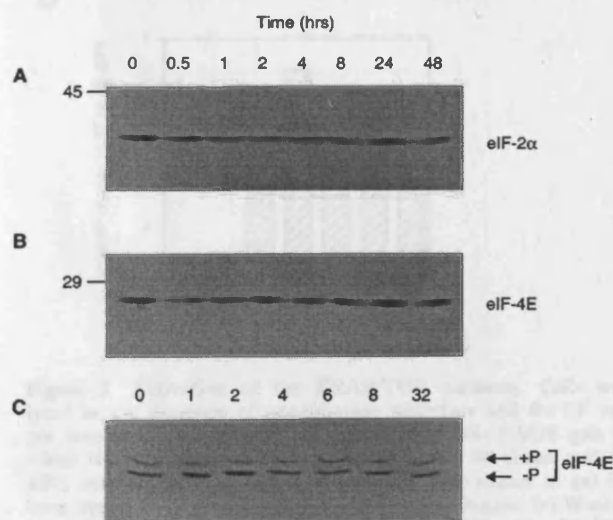
complex. eIF-4E, and thus complexes containing eIF-4E, can be partially purified by virtue of the fact that they bind to the m⁷GTP cap structure present at the 5′ end of eukaryotic messages. We therefore examined the association of eIF-4E with 4E-BP1 and with eIF-4G using m⁷GTP Sepharose affinity column chromatography (Figures 5c and d and 6). Complexes bound to the m⁷GTP Sepharose column were eluted and proteins were analysed by SDS–PAGE and Western blotting.

Appropriate regions of the resulting blots were probed with antibodies to eIF-4E and 4E-BP1 or eIF-4E and eIF-4G. After 1 h there was a large decrease in the association of 4E-BP1 with eIF-4E and by 2 h the level of 4E-BP1 associated with 4E fell to almost undetectable levels (Figure 5c), consistent

Figure 5 Activation of the FRAP/TOR pathway. Cells were lysed in the presence of phosphatase inhibitors and 8×10^5 cells per lane separated on 7.5% (**a**) and 15% SDS–PAGE gels (**b**) which were then probed with antibodies to p70 S6 kinase and 4E-BP1, respectively. The upper part of the blot shown in (**a**) has been overexposed to show the p85 form of the kinase. (**c**) Western blot showing the degree of association of 4E-BP1 with eIF-4E in complexes partially purified by m⁷GTP Sepharose affinity chromatography from samples taken in parallel to those analysed in (**b**). Samples were eluted from the column in the presence of an excess of m⁷GTP, precipitated and analysed on a 15% SDS–PAGE gel which was then Western blotted and the relevant portion of the blot probed with antibodies against eIF-4E and 4E-BP1 (**c**). (**d**) Laser densitometric analysis of the Western blots shown in (**c**)

with the decrease in levels of the dephosphorylated form of the 4E-BP1, the form which associates with eIF-4E, observed in parallel samples (Figure 5b). The apparent molecular weight of the 4E-BP1 isolated by m⁷GTP Sepharose chromatography is consistent with this being the dephosphorylated form of the protein (compare Figure 5b and c). Similar experiments were then performed to determine the degree of association of 4E with 4G (Figure 6). Treatment of the cells resulted in a large increase in the amount of 4G associated with 4E and a representative Western blot is shown (Figure 6a and b). The results from three such experiments were averaged (Figure 6c) and show that the eIF4G that is associated with eIF4E increases to 12 ($\pm$2.2)-fold by 4 h and starts to return to the uninduced level by 24 h which is in accordance with the time scale of induction of c-myc (Figure 1a). This demonstrates clearly that the dissociation of 4E-BP1 from eIF-4E following its phosphorylation results in increased 4F complex formation. These data support the hypothesis that the phosphorylation of 4E-BP1 and its subsequent dissociation from eIF-4E facilitates the translation of translationally repressed messages.

Both rapamycin and wortmannin block the phosphorylation of 4E-BP1 and abolish the translational up-regulation of c-myc

The immunosuppressant macrolide rapamycin has been shown to be a potent inhibitor of FRAP/TOR (Kunz et al., 1993; Sabatini et al., 1994) and binds to its target through interaction with FKBP12 (FK506-binding protein 12). Rapamycin therefore prevents the phosphorylation of both p70 S6 kinase and 4E-BP1 (Beretta et al., 1996; Chung et al., 1992; Price et al., 1992). Since our data thus far suggested that activation of the FRAP/TOR pathway may be involved in the c-myc response, we attempted to block the activation of this pathway using rapamycin and assess the effect on the translation of the c-myc mRNA. In addition to the use of rapamycin as a signalling inhibitor, experiments were performed in parallel using the specific inhibitor of phosphoinositide 3-kinases (PI 3-kinases), wortmannin, which is thought to block activation of the FRAP/TOR pathway by inhibiting an event upstream of the FRAP/TOR kinase (for review see Proud, 1996). More recently wortmannin has been shown to inhibit the serine-specific autokinase activity of mammalian TOR in vitro (Brunn et al., 1996). To examine the effect of these agents on the translational response, cell samples incubated with either wortmannin or rapamycin or untreated were taken at predetermined time intervals, subjected to SDS–PAGE, transferred to nitrocellulose and probed with antibodies for c-myc, α-tubulin, p70 S6 kinase or 4E-BP1 (Figure 7a). Exposure of cells to wortmannin and rapamycin decreased the induction of c-myc protein, by 39% and 36% respectively at 4 h and by 40% and 36% at 8 h (Figure 7a and b; representative blots are shown and these experiments were performed on at least three independent occasions). There was no corresponding change in the expression of the control protein α-tubulin (Figure 7a). In additional experiments performed we have observed inhibition of 50% or more by 4–8 h with rapamycin (data not shown). A comparison of the induction of c-myc mRNA (determined by Northern blot analysis on
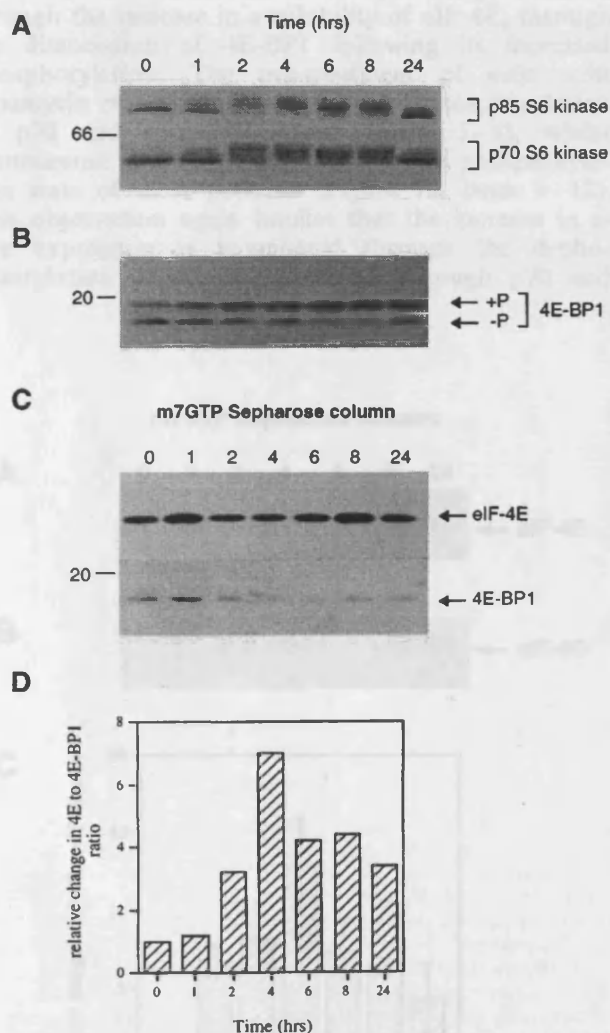
parallel samples from the same experiment), with the induction of c-*myc* protein shown in Figure 7a showed that the dissociation between protein and mRNA observed as normal in the control experiment (Figure 7c) was removed in the presence of both rapamycin and wortmannin (compare Figure 7b and c). Indeed, the c-*myc* protein induction was reduced to a level that can be accounted for by the increase in RNA expression alone. Thus, it appears that rapamycin and wortmannin remove the translational component of the c-*myc* induction. The inhibition of the c-*myc* response by these two compounds correlates directly with the inhibition of changes in the phosphorylation state of 4E-BP1 by both of these agents (Figure 7a, lanes 1 and 2, 5 and 6, 9 and 10). These results are consistent with the mechanism of this specific activation of translation of c-*myc* being mediated through the increase in availability of eIF-4E, through the dissociation of 4E-BP1 following its increased phosphorylation. The pre-treatment of cells with rapamycin resulted in the complete dephosphorylation of p70 and p85 S6 kinases (lanes 5 – 8), whilst wortmannin had very little effect on the phosphorylation state of these proteins (Figure 7a, lanes 9 – 12). This observation again implies that the increase in c-*myc* expression is augmented through the dephosphorylation of 4E-BP1, and not through p70 and

p85 S6 kinase phosphorylation, since the effects of wortmannin and rapamycin on the c-*myc* induction are identical whilst wortmannin, in this cellular system, does not block p70 S6 kinase action. It is interesting to note that while many authors have shown that inhibition of PI 3-kinase activity blocks the phosphorylation of p70 S6 kinase (Cheatham *et al.*, 1994; Chung *et al.*, 1994), the evidence presented here and evidence from other laboratories highlights situations where this is not in fact the case. In particular, it has been demonstrated using mutant PDGF receptors that activation of p70 S6 kinases can occur in the absence of PI 3-kinase activity (Ming *et al.*, 1994), and that phorbol ester-mediated p70 S6 kinase activation cannot be inhibited by wortmannin (Chung *et al.*, 1994). It seems likely therefore that in certain systems and with certain activators p70 S6 kinase can be activated by wortmannin-insensitive and thus probably PI 3-kinase-independent mechanisms. The role of PI 3-kinase in the activation of FRAP/TOR may therefore not be as straightforward as originally thought.

The reduction in the c-*myc* levels by rapamycin could in part be accounted for by the general effect on translation that this agent is known to have in B-cells. In some cellular systems it has been shown that rapamycin can block the shift of messages to polysomes in a selective manner (Jefferies *et al.*, 1994; Nielson *et al.*, 1995; Terada *et al.*, 1994) with only slight effects on general protein synthesis rates, however, in the B-cell line Ramos a 30% decrease in general protein synthesis rates was apparent at 3 – 6 h in the presence of rapamycin (Terada *et al.*, 1994). In our experiments the incorporation of [^{35}S]-methionine into protein during a time course of induction in the presence and absence of rapamycin shows that the induction in general protein synthesis was reduced by 37% at 3 – 4 h and by 46% at 7 – 8 h in the presence of 20 nM rapamycin (Figure 7d). Therefore, in our B-cell system, it is difficult to separate the general effects of rapamycin on protein synthesis from specific effects of this drug. However wortmannin had very little effect on general protein synthesis rates, decreasing the [^{35}S]-methionine incorporation by only 7.5% at 3 – 4 h and 32% at 7 – 8 h when compared to the untreated control cells (Figure 7d). In contrast, the c-*myc* response was reduced by 39% at 4 h in the presence of wortmannin (Figure 7a and b). These results therefore show clearly that wortmannin selectively blocks the translational increase in the level of c-*myc* protein as a direct result of inhibiting the phosphorylation of 4E-BP1. It can therefore be concluded that a large part of the c-*myc* translational response is mediated through activation of the FRAP/TOR signalling pathway resulting in the increased phosphorylation of 4E-BP1. The subsequent dissociation of this protein from eIF-4E thereby leads to increased initiation complex assembly and relieves the translational repression imposed on c-*myc* by its structured 5'UTR.
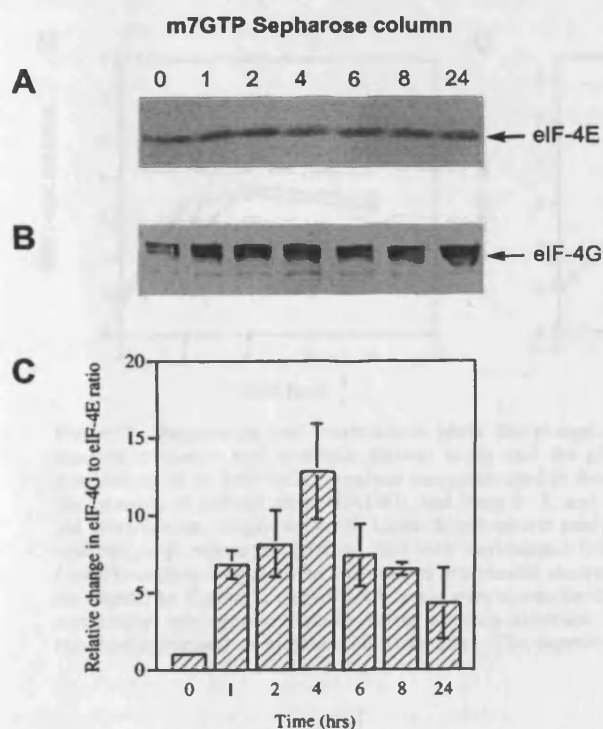

m7GTP Sepharose column

Figure 6 Increased association of eIF-4G with eIF-4E results from activation of FRAP/TOR. Experiments were performed as in Figure 5c and the relevant portions of the blots were probed with antibodies to eIF-4E (**a**) and eIF-4G (**b**). (**c**) Laser densitometric analysis of Western blots from that shown in (**a**) and (**b**) and from two other identical experiments demonstrating an increase in the eIF-4G to eIF-4E ratio which is indicative of increased formation of active eIF-4F complex. Results show the mean of three independent experiments and error bars indicate the standard deviation from the mean. (The time point at 8 h shows the mean of two experiments only)

Discussion

The results presented here demonstrate a serum-dependent translational induction of c-*myc* protein levels in EBV-immortalized B-cells mediated through activation of the FRAP/TOR signalling pathway and
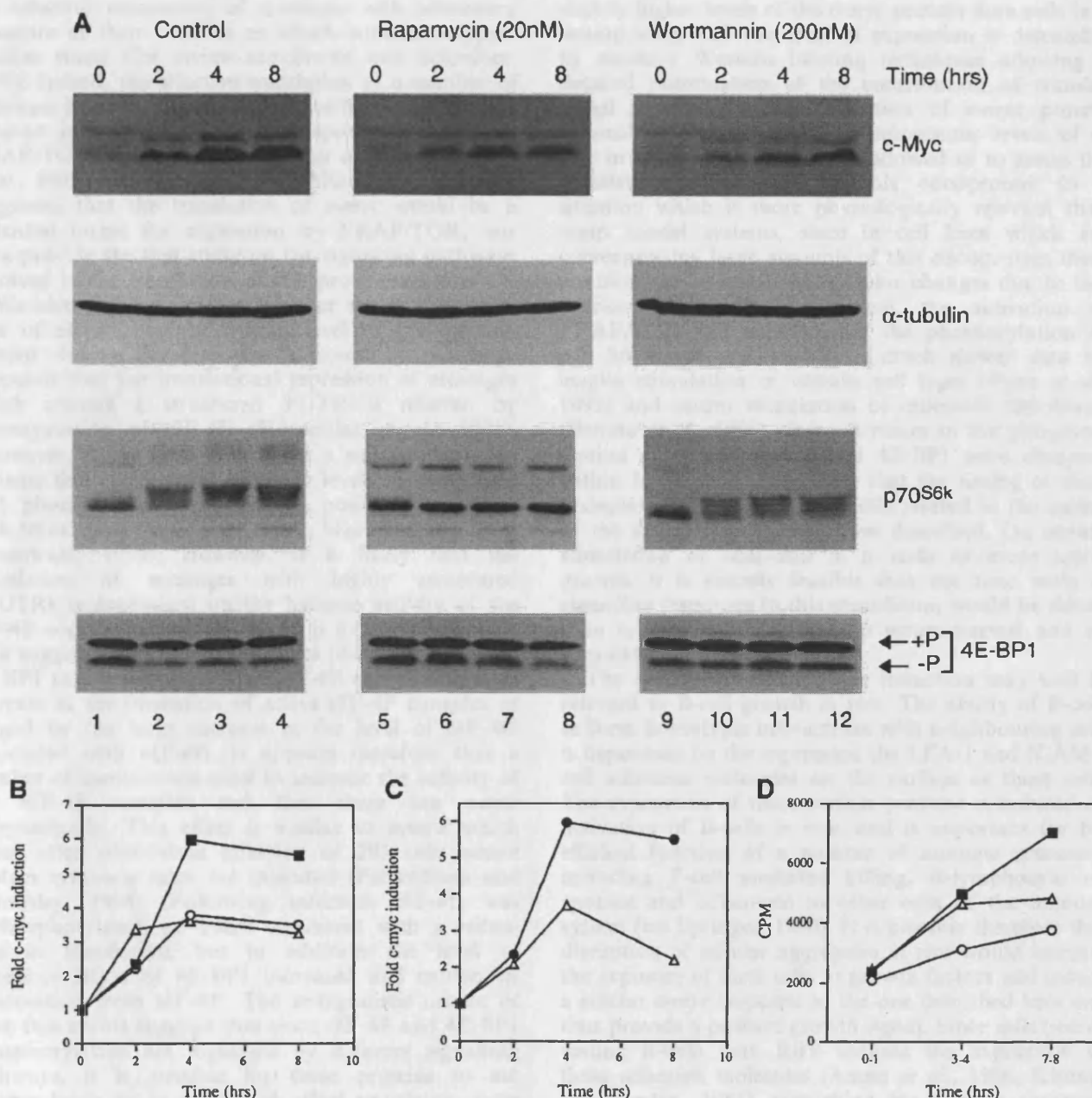
Figure 7 Rapamycin and wortmannin block the phosphorylation of 4E-BP1 and inhibit the c-*myc* response. (a) Western blot analysis of c-*myc* and α-tubulin protein levels and the phosphorylation states of p70 S6 kinase and 4E-BP1 during the serum stimulation of an EBV-LCL. Analysis was performed as described in Figures 1 and 5. Lanes 1–4 show cells pretreated for 30 min in the presence of solvent alone (DMSO), and lanes 5–8, and 9–12 show cells pre-treated in the presence of 20 nM rapamycin and 200 nM wortmannin, respectively. (b) Laser densitometric analysis of the c-*myc* blots shown in (a), treated with DMSO alone (closed squares), with rapamycin (circles), and with wortmannin (triangles). (c) A comparison of the c-*myc* protein (closed circles) and RNA (open triangles) induction for the control experiment shown in (a). Analysis was performed by Western and Northern blotting as in the legend to Figure 1. c-*myc* RNA levels were normalized to the GAPDH signal. (d) A comparison of the incorporation of [^{35}S]-methionine into protein (c.p.m.) during a serum induction in the presence of solvent alone (closed squares) and in the presence of rapamycin (circles) or wortmannin (triangles). The experiment was performed as in Figure 3

phosphorylation of 4E-BP1. c-*myc* protein levels rise typically 5.5–10-fold by 2–4 h post-stimulation with increases in mRNA expression reaching less than two-fold. Although increases in the overall level of incorporation of [^{35}S]-methionine into protein were also evident, these rises were insufficient to account for the induction in c-*myc* protein levels. We observed a decrease in the association of 4E-BP1 with eIF-4E following the phosphorylation of 4E-BP1 and a subsequent increase in the association of eIF-4E with

eIF-4G, and suggest that the selective translation of c-*myc* mRNA results from the increased availability of eIF-4E for initiation complex formation which in turn leads to the relief of the translational repression imposed on the c-*myc* message by its structured 5'UTR. Moreover, inhibition of the phosphorylation of 4E-BP1 by the signalling inhibitors rapamycin and wortmannin led to a significant reduction in c-*myc* protein levels. These data are consistent with current hypotheses on the role of the FRAP/TOR pathway in

the selective translation of messages with secondary structure in their 5'UTRs or which contain polypyrimidine tracts (for review see Brown and Schreiber, 1996). Indeed, the selective translation of a number of messages in both of these classes has been shown to be reduced in the presence of the specific inhibitor of FRAP/TOR, rapamycin (Jefferies et al., 1994; Nielson et al., 1995; Terada et al., 1994). Although it has been suggested that the translation of c-myc would be a potential target for regulation by FRAP/TOR, our data provide the first study on the signalling pathways involved in the translation of this proto-oncogene.

We observed no increase in either the phosphorylation of eIF-4E, or the overall level of this protein present during the response, although it has been proposed that the translational repression of messages which contain a structured 5'UTR is relieved by overexpression of eIF-4E (Koromilas et al., 1991). Moreover, it has been shown for a number of other systems that increases in both the levels of expression and phosphorylation of eIF-4E positively correlate with translation (Mao et al., 1992; Morley et al., 1991; Rosenwald, 1995). However, it is likely that the translation of messages with highly structured 5' UTRs is dependent on the helicase activity of the eIF-4F complex, of which eIF-4E is a component. Our data suggest that an increase in the phosphorylation of 4E-BP1 causes a liberation of eIF-4E and therefore an increase in the formation of active eIF-4F complex as judged by the large increase in the level of eIF-4G associated with eIF-4E. It appears therefore that a number of mechanisms exist to increase the activity of the eIF-4F complex and that these can occur independently. This effect is similar to events which occur after adenovirus infection of 293 cells where protein synthesis rates are inhibited (Feigenblum and Schneider, 1996). Following infection eIF-4E was dephosphorylated, an event consistent with a reduction in translation, but in addition the level of phosphorylation of 4E-BP1 increased and caused its dissociation from eIF-4E. The antagonistic nature of these two events suggests that since eIF-4E and 4E-BP1 phosphorylation are regulated by different signalling pathways, it is possible for these proteins to act independently or in concert to affect translation rates and that they are not always both phosphorylated in response to the same stimulus (Feigenblum and Schneider, 1996). The 2-3-fold increase in general protein synthesis observed here clearly shows that translation initiation is activated even without increases in the phosphorylation of eIF-4E.

Serum induction of c-myc has been well documented at the level of mRNA (Dean et al., 1986; Kelly et al., 1983; Nepveu et al., 1987). However, the contribution of a translational response to the induction of c-myc protein levels on exposure of quiescent cells to mitogens has been very difficult to quantify, since c-myc protein is undetectable by even sensitive ELISA techniques after the withdrawal of growth factors and the onset of quiescence (Waters et al., 1991). The serum response we have observed occurs in EBV-immortalized LCLs in the exponential phase of growth and appears to result from disruption of cellular clusters formed by these cells during their growth and subsequent increased exposure of these cells to serum. As these cells are continuously cycling they express

slightly higher levels of the c-myc protein than cells in a resting state, and this level of expression is detectable by sensitive Western blotting techniques allowing a detailed examination of the contribution of translational responses to the induction of c-myc protein expression. The detection of endogenous levels of c-myc in this cellular system has allowed us to assess the translational regulation of this oncoprotein in a situation which is more physiologically relevant than many model systems, since in cell lines which are overexpressing large amounts of this oncoprotein there are likely to be additional cellular changes due to this over-expression. In our system, the activation of FRAP/TOR and consequently the phoshorylation of p70 S6 kinase and 4E-BP1 is much slower than on insulin stimulation of various cell types (Price et al., 1992) and serum stimulation of quiescent fibroblasts (Beretta et al., 1996) where increases in the phosphorylation of p70 S6 kinase and 4E-BP1 were observed within 10-15 min. It is likely that the timing of these phosphorylation events is directly related to the nature of the serum response we have described. On serum-stimulation of cells still in a state of more active growth, it is entirely feasible that the time scale of signalling responses to this stimulation would be slower than in cells which have been serum-starved and re-stimulated.

The serum-dependent c-myc induction may well be relevant to B-cell growth in vivo. The ability of B-cells to form homotypic interactions with neighbouring cells is dependent on the expression the LFA-1 and ICAM-1 cell adhesion molecules on the surface of these cells. The expression of these surface proteins is induced on activation of B-cells in vivo, and is important for the efficient function of a number of immune processes, including T-cell mediated killing, B-lymphocyte responses and adherence to other cells of the immune system (see Springer, 1990). It is possible therefore that disruption of cellular aggregates in vivo would increase the exposure of these cells to growth factors and induce a similar c-myc response to the one described here and thus provide a positive growth signal. Since infection of resting B-cells with EBV induces the expression of these adhesion molecules (Aman et al., 1986, Kintner and Sugden, 1981), mimicking the normal processes involved in B-cell activation, the virus may be introducing a mechanism whereby disruption of the resulting cellular aggregates formed can provide a serum responsive growth-promoting c-myc induction. It is therefore possible that this response occurs in the EBV positive immunoblastic B-cell lymphomas which develop in immunosuppressed individuals, since the cells in these tumours display an LCL-like phenotype (Young and Rowe, 1992), and may even contribute to the progression of the disease.

It is clear that the c-myc induction in EBV-positive B-cells described herein, is selective, mediated largely at the level of translation, and the result of the activation of a signalling pathway known to play a role in the directed translation of translationally repressed messages. We have demonstrated recently that the c-myc 5'UTR contains an internal ribosome entry segment (IRES) implying that this mRNA can also be translated in cap-independent manner (Stoneley et al., 1998). It would be interesting therefore to direct future work towards examining the role of the c-myc IRES in

translational responses and the effect that this region has on the induction of c-myc expression. In addition it will be important to assess the effect of the activation of the FRAP/TOR pathway on the expression of other growth-related, translationally repressed and IRES containing genes in these systems.

Materials and methods

Cell culture

The cell lines GM0892A, GM03201 and GM1953 were obtained from the Human Genetic Mutant Cell Repository, Camden, New Jersey, USA, and represent Epstein-Barr virus immortalized B-cell lines established from normal healthy donors. Cells were maintained in suspension culture at 37°C and 5% CO_2 in RPMI 1640 medium (GIBCO–BRL) and 15% foetal calf serum (Advanced Protein Products). Serum stimulation experiments were performed by pelleting cells by centrifugation at 1300 r.p.m. for 5 min and resuspending them in fresh media containing the appropriate concentration of serum at 5×10^5 ml. For treatment with signalling inhibitors, cells were pre-incubated in serum-free media containing rapamycin (20 nM), wortmannin (200 nM), or an equivalent dilution of solvent (DMSO) for 30 min before the addition of serum. Cell viability was determined using trypan blue exclusion by adding an equal volume of 0.4% trypan blue stain to a cell suspension in PBS. For measurement of the rate of degradation of the c-myc protein cells were treated in culture with cycloheximide (50 μg/ml) and protein levels determined by SDS–PAGE and Western blotting. All experiments were performed on at least three independent occasions.

Determination of protein synthesis rates

For determination of protein synthesis rates in the presence of signalling inhibitors, cells were pelleted, resuspended at a concentration of 5×10^5/ml in serum-free media and then incubated for 30 min in the presence of inhibitor before the addition of serum to 15%. Cells were then divided into 4.5 ml aliquots in duplicate in 6-well dishes and 25 μCi of [35S]-methionine (NEN) added to the first time point for 1 h. [35S]-methionine was added to the remaining cells at 3 h and 7 h and labelling performed for 1 h. For protein synthesis determinations in the absence of inhibitors, cells were pelleted, resuspended in media containing 15% serum and experiments performed as described above. At the end of the labelling periods cells were pelleted, washed twice in PBS and then resuspended in a final volume of 1 ml of PBS. Cell suspensions were then spotted in triplicates of 20 μl on to a piece of 3MM filter paper (Whatman) divided into squares and the filter paper dried. Filters were washed for 3×15 min in 5% TCA and then 1×15 min in methanol before drying and cutting into squares. Radioactivity was measured by scintillation counting.

FACS analysis

Propidium iodide staining was performed to determine the cell cycle distribution of cell populations. Cells (2×10^6 per time point) were washed once in PBS and then resuspended in 200 μl PBS. Cells were fixed by the addition of 2 ml of ice-cold 70% ethanol, 30% PBS and incubated at 4°C for at least 30 min and usually overnight. The cells were then pelleted by centrifugation, resuspended in 800 μl PBS, and 100 μl of propidium iodide (400 μg/ml) and 100 μl of RNase A (1 mg/ml) added. Cells were then incubated at 37°C for 30 min before fluorescence analysis.

SDS–PAGE and Western blotting

For analysis of c-myc, α-tubulin, eIF-4E, eIF-4G and eIF-2α proteins, cell pellets were solubilized in electrophoresis buffer (50 mM Tris-HCl pH 6.8, 4% SDS, 10% 2-mercaptoethanol, 1 mM EDTA, 10% glycerol and 0.01% bromophenol blue) by sonication. Cell extracts (10^6 cells per lane) were then analysed by SDS-polyacrylamide gel electrophoresis on 7.5% or 10% 16 cm gels (BioRad) and proteins transferred to nitrocellulose (Schleicher and Schuell) by electroblotting in transfer buffer (0.2 M glycine, 20 mM Tris, 20% (v/v) methanol) for 1.5 h at 85 V. For analysis of the phosphorylation states of the 4E-BP1 and p70 S6 kinase proteins, cell pellets were solubilized in extraction buffer (50 mM Na β-glycerophosphate pH 7.4, 0.5 mM Na orthovanadate, 1 mM EDTA, 1 mM EGTA, 1 mM DTT, 1% Triton-X100 and 10% glycerol) with 1 μM microcystin, 10% aprotinin, 0.1 mM PMSF, 1 μg/ml leupeptin and 1 μg/ml N-α-p-Tosyl-l-lysine chloromethylketone (TLCK) added immediately before use. Cell extracts were centrifuged at 13 000 r.p.m. for 5 min to pellet cell debris and $0.5–1 \times 10^6$ cell equivalents of extract mixed with an equal volume of 2 × electrophoresis buffer, boiled and analysed by SDS-polyacrylamide electrophoresis. p70 S6 kinase proteins were analysed using 7.5% gels and transferred as described above. For analysis of 4E-BP1, samples were resolved on 15% gels, transferred for 2 h on to PVDF membrane (Gelman Sciences) and the membrane fixed in 0.05% glutaraldehyde in Tris-buffered saline containing 0.1% Tween-20 (TBS-T) for 30 min. Equal loading of protein was determined on all blots by staining with Ponceau S. Blots were blocked by incubation in 5% skimmed milk in TBST for 1–2 h and then probed with the relevant antibodies for 1 h at room temperature. c-myc protein was detected using the mouse monoclonal antibody 9E10 (generated by Dr T Harrison) at 1:400 dilution and α-tubulin proteins were detected using a mouse monoclonal antibody (Sigma) at 1:10 000. Rabbit polyclonal antibodies used to detect eIF-4E, eIF-2α, p70 S6 kinase, 4E-BP1, and eIF-4G were provided by Dr S Morley (4E and 4G), Dr N Redpath (p70 S6 kinase), Prof R Denton (4E-BP1), and Prof C Proud (eIF-2α) respectively, and were used at dilutions of 1:7000, 1:2000, 1:1000, and 1:2000 and 1:2000, respectively. Blots were then incubated with peroxidase-conjugated secondary antibodies raised against mouse or rabbit immunoglobulins and developed using the chemiluminescence reagent 'Illumin 8' (generated by Dr M Murray, Dept. of Genetics, Leicester University).

Isoelectric focusing

To determine the phosphorylation state of eIF-4E, non-phosphorylated and phosphorylated forms of the protein were separated using one-dimensional isoelectric focusing. Cell pellets were lysed in extraction buffer at a concentration of 2×10^7 cells/ml and prepared as for analysis by Western blotting. 20 μl of sample was mixed with the appropriate volume of 7 × isoelectric focusing sample buffer and urea added to a final concentration of 9M. Isoelectric focusing was performed essentially as described (Redpath, 1992), using a Biorad minigel apparatus with ampholytes in the pH range 3–10 (BioRad), and 0.01 M glutamic acid and 0.05 M histidine at the anode and cathode, respectively. Focused gels were then Western blotted for 30 min and probed for eIF-4E as described above.

m^7 GTP Sepharose affinity chromatography

eIF-4E containing protein complexes were isolated using an adaptation of a method previously described (Morley and Pain, 1995a). Cells (1×10^7 per time point) were pelleted by centrifugation, washed twice in PBS and then

resuspended in homogenization buffer (50 mM MOPS-KOH, pH 7.2, 50 mM NaCl, 50 mM NaF, 50 mM Na β-glycerophosphate, 5 mM EDTA, 5 mM EGTA, 14 mM 2-mercaptoethanol) containing freshly added 100 μM GTP, 2 mM benzamidine, 0.1 mM PMSF, 1 μM microcystin and 1 μg/ml leupeptin and TLCK. NP40 was then added to 0.5% and the cells lysed by vortexing. Cell debris was removed by centrifugation at 13000 r.p.m. for 5 min and the lysate loaded onto a 250 μl m⁷GTP Sepharose (Pharmacia) column equilibrated in buffer minus detergent. Following one wash of the column with 500 μl of buffer, bound complexes were eluted in 500 μl buffer containing 0.2 mM m⁷GTP (Sigma). Proteins were then precipitated by the addition of 500 μl of 7% trichloroacetic acid in the presence of cytochrome c (10 μg/ml) on ice. Precipitates were pelleted by centrifugation at 13 000 r.p.m. for 10 min, washed three times in acetone, and dried. Samples were solubilized in electrophoresis buffer and analysed for eIF-4E, eIF4-G and 4E-BP1 content by SDS–PAGE and Western blotting as described above

Northern blot analysis

Total cellular RNA was prepared and analysed by Northern blotting exactly as described previously (West et al., 1995). DNA probes used for the detection of c-myc and GAPDH mRNA species were also as described (West et al., 1995). In addition, a plasmid containing the α-tubulin cDNA (Villasante et al., 1986) was kindly provided by P Walden via Prof K Gull (University of Manchester), and an 839 and 738 bp region of the cDNA were isolated and used to detect the α-tubulin message.

Sucrose gradient density centrifugation and RNA detection

Sucrose gradient centrifugation was used to separate ribosomes into polysomal and monosomal forms, and these gradients were then fractionated with continuous monitoring at 260 nm and RNA isolated from each fraction as described previously (West et al., 1995). The distribution of individual mRNA species across these gradients was then determined by slot blot analysis and hybridization with specific cDNA probes. The c-myc, GAPDH, and α-tubulin probes were as described previously (West et al., 1995)

References

Allday MJ and Farrell PJ. (1994). J. Virol., 68, 3491–3498.
Aman P, Lewin N, Nordstrrum M and Klein G. (1986). Curr. Top. Microbiol. Immunol., 132, 266–271.
Beretta L, Gingras A, Svitkin YV, Hall MN and Sonenberg, N. (1996). EMBO J., 15, 658–664.
Blanchard J-M, Piechaczyk, M, Dani C, Chambard J-C, Franchi A, Pouyssegur J and Jeanteur P. (1985). Nature, 317, 443–445.
Brown EJ and Schreiber SL. (1996). Cell, 86, 517–520.
Brunn GJ, Williams J, Sabers C, Weiderrecht G, Lawrence JC and Abraham RT. (1996). EMBO J., 15, 5256–5267.
Bu X and Hagedorn, CH. (1991). FEBS Lett., 283, 219–222.
Cheatham B, Vlahos CJ, Cheatham L, Wang L, Blenis J and Kahn CR. (1994). Mol. Cell. Biol., 14, 4902–4911.
Cherney BW, Bhatia K and Tosato G. (1994). Proc. Natl. Sci. USA 91, 12967–12971.
Chung J, Grammer TC, Lemon KP, Kaziauskas A and Blenis J. (1994). Nature, 370, 71–75.
Chung J, Kuo CJ, Crabtree GR and Blenis J. (1992). Cell, 69, 1227–1236.
Cohen RB, Boal TR and Safer B. (1990). EMBO J., 9, 3831–3837.
Darveau A. Pelletier J and Sonenberg N. (1985). Proc. Natl. Sci. USA, 82, 2315–2319.
Dean M, Levine RA, Ran W, Kindy MS, Sonenshein GE and Campisi J. (1986). J. Biol. Chem., 261, 9161–9166.
Feigenblum D and Schneider RJ. (1996). Mol. Cell. Biol., 16, 5450–5457.
Flynn A and Proud CG. (1996). Eur. J. Biochem., 236, 40–47.
Gallie DR and Traugh JA. (1994). J. Biol. Chem., 269, 7174–7179.
Gray NK and Hentze MW. (1994). Mol. Biol. Reports, 19, 195–200.
Gregory CD, Murray RJ, Edwards CF and Rickinson AB. (1988). J. Exp. Med., 167, 1811–1824.

Gregory CD, Rowe M and Rickinson AB. (1990). J. Gen. Virol., 71, 1481–1495.
Hann SR and Eisenman RN. (1984). Mol. Cell. Biol., 4, 2486–2497.
Jefferies HB, Reinhard JC, Kozma SC and Thomas G. (1994). Proc. Natl. Acad. Sci. USA, 91, 4441–4445.
Jones J, Branda J, Johnston KA, Polymenis M, Gadd M, Rustgi A, Callanan L and Schmidt EV. (1996). Mol. Cell. Biol., 16, 4754–4764.
Jones N. (1996). Immunol., 89, 26–30.
Kelly K, Cochran BH, Stiles CD and Leder P. (1983). Cell, 35, 603–610.
Kintner C and Sugden B. (1981). Nature, 294, 458–460.
Koromilas AE, Lazaris-Karatzas A and Sonenberg N. (1991). EMBO J., 11, 4153–4158.
Kunz JR, Henriquez U, Schneider M, Deuter-Reinhard M, Movva NR and Hall MN. (1993). Cell, 73, 585–596.
Lazarus P. (1992). Oncogene, 7, 1037–1041.
Lin T-A, Kong X, Haystead TAJ, Pause A, Belsham G, Sonenberg N and Lawrence JC. (1994). Science, 266, 653–656.
Lin T-A, Kong X, Salteil AR, Blackshear PJ and Lawrence JC. (1995). J. Biol. Chem., 270, 18531–18538.
Lüscher B and Eisenmann RN. (1988). Mol. Cell. Biol., 8, 2504–2512.
Lyons RT, Nordeen SK and Young DA. (1980). J. Biol. Chem., 255, 6330–6334.
Manzella JM, Rychlik W, Rhoads RE, Hershey JWB and Blackshear PJ. (1991). J. Biol. Chem., 266, 2383–2389.
Mao X, Green JM, Safer B, Lindsten T, Frederickson RM, Miyamoto S, Sonenberg N and Thompson CB. (1992). J. Biol. Chem. 267, 20444–20450.
Marcu KB, Bossone SA and Patel AJ. (1992). Ann. Rev. Biochem., 61, 809–860.
Marshall CJ. (1996). FASEB, J., 10, 7–13.

Mendez R, Myers MG, White MF and Rhoads RE. (1996). *Mol. Cell. Biol.,* **16,** 2857–2864.

Ming X, Burgering BMT, Wennstrom S, Claesson-Welsh L, Heldin CH, Bos JL, Kozma SC and Thomas G. (1994). *Nature,* **371,** 426–429.

Morley SJ, Dever TE, Etchison D and Traugh JA. (1991). *J. Biol. Chem.,* **266,** 4669–4672.

Morley S and Pain VM. (1995a) *J. Cell. Sci.,* **108,** 1751–1760.

Morley SJ and Pain VM. (1995b) *Biochem. J.,* **312,** 627–635.

Morley SJ and Traugh JA. (1989). *J. Biol. Chem.,* **264,** 2401–2404.

Morley SJ and Traugh JA. (1990). *J. Biol. Chem.,* **265,** 10611–10616.

Nepveu A, Levine RA, Campisi J, Greenberg ME, Ziff EB and Marcu KB. (1987). *Oncogene,* **1,** 243–250.

Nielson FC, Ostergaard L, Nielson J and Christianson J. (1995). *Nature,* **377,** 358–362.

Parkin N, Darveau A, Nicholson R and Sonenberg N. (1988). *Mol. Cell. Biol,* **8,** 2875–2883.

Paulin FEM, West MJ, Sullivan NF, Whitney RL, Lyne L and Willis AE. (1996). *Oncogene,* **13,** 505–513.

Pause A, Belsham GJ, Gingras A-C, Donze O, Lin T-A, Lawrence Jr JC and Sonenberg N. (1994). *Nature,* **371,** 762–767.

Price DJ, Grove JR, Calvo V, Avruch J and Bierer BE. (1992). *Science,* **257,** 973–976.

Proud CG. (1994). *Nature,* **371,** 747–748.

Proud CG. (1996). *Trends Biochem. Sci.,* **21,** 181–185.

Redpath NT. (1992). *Anal. Biochem.,* **202,** 340–343.

Rosenwald IB. (1995). *Cancer Lett.,* **98,** 77–82.

Rosenwald IB, Rhoads DB, Callanan LD, Isselbacher KJ and Schmidt EV. (1993). *Proc. Natl. Acad. Sci. USA.* **90,** 6175–6178.

Rousseau D, Kaspar R, Rosenwald I, Gehrke L and Sonenberg N. (1996). *Proc. Natl. Acad. Sci. USA,* **93,** 1065–1070.

Sabatini DM, Erdjument-Bromage, H, Lui M, Tempst P and Snyder SH. (1994). *Cell,* **78,** 35–43.

Shindo H, Tani E, Matsumuto T, Hashimoto T and Furuyama J. (1993). *Acta Neuropath.,* **86,** 345–352.

Spotts GD and Hann SR. (1990). *Mol. Cell. Biol.,* **10,** 3952–3964.

Springer TA. (1990). *Nature,* **346,** 425–434.

Stoneley M, Paulin FEM, Le Quesne JPC, Chappell SA and Willis AE. (1998). *Oncogene,* **16,** 423–428.

Terada N, Patel HR, Takase K, Kohno K, Nairn AC and Gelfand EW. (1994). *Proc. Natl. Acad. Sci. USA,* **91,** 11477–11481.

Villasante A, Wang D, Dobner P, Dolph P, Lewis SA and Cowan NJ. (1986). *Mol. Cell. Biol.,* **6,** 2409–2419.

Von Manteuffel SR, Gingras A-C, Ming X-F, Sonenberg N and Thomas G. (1996). *Proc. Natl. Acad. Sci. USA,* **93,** 4076–4080.

Waters CM, Littlewood TD, Hancock DC, Moore JP and Evan GI. (1991). *Oncogene,* **6,** 797–805.

West MJ, Sullivan NF and Willis, AE. (1995). *Oncogene,* **11,** 2515–2524.

Young LS and Rowe M. (1992). *Sem. Cancer Biol.,* **3,** 273–284.